

# NANOTECH FRANCE 2016

International Nanotechnology Conference  
1 - 3 June 2016

Pôle Universitaire Léonard de Vinci, La Défense  
Paris - France

Organizer



**SETCOR**  
Conferences & Events

[www.sector.org](http://www.sector.org)

In Collaboration with



**edp sciences**

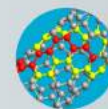
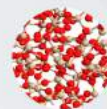
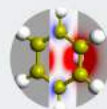
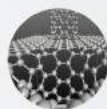
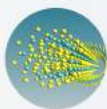
Joint Conference



# ATOMISTIX TOOLKIT

## Atomic-Scale Modeling Software for Nanotechnology

Atomistix ToolKit (ATK) offers unique capabilities for simulating electrical transport properties of nanodevices on the atomic scale. Based on an open architecture which integrates a powerful scripting language with a graphical user interface, ATK is a comprehensive platform for studies in nanoelectronics, using both accurate first-principles (DFT) and fast semi-empirical methods and classical potentials. Moreover, ATK includes a very advanced electrostatic model to allow realistic simulations of nanoscale transistor structures.



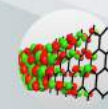
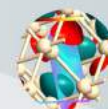
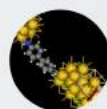
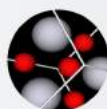
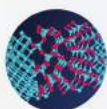
### Study

graphene & nanotubes  
nanowires  
magnetic tunnel junctions  
molecular electronics  
complex interfaces  
high-K dielectrics  
spintronics  
single-electron transistor  
phonons and phonon transport  
transistor DOS  
Nudged Elastic Band  
stress and strain  
topological insulators



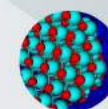
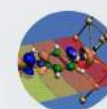
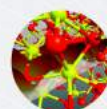
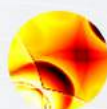
### Calculate

I-V curve  
transistor characteristics  
spin current  
Schottky barrier  
leakage current  
contact resistance  
tunnel magneto-resistance  
charge stability diagram  
classical potential  
Molecular Dynamics nanotube  
complex bandstructure  
transition states  
thermal transport  
spin transfer torque



ATK is also an ideal tool for educational courses in various subjects, from basic quantum mechanics to graduate courses in nanoelectronics. Special discounts are available for teaching licenses.

Since 2006, over 800 scientific articles have been published using ATK. The software is used by over 300 research groups at leading universities, government labs, and electronics companies around the world, in a wide range of application areas (see other side).



Download a free trial:

[www.quantumwise.com](http://www.quantumwise.com)

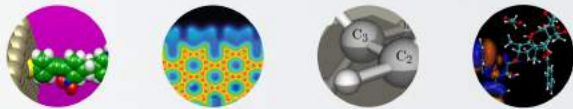


# Application areas

The unique capabilities of Atomistix ToolKit are currently being applied in a wide variety of areas, such as carbon and molecular electronics, nanowires, and spintronics devices, as well as for assessing the structural and electrical properties of new electronic materials like high-k dielectrics or organic electronic materials.

## Molecular Electronics

- Current-voltage (I-V) characteristics of rectifying molecular junctions (single molecules between metal electrodes), i.e. molecular diodes and switches. The active component can be an organic or organometallic molecule, a metallic nanocluster, etc.
- Resistivity of insulating or conducting molecular wires, free or attached to surfaces.
- Investigation of optical switches
- Inelastic spectroscopy.



## Bulk and nanoscale semiconductors

- Surface states in semiconducting nanowires.
- Leakage currents in ultra-shallow junctions with high/low-k dielectrics.
- Schottky barriers of complex interfaces.
- Activation energies of defect diffusion.
- Work function of nanostructured surfaces (nanoclusters, wires).
- Binding energies of defects in bulk semiconductors, nanowires, or nanotubes.
- Nonparabolicity parameters.
- Phonon limited mobility.



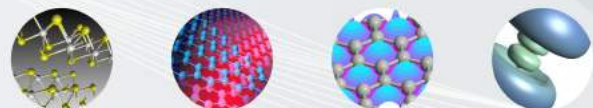
## Carbon-based Electronics

- Transport properties (conductance, I-V) of carbon or boron-nitride nanotubes, with or without defects and impurities.
- Graphene nanoribbons, e.g. for field-effect transistor applications; also bilayer structures.
- Multiwall nanotubes, for applications as nanoscale variable resistors or capacitors.
- Contact resistance and capacitance of metal, nanotube and graphene interfaces and junctions.
- I-V characteristics of functionalized nanotubes or graphene for sensor applications.



## 3-Terminal devices

- Advanced electrostatic model with dielectric and biased metallic region.
- Calculation of transistor characteristics.
- Charge stability diagrams of weakly coupled single-electron transistors in Coulomb blockade regime (sequential tunneling).



## Nanowires

- I-V characteristics of metallic nanowires and atomic point contacts.
- Electromigration and non-equilibrium current-induced forces in atomic wires.
- Mobility limited by random scattering.



## Magnetic systems and spintronics

- Spin tunneling mechanisms in magnetotunnel junction (MTJ) for MRAM/read applications.
- Spin torque transfer in MTJs.
- I-V characteristics of molecular spintronics structures.
- Non-collinear, including spin spin-orbit.
- Transport properties of magnetic metallic nanowires.



Computational science has become critical to scientific leadership, economic competitiveness, and national security. Breakthroughs and innovations will be won by those most skilled with advanced computing systems and computational science applications.

US President's Information Technology Advisory Committee

QuantumWise, Virtual NanoLab, Atomistix ToolKit, and NanoLanguage are registered trademarks used under licence.

© QuantumWise 2015

QuantumWise A/S

Fruebjergvej 3, Box 4  
DK-2100 Copenhagen  
DENMARK

Quantum  
Wise  
When every atom matters

[www.quantumwise.com](http://www.quantumwise.com)

[info@quantumwise.com](mailto:info@quantumwise.com)

+45 699 01 888

+45 698 02 801



# Registration Opening for all conferences Nanotech France 2016, EGF 2016, NanoMatEn 2016 and NanoMetrology 2016

May 31<sup>st</sup>, 2016

15:00-18:00	Registration / Welcoming Cocktail Reception	Registration Area
-------------	---	-------------------

## Nanotech France 2016 Sessions Program

June 1<sup>st</sup>, 2016

08:30-12:00	Registration	Registration Area
09:00-12:45	Nanotech Plenary Session I	Amphitheatre H
09:00-12:45	Joint Symposium on Functional Hybrids and Clay Nanomaterials	Room 261
12:00-14:00	Lunch Break / Exhibition / Poster Session I	Restaurant / Main Hall
14:00-16:00	Session I: Nanomaterials Fabrication / Synthesis	Room 211
	Session II - Nanomaterials synthesis and properties	Room 212
	Joint Symposium on Functional Hybrids and Clay Nanomaterials	Room 261
16:00-16:30	Coffee Break / Exhibition / Poster Session I	Main Hall
16:30-19:00	Session I: Nanomaterials Fabrication / Synthesis	Room 211
	Session II - Nanomaterials synthesis and properties	Room 212
	Joint Symposium on Functional Hybrids and Clay Nanomaterials	Room 261

June 2<sup>nd</sup>, 2016

09:15-12:45	Nanotech Plenary session II	Amphitheatre H
10:00-10:30	Coffee Break / Exhibition / Poster Session II	Main Hall
10:30-12:45	Session III: NanoBioMedecine /Nanosafety	Room 508
12:00-14:00	Lunch break / Exhibition / Poster session II	Restaurant / Main Hall
14:00-16:00	Session III: NanoBioMedecine /Nanosafety	Room 508
16:00-16:30	Coffee break / Exhibition / Poster session II	Main Hall
16:30 -19:00	Session III: NanoBioMedecine /Nanosafety	Room 508
18:30-20:30	Networking Cocktail – Meet Elsevier Team	Main Hall

June 3<sup>rd</sup>, 2016

09:00-10:00	Session IV: NanoElectronics/NanoPhotonics	Room 211
	Industrial session: InnovNano France 2016	Room 508
10:00-10:30	Coffee Break + Exhibition	Main Hall
10:30-13:00	Session IV: NanoElectronics/NanoPhotonics	Room 211
	Industrial session:InnovNano France 2016	Room 508



## NanoMetrology France 2016 Sessions Program

June 1 <sup>st</sup> , 2016		
08:30-12:00	Registration	Registration Area
09:00-12:45	Nanotech Plenary Session I	Amphitheatre H
10:30-11:00	Coffee Break / Exhibition / Poster Session II	Main Hall
11:00-12:45	Session I: Nanomaterials characterization	Room 508
	Symposium on Nanospectroscopy	Room 561
12:00 - 14:00	Lunch Break / Exhibition / Poster Session I	Restaurant / Main Hall
14:00 16:00	Session I: Nanomaterials characterization	Room 508
	Symposium on Nanospectroscopy	Room 561
16:00 -16:30	Coffee Break / Exhibition / Poster Session I	Main Hall
16:30 19:00	Session I: Nanomaterials characterization	Room 508
	Symposium on Nanospectroscopy	Room 561

June 2 <sup>nd</sup> , 2016		
09:15-12:45	Nanotech Plenary session II	Amphitheatre H
09:00-10:00	Symposium on Detection, location & quantification Nano	Room 511
10:00 - 10:30	Coffee Break / Exhibition / Poster Session II	Main Hall
10:30 -12:45	Symposium on Detection, location & quantification Nano	Room 511
12:00 -14:00	Lunch break / Exhibition / Poster session II	Restaurant / Main Hall
14:00 -16:00	Symposium on Detection, location & quantification Nano	Room 511
16:00 - 16:30	Coffee break / Exhibition / Poster session II	Main Hall
16:30 -19:00	Symposium on Detection, location & quantification Nano	Room 511
18:30 -20:30	Networking Cocktail – Meet Elsevier Team	Main Hall

# NanMaterials for Energy and Environment - NanoMatEn 2016 Sessions Program

June 1 <sup>st</sup> , 2016		
08:30-12:00	Registration / Welcome Coffee	Registration Area
09:00-12:45	Nanotech Plenary Session I	Amphitheatre H
12:00-14:00	Lunch Break / Exhibition / Poster Session I	Restaurant / Main Hall
June 2 <sup>nd</sup> , 2016		
08:30-12:45	Nanotech Plenary session II	Amphitheatre H
10:30-11:00	Coffee Break / Exhibition / Poster Session II	Main Hall
10:30-12:45	NanoMatEn 2016 Session I: NanoEnergy	Room 211
	NanoMatEn 2016 Session II: Nanotechnology for Environmental	Room 212
12:00-14:00	Lunch break / Exhibition / Poster session II	Restaurant / Main Hall
14:00-16:00	NanoMatEn 2016 Session I: NanoEnergy	Room 211
	NanoMatEn 2016 Session II: Nanotechnology for Environmental	Room 212
	Symposium on Nanotechnology for Photovoltaics	Room 260
16:00-16:30	Coffee break / Exhibition / Poster session II	Main Hall
16:30-19:00	NanoMatEn 2016 Session I: NanoEnergy	Room 211
	NanoMatEn 2016 Session II: Nanotechnology for Environmental	Room 212
	Symposium on Nanotechnology for Photovoltaics	Room 260
18:30-20:30	Networking Cocktail – Meet Elsevier Team	Main Hall
June 3 <sup>rd</sup> , 2016		
08:30-10:30	NanoMatEn 2016 Session III: Nanotechnology for water treatment	Room 561
10:30-11:00	Coffee Break / Exhibition	Main Hall
11:00-13:00	NanoMatEn 2016 Session III: Nanotechnology for water treatment	Room 561



## European Graphene Forum - EGF 2016 Sessions Program

June 1 <sup>st</sup> , 2016		
08:30-12:00	Registration / Welcome Coffee	Registration Area
09:00-10:30	EGF2016 Plenary Session I	Amphitheatre G
10:30-11:00	Coffee Break / Exhibition / Poster Session II	Main Hall
11:00-12:45	EGF2016 Plenary Session I	Amphitheatre G
12:45-14:00	Lunch Break / Exhibition / Poster Session I	Restaurant / Main Hall
14:00-16:00	EGF 2016- Session I: Graphene and 2D Materials Synthesis, characterization and properties	Amphitheatre G
16:00-16:30	Coffee Break / Exhibition / Poster Session I	Main Hall
16:30-19:00	EGF 2016- Session I: Graphene and 2D Materials Synthesis, characterization and properties	Amphitheatre G

June 2 <sup>nd</sup> , 2016		
09:15-12:45	EGF 2016 Plenary Session II	Amphitheatre G
10:30-11:00	Coffee Break / Exhibition / Poster Session II	Main Hall
10:30-12:45	EGF 2016 Plenary Session II	Amphitheatre G
12:00-14:00	Lunch break / Exhibition / Poster session II	Restaurant / Main Hall
14:00-16:00	EGF 2016- Session II: Graphene and 2D Materials characterization and properties	Amphitheatre G
	EGF 2016- Session III: Graphene and 2D Materials properties and applications	Room 561
16:00-16:30	Coffee break / Exhibition / Poster session II	Main Hall
16:30-19:00	EGF 2016- Session II: Graphene and 2D Materials characterization and properties	Amphitheatre G
	EGF 2016- Session III: Graphene and 2D Materials properties and applications	Room 561
18:30-20:30	Networking Cocktail – Meet Elsevier Team	Main Hall

June 3 <sup>rd</sup> , 2016		
08:30-10:00	EGF 2016- Session IV: Graphene and 2D Materials applications	Room 511
10:00-10:30	Coffee Break / Exhibition	Main Hall
10:30-13:00	EGF 2016- Session IV: Graphene and 2D Materials applications	Room 511

## Nanotech France 2016 Conference Preliminary Program

<b>June 1<sup>st</sup>, 2016</b> <b>Nanotech Plenary session I</b>		
<b>Amphitheatre H</b>		
<b>Session's Chairs:</b> <b>Prof. Jupille Jacques, Institut des Nanosciences de Paris - France.</b> <b>Prof. James M Hill, University of South Australia – Australia</b>		
<b>08:30-12:00 Conferences Registration</b>		
<b>09:00-09:30</b>	Club nanoMetrology: a French Initiative to improve the Reliability of Measurements at the Nanoscale. A review after 4 years. <b>G. Favre</b> , K. Aguir, D. Bernard, O. Bezencenet, J. Carimalo, N. Feltin, B. Gautier, A. Levenson, T. Macé, P. Maillot and J.-M. Moschetta	<b>Dr. Georges Favre</b> , Laboratoire national de métrologie et d'essais (LNE) – <b>France</b>
<b>09:30-10:00</b>	European standardization in nanotechnologies and relation with International work. How standardization can help industry and regulators in developing safe products? <b>P. Conner</b>	<b>Mr. Patrice Conner</b> , AFNOR Standardization, Management and Consumer Services Dep- <b>France</b>
<b>10:00-10:30</b>	Mathematical modelling in nanotechnology <b>J. Hill</b>	<b>Prof. James M Hill</b> , University of South Australia – <b>Australia</b>
<b>10:30-11:00 Coffee Break / Exhibition/ Posters Session I</b>		
<b>11:00-11:30</b>	Water collection/Repellency of Bioinspired Micro/Nano-structured Surfaces <b>Y. Zheng</b>	<b>Prof. Yongmei Zheng</b> , Beihang University – <b>China</b>
<b>11:30-12:00</b>	Ultrasonic Spray Coating as a versatile technique for the large area deposition of functional nanoparticles J. Stryckers and <b>W. Deferme</b>	<b>Prof. Wim Deferme</b> , Hasselt University - <b>Belgium</b>
<b>12:45-14:00 Lunch Break / Exhibition / Posters session I</b>		

<b>June 1<sup>st</sup>, 2016</b> <b>Session I: Nanomaterials Fabrication / Synthesis</b>		
<b>Conference Room 211</b>		
<b>Session's Chairs:</b> <b>Prof. Jacques Jupille, Institut des Nanosciences de Paris – France/ Prof. Nicolas Fressengeas, Lorraine University – France/ Dr. Valentina Beghetto, Ca' Foscary, University of Venice – Italy / Prof. Valentin Rodionov, King Abdullah University of Science and Technology - Saudi Arabia</b>		
<b>14:00-14:15</b>	Rational Synthesis of Chirality-Pure Single Walled Carbon Nanotube <b>K.Yu. Amsharov</b>	<b>Dr. Konstantin Amsharov</b> , University of Erlangen-Nürnberg – <b>Germany</b>
<b>14:15-14:30</b>	New frontiers and technologies for advanced materials <b>V. Beghetto</b> , L. Agostinis, R. Taffarello and R. Samiolo	<b>Dr. Valentina Beghetto</b> , Ca' Foscary, University of Venice - <b>Italy</b>
<b>14:30-14:45</b>	Weak interactions for strong complexation between DNA nano-rods and lipids <b>L. Navailles</b> , K. Bougis, R. Leite Rubim, N. Ziane, J. Peyencet, A. Bentaleb, A. Février, B.B. Gerbelli, C.L.P. Oliveira, A. de Oliveira, . Schoentgen, G. Tonelli, P. Barthélémy and F. Nallet	<b>Dr. Laurence Navailles</b> , CNRS/ Bordeaux University, <b>France</b>



14:45-15:00	Repeat proteins as template to organize photoactive molecules <b>S. Hernández Mejías</b> , J. López-Andarias, K. Erazo, C. Atienza, N. Martín and A.L. Cortajarena	<b>Ms. Sara Hernández</b> , IMDEA-Nanociencia, Madrid - Spain
15:00-15:15	Chemical Reactions Directed Evolution of Complex Peptide Nanostructures <b>A.K. Das</b>	<b>Dr Apurba K. Das</b> , Indian Institute of Technology Indore- India
15:15-15:30	Metal nanoparticles for optical limiting prepared via citrate reduction <b>C. S. Hege</b> , S. Dengler and B. Eberle	<b>Ms. Cordula Hege</b> , Fraunhofer IOSB – Germany
15:30-15:45	Shape and Pore Size Controlled Scalable Synthesis of Functional Oxide Nanostructures through Exothermic Chemical Reactions <b>A. Voskanyan</b> and K.Y. Chan	<b>Mr. Albert Voskanyan</b> , The University of Hong Kong - Hong Kong
15:45-16:00	Ultrasonic Spray Coating as a scale-up technique for the deposition of hybrid magnetic-plasmonic nanocomposites <b>J. Stryckers</b> , T. Swusten, W. Brullot, J. D'Haen, T. Verbiest and W. Deferme	<b>Mr. Jeroen Stryckers</b> , Hasselt University - Belgium
16:00-16:30	<b>Coffee Break / Exhibition/ Posters Session I</b>	
16:30-16:45	The Development and Application of Vacuum-interconnected Technology for Nanofabrications <b>S. A. Ding</b> and H. Yang	<b>Dr. Sunan Ding</b> , SuZhou Institute of Nano-Tech and Nano-Bionics / Chinese Academy of Sciences - China
16:45-17:00	Functionalization of single wall carbon nanotube for cesium sorption <b>H. Draouil</b> , L. Alvarez, J. Cambedouzou, M. A. Zaibi and J.-L. Bantignies	<b>Ms. Hajer Draouil</b> , Tunis University - Tunisia
17:00-17:15	Development of a new direct liquid injection system for nanoparticle deposition by chemical vapor deposition using nanoparticle solutions <b>M.Vervaele</b> , B. De Roo, M.Rajala, H.Guillon, J.W.Seo and J.P.Locquet	<b>Mr. Mattias Vervaele</b> , KU Leuven - Belgium
17:15-17:30	Composite production for Cold Gas Spray and photocatalytic behavior of the multifunctional coatings <b>S. Dosta</b> , M. Robotti, I. G. Cano, N. Cinca, A. Concustell, J. M. Guilemany	<b>Dr. Sergi Dosta</b> , University of Barcelona - Spain
17:30-17:45	Application of Spark discharge method for in situ synthesis of copper nano particles on cotton fabrics <b>S. Shahidi</b> , A.Jamali 2, S.D. Sharifi and H. Ghomi	<b>Dr. Sheila Shahidi</b> , Islamic Azad University- Iran
17:45-18:00	Controlled resonance energy transfer under one- and two-photon excitations in a hybrid material engineered from quantum dots and the photosensitive protein bacteriorhodopsin <b>V. Krivenkov</b> , P. Samokhvalov, R. Bilan, D. Solovyeva, A. Chistyakov and I. Nabiev	<b>Mr. Victor Krivenkov</b> , National Research Nuclear University - Russian Federation
18:00-18:15	Microwave Assisted Synthesized ZnO nanorods arrays on Tetrapak Substrate <b>A.Pimental</b> , B. Coelho, S. Ferreira, A. Araújo, D. Nunes, M. Oliveira, R.Franco, H. Águas, R. Martins and E. Fortunato	<b>Dr. Ana Pimentel</b> , Universidade NOVA de Lisboa - Portugal
18:15-18:30	Fabrication of Metal Nanotubes via Short-Circuit Diffusion Process and The Diffusion Model <b>S. Baylan</b> , E. Rabkin and G. Richter	<b>Mrs. Semanur Baylan</b> , Max Planck Institute for Intelligent Systems- Germany
18:30-18:45	Design and characterization of nanowired microwave devices in substrate integrated waveguide technology <b>V. Van Kerckhoven</b> , L. Piraux and I. Huynen	<b>Mr. Vivien Van Kerckhoven</b> , Université catholique de Louvain - Belgium
18:45-19:00	G-doping in Thin Si Nano-grating Layers A. Tavkhelidze, L. Jangidze, <b>M. Mebonia</b> , G. Skhiladze, D. Ursutiu, C. Samoila, Z. Taliashvili, and L. Nadaraia	<b>Mr. Mikheil Mebonia</b> , Ilia State University- Germany

June 1<sup>st</sup>, 2016

Session II - Nanomaterials synthesis and properties

Conference Room 212

Session's Chairs:

Prof. Wim Deferme, Hasselt University – Belgium/ Prof. Yongmei Zheng, Beihang University – China/ Dr. Karine Bonnot, French German Research Institute of Saint-Louis – France/ Prof. Tahar Laoui, King Fahd University of Petroleum and Minerals- Saudi Arabia

14:00-14:30	Surface-Engineered Mechanically Hard Tungsten Disulfide (WS <sub>2</sub> ) Inorganic Nanotubes (INTs-WS <sub>2</sub> )– Novel Chemically Tailored Nanoscale CNT-Replacement Inorganic “Nanofillers” <b>J.-P. Lellouche</b> , D. Raichman and J. Laloy	<b>Prof. Jean-Paul Lellouche</b> , Bar-Ilan University - Israel
14:30-14:45	Reinforcing Acrylonitrile Rubber With Graphene: Inspection of Mechanical, Thermal and Cure Kinetics Properties <b>B. Mensah</b> and C. Nah	<b>Mr. Bismark Mensah</b> , Chonbuk National University - Rep. of Korea
14:45-15:00	Development of Flexural Properties in Woven-fabric/Epoxy Resin CFRP Panels with Additional Nano Rubber Particle Reinforcement <b>J. Sirichantra</b> , T. Pullawan, P. Lamo and S. Kumwongwian	<b>Dr. Jariyavadee Sirichantra</b> , Ministry of Science and Technology - Thailand
15:00-15:15	The effect of dispersion method and processing condition on the structure properties of polystyrene/graphene oxide nanocomposites <b>Z. Mohammadsalih</b> , B.J. Inkson and B. Chen	<b>Mr. Zaid Mohammadsalih</b> , University of Sheffield - UK
15:15-15:30	Hollow Nanoparticles for Applications in Lightweight Nanocomposites <b>V. Rodionov</b> and T. Sainsbury	<b>Prof. Valentin Rodionov</b> , King Abdullah University of Science and Technology - Saudi Arabia
15:30-15:45	Functionalization and optical properties of inorganic liquid crystals <b>M. Thiriet</b> , K. Lahlil, J.P. Boilot, J. Peretti and T. Gacoin	<b>Ms. Maud Thiriet</b> , Ecole Polytechnique, CNRS – France
15:45-16:00	Chip Calorimetry for Investigating the Co-detection of Hexogen and Pentrite Vapors by Nanostructured Porous Materials <b>K. Bonnot</b> , L. Schlur and D. Spitzer	<b>Dr. Karine Bonnot</b> , French German Research Institute of Saint-Louis - France
16:00-16:30	<b>Coffee Break / Exhibition/ Posters Session I</b>	
16:30-16:45	Development of fire retardant treatment with silica nanoparticles to apply onto bio-based composite materials <b>M. Bourebrab</b> , G. Durand, A. Taylor, R. Hadden and L. Bisby	<b>Ms. Marion Bourebrab</b> , University of Edinburgh - UK
16:45-17:00	Resistive sensors from nanoparticle assembles <b>L. Baklouti</b> and F. Favier	<b>Ms Linda Baklouti</b> , University of Montpellier – France
17:00-17:15	Effect of nano Zinc oxide particles on weathering properties of epoxy coatings <b>D. Shalini</b> and A.S.Khanna	<b>Mrs. Dolai Shalini</b> , IIT Bombay – India
17:15-17:30	Facile Synthesis of Scalable Hierarchical Surfaced Titanium Di-oxide Hollow Sphere for Hydrogen Generation Application <b>K.K. Jeremy Ang</b> , B.Y.Liang Tan, J.Juay and D. Sun	<b>Mr. Koon Keong Jeremy Ang</b> , Nanyang Technological University – Singapore
17:30-17:45	Solid Cation-exchange Resin catalysed Esterification of Lactic Acid with Ethanol: A Novel Kinetic Study. <b>E. Okon</b> and G. Edward	<b>Mrs. Edidiong Okon</b> , The Robert Gordon University Aberdeen – UK
17:45-18:00	Resistive Switching in Self-ordered TiO <sub>2</sub> Nanocolumn Arrays <b>M. Marik</b> , M. Bendova, J. Hubalek and A. Mozalev	<b>Mr. Marian Marik</b> , Brno University of Technology - Czech Republic



18:00-18:15	Formulation and Characterization of Garlic oil nanoparticles with enhanced Anti-Microbial Activities <b>S. Fahmy</b> and W. Mamdouh	<b>Mr. Sherif Fahmy</b> , The American University in Cairo – <b>Egypt</b>
18:15-18:30	Neutron radiation resistance of ferroelectric copolymer filled with Al <sub>2</sub> O <sub>3</sub> and ZnO nanoparticles <b>S.Rouabah</b> , B. Vincent, D.Rouxel, A.Chaabi, S.Girard, P. Paillet and M. Gaillardin	<b>Ms. Sawsen Rouabah</b> , Jean Lamour Institute – <b>France</b>
18:30-18:45	The Synthesis of Blue Colored Zirconia and Its Application on Automotive Industry <b>A.Yurdakul</b> and H. Gocmez	<b>Dr. Arife Yurdakul</b> , Dumlupinar University- <b>Turkey</b>
18:45-19:00	Effect of nanoclay on short term water absorption and swelling of composites made by wood poplar flour and recycled polystyrene <b>A. Tavasoli</b> , A. Samariha, M. Nemati and Z. Masoomi	<b>Dr. Afshin Tavasoli</b> , Islamic Azad University- <b>Iran</b>

**June 1<sup>st</sup>, 2016**

**Nanotech France 2016: Joint Symposium on Functional Hybrids and Clay Nanomaterials**

**Conference Room 261**

**Session's Chairs:**

**Prof. Eduardo Ruiz-Hitzky and Dr. Pilar Aranda, Materials Science Institute of Madrid (ICMM-CSIC) - Spain**

**Prof. Alicia de Andrés, Materials Science Institute of Madrid (CSIC) - Spain**

**Dr Mercedes Vila, Ctechnano-coating technologies S.L - Spain**

**Dr. Vanessa Prevot, Blaise Pascal University - France**

09:00-09:05	Welcome from the symposium chairs	<b>Chairs</b>
09:05-09:40	Clay-graphene nanocomposites <b>E. Ruiz-Hitzky</b>	<b>Prof. Eduardo Ruiz-Hitzky</b> , Materials Science Institute of Madrid (ICMM-CSIC) – <b>Spain</b>
09:40-09:55	Graphene / Ru nanostructure transparent hybrid systems for sensing applications L. Álvarez-Fraga, <b>F. Jiménez-Villacorta</b> , E. Climent-Pascual, R. Ramirez-Jiménez, C. Prieto and A. de Andrés	<b>Dr. Felix Jimenez-Villacorta</b> , Materials Science Institute of Madrid (CSIC) – <b>Spain</b>
09:55-10:10	Thermal properties of LDPE Graphene filled nanocomposites designed for HVDC cable accessories. <b>K. Gaska</b> , R. Hafiizh Azhari, R. Kadar, M. Andersson and S. Gubanski	<b>Dr. Karolina Gaska</b> , Chalmers University of Technology – <b>Sweden</b>
10:10-10:30	<b>Coffee Break / Exhibition/ Posters session I</b>	
10:30-11:05	Multi-parameter monitoring of in vitro tissue models using organic electronics R.M Owens	<b>Dr. Roisin Owens</b> , Ecole des Mines de. St. Etienne – <b>France</b>
11:05-11:30	DNA-based bionanocomposites for gene transfer and biotechnological applications. <b>F.A.Castro-Smirnov</b> , O. Piétrement, P. Aranda, J. Ayache, E. Le Cam, J-R. Bertrand, B.S. Lopez and E.Ruiz-Hitzky	<b>Prof Fidel A. Castro-Smirnov</b> , University of Informatic Sciences – <b>Cuba</b>
11:30-11:55	In Vivo Multimodal Deep Tissue Imaging with Hybrid Nanostructures <b>D. H. Ortgies</b> , L. de la Cueva, B. del Rosal, F. Sanz-Rodríguez, N. Fernández, M. C. Iglesias-de la Cruz, G. Salas, D. Cabrera, F. J. Teran, D. Jaque and E. Martín Rodríguez	<b>Dr. Dirk Ortgies</b> , Autonomous University of Madrid – <b>Spain</b>
11:55-12:10	Magneto-photo-thermal Nanomaterials as Efficient Nanoheaters for Tumor Therapy <b>A. Espinosa</b> , R. Di Corato, J. Kolosnjaj-Tabi, M. Bugnet, G. Radtke, S. Neveu, G. A. Botton, P. Flaud, A. Abou-Hassan, T. Pellegrino and C. Wilhelm	<b>Dr Ana Espinosa</b> , Paris Diderot University - <b>France</b>

12:10-12:25	Adsorption of diclofenac pharmaceutical product onto clay mineral and organoclay derivatives <b>T. De Oliveira</b> and R.Guégan	<b>Mr. Tiago De Oliveira</b> , Institut des Sciences de la Terre d'Orléans – <b>France</b>
12:45-14:00	<b>Lunch Break / Exhibition / Posters session I</b>	
14:00-14:25	Sepiolite-Nanocellulose Assembly as new Nanofibrous Hybrid Materials <b>M. M. González del Campo, M. Darder, P. Aranda and E. Ruiz-Hitzky</b>	<b>Dr. Margarita Darder</b> , Materials Science Institute of Madrid, CSIC-Madrid - <b>Spain</b>
14:25-14:40	Multi-enzyme/layered double hydroxide-based biohybrids for the synthesis of chiral polyols in cascade reaction <b>F. Bruna Gonzalez</b> , M. De Sousa, M. Lorillière, G. Ali, T. Gefflaut, V. de Berardinis, L. Pollegioni, W.-D. Fessner, C. Forano, V. Prévot, C. Mousty, F.Charmantay and L. Hecquet	<b>Dr. Felipe Bruna Gonzalez</b> , Blaise Pascal University - <b>France</b>
14:40-14:55	Biohybrids based on zein and montmorillonite: preparation and use as nanofiller in clay-based bionanocomposites <b>A.C.S. Alcântara, M. Darder, P. Aranda and E. Ruiz-Hitzky</b>	<b>Dr. Pilar Aranda</b> , Materials Science Institute of Madrid, CSIC-Madrid - <b>Spain</b>
14:55-15:30	Hybrid Photonics for Energy Efficiency <b>P.G. Lagoudakis</b>	<b>Prof. Pavlos G. Lagoudakis</b> , University of Southampton - <b>UK</b>
15:30-15:55	Plasmon assisted Nd <sup>3+</sup> -based solid-state nanolaser <b>P. Molina, E. Yraola, M.O. Ramirez, C. Tserkezis, J.L. Plaza, J.Aizpurua, J.Bravo-Abad and L.E. Bausá</b>	<b>Prof. Luisa Bausá</b> , Autonomous University of Madrid – <b>Spain</b>
15:55-16:15	<b>Coffee Break /Exhibition/ Posters Session I</b>	
16:15-16:40	MoSi <sub>2</sub> -Si <sub>3</sub> N <sub>4</sub> Composite Absorber for Concentrated Solar Power (CSP) <b>A. Rodríguez-Palomo, D. Hernández-Pinilla, E. Céspedes, L. Álvarez-Fraga, F. Jiménez-Villacorta, R. Jiménez-Riobóo and C. Prieto</b>	<b>Prof. Carlo Prieto</b> , Materials Science Institute of Madrid (CSIC) – <b>Spain</b>
16:40-16:55	Hybrid photonic crystal LED renders 123% color conversion effective quantum yield <b>M. Brossard</b> , C. Krishnan, K.-Y. Lee, J.-K. Huang, C.-H. Lin, H.-C. Kuo, M. D. B. Charlton and P. G. Lagoudakis	<b>Dr. Mael Brossard</b> , University of Southampton – <b>UK</b>
16:55-17:10	ZnO-clay nanoarchitectures: preparation and uses as photocatalyst <b>M. Akkari, P. Aranda, H. Ben Rhaiem, A. Ben Haj Amara and E. Ruiz-Hitzky</b>	<b>Dr. Pilar Aranda</b> , Materials Science Institute of Madrid, CSIC-Madrid - <b>Spain</b>
17:10-17:40	Atomic and Molecular Layer Deposition of Hybrid Nanostructured Materials <b>M.Vila</b>	<b>Dr. Mercedes Vila Juárez</b> , CTECH Nano-Coating Technologies S.L – <b>Spain</b>
17:45-17:55	Maya Blue-Based Nanostructured Clay Materials for Colouring Geopolymers <b>C.M. Ouellet-Plamondon</b> , P. Aranda, A. Favier, G. Habert, H. Van Damme and E. Ruiz-Hitzky	<b>Prof. Claudiane Ouellet-Plamondon</b> , École de Technologie Supérieure – <b>Canada</b>
17:55-18:10	Multifunctional Metallic Janus MOF Particles Synthesized by the Desymmetrization at Interfaces Approach <b>A. Ayala</b> , I. Imaz and D. Maspoch	<b>Mr. Abraham Ayala Hernández</b> , Autonomous University of Barcelona - <b>Spain</b>
18:10-18:25	Nanoclays for adsorption of tartrazine: A sustainable application <b>C. del Hoyo Martínez</b> , M. S. Lozano García and V. Sánchez Escribano	<b>Prof. Carmen del Hoyo Martínez</b> , University of Salamanca – <b>Spain</b>
18:25-18:40	Study of synthetic talc growth by EXAFS: basic research to support technology transfer <b>A. Dumas</b> , M. Mizrahi, F. Martin, F. Requejo, M. Claverie, C. Aymonier	<b>Dr Angela Dumas</b> , Institut de Chimie de la Matière Condensée de Bordeaux (ICMCB) – <b>France</b>

**June 2<sup>nd</sup>, 2016**  
**Nanotech Plenary session II**

**Amphitheatre H**

**Session's Chairs:**  
**Prof. Jupille Jacques, Institut des Nanosciences de Paris – France/ Prof. Alejandro Pérez-Rodríguez, Catalonia Institute for Energy Research, IREC – Spain**

<b>09:15-10:00</b>	DNA-controlled fusion of liposomes O.Ries, P.Löffler and <b>S.Vogel</b>	<b>Prof Stefan Vogel</b> , University of Southern Denmark - Denmark
<b>10:00-10:30 Coffee Break / exhPosters Session</b>		
<b>10:30-11:15</b>	Meeting the needs for aged and released nanomaterials required for further testing <b>B. Nowack</b>	<b>Prof. Bernd Nowack</b> , Empa, Swiss Federal Laboratories for Materials Science and Technology - Switzerland
<b>11:15-12:00</b>	Resonant Raman scattering methodologies for assessment of nanometric layers in high efficiency chalcogenide solar cells M. Guc, D. Hariskos, W. Hempel, F. Oliva, L. Calvo-Barrio, T, Jawhari, V. Izquierdo-Roca and <b>A. Pérez-Rodríguez</b>	<b>Prof. Alejandro Pérez-Rodríguez</b> , Catalonia Institute for Energy Research, IREC - Spain
<b>12:00-12:30</b>	Publish books chapters with SETCOR, in collaboration with Elsevier.	<b>Mr Simon Holt/ Mr Matthew Deans</b> , Elsevier Publishing-UK
<b>12:45-14:00 Lunch Break/ Exhibition/ Posters session II</b>		

**June 2<sup>nd</sup>, 2016**  
**Session III: NanoBioMedecine/Nanosafety**

**Conference Room 508**

**Session's Chairs:**  
**Prof. Danail Hristozov, University Ca' Foscari Venice – Italy/ Dr. Nicklas Raun Jacobsen, National Research Centre for the Working Environment, Copenhagen – Denmark/ Prof. Kevin Braeckmans, Ghent University - Belgium**

<b>10:30-11:00</b>	Engineered cell wall binding domains of lysins for the multiplexed detection and rapid separation of food-borne pathogens M. Kong and <b>S. Ryu</b>	<b>Prof. Sangryeol Ryu</b> , Seoul National University - Republic of Korea
<b>11:00-11:15</b>	Room-temperature aqueous synthesis of ultra-small Cu <sub>2</sub> -xSe nanoparticles for highly efficient photoacoustic imaging-guided photothermal cancer therapy <b>S. Zhang</b> , J. Xiong, L. Zhang, Z. Li and S. Dou	<b>Mr. Shaohua Zhang</b> , University of Wollongong - Australia.
<b>11:15-11:30</b>	Selective cancer cell toxicity and radiosensitization using mixed-oxide high atomic number nanoparticles <b>S.Grellet</b> , S. Kaas, E. Crabb, S. Allman and J.Golding	<b>Ms Sophie Grellet</b> The Open University - UK
<b>11:30-11:45</b>	Doxorubicin-loaded BN Nanoparticles for Cancer Therapy <b>I.V. Sukhorukova</b> , I.Yu. Zhitnyak, A.M. Kovalskii, N.A. Gloushankova, D.V. Golberg and D.V. Shtansky	<b>Mrs. Irina Sukhorukova</b> , National University of Science and Technology-Russia
<b>11 :45-12:00</b>	Antimicrobial electrospun nanofibrous scaffolds for gingival fibroblast growth <b>A. Baranowska-Korczync</b> , M. Jasiurkowska-Delaporte, B. Grześkowiak, M. Jarek, A. Warowicka, B. M. Maciejewska, J. Jurga-Stopa and S. Jurga	<b>Dr. Anna Baranowska-Korczync</b> , Adam Mickiewicz University - Poland
<b>12:00-12:15</b>	Development of new biocompatible □-Ti coatings on Ti6Al4V for medical applications <b>E. Frutos</b> and T. Polcar	<b>Dr. Emilio Torres</b> , Czech Technical University in Prague - Czech Republic

12:15-12:30	Wound healing evaluation of collagen-laminin dermal matrix <b>E.H. Gokce</b> , S. Tuncay-Tanriverdi, İ. Eroglu, N. Tsapis, I. Tekmen, E. Fattal and O. Ozer	<b>Dr. Evren Homan Gökçe</b> , University of Ege- Turkey
12:30-12:45	Nanostructured Copper Hydroxide on Graphene Pore Structure for Non-enzymatic Electrochemical Glucose Sensor <b>I. Shackery</b> and S. C. Jun	<b>Mr. Iman Shackery</b> , Yonsei University, Seoul - Rep. of Korea
12:45-13:00	An innovative detection platform to support nanomedicine characterisation and development <b>C. Desmet</b> , A. Valsesia, R. La Spina, P. Urban, F. Rossi and P. Colpo	<b>Dr. Cloe Desmet</b> , European Commission Joint Research Centre – Italy
<b>12:45-14:00 Lunch Break / Exhibition / Posters session II</b>		
14:00-14:30	Highly controlled delivery of macromolecules and contrast agents in living cells by laser-induced vapour nanobubbles R. Xiong, F. Joris, L. Wayteck, K. Raemdonck, K. Peynshaert, I. Lentacker, A. G. Skirtach and <b>K. Braeckmans</b>	<b>Prof. Kevin Braeckmans</b> , Ghent University - Belgium
14:30-14:45	Imidazolium-derived nanostructures for drug delivery <b>M. Rodrigues</b> , E. Amirthalingam, D. Limón, A. Calpena, D. B. Amabilino and L. Pérez-García	<b>Dr. Mafalda Rodrigues</b> , Barcelona University – Spain
14:45-15:00	The development and evaluation of a novel hybrid PLGA nanoparticle-Pheroid® system with the potential to improve tuberculosis therapy <b>M.P. Chelopo</b> , L. Kalombo, J. Wesley-Smith, B. Naicker, M. Glyn, A. Grobler and R. Hayeshi	<b>Ms. Madichaba P Chelopo</b> , North-West University and CSIR - South Africa
15:00-15:15	A novel SPION-eicosane coating material for on-demand drug release triggered by magnetic hyperthermia <b>L. Che Rose</b> , A.G. Mayes and H. Suhaimi	<b>Dr Laili Che Rose</b> , Malaysia Terengganu University – Malaysia
15:15-15:30	Morphology effect of mesoporous silica nanoparticles on drug delivery <b>S. Rahmani</b> , L. Lichon, M. Maynadier, M. Garcia, M. Gary-Bobo, M. Ferid, C. Charnay and J.O. Durand	<b>Ms. Saher Rahmani</b> , Institut Charles Gerhardt Montpellier University - France
15:30-15:45	Application of samarium oxide to evaluate the in vivo bio-distribution of PLGA nanoparticles <b>V. Mandiwana</b> , L. Kalombo, J.R. Zeevaart and A. Grobler	<b>Ms. Vusani Mandiwana</b> , CSIR, North West University - South Africa
15:45-16:00	Efficient drug delivery with synthesized mitoxantrone-gold nanoparticle conjugates for in vitro breast cancer therapy <b>A. Jafarizad</b> , S. gharibian, G. Pavon-Djavid and D. Ekinci	<b>Dr. Abbas Jafarizad</b> , Sahand University of Technolog- Iran.
<b>16:00-16:30 Coffee Break / Exhibition / Posters Session II</b>		
16:30-17:00	Toxicology: Pulmonary and systemic toxicity caused by nanoparticles <b>NR. Jacobsen</b>	<b>Dr. Nicklas Raun Jacobsen</b> , National Research Centre for the Working Environment-Copenhagen - Denmark
17:00-17:15	Measurement of airborne engineered nanoparticles <b>M. Levin</b>	<b>Dr. Markus Levin</b> , National Research Center for the Working Environment - Denmark
17:15-17:30	Evaluation of Dithizone-Based Colorimetric Sensors for Silver Nanoparticles in Aqueous Media <b>N. Wasukan</b> , S. Srisung, M. Kuno, K. Kulthong and R. Maniratanachote	<b>Dr. Nootcharin Wasukan</b> , Srinakharinwirot University - Bangkok-Thailand
17:30-17:45	Drosophila melanogaster as a suitable in vivo model to determine potential side effects of nanomaterials <b>M. Alaraby</b> , A. Hernández and R. Marcos	<b>Mr. Mohamed Alaraby</b> , Autonomous University of Barcelona – Spain
17:45-18:00	Determination for Stability Constant of Silver-DMSA Nanoparticles <b>S. Srisung</b> , N. Wasukan, K. Kulthong and R. Maniratanachote	<b>Dr. Sujittra Srisung</b> , Srinakharinwirot University- Thailand
18:00-18:15	Legal Metrology Framework for Nanotechnology in Australia <b>S. Devasahayam</b>	<b>Dr. Sheila Devasahayam</b> , Federation University Australia, Victoria – Australia



18:15-18:30	Effects of Different Printing Ink Binders on Printability and Biodegradability of Polylactic Acid Film <b>S. Netpradit</b> , S. Binraman and C. Ladmai	<b>Dr. Suchapa Netpradit</b> , King Mongkut's University of Technology Thonburi - <b>Thailand</b>
18:30-18:45	Effect of the supply air supporting the shaping of the exhaust air flow during the processing of nanomaterials <b>T. Jankowski</b>	<b>Mr. Tomasz Jankowski</b> , Central Institute for Labour Protection – National Research Institute – <b>Poland</b>
18:45-19:00	High stability metal nanoparticles for healthcare applications <b>E. El-Meliegy</b>	<b>Prof. Emad El-Meliegy</b> , National Research Centre, Ceramics – <b>Egypt</b>
19:00-19:15	Overview of available data of occupational exposure to manufactured nanomaterials, approaches and needs <b>S. Bau</b> and O. Witschger	<b>Dr. Sébastien Bau</b> , Institut National de Recherche et de Sécurité- <b>France</b>

**June 3<sup>rd</sup>, 2016**

**Session IV: NanoElectronics/NanoPhotonics**

**Conference Room 211**

**Session's Chairs:**

**Prof. Philippe Godignon, CNM-CSIC Barcelone-Spain – France/ Prof. Aurica Farcas, "Petru Poni" Institute of Macromolecular Chemistry – Romania**

09:00-09:45	Nanoscale Magnetic Skyrmions- A New twist for Spintronics <b>R. Wiesendanger</b>	<b>Prof. Roland Wiesendanger</b> , University of Hamburg – <b>Germany</b>
09:45-10:00	Density of states and electrical properties of nanocrystalline Co <sup>2+</sup> and Ta <sup>5+</sup> substituted barium bismuth niobate <b>P. Dhak</b> , A.Kundu, M.K. Adak, D. Dhak and A.O. Sjøstad	<b>Dr. Prasanta Dhak</b> , University of Oslo – <b>Norway</b>
10:00-10:30	<b>Coffee Break / Exhibition</b>	
10:30-10:45	Self-powered high photoresponse ultraviolet photodetector based on dual ion beam sputtered Ga doped ZnO P. Sharma, R.Singh, R. Bhardwaj, and <b>S. Mukherjee</b>	<b>Prof. Shaibal Mukherjee</b> , Indian Institute of Technology, Indore – <b>India</b>
10:45-11:00	Perovskite Oxide Spin Filters <b>B. Prasad</b> and M.G. Blamire	<b>Dr. Bhagwati Prasad</b> , Max Planck Institute for Solid State Research- Stuttgart - <b>Germany</b>
11:00-11:15	New fundamental effects in single molecular circuitry <b>A.C. Aragonès</b> , N. Darwish, F. Sanz, E. Ruiz and I.Díez-Pérez	<b>Mr. Albert Aragonès</b> , University of Barcelona - <b>Spain</b>
11:15-11:30	Synaptic Weight Modulation and Logic Function Learning with Electro-grafted Nano Organic Memristors <b>Y-P. Lin</b> , C.H. Bennett, D. Chabi, D. Vodenicarevic, D. Querlioz, T. Cabaret, A. Balan, B. Jousset, C. Gamrat, J-O. Klein and V. Derycke	<b>Dr. Yu-Pu Lin</b> , CEA Saclay - <b>France</b>
11:30-11:45	Quantum Interference Effect In Anthraquinone Solid State Junctions <b>M. L. Della Rocca</b> , C. Bessis, C. Barraud, P. Martin, J.-C. Lacroix, T. Markussen and P. Lafarge	<b>Dr. Maria Luisa Della Rocca</b> , Paris Diderot University - <b>France</b>
11:45-12:00	Impact of Surface Modification of ITO Bottom Electrode on Switching Characteristics of ZnO-based Transparent Resistive Memory Devices Fabricated on Polymer Substrate <b>F. M. Simanjuntak</b> and T. Y. Tseng	<b>Mr. Firman Mangasa Simanjuntak</b> , National Chiao Tung University – <b>Taiwan</b>
12:00-12:15	Synthesis of ZrO <sub>2</sub> films by spray pyrolysis ultrasonic presenting the up conversion phenomenon <b>P. E. Ortiz-Ortega</b> and M García-Hipólito	<b>Mr. Pedro Enrique Ortiz Ortega</b> , National Autonomous University of Mexico - <b>Mexico</b> .

12:15-12:30	Conjugated Polyrotaxanes: A Critical Assessment of Photo-physical Properties in Correlation with the Effect of the Nature of Host Molecules Encapsulation <b>A. Farcas</b> , A.-M. Resmerita and P.-H. Aubert	<b>Prof. Aurica Farcas</b> , "Petru Poni" Institute of Macromolecular Chemistry – <b>Romania</b>
12:30-12:45	Designing High Performance Digital Logic NOT Gate Using Single Electron Box (SEB) Nano-Devices <b>D. Bahrepour</b>	<b>Dr. Davoud Bahrepour</b> , Islamic Azad University- <b>Iran</b>
12:45-13:00	Use of Nanobiomechanics robots to tackle HIV virus <b>A. Vohra</b>	<b>Mr. Amit Vohra</b> , Bharat Electronics Limited- <b>India</b>

**June 3<sup>rd</sup>, 2016**  
**InnovNanoFrance 2016 : Industrial Session**

**Conference Room 508**

**Session's Chairs:**  
**Dr. Julio Gomez, CEO, Avanzare Innovacion Tecnologica S.L.- Spain**

09:00-9:30	Graphene based supercapacitors: results and perspectives <b>P. Bondavalli</b> and G. Pognon	<b>Dr. Paolo Bondavalli</b> , Head of Nanomaterial topic team, Thales Research and Technology – <b>France</b>
09:30-09:00	Graphene Roadmap: Wafer Scale Integration <b>Mr Iñigo Charola</b>	<b>Mr. Iñigo Charola</b> , Business Development Director- Graphenea - <b>Spain</b>
<b>10:00-10:30 Coffee Break / Exhibition</b>		
10:30-11:00	Static Multiple Light Scattering to monitor protein aggregation and pigments dispersibility <b>C. Tisserand</b> , G. Brambilla, P. Bru and G. Meunier	<b>Dr. Christelle Tisserand</b> , Formulation Company – <b>France</b>
11:00-11:30	Bulk graphene production and application in composites, energy and coatings <b>J. Gomez</b> , J. Perez and E. Villaro	<b>Dr. Julio Gomez</b> , CEO- Avanzare Innovacion Tecnologica S.L.- <b>Spain</b>
11:30-12:00	Graphene: the early commercialisation prospects <b>R. Gibbs</b>	<b>Mr. Ray Gibbs</b> , CEO- Hatydale Graphene Industries Plc- <b>UK</b>
12:00-12:30	3D Printing Sets New Standards in Microfabrication <b>A. Legant</b>	<b>Mr. Alexander Legant</b> , Nanoscribe GmbH, Eggenstein, Leopoldshafen – <b>Germany</b>
12:30-13:00	Graphene grown on SiC substrates for applications in electronics <b>L. Serrano</b> , A. García-García, A. Ballestar, J. M. de Teresa, M. R. Ibarra and P. Godignon	<b>Dr. Luis Serrano</b> , Graphene Nanotech (GPNT) - <b>Spain</b>

**Posters Session I: June 1<sup>st</sup> 2016**

**Nanotech France 2016: Nanomaterials synthesis, characterization/Nanometrology and properties**

**Exhibition and Poster Hall**

N.	Title	Author/Affiliation/Country
1	Organic solvent resistant polyelectrolyte multilayers : effect of the sulfonic to carboxylic content <b>P. Argkarawanitnan</b> and S. T. Dubas	<b>Ms. Patsarat Argkarawanitnan</b> , Chulalongkorn University, Bangkok – <b>Thailand</b>
2	Solvothetmal hot injection synthesis of AgNi nanoalloy <b>V. Vykoukal</b> , J. Bursik, P. Roupčová and J. Pinkas	<b>Mr. Vit Vykoukal</b> , Masaryk University - <b>Czech Republic</b>
3	Layer-by-Layer Deposition of Photocatalysts on PU foam <b>C. Wechwithayakhlung</b> and S. Dubas	<b>Ms. Chayanit Wechwithayakhlung</b> , Chulalongkorn University, Bangkok – <b>Thailand</b>

4	Thickness dependent optical properties of the large area synthesized few layers MoSe <sub>2</sub> on SiO <sub>2</sub> and Al <sub>2</sub> O <sub>3</sub> substrates by Molecular Beam Epitaxy <b>Y. H. Choi</b> , D. H. Lim, J. H. Jung, K. -H. Yoo, B. -Y. Yoo and M. -H. Cho	<b>Mr. Yoonho Choi</b> , Yonsei University, Seoul - <b>Republic of Korea</b>
5	Influence of superficial morphology in the growth of zinc oxide nanowires <b>Arana J A</b> , Monroy B M and Santana G	<b>Mr. Julio Alejandro Arana Trenado</b> , National Autonomous University of Mexico - <b>Mexico</b> .
6	Plasma functionalized POSS / PDMS nano-composite membranes for solvent separation by pervaporation <b>X. Chen</b> , Z. Chen, R. d'Agostino, L. F. Dumée, X. J. Dai and K. Magniez	<b>Mr Xiao. Chen</b> , Deakin University - <b>Australia</b>
7	New molecular precursors for AgCu nanoalloy preparation V.Vykoukal, J. Bursik, P.Roupcova, V. Halasta and <b>J. Pinkas</b>	<b>Prof. Jiri Pinkas</b> , Masaryk University - <b>Czech Republic</b>
8	Influence of nano-particles on the surface morphology and properties of fouling release coatings based on polydimethylsiloxane <b>Z. Zhang</b> , H. Zhou and Y. Qi	<b>Prof. Zhanping Zhang</b> , Dalian Maritime University – <b>China</b>
9	Effect of operating conditions on adhesion strength of Cu/AlN laminate fabricated by High Vacuum Surface Controlled Direct Bonding <b>S-C. Lim</b> and K.B. Jang	<b>Dr. Sung-Chul Lim</b> , Korea Institute of Industrial Technology, Songdo-dong – <b>Rep. of Korea</b>
10	Enhancement of the TFT's performance by slight phosphorus doping: Lower density of states within the grain boundaries and higher stability <b>M. Zaghdoudi</b> , R.Rogel, T.Mohammed-Brahim and H. Ezzaouia	<b>Mrs. Mariem Zaghdoudi</b> , Institute of Environmental Science and Technology – <b>Tunisia</b>
11	The Green Synthesis, Characterization, and Antioxidant Activities of Silver Nanoparticles Synthesized from <i>Asphodelus aestivus</i> Aqueous Extract <b>B. Kivçak</b> , T. Erdoğan, P. Taştan, B. Sümer Tüzün and M. Özyazıcı	<b>Prof. Bijen Kivçak</b> , Ege University, Izmir – <b>Turkey</b>
12	Synthesis of Monodisperse Gold Nanoparticles for Plasmonics <b>S. Marguet</b> , J. Caron, A. Habert and M. Khaywah	<b>Dr. Sylvie Marguet</b> , CNRS/CEA Saclay – <b>France</b>
13	Enhanced Mass Activity of Pt as Au@Pt Nanoparticles on reduced Graphene Oxide Support for Methanol and Ethanol Oxidation <b>P. Gnanaprakasam</b> , S. E. Jeena and T. Selvaraju	<b>Mr. P. Gnanaprakasam</b> , Karunya University- <b>India</b>
14	Formation of Germanium Analog of The Tubular Aluminosilicate imogolite Containing Fe <b>M. Ookawa</b> , E. Kato, M. Watanabe, K. Osada, M. Yoshikawa and S. Yamane	<b>Dr. Masashi Ookawa</b> , National Institute of Technology, Numazu College – <b>Japan</b>
15	Dispersion Characteristics of Layered Double Hydroxides in the presence of amphiphilic macroRAFT agents <b>M. Pavlovic</b> , V. Prevot, E. Bourgeat-Lami and I. Szilagyí	<b>Mr. Marko Pavlovic</b> , University of Geneva - <b>Switzerland</b>
16	Tuning the structure and the mechanical properties of epoxy-silica sol-gel hybrid materials B. Domènech, <b>I. Mata</b> and E. Molins	<b>Dr. Ignasi Mata</b> , Materials Science Institute -Barcelona (ICMAB-CSIC) - <b>Spain</b> .
17	High performance Transparent Electrode Consisting of Silver and Graphene Hybrid Structure Fabricated by Near-Field Electro-Spinning <b>D. H. Youn</b> , Y. J. Yu, S. J. Yun, H. K. Choi, J. S. Choi, G. H. Kim and C. G. Choi	<b>Dr. Doo-Hyeb Youn</b> , Electronics and Telecommunications Research Institute- <b>Republic of Korea</b>
18	Plasmonic Ag ultrafine nanoparticle-graphene substrates for Raman enhancement <b>E.Climent-Pascual</b> , F. Jimenez-Villacorta, L. Álvarez-Fraga, R. Ramírez-Jiménez, C. Prieto and A. De Andrés	<b>Dr. Esteban Climent-Pascual</b> , ICMM-CSIC - <b>Spain</b>
19	Self-cleaning Properties of Nanostructured Polypropylene Foils Fabricated by Roll-to-Roll Extrusion Coating <b>A. Telecka</b> and R. Taboryski	<b>Ms. Agnieszka Telecka</b> , Danish Technical University Nanotech DTU – <b>Denmark</b>

20	Chemical and electronic structure profiling in the top few nanometers of hydrothermally prepared and plasma hydrogenated ZnO nanorods <b>M. Al-Saadi</b>	<b>Mr. Mubarak Al-Saadi</b> , Sultan Qaboos University (SQU) - <b>Oman</b>
21	Fluorescent Photosensitive Vitroceramics with Silver and Samarium Additives: Improvement of Writing Accuracy and Efficiency for 3D Optical Storage Media <b>C. Busuioc</b> , S. Jinga and E. Pavel	<b>Dr. Cristina Busuioc</b> , Polytechnic University of Bucharest - <b>Romania</b>
22	Transparent and Hard PTFE-like Coatings by RF magnetron Sputtering of PTFE Polymer Target <b>Y. S. Song</b> and J. Kim	<b>Dr. Young Sik Song</b> , KITECH-Surface Technology R&BD Group-Incheon - <b>Republic of Korea</b>
23	Mathematical Modeling Process of Sedimentation Magnetic Nanoparticles on the Walls of Blood Vessels <b>M.A. Shumova</b> , D.V. Korolev, O.A. Smolyanskaya and S.A. Chivilikhin	<b>Mrs. Maria Shumova</b> , ITMO University, Saint-Petersburg - <b>Russian Federation</b>
24	Grown of silicon nanowires for possible solar cell applications <b>J. Salazar</b> , G. Santana and B. M. Monroy	<b>Ms. Jenifer Salazar</b> , National Autonomous University of Mexico – <b>Mexico</b>
25	Applications of Positron Probe in polymer nanocomposites G.B.Xie, J.Zhong, S.Gao and <b>B. Wang</b>	<b>Prof. Bo Wang</b> , Wuhan University – <b>China</b>
26	Modeling and Simulation of P-Type Cu <sub>2</sub> O Thin-Film Transistors Using COMSOL Multiphysics <b>S. Alsharif</b> , H. Farhan and H. Aljawhari	<b>Mrs. Sarah Alsharif</b> , King Abdulaziz University - <b>Saudi Arabia</b>
27	MoN-decorated Nitrogen Doped Carbon Nanotubes Anode With High Lithium Storage Performance <b>S.M. Abbas</b> , Z. Rehman, A. Rehman and N. Ahmad	<b>Mr. Syed Mustansar Abbas</b> , National Centre for Physics, Islamabad - <b>Pakistan</b>
28	Low Frequency Noise Spectroscopy in n-channel UTBOX de-vices with 20 nm Si film <b>B. Nafaa</b> , B. Cretu, N. Ismail, O. Touayar, E. Simoen, J.-M. Routoure, R. Carin, M. Aoulaiche and C. Claeys	<b>Ms. Beya Nafaa</b> , Institut National de Sciences Appliquées et de Technologie- <b>Tunisia</b>
29	Aluminum oxide nanopores and nanowires <b>F. Flores-Gracia</b> , J. Martínez-Juárez, J.A. Luna-López, R.R. González-Jiménez	<b>Dr. Francisco Flores</b> , Autonomous University of Puebla- <b>Mexico</b>

## Posters Session II: June 2<sup>nd</sup>, 2016

### Nanotech France 2016: NanoBioMedecine/Nanosafety

#### Exhibition and Poster Hall

1	Investigation of Biomolecule Release Behaviours From Titanium Surfaces with Controllable Porosity <b>C. Bayram</b>	<b>Mr. Cem Bayram</b> , Hacettepe University - <b>Turkey</b>
2	UV Crosslinkable PLGA-b-PEG Nanoparticle Integrated Gel Networks for Topical Drug Delivery <b>M. Gultekinoglu</b> , I. Eroglu, C. Bayram, E.A. Aksoy and K. Ulubayram	<b>Mrs. Merve Gultekinoglu</b> , Hacettepe University - <b>Turkey</b>
3	New Outlook on Parkinson's Treatment: A Dual Targeting Nanoparticle Complex for More Efficient Delivery of Curcumin Improves Neuroprotection <b>N. Beals</b> , P. Kharel, W. Geldenhuys and S. Basu	<b>Mr. Nathan Beals</b> , Kent State University- <b>USA</b>
4	Biodegradable mesoporous silica nanoparticles from synthesis to anti-cancer application <b>S. Seré</b> , J. Belmans, B. De Roo, M. Vervaele, S. Van Gool and J. P. Locquet	<b>Ms. Stephanie Seré</b> , KU Leuven- <b>Belgium</b>
5	Formulation and Characterization of Liposomes Loaded with Resveratrol using Plackett-Burman Experimental Design <b>S. Al-Edresi</b> , S. Freeman, H. Aojula and J. Penny	<b>Mr. Sarmad Al-Edresi</b> , University of Manchester- <b>United Kingdom</b>
6	Biological interactions monitoring of B-16 Melanoma cells using electrochemical impedance spectroscopy <b>C. Marculescu</b> , B. Tincu, A. Avram, T. Burinaru, C. Voitincu and M. Avram	<b>Dr. Catalin Marculescu</b> , National Institute for Research and Development in Microtechnologies – Bucharest- <b>Romania</b>



7	Formulation and In Vitro Evaluation of Simvastatin Loaded Nanostructured Lipid Carriers <b>D. Örgül</b> , H. Eroğlu and S. Hekimoğlu	<b>Mrs. Dilara Örgül</b> , Hacettepe University- <b>Turkey</b>
8	Kinetics of mRNA Onset Time in Single Cell Arrays <b>N. Mehrotra</b> , A.Reiser, R. Krzyszton and J.O. Rädler	<b>Ms. Neha Mehrotra</b> , Ludwig-Maximilians-University-Munich- <b>Germany</b>
9	Magnetocloric effect for inducing hypothermia as new therapeutic strategy for stroke <b>R. Iglesias</b> , A. Vieites-Prado, B. Argibay, F. Campos, M. Bañobre-López, T. Sobrino, J. Rivas and J. Castillo	<b>Dr.Ramón Iglesias</b> , University of Santiago de Compostela- <b>Spain</b> .
10	Lipid membrane anchors in Lipid-Nucleic acid (LiNA) conjugates for liposome fusion <b>O. Ries</b> , P.M. G. Löffler and S.Vogel	<b>Dr. Oliver Ries</b> , University of Southern Denmark- <b>Denmark</b>
11	One-pot Solventless Preparation of PEGylated Black Phosphorus Nanoparticles for Photoacoustic Imaging and Photo-thermal Therapy of Cancer <b>C. Sun</b> , C. Zhao and Z. Li	<b>Ms. Caixia Sun</b> , East China University of Science and Technology Shanghai- <b>China</b>
12	The ultra-structural analysis of antibody conjugated gold nanoparticles on fiber optic particles plasmon resonance (FOPPR) enabled bio-sensor <b>C-Y. Hsieh</b> , Y-N. Wu, S-R. Wu, C-Y. Chiang and L-K. Chau	<b>Ms. Ching-Yi Hsieh</b> , National Cheng Kung University- <b>Taiwan</b>
13	In situ Synthesis of Nano-copper on Denim Garment for Antibacterial Purposes <b>D. Zarbaf</b> , M. Montazer and A. Sadeghian Maryan	<b>Mr. Dara Zarbaf</b> , Islamic Azad University- Tehran- <b>Iran</b>
14	Filtering Pigments from honey by nanofiber membrane <b>F.Azizzadeh</b> and F. Altay	<b>Mrs. Farzaneh Azizzadeh</b> , Istanbul Technical University - <b>Turkey</b>
15	Physicochemical and mechanical characterization of electrospun poly-ε-caprolactone nanofibers loaded with cilostazol <b>M. Rychter</b> , A. Baranowska-Korczyk, M. Jarek, B.M. Maciejewska, L. Emerson Coy and J. Lulek	<b>Mr. Marek Rychter</b> , Poznań University of Medical Sciences- <b>Poland</b>

### Posters Session II: June 2<sup>nd</sup>, 2016

#### Nanotech France 2016: Nanoelectronics/ NanoPhotonics

#### Exhibition and Poster Hall

N.	Title	Author/Affiliation/Country
1	Green Emissive Perovskite Light-Emitting Diodes Via Morphological Control of Perovskite Films <b>M. H. Song</b> and J. C. Yu	<b>Prof. Myoung Hoon Song</b> , Ulsan National Institute of Science and Technology (UNIST)- <b>Republic of Korea</b>
2	Influence of electrical pulses on lithium cobalt oxide thin films : memristive behaviour and potential applications <b>V. S. Nguyen</b> , V. H. Mai, A. Moradpour,..P.Chrétien and O. Schneegans	<b>Mr. Van Son Nguyen</b> , Paris Sud University - <b>France</b>
3	Al <sub>2</sub> O <sub>3</sub> passivation effect in HfO <sub>2</sub> -Al <sub>2</sub> O <sub>3</sub> laminate structures grown on InP substrates <b>H-K. Kang</b> , Y-S. Kang, D-K. Kim, M. Back, Y-S. An, J-D. Song, H. Kim and M-H. Cho	<b>Mr. Hang-Kyu Kang</b> , Yonsei University-Seoul - <b>Republic of Korea</b>
4	Flexible Microelectrode Patterning with Thin Polymer Stencils Prepared using PEGDA/Silicate Nanocomposites <b>Y.H. Kim</b> , Y.K. Lee, T.Kim, S.Goel, H.J. Kim and S-J. Choi	<b>Dr. Young Ho Kim</b> , Daegu-Gyeongbuk Medical Innovation Foundation, Daegu - <b>Republic of Korea</b>
5	Molecular switches - from STM-induced single molecule chemistry to switching of entire layers <b>T.Leoni</b> , T.Lelaidier, A.Thomas, O.Siri and C.Becker	<b>Dr. Thomas Leoni</b> , Aix Marseille University - <b>France</b>

# NanoMetrology France 2016 Preliminary Program

June 1<sup>st</sup>, 2016

Session I: Methodologies for nanomaterials characterization

Conference Room 508

Session Chairs:

**Dr. Georges Favre, Laboratoire national de métrologie et d'essais(LNE) - France**  
**Prof. James M. Hill, University of South Australia - Australia**

11:00-11:30	Exact solutions for the axial pressure profiles in channels with Maxwell slip flow <b>A. C. Hoffmann</b> , S. Karakitsiou and B. Holst	<b>Prof. Alex Christian Hoffmann</b> , University of Bergen - Norway
11:30-12:00	Dynamic identification of perforated MEMS devices by the continuous wavelet transform <b>J. Lardiès</b> and T.P. Le	<b>Prof. Joseph Lardies</b> , FEMTO-ST Institute- Bourgogne Franche-Comté University - France
12:00-12:30	General atomistic approach for modeling metal-semiconductor interfaces using density functional theory and non-equilibrium Green's function <b>D. Stradi</b> , U. Martinez, A. Blom, M. Brandbyge and K. Stokbro	<b>Dr. Daniele Stradi</b> , Quantumwise-Danemark
12:30-12:45	Sidewall Roughness of Nanoelectronic and Nanophotonic Structures: Metrological Challenges and their Critical Role in Applications <b>V. Constantoudis</b> , G. Patsis and E. Gogolides	<b>Dr. Vassilios Constantoudis</b> , NCSR Demokritos/ Nanometrisis-Greece
12:45-14:00	<b>Lunch Break / Exhibition / Poster Session I</b>	
14:00-14:30	Implementation of Process Analytical Technology for the multi-sectoral manufacturing of nanoparticles by wet milling <b>C. Vairon</b> , D. Bordeaux and A. Blasco	<b>Ms. Celine Vairon</b> , SDTech company - UK
14:30-14:45	A SAXS/WAXS Laboratory Instrument for Nanomaterials characterization <b>O. Taché</b> , A. Thill, D. Carrière, F. Testard and O. Spalla	<b>Mr. Olivier Taché</b> , LIONS, NIMBE, CEA Paris Saclay University- France
14:45-15:00	MEMS for in-situ TEM nanoscience on dry and wet samples <b>L. Jalabert</b> , T. Ishida, T. Sato, M. Egawa, G. Valet, S. Volz and H. Fujita	<b>Dr. Laurent Jalabert</b> , LAAS-CNRS-France
15:00-15:15	Characterization of nanomaterials by A4F-UV-MALLS-ICPMS, Sp-ICPMS and DLS: Application to foodstuff, consumer products, environmental and medicinal samples <b>M. Menta</b> , I. de La Calle and M. Klein	<b>Dr. Mathieu Menta</b> , Ultra-Traces Analyses Aquitaine (UT2A)- Pau - France
15:15-15:30	Design of experiment for uncertainty evaluation of nanoparticle diameter measurements with AFM <b>B. De Boeck</b> , J. Pétry, N. Sebaihi and M. Dobre	<b>Dr. Bert De Boeck</b> , FPS Economy (NMI Belgium)-Belgium
15:30-15:45	Local resistance imaging on soft materials by conducting probe atomic force microscopy in intermittent contact mode <b>A. Vecchiola</b> , P. Chrétien, K. Bouzehouane, O. Schneegans, P. Seneor, S. Tatay and F. Houzé	<b>Dr. Aymeric Vecchiola</b> , Unité Mixte de Physique CNRS/Thales - France
15:45-16:00	Continuous monitoring of tip radius during atomic force microscopy imaging using higher harmonics E. Rull Trinidad, F. Gramazio, M. Lorenzoni, F. Pérez Murano, U. Staufer and <b>J. Fraxedas</b> <sup>2</sup>	<b>Dr. Jordi Fraxedas</b> , Catalan Institute of Nanoscience and Nanotechnology (ICN2) - Spain
16:00-16:30	<b>Coffee Break / Exhibition/ Posters Session I</b>	

16:30-16:45	Measurement uncertainty evaluation of a metrological AFM by modeling its position measurement system <b>P. Ceria</b> , S. Ducourtieux, Y. Boukellal and A. Allard	<b>Mr. Paul Ceria</b> , LNE- Laboratoire National de metrologie et d'Essais- <b>France</b>
16:45-17:00	Quantitative X-ray Resolution of the Atomic Structure of Metal Oxide Nanotubes: the Imogolite Case M.-S. Amara, S. Rouzière, E. Paineau, E. Poli, J. D. Elliott, G. Teobaldi and <b>P. Launois</b>	<b>Dr. Pascale Launois</b> , Paris Sud University- <b>France</b>
17:00-17:15	Water in Single-Walled Carbon Nanotubes: structural and dynamical analyses <b>E. Paineau</b> , S. Dalla-Bernardina, J.B. Brubach, S. Rouzière, P. Judeinstein, S. Rols, P. Roy and P. Launois	<b>Dr. Erwan Paineau</b> , Paris Sud University - <b>France</b>
17:15-17:30	An Accurate Reconvergent Fanout Aware Algorithm for nano-Circuits Reliability Ranking <b>W. Ibrahim</b> and H. Amer	<b>Prof. Walid Ibrahim</b> , UAE University - <b>UAE</b>
17:30-17:45	Modeling and Analysis of scatterometry with high-harmonic-generation EUV source <b>Y-S. Ku</b> , Y-C. Chen, C-L. Yeh, Y-C. Hsieh, C-H. Cho and C-W. Lo	<b>Dr. Yi-sha Ku</b> , Industrial Technology Research Institute - <b>Taiwan</b>
17:45-18:00	Influence of the probe-surface contact area on AFM tribological investigation of nanopatterned Si surfaces <b>A. Rota</b> , E. Serpini, G. C. Gazzadi and S. Valeri	<b>Dr. Alberto Rota</b> , CNR Nanoscience Institute-Modena - <b>Italy</b>
18:00-18:15	Simultaneous Topographical, Spectroscopic and Electrical Map-ping at the Nanoscale <b>A. Zoladek-Lemanczyk</b> , N. Kumar, A.A. Y, Guilbert, S.M. Tuladhar, T. Kirchartz, B.C. Schroeder, I. McCulloch, J. Nelson, D. Roy and F. A. Castro	<b>Dr. Alina Zoladek-Lemanczyk</b> , National Physical Laboratory- <b>UK</b>
18:15-18:30	Interaction between Hybrid Inclusions mediated by surfactant membranes <b>E. Azar</b> and D. Constantin	<b>Mrs. Elise Azar</b> , Paris Sud University-France
18:30-18:45	Micro to Atomic Scale Observations on Nano-sized Y-TZP Powder Produced by One-Step Hydrothermal Route A. Yurdakul, H. Gocmez and <b>H. Yurdakul</b>	<b>Dr. Hilmi Yurdakul</b> , Dumlupinar University- <b>Turkey</b>
18:45-19:00	First steps towards instantaneous positioning of Nanorobots equipped with graphene antenna in large scaled nano-systems <b>D. Moffo</b> and P. Canalda	<b>Mr. Dernas Moffo</b> , University of Bourgogne-Franche-Comté- <b>France</b>

**June 1<sup>st</sup>, 2016**

**Nanometrology France 2016: Symposium on Nanospectroscopy**

**Conference Room 561**

**Chairs: Prof. Pierre-Michel Adam University of technology of Troyes- France**

11:00-11:30	Nanospectroscopy of optical antennas and coupled hybrid antenna-nanoemitter-structures <b>M. Fleischer</b>	<b>Prof. Monika Fleischer</b> , Institute for Applied Physics-Eberhard Karls University, Tübingen - <b>Germany</b>
11:30-12:00	Nanospectroscopy with Silver Nanowires <b>S. Mackowski</b>	<b>Prof. Sebastian Mackowski</b> , Nicolaus Copernicus University- <b>Poland</b>
12:00-12:30	Addressing Challenges in Fabrication of Nanoscale Interstices at Molecular resolutions for Nanospectroscopies <b>S. Krishnamoorthy</b>	<b>Dr. Sivashankar Krishnamoorthy</b> , Luxembourg Institute of Science and Technology- <b>Luxembourg</b>
12:30-12:45	Real-time sensing of chemical and biological species into individual cells with single-molecule resolution <b>P. Actis</b>	<b>Dr. Paolo Actis</b> , BioNano Consulting /School of Electronic and Electrical Engineering, University of Leeds- <b>United Kingdom</b>

12:45-14:00 Lunch Break / Exhibition / Poster Session I		
14:00-14:30	Resonant Surface-enhanced Raman Scattering by Optical Phonons in CdSe Nanocrystals on Metal Nanocluster Arrays A.G. Milekhin, V.M. Dzhagan and <b>D.R.T. Zahn</b>	<b>Prof. Dietrich R.T. Zahn</b> , Chemnitz University of Technology- <b>Germany</b>
14:30-14:45	Approaching single molecule detection using plasmonic nanogaps A.R. L. Marshall, J. Stokes, <b>J-S. Bouillard</b> and A.M. Adawi	<b>Dr. Jean-Sebastien Bouillard</b> , University of Hull - <b>United Kingdom</b>
14:45-15:00	Colloidal Gold Nanostructures for Plasmonics <b>M. Y. Khaywah</b> and S. Marguet	<b>Dr. Mohammad Yehia Khaywah</b> , CNRS/CEA Saclay - <b>France</b>
15:00-15:15	Intermixing length measurement with up to sub-nm accuracy by XEDS spectrum imaging E Carbo-Argibay, C. Afonso, M. S. Claro and <b>D. G. Stroppa</b>	<b>Dr. Daniel Stroppa</b> , International Iberian Nanotechnology Laboratory - <b>Portugal</b> .
15:15-15:30	High resolution solid state NMR spectroscopy in surface organometallic chemistry: access to molecular understanding of active sites of well-defined heterogeneous catalysts. <b>E.Abou-Hamad</b> and J-M. Basset	<b>Dr. Edy Abou Hamad</b> , King Abdullah University of Science and Technology (KAUST) - <b>Saudi Arabia</b>
15:30-16:00	Aluminum plasmonics for UV nanooptics <b>J. Martin</b> , D. Khlopin, F. F. Zhang, Silvère Schuermans, D. Gérard, J. Proust and J. Plain	<b>Dr. Jérôme Martin</b> , de Technologie University of Troyes - <b>France</b>
16:00-16:30 Coffee Break / Posters Session I		
16:30-16:45	Scanning Tunneling Spectroscopy approaches for Nano-structures characterization <b>B. Naydenov</b> , J.Li, P. Barimar, and J.J. Boland	<b>Dr. Borislav Naydenov</b> , Trinity College Dublin - <b>Ireland</b>
16:45-17:00	Material optical properties by spectroscopic ellipsometry of thin particulate films O. Zhuromskyy, S. Golkar, I. Spies, R. Klupp-Taylor, U. Peschel,	<b>Dr Oleksandr Zhuromskyy</b> , Erlangen-Nürnberg University- <b>Germany</b>
17:00-17:15	Investigations and Conclusions regarding Metrological Fundamentals for 'true' Nanovolume Spectroscopy. <b>N. MacMillan</b>	<b>Mr. Norman McMillan</b> , Institute of Technology Carlow - <b>Ireland</b>
17:15-17:30	Emerging Applications of Nanoscale Zinc Oxide <b>D. Rogers</b> , V. E. Sandana, F. H. Teherani and P. Bove.	<b>Dr. David Rogers</b> , Nanovation Company - <b>France</b>
17:30-17:45	Investigation of Diamond-Like Carbon Films Physical Properties Using Multifractal Analysis <b>N. Margaryan</b> , Zh. Panosyan, A.Mailyan and S. Voskanyan	<b>Mr. Narek Margaryan</b> , National Polytechnic University of Armenia – <b>Armenia</b>

**June 2<sup>nd</sup>, 2016**

**Nanometrology France 2016:**

**Symposium on Detection, location & quantification of nanomaterials and by-product released from nano-enable products**

**Conference Room 511**

**Session Chairs:**

**Prof. Jean-Yves Bottero, CNRS-CEREGE-France and Duke University - USA**

09:00-09:30	Towards a Better Understanding of Interaction Mechanisms and Thermodynamic Properties of Nanomaterials Interacting with BioMacromolecules. <b>S. Stoll</b> , F. Loosli, O. Oriekhova, F. Carnal and A. Clavier	<b>Dr. Serge Stoll</b> , Institute F.-A. Forel, University of Geneva - <b>Switzerland</b>
-------------	---	---



<b>09:30-10:00</b>	Silver Nanoparticles in managed waste facilities: From metallic to sulfidic and back again. <b>R. Kaegi</b> , C. Meier, A. Voegelin, A. Pradas del Real, G. Sarret, and C.R. Mueller	<b>Dr. Ralf Kaegi</b> , Eawag, Swiss Federal Institute of Aquatic Science and Technology - <b>Switzerland</b>
<b>10:00-10:30 Coffee Break / Posters Session II</b>		
<b>10:30-11:00</b>	Rules and rates of release from nano-enabled products <b>N. Neubauer</b>	<b>Dr. Nicole Neubauer</b> , BASF SE, Company – <b>Germany</b>
<b>11:00-11:30</b>	Response of microbial communities and plant to metal oxide- and carbon-based nanomaterials in a plant-soil-based system <b>C. Santaella</b> , B. Collin, M. Hamidat, M. Barakat, P. Ortet and W. Achouak	<b>Dr. Catherine Santaella</b> , CNRS Marseille/ CEA Cadarache- <b>France</b>
<b>11:30-11:50</b>	Effect of chemical transformations of silver in nanoAg-enabled textiles on their antimicrobial efficacy and release <b>G. Lowry</b> and T. Dankovich	<b>Prof. Gregory Lowry</b> , Carnegie Mellon University - <b>USA</b>
<b>11:50-12:10</b>	Multi-scale X-ray computed-tomography for the 3D detection and location of nanomaterials in manufactured materials and complex media <b>P. Chaurand</b> , D. Borschneck, V. Vidal, C. Levard, L. Scifo, J. Perrin and J. Rose	<b>Mrs. Perrine Chaurand</b> , CEREGE-Aix-Marseille University- <b>France</b>
<b>12:10-12:30</b>	Indoor mesocosms: an integrated approach to assess the environmental risks of nanomaterials <b>M. Auffan</b> , M. Tella, L. Brousset, C. Santaella, J. Rose, A. Thiéry, J.Y. Bottero	<b>Dr. Melanie Auffan</b> , CEREGE/CNRS-Aix-Marseille University- <b>France</b>
<b>12:30-12:45</b>	Effect of nanoceria biotransformation in activated sludge on the microbiota associated to canola roots <b>B. Collin</b> , E. Doelsch, M. Auffan, N. Roche, M. Barakat, P. Ortet, W. Achouak and C. Santaella	<b>Dr. Blanche Collin</b> , Aix-Marseille University- <b>France</b>
<b>12:45-14:00 Lunch Break / Exhibition / Posters session II</b>		
<b>14:00-14:30</b>	Some challenges and solutions for detecting engineered nanoparticles in environmental samples M. Hadioui, K. Proulx, L. Frechette-Viens, T. Theoret and <b>K.J. Wilkinson</b>	<b>Prof. Kevin Wilkinson</b> , University of Montreal – <b>Canada</b>
<b>14:30-14:45</b>	Behavior of Engineered CeO <sub>2</sub> Nanoparticles Released in Aquatic Systems <b>O. Oriekhova</b> and S. Stoll	<b>Ms. Olena Oriekhova</b> , Institute F.-A. Forel, University of Geneva - <b>Switzerland</b>
<b>14:45-15:00</b>	Elucidation of standard specimen preparation techniques of nano-enabled products for characterization using field-emission scanning electron microscope <b>A. Sohrabi</b>	<b>Dr. Abouzar Sohrabi</b> , Sharif University of Technology, Tehran – <b>Iran</b>
<b>15:00-15:15</b>	Influence of nano-TiO <sub>2</sub> with Different Crystalline Phases on Bioaccumulation of Perfluorooctanesulfonate by Fishes Living in Different Water Layers <b>L.Y. Zhu</b> and L.W. Qiang	<b>Prof. Lingyan Zhu</b> , Nankai University - <b>China</b>
<b>15:15-15:30</b>	Assessing the heteroaggregation of manufactured nanoparticles with naturally occurring colloids in a typical surface water D. Slomberg, <b>J. Labille</b> , A. Praetorius, C. Harns, J-Y. Bottero, P. Ollivier, M. Scheringe <sup>2</sup> , N. Sani-Kast, S. Iliina and J. Brant	<b>Dr. Jerome Labille</b> , CEREGE, Aix-Marseille University- <b>France</b>
<b>15:30-15:45</b>	Behavior of engineered nanomaterials from marketed tiles under standardized abrasion conditions. <b>C. Bressot</b> , O. Aguerre-Chariol, C., Pagnoux and M., Morgeneyer	<b>Mr. Christophe Bressot</b> , Institut National de l'Environnement Industriel et des Risques (INERIS), Limoges - <b>France</b>
<b>15:45-16:00</b>	Marine plastic litters: the unanalyzed nano-fraction J. Gigault, <b>B. Pedrono</b> , B. Maxit and A. Ter Halle	<b>Mr. Boris Pedrono</b> , Cordouan Technologies, Pessac - <b>France</b>

16:00-16:30	Coffee Break / Exhibition/ Posters Session II	
16:30-16:45	Challenges on fate, behavior and effects of nanomaterials in the marine environment <b>C. Mouneyrac</b>	<b>Prof. Catherine Mouneyrac</b> , Université Catholique de l'Ouest-France
16:45-17:00	Sulfidation pathways of Silver Nanoparticles in the presence of Humic Acid <b>B. Thalmann</b> , A. Voegelin, E. Morgenroth and R. Kaegi	<b>Dr. Basilius Thalmann</b> , Eawag, Swiss Federal Institute of Aquatic Science and Technology - Switzerland
17:00-17:15	Mechanism of CuO/ZnO nanoparticle sulfidation: Insights from electron microscopy <b>A. Gogos</b> , B. Thalmann and R. Kaegi	<b>Dr. Alexander Gogos</b> , Eawag, Swiss Federal Institute of Aquatic Science and Technology - Switzerland
17:15-17:30	Development of the first generation of hybrid metrology algorithms dedicated to nanoparticles measurement with AFM and SEM techniques A.Dervillé, A.Delvallée, S.Martinez, ...,L.Devuille, Y.Zimmermann, <b>J.Foucher</b> and G.Favre	<b>Dr. Johann Foucher</b> , POLLEN Metrology Company - France
17:30-17:45	Toward the direct quantification of dissolution and aggregation of AgNPs using AF4-UVD-MALLS-ICP-MS and Cryo-TEM analysis <b>I.A.M Worms</b> , A. Arnould, R. Soulas, J-F. Damlencourt, S. Motellier, E. Mintz, I. Michaud-Soret and D. Truffier-Boutry	<b>Dr. Isabelle Worms</b> , CEA, Grenoble,DRF/BIG/LCBM/BioMet - France
17:45-18:00	Particle Size Distribution Analysis of Complex Fe <sub>2</sub> O <sub>3</sub> Nano-particle Aggregates Embedded in High Density Polyethylene Matrix <b>T. Uusimäki</b> , T. Wagner, E. Verleysen, J. Mielke, P. Müller and R.Kägi	<b>Dr. Toni Uusimäki</b> , ETH- Eawag-Switzerland
18:00-18:15	Combination of micro- and nano- computed X-ray tomography for the characterization of nanomaterial-plant interactions C. Levard, A.E. P. del Real, A. Avellan, <b>F. Schwab</b> , P. Chaurand, D. Borschneck, V. Vidal, M. Auffan, G. Sarret and J. Rose	<b>Dr. Fabienne Schwab</b> , Aix-Marseille University-CNRS- France
18:15-18:30	Piezo-Resistive Sensing Active (PRSA) Probes integrated into a Nanomeasuring Machine (NMM-1) <b>A. El Melegy</b> , T. Hausotte, M. A. Younes and M. Amer	<b>Dr. Ahmed El Melegy</b> , FAU Erlangen-Nürnberg University - Germany
18:30-18:45	One pot Green synthesis of fluorescent Zinc oxide nanoparticles and its biological effects <b>A. Mallick</b> , P. Kumari, S.K.Verma	<b>Dr. Muhammad Anwar Mallick</b> , Vinoba Bhave University- India
18:45-19:00	Adsorption properties of DOX antibiotic from aqueous solutions onto pristine and magnetized carbon nanotubes. <b>A. Terechshenko</b> , K.Korzhybayeva, M.R.Babaa, Jorge O. Oña-Ruales and Z. Bakenov	<b>Ms. Alina Terechshenko</b> , Nazarbayev University- Kazakhstan

# NanoMaterials for Energy and Environment - NanMatEn 2016 Preliminary Program

**June 2<sup>nd</sup>, 2016**  
**NanoMatEn 2016 Session I: NanoEnergy**

**Conference Room 211**

**Session Chairs:**  
**Prof. Je-Lueng Shie, National I-Lan University – Taiwan**  
**Prof. Nicolas Fressengeas, Lorraine University – France**

<b>10:30-11:00</b>	Multi-functional Thin Films for Solar Energy Utilization <b>J. He</b>	<b>Prof. Junhui He</b> , Technical Institute of Physics and Chemistry, Chinese Academy of Sciences - <b>China</b> .
<b>11:00-11:30</b>	Comparative study of PN, PIN and new Schottky based InGaN thin films solar cells A. Adaine, S. Ould Saad Hamady and <b>N. Fressengeas</b>	<b>Prof. Nicolas Fressengeas</b> , Lorraine University - <b>France</b>
<b>11:30-12:00</b>	Hybrid Heterojunction PEDOT:PSS/GaAs Thin Film Solar Cells Via Wafer-Bonding Technique <b>K.W. Sun</b>	<b>Prof. Kien Wen Sun</b> , National Chiao Tung University - <b>Taiwan</b>
<b>12:00-12:15</b>	Role of methylammonium molecules on the electronic transport properties of organometallic perovskite CH <sub>3</sub> NH <sub>3</sub> PbI <sub>3</sub> <b>G. R. Berdiyrov</b> , F. El-Mellouhi, M. E. Madjet, F. H. Alharbi, and S. N. Rashkeev	<b>Dr. Golibjon Berdiyrov</b> , Qatar Environment and Energy Research Institute - <b>Qatar</b>
<b>12:15-12:30</b>	Surface Modification for Enhancing Perovskite Solar Cell Performance <b>W. Yu</b> , Tom Wu and Aram Amassian	<b>Dr. Weili Yu</b> , King Abdullah University of Science and Technology - <b>Saudi Arabia</b> .
<b>12:30-12:45</b>	The TiO <sub>2</sub> -dye interface in DSSCs: comparing single crystals and thin films and deposition methods, sensitized in UHV and liquid solution <b>Z. Besharat</b> , R. Alvarez Asencio, M. Götelid, M. Johnson and M. W. Rutland	<b>Ms. Zahra Besharat</b> , KTH Royal Institute of Technology - <b>Sweden</b>
<b>12:45-14:00</b>	<b>Lunch Break / Exhibition / Posters session II</b>	
<b>14:00-14:15</b>	Photoelectric and Photothermoelectric Material of SBA-15/K-OMS-2 on Photoelectrochemical Solar Cell Application C-H. Lee, <b>J-L. Shie</b> , Y. Li and C-Y. Chang	<b>Prof. Je-Lueng Shie</b> , National I-Lan University - <b>Taiwan</b>
<b>14:15-14:30</b>	Aluminum-Carbon Nanotube Nanocomposite for Silicon Solar Cell Back Metallization K. El-Rafei, <b>A. Esawi</b> , O. Tobail and A. Klingner	<b>Dr. Amal Esawi</b> , The American University in Cairo - <b>Egypt</b>
<b>14:30-14:45</b>	Co-based mesoporous spinels for oxygen evolution reaction in alkaline medium <b>A. Habrioux</b> , I. Abidat, C. Canaff, D. Dambournet, C. Comminges, T. Napporn and K.B. Kokoh	<b>Dr. Aurélien Habrioux</b> , University of Poitiers - <b>France</b>
<b>14:45-15:00</b>	Coupled surface-plasmon/thermoelectric power generators based on TCO nanowires A. Catellani, A. Ruini, M. Buongiorno Nardelli and <b>A. Calzolari</b>	<b>Dr. Arrigo Calzolari</b> , CNR-NANO Istituto Nanoscienze, Centro S3 - <b>Italy</b>
<b>15:00-15:15</b>	Core-shell Ni-NiF <sub>2</sub> as cathode materials for secondary lithium batteries <b>L. Doubtsof</b> , L. Jouffret, P. Bonnet and K. Guerin	<b>Mrs. Lea Doubtsof</b> , Institut de Chimie de Clermont-Ferrand. Clermont University - <b>France</b>
<b>15:15-15:30</b>	Ultra-Thin copper oxide nanowires grown by atmospheric pressure afterglow for water splitting application <b>A. Imam</b> , T. Gries, K. Hussein and T. Belmonte	<b>Mr. Abdallah Imam</b> , Lorraine University - <b>France</b>

15:30-15:45	Energy transfer between up-converting nanocrystals and organic polymer <b>J. Grzelak</b> , K. Ciszak, M. Nyk, D. Piatkowski and S. Mackowski	<b>Ms. Justyna Grzelak</b> , Nicolaus Copernicus University - <b>Poland</b>
15:45-16:00	Energy Harvesting with Decorative Colour Specific Windows <b>B. Fisher</b> , E. New, D. Kutsarov, V. Stolojan and S. R. P. Silva	<b>Mr. Brett Fisher</b> , University of Surrey - <b>UK</b>
<b>16:00-16:30 Coffee Break / Exhibition / Posters Session II</b>		
16:30-16:45	Enhanced Thermal Conductivity of Nanofluids Containing Two-Dimensional Materials <b>D. Lee</b> , G. Lee, J-J. Park and M. Lee	<b>Dr. Dongju Lee</b> , Korea Atomic Energy Research Institute – <b>Republic. of Korea</b>
16:45-17:00	Nanofluids with enhanced thermal properties: an experimental and theoretical analysis <b>J. Navas</b> , A. Sánchez-Coronilla, E.I. Martín, R. Gómez-Villarejo, ..., C. Fernández-Lorenzo and J. Martín-Calleja	<b>Dr. Javier Navas</b> , Cádiz University - <b>Spain</b>
17:00-17:15	New Composites “LiCl/vermiculite” for Sorptive Heat Storage <b>A.D. Grekova</b> , L.G. Gordeeva and Y.I. Aristov	<b>Dr. Alexandra Grekova</b> , Novosibirsk State University - <b>Russian Federation</b>
17:15-17:30	Pseudocapacitive Study of Nickel Oxide Nanomaterials for Electrochemical Energy storage <b>L. Meda</b> , J. Adkins and C. Arnold	<b>Dr. Lamartine Meda</b> , Xavier Univresity of Louisiana- <b>USA</b>

**June 2<sup>nd</sup>, 2016**

**NanoMatEn 2016 Session II: Nanotechnology for Environmental applications**

**Conference Room 212**

**Session Chairs: Prof. Joydeep Dutta, KTH Royal Institute of Technology – Sweden/  
Prof. M. Carmen Hermosin, IRNAS-CSIC-Sevilla- Spain/ Prof. Tahar Laoui, King Fahd University  
of Petroleum and Minerals- Saudi Arabia**

10:30-11:00	Effect of Sb segregation on conductance and catalytic activity at Pt/Sb-doped SnO <sub>2</sub> interface: a synergetic computational and experimental study Q.Fu, L.C. Colmenares Rausseot, <b>U.Martinez</b> , P.I.Dahl, J.M.García Lastra, P.E. Vullum, I-H. Svenum and T.Vegge	<b>Dr. Umberto Martinez</b> , Quantumwise - <b>Danemark</b>
11:00-11:15	Au@Pt Core-shell Mesoporous Nanoballs and Nanoparticles as Efficient Electrocatalysts for formic acid and glucose oxidation <b>T.W. Napporn</b> , Y. Holade, A. Lehoux, H. Remita and K. B. Kokoh	<b>Dr. Teko W. Napporn</b> , Poitiers University- <b>France</b>
11:15-11:30	First insight into fluorinated Pt/carbon aerogels as more corrosion-resistant electrocatalysts for Proton Exchange Membrane Fuel Cells Cathodes <b>Y. Ahmad</b> , S. Berthon-Fabry, L. Dubau, K.Guerin and M. Chatenet	<b>Dr. Yasser Ahmad</b> , Blaise Pascal University- <b>France</b>
11:30-11:45	Label-Free Surface Plasmon Resonance Biosensing with Titanium Nitride Thin film S.P. Ng, G. Qiu, Z. Deng and <b>C.M.L. Wu</b>	<b>Prof. Chi-Man Wu</b> , City University of Hong Kong - <b>China</b>
11:45-12:00	Effect of calcination temperature on photocatalytic activity of TiO <sub>2</sub> /Bi <sub>2</sub> O <sub>3</sub> Nanofibers in the photodegradation of Acid Orange 7 (AO7) under visible light irradiation <b>J.Jermyn</b> , S.SiangLee, Benny Y.Liang Tan, H.Bai and D. Delai Sun	<b>Mr. Jermyn Juay</b> , Nanyang Technological University - <b>Singapore</b>
12:00-12:15	Facile Synthesis of Highly Efficient One-Dimensional Plasmonic Photo-catalysts <b>J. Xiong</b> and Z. Li	<b>Ms. Jinyan Xiong</b> , The University of Wollongong- <b>Australia</b> .



12:15-12:30	Analytical TEM study on the behavior of CeO <sub>2</sub> nanoparticles in Sb-V-CeO <sub>2</sub> /TiO <sub>2</sub> catalysts for NH <sub>3</sub> -SCR <b>Y.E. Jeong</b> , P.A.Kumar, K-Y. Lee and H.P. Ha	<b>Ms. Young Eun Jeong</b> , Korea Institute of Science and Technology- Seoul- <b>Republic of Korea</b>
12:30-12:45	Photodegradation of Ofloxacin with nano-go/m Composite and it's reuse <b>P. Alicanoğlu</b> and D. T. Sponza	<b>Mrs. Pelin Alicanoglu</b> , Pamukkale University-Turkey
<b>12:45-14:00 Lunch Break / Exhibition / Posters session II</b>		
14:00-14:15	Nanostructures as Catalysts for H <sub>2</sub> O <sub>2</sub> Electrogeneration and Degradation of Organic Pollutants <b>M. C. Santos</b>	<b>Prof. Mauro Santos</b> , ABC Federal University - <b>Brazil</b>
14:15-14:30	Designing efficient bimetallic photocatalysts for hydrogen production <b>E. Aronovitch</b> , P.Kalisman, L. Houben, L. Amirav and M.Bar-Sadan	<b>Mr. Eran Aronovitch</b> , Ben-Gurion University of the Negev- <b>Israel</b>
14:30-14:45	Enhancing Cuprous Oxide Stability for Hydrogen Evolution <b>J. Azevedo</b> , S.D. Tilley, M. Schreier, M. Stefik, L. Steier, P. Dias, C.T. Sousa, J.P. Araújo, M.T. Mayer, M. Graetzel and A. Mendes	<b>Mr. João Azevedo</b> , LEPABE-Porto University - <b>Portugal</b>
14:45-15:00	Preparation of Basic Type of Activated Alumina Supports for using in Production and Separation of Hydrogen M. Duran and <b>F.N. Tüzün</b>	<b>Dr. Fatma Nihal Tuzun</b> , Hitit University - <b>Turkey</b>
15:00-15:15	On the applicability of Johnson-Mehl-Avrami-Kolmogorov (JMAK) approach in explaining the hydrogen sorption kinetics in nanocrystalline magnesium hydride <b>S. Shrinivasan</b> , A. Gangrade, N.K. Gor, H.-Y. Tien, M. Tanniru, F. Ebrahimi and S.S.V. Tatiparti	<b>Prof. Sankara Sarma Tatipari</b> , Indian Institute of Technology Bombay - <b>India</b> .
15:15-15:30	Improving the Adhesion Capacity of Foliar Nitrogen Fertilizer through Nano networks <b>D. Cai</b> , N. Zhong, P. Zhao and Z. Wu	<b>Dr. Dongqing Cai</b> , Hefei Institutes of Physical Science, Chinese Academy of Sciences - <b>China</b>
15:30-15:45	Development of an "anti-bug" Bicomponent Fibre <b>M. Bischoff</b> , G. Seide and T. Gries	<b>Mrs. Merle Bischoff</b> , Institut für Textiltechnik, RWTH Aachen University- <b>Germany</b>
15:45-16:00	Molecularly Imprinted Polymer Nano layers for the electrochemical detection of pesticides <b>S. Bouden</b> , V. Bertagna, B. Cagnon and C. Vautrin-UI	<b>Dr. Sarra Bouden</b> , Orléans University- <b>France</b>
<b>16:00-16:30 Coffee Break / Exhibition/ Posters Session II</b>		
16:30-16:45	Carbon Nanofibers-Ionic Liquid Composite Sensors For Detection of Trace Heavy Metals <b>L. Oularbi</b> , M. El Rhazi and M. Turmine	<b>Mr. Larbi. Oularbi</b> , University Hassan II Casablanca, <b>Morocco</b> / Sorbonne University, UPMC University- <b>France</b>
16:45-17:00	Zero valent iron nanoparticles for remediation of soils contaminated with heavy metals O. Cortes, S.Machado, N.Vital, <b>H.Gouveia</b> , V.Correia,T. Albergaria and C. Delerue Matos	<b>Dr. Helena Gouveia</b> , ISQ, Taguspark -Oeiras- <b>Portugal</b>
17:00-17:15	Development of nano-porous geopolymer for passive cooling systems <b>M. Alshaaer</b> , J. Alkafawein, Y. Al-Fayez, T. Fahmy, M. Zamorano Toro and M. Martín Morales	<b>Prof. Mazen Alshaaer</b> , Prince Sattam Bin Abdulaziz University- <b>Saudi Arabia</b>
17:15-17:30	Novel Zeolite-Polyurethane Membrane for Environmental Applications <b>H.Shehu</b> and E.Gobina	<b>Ms. Habiba Shehu</b> , Robert Gordon University-Aberdeen- <b>United Kingdom</b>
17:30-17:45	Flue Gases Capturing Capacity of Nano-porous organic Ma-terials <b>R. Ullah</b> , M. Atilhan and C.T. Yavuz	<b>Dr. Ruh Ullah</b> , Qatar University- <b>Qatar</b>

**June 2<sup>nd</sup>, 2016**  
**NanoMatEn 2016- Symposium on Nanotechnology for Photovoltaics**

**Conference Room 260**

**Session Chairs:**  
**Prof. Alejandro Perez-Rodriguez, IREC- Catalonia Institute for Energy Research - Spain**

<b>14:00-14:45</b>	High efficiency thin film photovoltaic cells in novel light confinement architectures	<b>Prof. Jordi Martorell</b> - ICFO - Barcelona- <b>Spain</b>
<b>14:45-15:30</b>	Nano-architectures and organic-inorganic hybrid material combinations for novel photovoltaic device concepts <b>S. Christiansen</b> , S. Schmitt, S. Jäckle, G. Sarau, M. Göbelt, R. Keding, M. Mattiza, B. Hoffmann and M. Latzel	<b>Prof. Silke Christiansen</b> , Helmholtz Zentrum für Materialien und Energie, HZB (Berlin), Germany- <b>Germany</b>
<b>15:30-15:45</b>	Metal Oxide Nanorod Arrays Fabricated by Solution Processes for Applications in Hybrid Photovoltaic Cells <b>S. Chuangchote</b> , W.Arpavate, N.Laosiripojana and T. Sagawa	<b>Dr. Surawut Chuangchote</b> , King Mongkut's University of Technology Thonburi- <b>Thailand</b>
<b>15:45-16:00</b>	Boosting impact of nanometric Ge layers on the synthesis and performance in Cu <sub>2</sub> ZnSnSe <sub>4</sub> solar cells <b>P.Pistor</b> , S.Giraldo, M.Neuschitzer, M. Placidi A.Pérez-Rodriguez and E.Saucedo	<b>Dr. Paul Pistor</b> , Catalonia Institute for Energy Research- (IREC) - <b>Spain</b>
<b>16:00-16:30 Coffee Break / Exhibition / Posters session II</b>		
<b>16:30-16:45</b>	Thin Epitaxial Silicon Foils Using Porous-Silicon-Based Lift-Off for Photovoltaic Application <b>I. Gordon</b>	<b>Dr. Ivan Gordon</b> , Photovoltaics Department IMEC-Leuven- <b>Belgium</b>
<b>16:45-17:15</b>	Photon managements by employing one- and two-dimensional structures for optoelectronic devices J-H. He, and <b>J.R.D.Retamal</b>	<b>Dr. Jose Ramon Duran Retamal</b> , King Abdullah University of Science & Technology, <b>Saudi Arabia</b>
<b>17:15-17:30</b>	Electric and Photovoltaic Behavior of Novel Few Layer $\alpha$ -MoTe <sub>2</sub> / MoS <sub>2</sub> Dichalcogenide Heterojunction <b>A.Pezeshki</b> and S. Im	<b>Mrs. Atiye Pezeshki</b> , Yonsei University- Seoul - <b>Republic od Korea</b>
<b>17:30-17:45</b>	Zinc selenide as a potential Cd-free buffer nanolayer for CZTSe solar cells <b>M.Placidi</b> , M. Espindola-Rodriguez, H. Xie, F. Oliva, Y. Sanchez, M. Neuschitzer, S. Giraldo, I. Becerril-Romero, P. Pistor, V. Izquierdo-Roca, E. Saucedo and A. Pérez-Rodríguez	<b>Dr. Marcel Placidi</b> , Catalonia Institute for Energy Research (IREC) - <b>Spain</b>
<b>17:45-18:00</b>	SURMOFs and CNCs as novel tuneable Materials for Optical, Photonic as well as for Solar Energy Materials <b>E. Redel</b>	<b>Dr. Engelbert Redel</b> , Karlsruhe Institute of Technology (KIT) - <b>Germany</b>

**June 3<sup>rd</sup>, 2016**  
**NanoMatEn 2016- Session III: Nanotechnology for water treatment**

**Conference Room 561**

**Session Chairs:**  
**Prof. Joydeep Dutta, KTH Royal Institute of Technology - Sweden**  
**Dr. Alberto Figoli, Institute on Membrane Technology (CNR-ITM) - Italy**

<b>08:30-09:15</b>	Nanotechnology for cleaning water: redox reactions the way out?	<b>Prof. Joydeep Dutta</b> , KTH Royal Institute of Technology - <b>Sweden</b>
<b>09:15-09:30</b>	Nanostructured membranes for water desalination: an overview <b>M.Faccini</b> and M. Boerrigter	<b>Dr. Mirko Faccini</b> , LEITAT Technological Center- <b>Spain</b>

09:30-09:45	Decontamination of wastewater using nanocarbon compounds insert in diatomite mesoporous structure E. Flores, O. Enriquez, J. De la Cruz, A. López, G.Poma and <b>M.Quintana</b>	<b>Dr. Maria Quintana</b> , Engineering and Technological University, Lima - <b>Peru</b>
09:45-10:00	Functionalization of glassy carbon electrode by amines electrochemical oxidation for micro-pollutants detection in water D. Pally, M. Alaaeddine, B. Cagnon, <b>V. Bertagna</b> , R. Benoit, F. Podvorica and C. Vautrin	<b>Dr. Valerie Bertagna</b> , University of Orleans - <b>France</b>
<b>10:00-10:30 Coffee Break / Exhibition</b>		
10:30-11:00	PVDF UF hollow-fiber membrane production as pre-treatment system in Water Desalination Reverse Osmosis Unit <b>A. Figoli</b> , O. Saoncella, S. Xue, S. Simone, F.Galiano, M. Boerrigter, C. Chaumette, M. Faccini and E. Drioli	<b>Dr. Alberto Figoli</b> , Institute on Membrane Technology (CNR-ITM) - <b>Italy</b>
11:00-11:15	Development of Alumina-Carbon Nanotubes Porous Membranes Using Spark Plasma Sintering Process for Water Purification <b>T. Laoui</b> , H. K. Shahzad, M. A. Hussein, F. Patel, N. Al Aqeeli and M. A. Atieh	<b>Prof. Tahar Laoui</b> , King Fahd University of Petroleum and Minerals- <b>Saudi Arabia</b>
11:15-11:30	The efficient separation of oil-water emulsions with a flexible, superhydrophilic and self-cleaning TiO <sub>2</sub> /Fe <sub>2</sub> O <sub>3</sub> membrane <b>B.Y.L. Tana</b> , J. Juaya, J.K.K. Anga, Z.Liub and D. Suna	<b>Mr. Benny Tan</b> , Nanyang Technological University - <b>Singapore</b>
11:30-11:45	Nanostructure formation, characterization and application of ba-nana peels nanosorbent in mine water treatment <b>O. Atiba-Oyewo</b> , M.S. Onyango and C. Wolkersdorfer	<b>Ms. Opeyemi Atiba-Oyewo</b> , Tshwane University of Technology - <b>South Africa</b>
11:45-12:00	Fabrication of hematite photoanode for solar water splitting by using pulsed laser deposition <b>C-P.Yen</b> , Y-J. Li, S-J. Luo, J.Wang, C-J.Tseng and S-Y Chen	<b>Mr. Chih-ping Yen</b> , National Taiwan University - <b>Taiwan</b>
12:00-12:15	Molecular Dynamics-Continuum Hybrid Simulation of Water Transport through Carbon Nanotube Membranes <b>A. Kudaikulov</b> , A. Kaltayev and C. Jossierand	<b>Mr. Aziz Kudaikulov</b> , Al-Farabi Kazakh National University - <b>Kazakhstan</b>
12:15-12:30	Titanium Dioxide-Based Nanocatalysts Constructed from Natural Sources for Photocatalytic Wastewater Treatment <b>P. Kemacheevakul</b> and S.Chuangchote	<b>Dr. Patiya Kemacheevakul</b> , King Mongkut's University of Technology - <b>Thailand</b>
12:30-12:45	Magnetic Nanoparticles Stabilized by Lignocellulosic Waste as Green Adsorbent For Cr(VI) Removal from Waste Water <b>I.L.A. Ouma</b> , A.E. Ofomaja and E.B. Naidoo,	<b>Ms. Linda Ouma</b> , Vaal University of Technology- <b>South Africa</b>

## Posters Session II: June 2<sup>nd</sup>, 2016

### NanoMatEn 2016

#### Exhibition and Poster Hall

N.	Title	Author/Affiliation/Country
1	Solar charged redox flow battery <b>K. Wedege</b> , J. Azevedo, A. Khataee, A. Mendes and A. Bentien	<b>Ms. Kristina Wedege</b> , Aarhus University - <b>Denmark</b>
2	Novel Methods for the Deposition of Solution-Processed CdTe Inks for Photovoltaic Applications <b>J.C. Russell</b> , J.M. Kurley, H. Zhang and D. Talapin	<b>Mr Jake Russell</b> , University of Chicago - <b>USA</b>
3	Enhancement of power conversion efficiency of dye-sensitized solar cells via incorporation of GaN semiconductor materials synthesized in hot-wall CVD furnace. <b>M. Baisariyev</b> , R.Iskakov, G. Sugurbekova	<b>Mr. Murat Baisariyev</b> , Nazarbayev University - <b>Kazakhstan</b>

4	Fabrication of Hierarchical Nanostructures for Perfect Anti-reflection Coating S.J. Cho and <b>T. An</b>	<b>Prof. Taechang An</b> , Andong National University - <b>Republic of Korea.</b>
5	Modeling infrared radiation transport in insulating dielectric nanocomposites to minimize radiative thermal losses <b>J.Tang</b> , V.Thakore and T.Ala-Nissilä	<b>Ms. Janika Tang</b> , Aalto University - <b>Finland</b>
6	Numerical Investigations of Heat Transfer in Rectangular Micro-Channels during Single Phase Fluid Flow using Cooling Nanoliquids <b>L. Snoussi</b> , N. Ouerfelli, F.B.M. Belgacem and A. Guizani	<b>Dr. Lotfi Snoussi</b> , Research and Technologies Centre of Energy – <b>Tunisia</b>
7	The performance fo Zn/Ni battery using NixZn(1-x)O as anodic material to suppress Zn dendrite <b>Y. Im</b> , K;Su Park, T.W. Cho, J-S. Lee and M.Kang	<b>Mr. Younghwan Im</b> , Yeungnam University - <b>Republic of Korea</b>
8	Kinetic mechanisms of hydrogen sorption in nanocrystalline magnesium (hydride) <b>S. Shrinivasan</b> , A. Gangrade, N.K. Gor, H.-Y. Tien, M. Tanniru, F. Ebrahimi and S.S.V. Tatiparti	<b>Ms. Sweta Shrinivasan</b> , Indian Institute of Technology Bombay – <b>India</b>
9	Hydrogen production from propane steam reforming over 30NiFe1-xO/70Al2O3 catalysts <b>Kang Min Kim</b> <sup>1</sup> , Byeong Sub Kwak <sup>1</sup> , No-Kuk Park <sup>2</sup> , Tae Jin Lee <sup>2</sup> , Misook Kang <sup>*1</sup>	<b>Mr. Kang Min Kim</b> , Yeungnam University - <b>Republic of Korea</b>
10	Hydrogen production by propane steam reforming over transition metal (A = Fe, Co, Ni, Cu) in Mn-based metal oxide structure <b>J. Yeon Do</b> and M. Kang	<b>Ms. Jeong Yeon Do</b> , Yeungnam University - <b>Republic of Korea</b>
11	Three-metallic Mn-based Ni1-XCoXMnO4/γ-Al2O3 (X=0.2, 0.3, 0.4, 0.5) catalysts for hydrogen production via steam reforming of propane gas <b>S.W. Jo</b> and M. Kang	<b>Mr. SeungWon Jo</b> , Yeungnam University - <b>Republic of Korea</b>
12	Effective hydrogen production from propane stream reforming on Co/Cex/γ-Al2O3 <b>M.Park</b> and M.Kang	<b>Mr. Minkyu Park</b> , Yeungnam University - <b>Republic of Korea.</b>
13	Oxygen Reduction Reaction Catalyzed by Manganese Dioxide Nanoflowers <b>L.R. Aveiro</b> , V.S. Antonin, A.G.M. da Silva, E. G. Candido, P.H.C.Camargo and M.C. dos Santos	<b>Mrs. Luci Aveiro</b> , ABC Federal University - <b>Brazil</b>
14	W@Au nanostructures as catalysts for H2O2 electrogeneration <b>V. S. Antonin</b> , L.S. Parreira, F.L. Silva, R.B. Valim, P. Hammer, M.R.V. Lanza and M. C. Santos	<b>Ms. Vanessa Antonin</b> , ABC Federal University - <b>Brazil</b>
15	Selective removal of lead using a nanocompound basedon diatomite and graphene oxide <b>E. Flores</b> , O. Enriquez, J. De la Cruz, A. López, G. Poma and M. Quintana	<b>Ms. Elena Flores</b> , Universidad de Ingenieria y Tecnologia - <b>Peru</b>
16	Hybrid Nanocomposite of Nanocellulose-Silver Nanoparticles-Graphene Oxide for Environmental Remediation Purposes <b>S.W. Chook</b> ,C.H. Chia and S. Zakaria	<b>Dr. Soon Wei Chook</b> , National University of Malaysia (UKM) – <b>Malaysia</b>
17	Study of degradability of starch-based films mixing with nano-Titanium dioxide <b>J. Komastitaya</b> , S. Mataweechotikul and A. Simprasert	<b>Dr. Juntira Komastitaya</b> , King Mongkut University of Technology Thonburi-Bangkok- <b>Thailand</b>
18	Synthesis and Characterization of Superparamagnetic Magnetite/Modified Magnetite Nano-Particles (Fe3O4@SiO2@L) H. Çiftci, <b>B. Ersoy</b> and A. Evcin	<b>Prof. Bahri Ersoy</b> , Afyon Kocatepe University- <b>Turkey</b>
19	Determination of the equilibrium constant of 1,3,5-nickel bencenotricarboxylate, Ni-HKUST-1 <b>J. Vargas</b> , J. Balmaseda and R. Salcedo	<b>Ms. Jaquebet Vargas Bustamante</b> , Universidad Nacional Autónoma de México- <b>Mexico</b>
20	Nanocomposite films as a gas sensor for organic compounds <b>S.Ali</b> , B. Horrocks and A. Houlton	<b>Mrs. Shams Ali</b> , Newcastle University- <b>United Kigndom</b>
21	Synthesis and characterization of ZnO-Ag nanoparticles supported on MCM-41 as a photocatalyst for degradation Congo Red <b>E. M. Barrera-Rendón</b> , G. García-Rosales and J. Jiménez-Becerril	<b>Ms. Eva M. Barrera Rendón</b> , Toluca Technology Institute- <b>Mexico</b>

<b>22</b>	Synthesis and Evaluation of a Carbon-TiO <sub>2</sub> -CeO <sub>2</sub> composite for the degradation of phenol <b>Y. Lara-Lopez</b> , G. García-Rosales and J. Jiménez-Becerril	<b>Ms. Yoselin Lara-Lopez</b> , Toluca Technology Institute- <b>Mexico</b>
<b>23</b>	Low Cost and Free TCO Porous Coal as a Counter Electrode (CE) for Dye Sensitized Solar Cell (DSSC) <b>M.Y. Feteha</b> , S. Ebrahim and L. Saad	<b>Dr. Mohamed Feteha</b> , Alexandria University- <b>Egypt</b>
<b>24</b>	Facile formation of fullerene nanostructures and their application to polymer solar cells <b>S. Woo</b> , W.-H. Kim and S.-J. Sung	<b>Dr. Sungho Woo</b> , Daegu Gyeongbuk Institute of Science & Technology- <b>Republic of Korea</b>
<b>25</b>	Comparison of the systemic nanoherbicide Imazamox-LDH obtained by direct synthesis and reconstruction: preliminary results R. Khatem, A. Bakhti and <b>M.C. Hermosin</b>	<b>Prof. M. Carmen Hermosin</b> , IRNAS-CSIC-Sevilla- <b>Spain</b>
<b>26</b>	Polymer optimised dewatering of sludge using Geotubes, a systematic approach <b>H. Haase</b> , W. Lieske, T. Schanz and H. Dehn	<b>Mr. Wolfgang Lieske</b> , Ruhr-University- <b>Germany</b>



# European Graphene Forum – EGF 2016

## Preliminary Program

June 1 <sup>st</sup> , 2016 EGF 2016- Plenary session I		
Amphitheatre G		
Session's Chairs: Dr Cinzia Casiraghi, University of Manchester- UK Prof. Giancarlo Faini, Laboratoire de Photonique et de Nanostructures, CNRS - France		
09:00-9:40	Supramolecular approaches to 2-D materials: from complex structures to sophisticated functions <b>P.Samori</b>	<b>Prof. Paolo Samori</b> , Starsbourg University - France
09:40-10:20	Water-based 2D-crystal Inks: from Production to Devices <b>C. Casiraghi</b>	<b>Dr. Cinzia Casiraghi</b> , University of Manchester- U K
10:30-11:00 Lunch Break / Exhibition / Posters Session I		
11:00-11:30	PN Junction Based Devices in Ultra-Clean Graphene P. Rickhaus, M-H. Liu, P. Makk, M. Jung, C. Handschin, S. Zihlmann, E. Tovari, R. Maurand, M. Weiss, K. Richter and <b>C. Schönenberger</b>	<b>Prof. Christian Schönenberger</b> , University of Basel - Switzerland
11:30-12:00	2-D Nanocarbons: Attraction, Reality and Future <b>Z. Liu</b>	<b>Prof Zhongfan Liu</b> , Peking University- Beijing - China
12:00- 12:30	Effects of morphology and surface chemistry of graphite nanoplates on dispersion and network formation in polypropylene melts R. M. Santos and <b>J. A. Covas</b>	<b>Prof. José Covas</b> , University of Minho - Portugal
12:30-12:45	Exploring Graphene Plasmonics for Novel Applications: From Tunable Absorption Enhancement to Strong Optical Forces <b>J. Zhang</b> , W. Liu, Z. Zhu, C. Guo, K. Liu, X. Yuan and S. Qin	<b>Dr. Jianfa Zhang</b> , National University of Defense Technology- China
12:45-13:00	Scalable Few Layer Graphene Production by Graphite Exfoliation in Liquids <b>C. Damm</b> , T. J. Nacken, H. Xing, Y. Hambal and W. Peukert	<b>Dr. Cornelia Damm</b> , University Erlangen-Nürnberg- Germany
12:45-14:00 Lunch Break / Exhibition / Posters Session I		
EGF 2016- Session I: Graphene and 2D Materials Synthesis, characterization and properties		
Session's Chairs: Prof Zhongfan Liu, Peking University, Beijing – China/ Prof. Andrey Chuvilin, CIC nanoGUNE – Spain		
14:00-14:15	CVD-grown large-area monolayer MoS <sub>2</sub> using H <sub>2</sub> S <b>D. Dumcenco</b> , D. Ovchinnikov, O. Lopez-Sanchez, P. Gillet, D. T. L. Alexander, S. Lazar, A. Radenovic and A. Kis	<b>Dr. Dumitru Dumcenco</b> , EPFL - Switzerland
14:15-14:30	Centimeter-scale synthesis of ultrathin layered MoO <sub>3</sub> by van der Waals epitaxy <b>A.J. Molina-Mendoza</b> , J.L. Lado, J. Island, M. Angel Niño, L. Aballe, M. Foerster, F.Y. Bruno, H.S. J. van der Zant, G. Rubio-Bollinger, N. Agraït, E.M. Perez, J. Fernández-Rossier and A. Castellanos-Gomez	<b>Mr. Aday J Molina-Mendoza</b> , Universidad Autonoma de Madrid - Spain
14:30-14:45	Plasma-assisted CVD graphene synthesis and characterization on nickel substrates <b>P. Pop-Ghe</b> , L. Krückemeier, N. Wöhrle and V. Buck	<b>Ms. Patricia Pop-Ghe</b> , University of Duisburg - Essen- Germany
14:45-15:00	A Record-Breaking mobility for CVD Graphene by suppressing the effect of charged impurities <b>R. Nashed</b> , K. Brenner and A. Naeemi	<b>Mr. Ramy Nashed</b> , Georgia Institute of Technology – USA
15:00-15:15	Chemical Kinetics during CVD Growth of Graphene <b>S. Farhat</b> , I. Hinkov, H-A. Mehedi and A. Gicque	<b>Dr. Farhat Samir</b> , CNRS LSPM-Paris 13 University- France

<b>15:15-15:30</b>	Optimized Synthesis of Graphene by Cobalt-Catalyzed Decomposition of Methane with Plasma-Enhanced CVD <b>H.-A. Mehedi</b> , B. Baudrillart, D. Alloyeau, C. Ricolleau, J. Lagoutte, A. Gicquel and S. Farhat	<b>Dr. Hasan Al Mehedi</b> , CNRS LSPM-Paris 13 University- <b>France</b>
<b>15:30-15:45</b>	Tuning the nature of nitrogen atoms in N-containing RGO: Enhanced thermal oxidation stability by nitrogen doping <b>S. Sandoval</b> , N. Kumar, A. Sundaresan, C. N. R. Rao, A. Fuertes and G. Tobias	<b>Ms. Stefania Sandoval Rojano</b> , Institute of Materials Science of Barcelona - <b>Spain</b>
<b>15:45-16:00</b>	Towards High Quality Graphene Flakes by Electrochemical Exfoliation of Graphite With Multifunctional Electrolytes <b>J.M. Munuera</b> , J.I. Paredes, S. Villar-Rodil, M. Ayán-Varela, A. Martínez-Alonso and J.M.D. Tascón	<b>Mr. Jose Munuera</b> , Instituto Nacional del Carbón, INCAR-CSIC - <b>Spain</b>
<b>16:00-16:15</b>	Deoxygenation of Graphene Oxide by Metalorganic Compounds <b>N. Jalagonia</b> , T. Kuchukhidze, N. Jalabadze, V. Tsitsishvili and R.Chedia	<b>Mrs. Natia Jalagonia</b> , Ilia Vekua Sukhumi Institute of Physics and Technology, Tbilisi - <b>Georgia</b>
<b>16:15-16:30 Coffee Break / Exhibition / Posters Session I</b>		
<b>16:30-16:45</b>	Functionalization of Graphene by [2+1] Cycloaddition Reaction at Ambient Conditions A. Faghani, R. Haag and <b>M. Adeli</b>	<b>Prof. Mohsen Adeli</b> , Free University of Berlin - <b>Germany</b> .
<b>16:45-17:00</b>	A facile and scalable way to produce reduced graphene oxide/epoxy nanocomposites <b>G.B. Olowjoba</b> , S. Kopsidas, S.Eslava, E.S. Gutierrez, A.J. Kinloch, C.Mattevi, V.G. Rocha and A.C. Taylor	<b>Dr. Ganiu B. Olowjoba</b> , Imperial College London, London - <b>UK</b>
<b>17:00-17:15</b>	Benzoxazine-functionalized graphene oxide for synthesis of new nanocomposites <b>I. Biru</b> , C. Damian, S. A. Garea and H. Iovu	<b>Mrs. Luliana Biru</b> , University Politehnica of Bucharest - <b>Romania</b>
<b>17:15-17:30</b>	Electrodeposition process of graphene nano-plates on open-cells aluminum foams – a critical review <b>A. Simoncini</b> , V. Tagliaferri and N. Ucciardello	<b>Mr. Alessandro Simoncini</b> , University of Rome "Tor Vergata" - <b>Italy</b>
<b>17:30-17:45</b>	Optimization of In-Situ Polymerization Process of Graphene Nano-Platelet Composites <b>B. Yang</b> , J. Doucette and P. Mertiny	<b>Mr. Bo Yang</b> , University of Alberta - <b>Canada</b>
<b>17:45-18:00</b>	Multilayered Membranes based on Graphene and Natural Polymers for Biomedical Applications <b>M. C. Paiva</b> , E. Cunha, D. Moura, C. Silva, M. F. Proença and N. Alves	<b>Dr. Maria Paiva</b> , University of Minho- <b>Portugal</b>
<b>18:00-18:15</b>	Antimicrobial properties of RGO modified with Polysulfone Brushes and their nanocomposites <b>J.Peña-Bahamonde</b> , H.Nguyen, V.San Miguel, J.C.Cabanelas and D. Rodrigues	<b>Mrs. Janire Pena Bahamonde</b> , University Carlos III Madrid- <b>Spain</b>
<b>18:15-18:30</b>	Room-temperature positive magnetoresistance in functionalized graphene grown by CVD <b>O.V. Kononenko</b> , V. N. Matveev, V.I. Levashov and V.T. Volkov	<b>Dr. Oleg Kononenko</b> , Institute of Microelectronics Technology and High Purity Materials- <b>Russian Federation</b>
<b>18:30-18:45</b>	Defects in irradiated graphene on metallic substrates <b>I. Shchedrina</b> , C. Corbel, N. Ollier, O. Cavani, T. Wade, M. Konczykowski, J-P. Renault, J. Ghilan, H. Randriamahazaka, C.S. Cojocar, I. Florea and B. Geffroy	<b>Dr. Irina Shchedrina</b> , Ecole polytechnique - <b>France</b>
<b>18:45-19:00</b>	High porosity Graphene/Fe <sub>3</sub> O <sub>4</sub> scaffolds for Electromagnetic Interference Shielding <b>M. González</b> , J. Pozuelo and J. Baselga	<b>Mrs. Marta González</b> , University Carlos III of Madrid- <b>Spain</b>
<b>19:00-19:15</b>	Effect of Post-Exfoliation Annealing and Ultrasonic Treatments on Mechanically Exfoliated MoS <sub>2</sub> <b>P. Budania</b> , N. Mitchell and D. McNeill	<b>Ms. Prachi Budania</b> , Queen's University, Belfast – <b>UK</b>

June 2<sup>nd</sup> , 2016

EGF 2016- Plenary session II

Amphitheatre G

Session's Chairs:

**Prof. Giancarlo Faini, Laboratoire de Photonique et de Nanostructures, CNRS – France**  
**Dr. Konstantin Amsharov, University of Erlangen-Nürnberg – Germany/ Prof. Alberto Fina, Polytechnic University of Turin – Italy**

08:30-9:15	2D Materials: technology, standards and science <b>A.H. Castro Neto</b>	<b>Prof. Antonio H. Castro Neto</b> , National University of Singapore - <b>Singapore</b>
09:15-10:00	Graphene-based Platforms for Biosensing Applications <b>A. Merkoçi</b>	<b>Prof. Arben Merkoçi</b> , ICN2/CSIC/The Barcelona Institute of Science and Technology - <b>Spain</b>
10:00-10:30 Coffee Break / Exhibition / Posters Session II		
10:30-11:00	Carbon Based Nano-Materials/Devices <b>K.S. Kim</b>	<b>Prof Kwang S. Kim</b> , Ulsan National Institute of Science and Technology - <b>Korea</b>
11:00-11:30	Reaction kinetics of Stone - Wales rotation in graphene <b>A. Chuvilin</b> , S. T. Skowron, V. O. Koroteev, M. Baldoni, S. Lopatin, A. Zurutuza and E. Bichoutskaia	<b>Prof. Andrey Chuvilin</b> , CIC nanoGUNE – <b>Spain</b>
11:30-12:00	Ultrafast Generation of Plasmon Polaritons in High Mobility Graphene <b>D.N. Basov</b>	<b>Prof. Dmitri Basov</b> , University of California and Columbia University - <b>USA</b>
12:00-12:30	Design and fabrication of Graphene based platforms for Raman sensing L. Álvarez-Fraga, F. Jimenez-Villacorta, E. Climent-Pascual, R. Ramírez-Jiménez, C. Prieto and <b>A. de Andrés</b>	<b>Prof. Alicia de Andrés</b> , Materials Science Institute of Madrid (CSIC) – <b>Spain</b>
12:30-12:45	Imaging and spectroscopy on the 10-nm length scale <b>M. Eisele</b>	<b>Mr. Max Eisele</b> , Neaspec GmbH- <b>Germany</b>

12:45-14:00 Lunch Break / Exhibition / Posters session II

EGF 2016- Session II: Graphene and 2D Materials characterization and properties

**Chairs: Giancarlo Faini, Laboratoire de Photonique et de Nanostructures, CNRS – France/ Dr. Konstantin Amsharov, University of Erlangen-Nürnberg – Germany/ Prof. Alberto Fina, Polytechnic University of Turin – Italy**

14:00-14:40	Graphene nanoplatelets for thermally conductive polymer nano-composites via melt reactive extrusion <b>A. Fina</b> , S. Colonna, O. Monticelli, M. Tortello, R.S. Gonnelli, J. Gomez, M. Pavese, F. Giorgis and G. Saracco	<b>Prof. Alberto Fina</b> , Polytechnic University of Turin - <b>Italy</b>
14:40-15:00	Reduced Graphene Oxide Enhances Horseradish Peroxidase Stability by Serving as Radical Scavenger and Redox Mediator <b>C. Zhang</b> , S. Chen, P.J. J. Alvarez and W. Chen	<b>Prof. Chengdong Zhang</b> , Nankai University- <b>China</b>
15:00-15:30	Ab-initio calculations and simple models of electronic excitations in 2D materials and heterostructures <b>K.S.Thygesen</b>	<b>Prof. Kristian.S. Thygesen</b> , Technical University of Denmark- <b>Denmark</b>
15:30-15:45	Mechanical Property Enhancement of In-Situ Synthesized Three-Dimensional Network Graphene Reinforced Copper Nanocomposites <b>X. Zhang</b> , C.N.He and N.Q. Zhao	<b>Mr. Xiang Zhang</b> , Tianjin University- <b>China</b>
15:45-16:00	Next-Generation of Graphene Composites: Surface-Modified GO with Tunable Flake Orientation <b>M. Wåhlander</b> , F. Nilsson, A. Carlmark, S. Edmondson and E. Malmström	<b>Mr. Martin Wåhlander</b> , KTH Royal Institute of Technology - <b>Sweden</b>

16:00-16:30 Coffee Break / Exhibition / Posters session II		
16:30-16:45	Tunable Magnetism of Adatoms adsorbed on Bilayer Graphene <b>D. Nafday</b> , M. Kabir and T. Saha Dasgupta	<b>Ms. Dhani Nafday</b> , S.N. Bose National Center for Basic Sciences- Kolkata-India
16:45-17:00	Ultrafast optics in graphene <b>K. Liu</b> , J.F. Zhang, Z.H. Zhu, C.C. Guo, X.D. Yuan, W.M. Ye and S.Q. Qin	<b>Prof. Ken Liu</b> , National University of Defense Technology- China
17:00-17:15	Graphynes: from Competitors to Graphene to Atomic Sieves and Scatter <b>F. Viñes</b> , M. Manadé, S. Kim, P. Gamallo, J.Y. Lee and F. Il-Ias	<b>Dr. Francesc Viñes</b> , Barcelona University- Spain
17:15-17:30	Combination of the PDCs Route with the SPS Process to Easily Obtain Large and Pure h-BN Nanosheets Y. Li, S. Yuan, <b>P. Steyer</b> , B. Toury, V. Garnier, A. Brioude and C. Journet	<b>Dr. Philippe Steyer</b> , INSA Lyon- France.
17:30-17:45	Graphene based Electrically Tunable Hybrid Plasmonic-photonic Waveguide with Low-loss and Nano-scale Optical Confinement L.Singh ,Sulabh and <b>M. Kumar</b>	<b>Dr Mukesh Kumar</b> , Indian Institute of Technology-Indore- India
17:45-18:00	Electrochemically exfoliated graphite for solution-processed transparent conductive electrodes. <b>A.Ly</b> , P. Viville and R. Lazzaroni	<b>Mr. Ahmadou Ly</b> , Mons University- Belgium
18:00-18:15	Discontinuous bilayer graphene chemiresistors <b>P. Krauss</b> and J. J. Schneider	<b>Mr Peter Krauss</b> , Technische Universität Darmstadt -Germany
18:15-18:30	Spin noise in graphene detected via cross-correlation <b>S. Omar</b> , I.J. Vera-Marun, M.H.D. Guimarães, A. Kaverzin and B.J. van Wees	<b>Mr. Siddhartha Omar</b> , University of Groningen- The Netherlands
18:30-18:45	Graphene oxide framework membranes: Control the 2D interspacing toward strict molecular sieving <b>G. Zeng</b> , G. Li, B. Qi, X. He, Y. Zhang and Y. Sun	<b>Dr. Gaofeng Zeng</b> , Shanghai Advanced Research Institute, Chinese Academy of Sciences - China
18:45-19:00	Hydrogen-decorated stabilization and thermal conductivity of penta-silicene: A first principles calculation <b>H. K. Liu</b> , Y. Lin and M. Hu	<b>Mr. Huake Liu</b> , RWTH Aachen University- Germany
19:00-19:15	Enhancing the performance of dye-sensitized solar cells by incorporating various ratios of platinum and reduced graphene oxide thin film as a counter electrode <b>N. Ahmad-Ludin</b> , A. Bolhan, M. Y. Sulaiman, M. S. Suait, M. A. Mat-Teridi, M. A. Ibrahim, S. Sepeai, K. Sopian and H. Arakawa	<b>Dr. Norasikin Ahmad Ludin</b> , Kebangsaan University – Malaysia

**June 2<sup>nd</sup>, 2016**

**EGF 2016- Session III: Graphene and 2D Materials properties and applications**

**Conference Room 561**

**Session's Chairs:**

**Dr Cinzia Casiraghi, University of Manchester- UK**

**Prof. Alicia de Andrés, Materials Science Institute of Madrid (CSIC), Spain**

14:00-14:30	Platinum-Gold Alloy Nanoparticles Decorated Crumpled Graphene for Electrocatalyst <b>H.D. Jang</b> , S.K. Kim, J-H. Choi and H.Chang	<b>Prof. Hee Dong Jang</b> , Korea Institute of Geoscience and Mineral Resources - Republic of Korea
14:30-15:00	Graphene Transistor Monitoring Properties of Functional Oxides <b>D.Suh</b>	<b>Prof. Dongseok Suh</b> , Sungkyunkwan University - Republic of Korea

15:00-15:15	Infrared spectroscopy of closely aligned heterostructures of graphene and hexagonal boron nitride <b>D.S.L. Abergel</b> and M. Mucha-Kruczyński	<b>Dr. David Abergel</b> , Nordita, KTH Royal Institute of Technology and Stockholm University- <b>Sweden</b>
15:15-15:30	Anisotropy of Unstrained Pristine Graphene <b>G. Shpenkov</b>	<b>Dr. Georgi Shpenkov</b> , Academy of Computer Science and Management- <b>Poland</b>
15:30-15:45	Temperature dependent fracture of defected graphene sheets: a Molecular Dynamics study <b>S. Nasiri</b> and M. Zaiser	<b>Mrs. Samaneh Nasiri</b> , Friedrich-alexander University- <b>Germany</b>
15:45-16:00	Graphene: A Tunable Kerr Nonlinear Medium <b>B. Semnani</b> , A.H. Majedi and S. Safavi-Naeini	<b>Mr. Behrooz Semnani</b> , University of Waterloo- <b>Canada</b>
<b>16:00-16:30 Coffee Break / Exhibition / Posters session II</b>		
16:30-16:45	Substantial improvement of graphene-enhanced raman scattering through strain engineering of graphene G. Dobrik, P. Nemes-Incze, L.P. Biró and <b>L. Tapasztó</b>	<b>Dr. Levente Tapasztó</b> , Centre For Energy Research Hungarian Academy of Sciences- <b>Hungary</b>
16:45-17:00	Evaluation of Graphene Suspensions <b>T.J. Nacken</b> , C. E. Halbig, C. Damm, J. Walter, S. Eigler and W. Peukert	<b>Mr. Thomas Nacken</b> , University Erlangen-Nürnberg - <b>Germany</b> .
17:00-17:15	Pt nanoparticles supported on rGO/SiC hybrid material as a cathode catalyst in DMFC <b>B. Ozdincer</b> , K. K. Maniam and S. M. Holmes	<b>Mr. Baki Ozdincer</b> , The University of Manchester – <b>UK</b>
17:15-17:30	Graphene based coatings against corrosion <b>K.S. Aneja</b> , S. Bohm, A.S. Khanna and M. Thompson	<b>Mr. Karanveer. S. Aneja</b> , Indian Institute of Technology Bombay - <b>India</b>
17:30-17:45	Impact of reduction degree of graphene oxide on the photocatalytic activity of graphene oxide/TiO <sub>2</sub> nanotubes <b>M. Hamandi</b> , G. Berhault, C. Guillard and H. Kochkar	<b>Mrs. Marwa Hamandi</b> , Claude Bernard University Lyon – <b>France</b>
17:45-18:00	Fabrication of Graphene oxides (GO) based rGO-TiO <sub>2</sub> /Fe <sub>3</sub> O <sub>4</sub> nanocomposites for the removal of Methylene Blue and Arsenic(III) from Wastewater <b>P. Benjwal</b> , M. Kumar, P. Chamoli and K.K. Kar	<b>Ms. Poonam Benjwal</b> , Indian Institute of Technology Kanpur- <b>India</b>
18:00-18:15	Graphene nanoplatelets biocompatibility is improved by surface adsorption of polymers A. Pinto, A. Moreira, F. Magalhães and <b>I. Gonçalves</b>	<b>Dr. Inês C. Gonçalves</b> , University of Porto- <b>Portugal</b>
18:15-18:30	Functionalization of graphene field-effect transistor channel for ischemic stroke biomarker detection <b>P. D. Cabral</b> , E. Fernandes, F. Cerqueira, G. Machado Jr., J. Borme and P. Alpuim	<b>Ms. Patricia Cabral da Silva</b> , International Iberian Nanotechnology Laboratory- <b>Portugal</b>
18:30-18:45	A Novel SPR biosensor chip with Graphene Oxide Linking Layer <b>Yu.V. Stebunov</b> , O.A. Aftenieva, A.V. Arsenin and V.S. Volkov	<b>Mr. Yury Stebunov</b> , Moscow Institute of Physics and Technology- <b>Russian Federation</b>
18:45-19:00	Heartbeat resistive sensor based on graphene nanobelt thin films A. Alaferdov, R. Savu, S. Rackauskas, T. Rackauskas, E. Joanni and <b>S A. Moshkalev</b>	<b>Dr. Stanislav Moshkalev</b> , UNICAMP, Center for Semiconductor Components- <b>Brazil</b>
19:00-19:15	The potential of graphene based active components in silicon photonic systems <b>D. Schall</b> , and D. Neumaier	<b>Mr. Daniel Schall</b> , AMO GmbH-Aachen- <b>Germany</b>
19:15-19:30	Few-Layer Graphene Langmuir Nanofilm Decorated by Palladium Nanoparticles for NO <sub>2</sub> and H <sub>2</sub> Gas Sensing <b>D. Kostiuik</b> , S. Luby, M. Demydenko, Y. Halahovets, P. Siffalovic, K. Vegso, J. Ivanco, M. Jergel, M. Kotlar, R. Redhammer and E. Majkova*	<b>Dr. Dmytro Kostiuik</b> , Slovak Academy of Sciences- <b>Slovakia</b>



**June 3<sup>rd</sup>, 2016**  
**EGF 2016- Session IV: Graphene and 2D Materials applications**

**Conference Room 511**

**Session's Chairs:**  
**Prof Valerio Pruneri, ICFO-The Institute of Photonic Sciences and ICREA- Spain**  
**Prof. Thomas Mueller, Institute of Photonics, Vienna University of Technology – Austria**

<b>08:30-09:00</b>	Radionuclide Therapy with Neutron-Activated Graphene Oxide Nanoplatelets <b>J Kim and M. Jay</b>	<b>Prof. Michael Jay</b> , University of North Carolina- <b>USA</b>
<b>09:00-09:30</b>	Thixotropic Properties of Graphene Oxide/Hydrogel for 3D Bioprinting H. Li and <b>L. Li</b>	<b>Prof. Lin Li</b> , Nanyang Technological University- <b>Singapore</b>
<b>09:30-10:00</b>	Graphene for transparent electrodes and sensing applications <b>V.Pruneri</b>	<b>Prof. Valerio Pruneri</b> , ICFO- The Institute of Photonic Sciences and ICREA- <b>Spain</b>
<b>10:00-10:30 Coffee Break / Exhibition</b>		
<b>10:30-11:00</b>	Ballistic transport regimes in hBN-encapsulated graphene devices <b>J.Wallbank</b> and V. Falko	<b>Dr. John Wallbank</b> , National Graphene Institute, University of Manchester - <b>UK</b>
<b>11:00-11:30</b>	Optoelectronics with atomically thin materials <b>T.Mueller</b>	<b>Prof. Thomas Mueller</b> , Institute of Photonics, Vienna University of Technology - <b>Austria</b>
<b>11:30-12:00</b>	Nonlinear Electrodynamics and Optics of Graphene <b>S.A. Mikhailov</b>	<b>Dr. Sergey Mikhailov</b> , University of Augsburg - <b>Germany</b>
<b>12:00-12:30</b>	Graphene membranes and their use as pressure sensors <b>H.S.J. van der Zant</b>	<b>Prof. Herre S.J. van der Zant</b> , Delft University of Technology - <b>The Netherlands</b>
<b>12:30-13:00</b>	Functionalized graphene for flexible light-emitting devices E;T;Alonso, G;Karkera, G;F. Jones, S;Russo, <b>M.F. Craciun</b>	<b>Prof. Monica F. Craciun</b> , University of Exeter - <b>UK</b>

**Posters Session II: June 2<sup>nd</sup>, 2016**  
**European Graphene Forum - EGF 2016**

**Exhibition and Poster Hall**

<b>N.</b>	<b>Title</b>	<b>Author/Affiliation/Country</b>
<b>1</b>	Formation of Continuous Few-layer MoS <sub>2</sub> Nanosheet Film for Sensing and Detection Applications <b>M.Demydenko</b> , M.Jergel, D.Kostiuk, Y.Halahovets, M.Kotlar, P.Siffalovic, K.Vegso and E.Majkova	<b>Dr. Maksym Demydenko</b> , Slovak Academy of Sciences - <b>Slovakia</b>
<b>2</b>	Grain Boundary Structures and Electronic Properties of Hexagonal Boron Nitride on Cu (111) <b>Q. Li</b> , Y. Zhang and <b>Z. Liu</b>	<b>Ms. Qiucheng Li</b> , Peking University, Beijing - <b>Republic of China</b>
<b>3</b>	Large-scale Synthesis of Defects-selective Graphene Quantum Dots for Cell Imaging by Ultrasonic-assisted Liquid-Phase Exfoliation <b>L. Lu</b> and Y.T. Pei	<b>Mr. Liqiang Lu</b> , University of Groningen - <b>Netherlands</b>
<b>4</b>	CVD growth of large single crystal graphene <b>L. Lin</b> , H. Ren, J. Li, N. Kang, H. Q. Xu, H. Peng and Z. Liu	<b>Mr. Li Lin</b> , Peking University- <b>China.</b>
<b>5</b>	Fabrication and Characterization of Near Infrared Detectors based on MoS <sub>2</sub> Few-layers Grown with Chemical Vapor Deposition X. Wang, L.L. Shiau and <b>B.K. Tay</b>	<b>Prof. Beng Kang Tay</b> , Nanyang Technological University- <b>Singapore</b>

6	Silver/nitrogen-doped reduced graphene oxide as an electrocatalyst for oxygen reduction in alkaline medium L.T. Soo, <b>K.S. Loh</b> , A.B. Mohamad, W.R.W. Daud and W.Y. Wong	<b>Dr. Kee Shyuan Loh</b> , Kebangsaan Malaysia University- <b>Malaysia</b>
7	Adsorption Abilities of TiO <sub>2</sub> -R-OH-rGO Nanocomposites <b>E. Kusiak-Nejman</b> , A. Wanag, J. Kapica-Kozar, Ł. Kowalczyk, A.W. Morawski, L. Lipińska and M. Aksienionek	<b>Dr. Ewelina Kusiak-Nejman</b> , West Pomeranian University of Technology- <b>Poland</b>
8	Preparation and Tribological Performance of Nickel-Graphene Oxide Composite Coatings <b>S. Qi</b> , X. Li and H. Dong	<b>Mr Shaojun Qi</b> , University of Birmingham- <b>United Kingdom</b>
9	One - pot preparation of SERS nanocomposites of silver and graphene oxide with tunable properties <b>M.O. Volodina</b> , A.V. Sidorov, E.A. Eremina and E.A. Goodilin	<b>Mrs. Mariia Volodina</b> , Lomonosov Moscow State University- <b>Russian Federation</b>
10	Reduced graphene oxide on/in metallic substrates: coating and composite M.A.Rodríguez-Escudero, A.Argumanez, I. Llorente, O. Caballero-Calero, M.S. MartínGonza-lez, R. Fernandez and <b>M.C.García-Alonso</b>	<b>Mrs. M Cristina Garcia-Alonso</b> , The Spanish National Research Council (CSIC)- <b>Spain</b>
11	High orientation degree of graphene nanoplatelets in spark plasma sintered silicon nitride composites <b>O. Tapasztó</b> , L. Tapasztó, V. Puchy, J. Dusza, C. Balázs and K. Balázs	<b>Dr. Orsolya Tapasztó</b> , Center for Energy Research, Institute of Technical Physics and Materials Sciences- <b>Hungary</b>
12	Observation of Alkali Metal Adsorption on Freestanding Graphene by Means of LEEPS Microscopy <b>M. Lorenzo</b> , J. Vergés, C. Escher, J.-N.Longchamp and H.-W. Fink	<b>Ms. Marianna Lorenzo</b> , University of Zurich- <b>Switzerland</b>
13	3D nanodendrites consisting of Pd and N-doped carbon nanoparticles as bifunctional catalyst <b>H. K. Sadhanala</b> , R. Nandan, and K. K. Nanda	<b>Mr. Hari Krishna Sadhanala</b> , Indian Institute of Science- Bangalore- <b>India</b> .
14	Graphene growth and transfer towards flexible substrates for microwave applications <b>J. Njeim</b> , A. Madouri, A. Cavanna, P. Chrétien, A. Jaffré, Z. Ren and D. Brunel	<b>Ms. Joanna Njeim</b> , Pierre et Marie Curie University- <b>France</b>
15	Multi-layered graphene interface for enhancing the stretchability of brittle conductive layers S. Won, <b>Y. Hwangbo</b> , K-S. Kim, H-J. Lee and J-H. Kim	<b>Dr. Yun Hwangbo</b> , Korea Institute of Machinery & Materials (KIMM)- <b>Republic of Korea</b>
16	Experimental study of the electrical properties of multilayer graphene-fullerene C60-multilayer graphene junctions <b>E. Benítez</b> and D. Mendoza.	<b>Mr. Erick Benitez</b> , National Autonomous University of Mexico - <b>Mexico</b> .
17	Spin transport in fully hexagonal boron nitride encapsulated graphene <b>M. Gurram</b> , S. Omar, S. Zihlmann, P. Makk, C. Schönenberger and B.J. van Wees	<b>Mr. Mallikarjuna Gurram</b> , University of Groningen- <b>The Netherlands</b>
18	Ultra-Broadband Strong Absorption Enhancement in Graphene with Plasmonic Light Trapping <b>F. Xiong</b> and J. Zhang	<b>Mr. Xiong Feng</b> , National University of Defense Technology- <b>China</b>
19	Novel Aerosol Synthesis of Pt Nanoparticles-Laden Graphene via Microwave Plasma Spray Pyrolysis and Their Enhanced Methanol Oxidation Reaction <b>H. Chang</b> , E.H. Jo, S.K. Kim and H.D. Jang	<b>Dr. Hankwon Chang</b> , Korea Institute of Geoscience & Mineral Resources- <b>Republic of Korea</b>
20	Diverse anisotropy of phonon transport in two-dimensional group IV-VI compounds: A comparative study <b>G. Qin</b> and M. Hu	<b>Mr. Guangzhao Qin</b> , RWTH Aachen University- <b>Germany</b>
21	Effect of modified Graphene and Montmorillonites and their mixtures on the properties of biodegradable PLA/PCL blend <b>A. Habi</b> , B.S.Bouakaz, Y. Grohens and I. Pillin	<b>Dr. Abderrahmane Habi</b> , A. Mira de Béjaia University - <b>Algeria</b> .
22	Magneto-optical characterization of super-lattices in graphene <b>T. Wolf</b> , I. P. Levkivskyi, O. Zilberberg and G. Blatter	<b>Mr. Tobias Wolf</b> , ETH Zurich- <b>Switzerland</b>
23	Conference topic: applications of graphene in biomedical area Graphene Oxide Based Sensing of Small Molecules <b>O.A. Aftenieva</b> , Yu.V. Stebunov and A.V. Arsenin	<b>Ms. Olha Aftenieva</b> , Moscow Institute of Physics and Technology- <b>Russian Federation</b>
24	Development of Graphene-based Barriers for Solar Cells <b>G. Rossi</b> , M.Sarno, C.Cirillo and L. Incarnato	<b>Dr. Gabriella Rossi</b> , University of Salerno - <b>Italy</b>

**Posters Session I: June 1<sup>st</sup>, 2016**

**Nanotech France 2016:  
NanoMaterials synthesis,  
characterization/  
Nanometrology and properties**

# Organic solvent resistant polyelectrolyte multilayers : effect of the sulfonic to carboxylic content

P. Argkarawanitnan,<sup>1,2,\*</sup> S. T. Dubas,<sup>1,2</sup>

<sup>1</sup>Petroleum and Petrochemical college, Chulalongkorn University

<sup>2</sup>Center of Excellence on Petrochemical and Materials Technology

## Abstract:

The utilization of non-polar solvent in microfluidic devices have been limited by the swelling of PDMS chips. Our group has recently reported the layer-by-layer deposition of polyelectrolyte multilayers that could protect PDMS against chloroform vapor for several hours without swelling. In this work, we used a copolymer of polystyrene sulfonic acid and poly maleic acid with various ratio of sulfonic to acrylic. While Poly (diallyl dimethyl ammonium chloride) PDADMAC was used as poly cation, 4 different polyelectrolytes were used as poly anion. Pure PSS (100% sulfonic) Poly(4-styrenesulfonic acid-co-maleic acid) ratio 3:1 (75% sulfonic 25% carboxylic) and 1:1 (50% sulfonic 50% carboxylic) and pure Poly(acrylic acid) (100% carboxylic) were used as a polyanionic. The effect of the number of layer and the carboxylic/sulfonic ratio on the solvent resistance of the substrate. UV-Vis spectrophotometer was used to monitor the opacity/transparency of the substrate after exposed to acetone. Results show that the higher carboxylic content provide the best solvent resistance. These result could simplify the utilisation of organic solvent in microfluidic applications.

**Keywords:** Solvent resistance, Polyelectrolyte multilayers, layer-by-layer

## References:

Decher, G. (1997), Fuzzy nanoassemblies: Toward layered polymeric multicomposites, *Science*, 27, 1232-1237.

Rajendrani M. (2007), When PDMS isn't the best, *Anal. Chem. Soc.*, 3248-3253.

Panittamat K., Adisorn T., Stephan T. D., Luxsana D. (2011), Polyelectrolyte multilayers coating for organic solvent resistant microfluidics chip, *Mat. Lett.*, 65, 3629-3623.

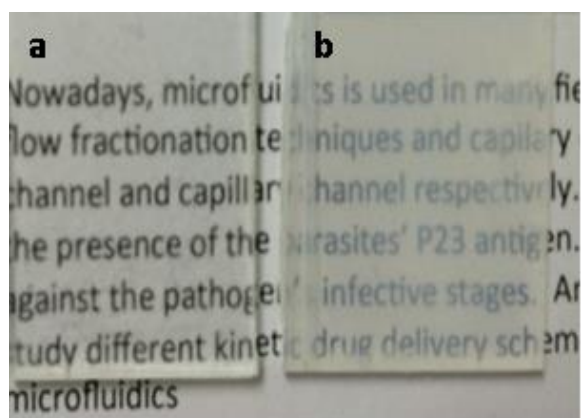


**Figure 1:** Figure illustrating the digital photograph of PMMA substrate in acetone for 5 min (a) PDADMAC/PAA, (b) Reference

# Solvothermal hot injection synthesis of AgNi nanoalloy

Vit Vykoukal<sup>1</sup>, Jiri Bursik<sup>2</sup>, Pavla Roupcova<sup>2</sup>, Jiri Pinkas<sup>1\*</sup>

<sup>1</sup> Masaryk University, Faculty of Science, Department of Chemistry, Kotlarska 2, 611 37 Brno, Czech Republic

<sup>2</sup> Institute of Physics of Materials, ASCR, Zizkova 22, 616 62 Brno, Czech Republic [jpinkas@chemi.muni.cz](mailto:jpinkas@chemi.muni.cz)

## Abstract:

Nanomaterials and especially their preparation by chemical approach is a very active field of materials research. The synthesis of nanoalloys is one integral part of nanoscience and development of efficient methods is a challenging task due to their chemical, phase, and morphological variability. In case of metal nanoalloys we can observe many interesting properties such as depression of melting point,<sup>1,2</sup> plasmon resonance,<sup>3,4</sup> catalytic activity,<sup>5</sup> and phase separation.<sup>6</sup> Nanoalloys can be prepared by many approaches, but highly advantageous is the solvothermal synthesis, specifically in oleylamine.<sup>5,7</sup> The hot injection technique appears to be the best for ensuring homogeneous conditions for nanoparticles nucleation and growth.

AgNi nanoparticles were prepared by injection of an oleylamine solution (4 cm<sup>3</sup>) of AgNO<sub>3</sub> and Ni(acac)<sub>2</sub> (different molar ratios, 4 mmol total amount) to a mixture of oleylamine (16 cm<sup>3</sup>) and octadecene (20 cm<sup>3</sup>) at 230 °C. After 10 minutes, the reaction mixture was cooled down to room temperature in a water bath. Then 20 cm<sup>3</sup> of acetone was added to precipitate nanoparticles and the suspension was centrifuged. The precipitate was washed by a mixture of hexane and acetone (1:3 volume ratio). This procedure was repeated twice and finally the precipitate was dispersed in hexane and characterized.

Dynamic Light Scattering (DLS), Transmission Electron Microscopy (TEM), Elemental analyses (ICP OES), and Small-Angle X-ray Scattering (SAXS) analyses were performed for determination of chemical composition, average size, size distribution, and shape of the prepared nanoparticles. Plasmon resonances were observed and we found that the intensity of plasmon resonance was dependent on the molar ratio of AgNi in the particles. HT-XRD was carried out and we observed a phase separation in the prepared nanoalloy. Magnetic properties and their dependence on temperature were also characterized and the results are in a good agreement with the HT-XRD characterization.

## Acknowledgements

This research has been financially supported by the Ministry of Education, Youth and Sports of the Czech Republic under the project CEITEC 2020 (LQ1601). Authors thank the X-ray Diffraction and Bio-SAXS Core Facility of CEITEC.

**Keywords:** nanomaterials, nanoalloy, silver, nickel, DLS, SAXS

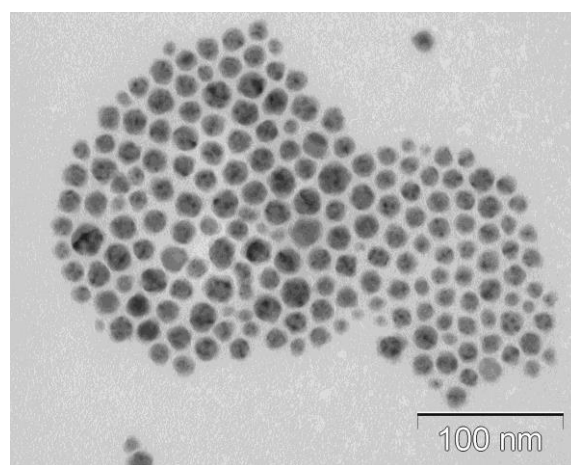


**Figure 1:** TEM image of AgNi nanoalloy

## References:

1. Zou, C.; Gao, Y.; Yang, B.; Zhai, Q. *J. Mater. Sci.: Materials in Electronics* **2009**, *21* (9), 868–874.
2. Jiang, H.; Moon, K.; Hua, F.; Wong, C. P. *Chem. Mater.* **2007**, *19* (18), 4482–4485.
3. Link, S.; El-Sayed, M. A. *Annu. Rev. Phys. Chem.* **2003**, *54*, 331–366.
4. Gonzalez, C. M.; Liu, Y.; Scaiano, J. C. *J. Phys. Chem. C* **2009**, *113* (27), 11861–11867.
5. Zhang, Y.; Huang, W.; Habas, S. E.; Kuhn, J. N.; Grass, M. E.; Yamada, Y.; Yang, P.; Somorjai, G. A. *J. Phys. Chem. C* **2008**, *112* (32), 12092–12095.
6. Sopousek, J.; Zobac, O.; Bursik, J.; Roupcova, P.; Vykoukal, V.; Brož, P.; Pinkas, J.; Vrestal, J. *J. Phys. Chem. Chem. Phys.* **2015**.
7. Sopousek, J.; Pinkas, J.; Broz, P.; Bursik, J.; Vykoukal, V.; Skoda, D.; Styskalík, A.; Zobac, O.; Vrestal, J.; Hrdlicka, A.; Simbera, J. *J. Nanomaterials* **2014**, *2014*, 1–13.



# Layer-by-Layer Deposition of Photocatalysts on PU foam

C. Wechwithayakhlung, S. Dubas,

Chulalongkorn University, Petroleum and Petrochemical College, Bangkok, Thailand

## Abstract:

Photocatalytic reactions of semiconductor such as  $\text{TiO}_2$  and  $\text{ZnO}$  have been intensely studied mainly for cleaning organic compound in waste water and in air. Zinc oxide is a promising material in environmental application due to its high catalytic efficiency and it has also been proposed for water splitting applications as it can be activated in ambient light. Recently metallic nanoparticles have been found to enhance the photocatalytic activity of  $\text{ZnO}$ . In this work we investigated the effect of the layer by layer co-deposition of  $\text{ZnO}$  catalyst with silver nanoparticles. The  $\text{ZnO}$  and  $\text{Ag}$  nanoparticles were synthesized in a single batch using an acrylated polyelectrolyte as single ligand. The particle were then successfully deposited on polyurethane (PU) foam by layer-by-layer (LbL) self-assembly technique using a Poly(diallyldimethylammonium chloride) (PDADMAC) and a poly(4-styrene sulfonate) (PSS) as primer layer. The anionic silver and  $\text{ZnO}$  were deposited in alternance with PDADMAC to form a catalytic layer on the PU foam. Evidence of the LbL growth of  $\text{ZnO}/\text{Ag}$  films was provided by UV-visible spectroscopy. The photocatalytic activities of the films were investigated over the degradation of methyl violet dye under UV-Vis irradiation. The presence of silver nanoparticles was found to enhance the dye degradation rate when compare with  $\text{ZnO}$  alone. This work provides a simple method for the incorporation of both silver and  $\text{ZnO}$  on porous PU foam for enhances activity and recovery.

**Keywords:** layer-by-layer technique, polyelectrolyte multilayers, zinc oxide, photocatalytic applications.

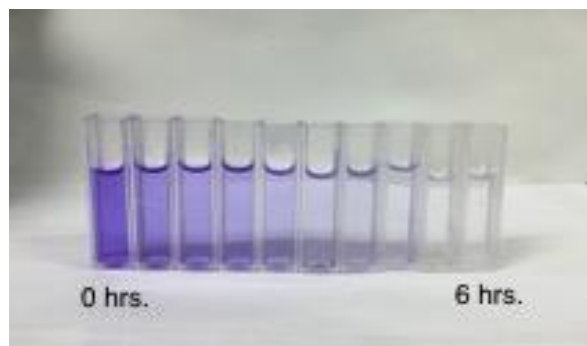


**Figure 1:** Figure illustrating the photocatalytic degradation of 5 ppm methyl violet dye under 6 hours of UV-Vis irradiation using  $\text{Ag}/\text{ZnO}$  bilayers immobilized on PU foam by LbL self-assembly technique.

## References:

1. Kotov, N. A., Dekany, I., Fendler, J. H. (1995). Layer-by-layer self-assembly of polyelectrolyte-semiconductor nanoparticle composite films. *The Journal of Physical Chemistry*, 99(35), 13065-13069.
2. Priya, D. N., Modak, J. M., & Raichur, A. M. (2009). LbL fabricated poly (styrene sulfonate)/ $\text{TiO}_2$  multilayer thin films for environmental applications. *ACS applied materials & interfaces*, 1(11), 2684-2693.
3. Zhai, H., Wang, L., Sun, D., Han, D., Qi, B., Li, X., ... Yang, J. (2015). Direct sunlight responsive  $\text{Ag}-\text{ZnO}$  heterostructure photocatalyst: Enhanced degradation of rhodamine B. *Journal of Physics and Chemistry of Solids*, 78, 35-40.

# Thickness dependent optical properties of the large area synthesized few layers MoSe<sub>2</sub> on SiO<sub>2</sub> and Al<sub>2</sub>O<sub>3</sub> substrates by Molecular Beam Epitaxy

Y. H. Choi<sup>1</sup>, D. H. Lim<sup>1</sup>, J. H. Jung<sup>1</sup>, K. -H. Yoo<sup>1</sup>, B. -Y. Yoo<sup>2</sup>, M. -H. Cho<sup>1\*</sup>

<sup>1</sup> Institute of Physics and Applied Physics, Yonsei University, Seoul, 120-749, Republic of Korea

<sup>2</sup> Department of Materials Engineering, Hanyang University, Gyeonggi-do 426-791, Rep. of Korea

\*Corresponding Author's E-mail: mh.cho@yonsei.ac.kr

## Abstract:

Transition metal dichalcogenides (TMDCs) has been explored as promising optoelectronic device because they are direct band gap and sub nanometer thickness. We studied molecular beam epitaxy (MBE) method for large area MoSe<sub>2</sub> facilitating a direct exfoliation-less device fabrication. We evaporated Mo element by e-beam and Se element by Knudsen cell. We investigated the chemical composition of the few layers film by high resolution X-ray photoelectron spectroscopy (HRXPS) and confirmed the optical band gap by photoluminescence (PL). To confirm the film thickness, we performed atomic force microscopy (AFM) and Raman spectroscopy. In addition, PL and Raman mapping were examined to show the uniform large area MoSe<sub>2</sub> film. With spectroscopic ellipsometry measurement (SE), we studied MoSe<sub>2</sub> optical properties, refractive index, extinction coefficient, and dielectric. Temperature dependent PL emission from the as-grown MoSe<sub>2</sub> thin film showed trion, exciton and optical bandgap change. In order to investigate the quality of the film, we studied high resolution transmission electron microscopy (HRTEM) with top view and vertical view. Finally, we have synthesized MoSe<sub>2</sub> on Al<sub>2</sub>O<sub>3</sub> with the same method, resulting in successful epitaxial growth for large area MoSe<sub>2</sub>.

**Keywords:** MoSe<sub>2</sub>, Molecular beam epitaxy, Photoluminescence, Raman spectroscopy, High resolution transmission electron microscopy, Spectroscopy Ellipsometry

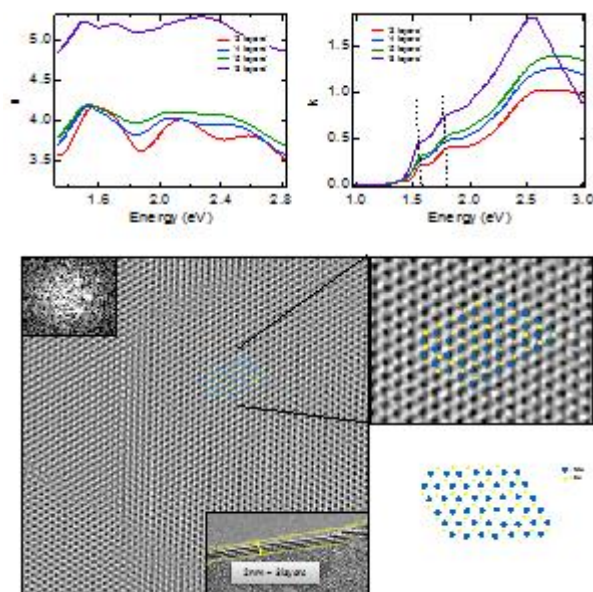


**Figure 1:** Figure shows thickness dependent optical properties, refractive index and extinction coefficient. And high resolution transmission electron microscopy with top view shows high quality MoSe<sub>2</sub>

## References:

Xin Lu, M. Iqbal Bakti Utama, Junhao Lin, Xue Gong, Jun Zhang, Yanyuan Zhao, Sokrates T. Pantelides, Jingxian Wang, Zhili Dong, Zheng Liu, Wu Zhou, and Qihua Xiong, (2014), Large-Area Synthesis of Monolayer and Few-Layer MoSe<sub>2</sub> Films on SiO<sub>2</sub> Substrates, Nano Lett. 14, 2419–2425

# Influence of superficial morphology in the growth of zinc oxide nanowires

Arana J A<sup>1\*</sup>, Monroy B M<sup>1</sup>, Santana G<sup>1</sup>

<sup>1</sup>Instituto de Investigaciones en Materiales, Universidad Nacional Autónoma de México, Ciudad universitaria, Coyoacán 04510, México D. F., México

## Abstract

For many opto–electronic applications the use of transparent electrodes. They consist of Ta transparent conducting oxide (TCO) [1]. These materials can be considered as the conjunction of different materials properties into just one, in this case, conductivity strongly coupled to transmittance [2]. The challenge is to obtain materials that are transparent but at the same time electrically conductors. TCOs are usually polycrystalline or amorphous materials. They show a resistivity of  $10^{-3}\Omega\text{cm}$  or smaller and an average transmittance up to 80% in the visible range [1].

Aluminum-doped zinc oxide thin films (*ZnO:Al*, AZO), have been investigated due to their high transmittance, possibility to obtain low resistivity, large stability under hydrogen plasma treatment [3], abundance and low cost [4].

AZO films have a large number of applications, mainly in opto – electronic field, where it is used in LEDs, transparent transistors, photovoltaic cells and memory devices [5].

Currently, nanostructures of ZnO are under investigation, one of these nanostructures are ZnO nanowires (NWs). They are considered as channel structures of low absorption, emission, also as electrons, holes and photons transporters [6]. This feature is quite suitable for both optics and electronics applications.

This work focuses on the study of superficial morphology influence in *ZnO* NWs growth. From an AZO TCO layer (also known as “seed layer”), *ZnO* NWs were grown using VLS technique (vapor – liquid – solid) via a catalyst, gold (*Au*) in this case. According to the main goal, seed layers were grown by different techniques, spray pyrolysis and sputtering, to compare their properties and influence on the ZnO NWs growth.

## References

1. Minami T “Transparent conducting oxide for semiconductors for transparent electrodes” *Semicond. Sci. Technol.* 20 S35 – S44, 2005.
2. Exarhos G J and Zhou X – D “Discovery – based design of transparent conducting oxide films” *Thin Solid Films* 515 7025 – 7052, 2007.
3. Chang J F and Hon M H “The effect of deposition temperature on the properties of Al – doped zinc oxide thin films” *Thin Solid Films* 386 79 – 86, 2001.
4. Jiang X, Wong F L, Fung M K and Lee S T “Aluminium – doped zinc oxide films as transparent conductive electrode for organic light – emitting devices” *Appl. Phys. Lett.* 83 9, 2003.
5. Moezzi A, McDonagh A M and Cortie M B “Zinc oxide particles: Synthesis, properties and applications” *Chemical Engineering Journal* 185 – 186 1 – 22, 2012.
6. Cui J “Zinc oxide nanowires” *Materials Characterization* 64 43 – 52, 2012.

# Plasma functionalized POSS / PDMS nano-composite membranes for solvent separation by pervaporation

Xiao. Chen<sup>1\*</sup>, Zhiqiang. Chen<sup>1</sup>, Riccardo. d'Agostino<sup>2</sup>, Ludovic. F. Dumée<sup>1</sup>, Xiujuan. J. Dai<sup>1</sup> and Kevin. Magniez<sup>1</sup>

<sup>1</sup>Institute for Frontier Materials, Deakin University., Waurn Ponds 3216, VIC, Australia

<sup>2</sup>Institute of Nanotechnology, CNR, Department of Chemistry, University of Bari, via E. Orabona 4, 70121 Bari, Italy

## Abstract:

Polyhedral oligomeric silsesquioxanes (POSS) are a class of silicon based nano-caged materials which acts as highly crystalline, 3 – dimensional building blocks with potential for the design of advanced functional separation materials [1]. The incorporation of POSS into nano-composite membranes provide enhanced thermal and mechanical properties, as well as a controlled degree of the free volume distribution at the polymer matrix / particle interface [2]. The presence of the smartly functionalized POSS, exhibiting specific corner functional groups, may also alter the degree of cross-linking of the polymer matrix by covalently bonding the POSS with the polymer, this offering a stable and dense material desirable for pervaporation application [2]. However, a major challenge faced to the incorporation of nano-materials in general across nano-composites relates to kinetic agglomerations and cluster formation and thus to inhomogeneous distribution of the particles across the matrix. This may be due to the large aspect ratio and strong repulsive interactions between the nano-materials and the polymer chains [2]. In this work, a novel plasma gas functionalisation technique was developed on POSS nano-materials to allow for the design of POSS exhibiting controlled densities of functional groups [3, 4]. This technique is more environmentally friendly and offers a higher yield than conventional liquid based functionalization routes. Here, controllable amounts of primary amine groups were introduced onto the corner sites of octa-methyl POSS through a combined continuous wave (CW) and pulsed (P) plasma treatment. The functionalized POSS were then incorporated in a poly(methylsiloxane) (PDMS) matrix by physical blending prior to curing. A range of curing and preparation conditions, including temperature, POSS loading and cast film thicknesses were trialed to evaluate the impact of individual parameters on the final membrane properties. The presence of the functionalized POSS is found to increase the perme-

ation rates of ethanol upon ethanol/water separation tests in a pervaporation mode and to lead to enhanced selectivity when compared to the bare PDMS membrane materials. The factors which influence the performance of the nano-composite membranes will be discussed along with a focus on the interaction between the POSS nano-particle and polymer matrix. This study opens up routes to the design of high flux and high selectivity membrane for solvent separation.

**Keywords:** POSS corner functionalization, nano-composite membrane, pervaporation, solvent separation

## References:

- [1] Cordes, D.B., P.D. Lickiss, and F. Rataboul. (2010), Recent Developments in the Chemistry of Cubic Polyhedral Oligosilsesquioxanes. *Chemical Reviews.*, 110(4), 2081-2173.
- [2] Konietzny, R., et al. (2014), POSS-hybrid membranes for the removal of sulfur aromatics by pervaporation. *Separation and Purification Technology.*, 123, 172-183.
- [3] Chen, Z., et al. (2012), Practical Amine Functionalization of Multi-Walled Carbon Nanotubes for Effective Interfacial Bonding. *Plasma Processes and Polymers.*, 9(7), 733-741.
- [4] Chen, X., Chen, Z., Dumée, L. F., Dai, X. J., Magniez, K. (2015), Functionalisation of octa-methyl polyhedral oligomeric silsesquioxane (POSS) by sequential continuous wave and pulsed plasma mode treatments, in *22nd International Symposium on Plasma Chemistry.*, Antwerp, Belgium, P-II-7-4.

# New molecular precursors for AgCu nanoalloy preparation

Vit Vykoukal<sup>1</sup>, Jiri Bursik<sup>2</sup>, Pavla Roupčová<sup>2</sup>, Vitezslav Halasta, Jiri Pinkas<sup>1\*</sup>

<sup>1</sup> Masaryk University, Faculty of Science, Department of Chemistry, Kotlarska 2, 611 37 Brno, Czech Republic

<sup>2</sup> Institute of Physics of Materials, ASCR, Zizkova 22, 616 62 Brno, Czech Republic  
[jpinkas@chemi.muni.cz](mailto:jpinkas@chemi.muni.cz)

## Abstract:

Nanoparticles preparation by bottom-up methods depends strongly on using molecular precursors and the type and nature of precursors have a decisive effect of their formation and properties. They can greatly affect their resulting size, size distribution, shape<sup>1</sup> and optical properties.<sup>2</sup> In case of Cu, Ag, and Cu/Ag nanoparticles we can observe plasmon resonances and their close connection with the size, shape and distribution of sizes.

We synthesized several new copper precursors by reduction of Cu(II) salts of carboxylic acids by triphenylphosphine.<sup>3</sup> This approach was also used for the CuAg nanoalloy from a single source precursor. The molecular structures of new precursors were completely characterized by single crystal X-ray diffraction analyses. We examined also chemical, spectroscopic, and thermal properties of prepared precursors.

CuAg alloy nanoparticles were prepared by solvothermal hot-injection technique<sup>4,5</sup> from the new precursors based on Cu(I) complexes. Variations in resulting properties of prepared nanoalloys, specially optical properties, were observed for different copper precursors.

**Acknowledgements.** This research has been financially supported by the Ministry of Education, Youth and Sports of the Czech Republic under the project CEITEC 2020 (LQ1601).

Authors thank the X-ray Diffraction and Bio-SAXS Core Facility of CEITEC.

**Keywords:** new precursors based on Cu(I), XRD, nanoalloy, copper, silver

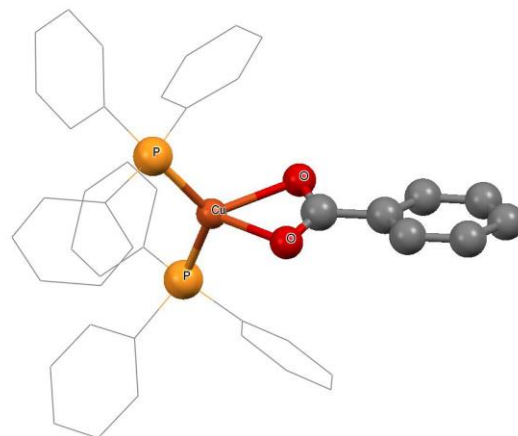


**Figure 1:** Molecular structure of bis(triphenylphosphine)copper(I) benzoate

## References:

1. Xia, Y.; Xiong, Y.; Lim, B.; Skrabalak, S. E. *Angew. Chem. Int. Ed.* **2009**, *48* (1), 60–103.
2. Link, S.; El-Sayed, M. A. *Annu. Rev. Phys. Chem.* **2003**, *54*, 331–366.
3. Adner, D.; Mockel, S.; Korb, M.; Buschbeck, R.; Rüffer, T.; Schulze, S.; Mertens, L.; Hietschold, M.; Mehring, M.; Lang, H. *Dalton Trans.* **2013**, *42* (44), 15599.
4. Zhang, Y.; Huang, W.; Habas, S. E.; Kuhn, J. N.; Grass, M. E.; Yamada, Y.; Yang, P.; Somorjai, G. A. *J. Phys. Chem. C* **2008**, *112* (32), 12092–12095.
5. Sopousek, J.; Pinkas, J.; Broz, P.; Bursik, J.; Vykoukal, V.; Skoda, D.; Styskalík, A.; Zobac, O.; Vrestal, J.; Hrdlicka, A.; Simbera, J. *J. Nanomaterials* **2014**, *2014*, 1–13.



# Influence of nano-particles on the surface morphology and properties of fouling release coatings based on polydimethylsiloxane

Zhanping ZHANG<sup>a</sup>, Hongfei ZHOU, Yuhong QI

Department of Materials Science & Engineering, Dalian Maritime Univ., Dalian 116026, China

## Abstract:

Silicone fouling release coatings for ships are not only safe and non-toxic for marine environment, but also have excellent property of fouling-release, drag-reduction and energy-saving. However they are attached more easily than toxic anti-fouling coatings by marine organism. It limits its promotion and wide application in ship's industry. In order to further improve the antifouling performance, some technical methods, such as building surface of the bionic structure, controlling chemical and physical properties, mixing nano-particles into paint to control surface morphology and hydrophobicity, etc. are investigated in recent years. Latter is considered as one cheap and convenient method. But, it needs further investigated what kind of micro/nano powders with what kind of shape and dimension can has better effect. Six different kinds of micro/nano powders with typical form are chosen to prepare silicone fouling release coatings in this article. They are respectively multi-walled carbon nanotubes(MWCNTs), nano titanium dioxide(NTD) and calcium sulphate whisker(CSW), micaceous iron oxide(MIO), tourmaline(TML) and iron oxide red(IOR). Every silicone coating was prepared with same formula and quality percentage of 1.5% powder. The powder's size and morphology measured by laser particle size analyzer and scanning electron microscope. The surface morphology and roughness of composite coatings were investigated by confocal laser scanning microscope. Based on the contact angle measurement of diiodomethane and water, the coating surface free energy was estimated by Owens two liquid method. All panels of coatings were tested by immersion in the yellow sea at Lushun port for evaluating the anti-fouling property, the resistance torque of coating in seawater was measured using rotating disk specimen in the laboratory. The results show that the water contact Angle and surface roughness are the highest coating of multi-walled carbon nanotubes, its shaw hardness, the polar force component of the surface free energy and resistance torque are the lowest. After the immersion test of a biological growth season, Multi-

walled carbon nanotube coating showed the best antifouling and drag reduction performance.

**Keywords:** MCNTs; nano; PDMS; particle; fouling release coating

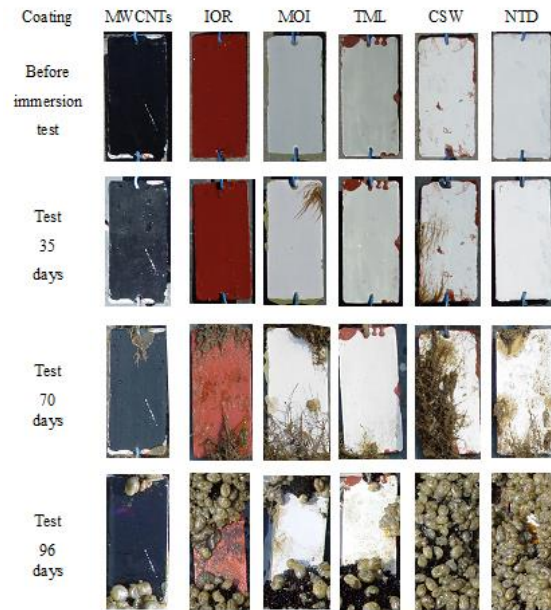


**Figure 1:** Morphology and marine fouling organism during immersion test.

## References:

1. James, C. Maureen, C. (2011) Trends in the development of environmentally friendly fouling-resistant marine coatings, *Nat Commun.* 244(2), 1–10
2. Chelsea, M. Scott, C. Anthony, B. (2010), Non-toxic antifouling strategies, *Materials Today*, 3(4), 36-44.

# Effect of operating conditions on adhesion strength of Cu/AlN laminate fabricated by High Vacuum Surface Controlled Direct Bonding

Sung-Chul Lim<sup>1\*</sup>, Kyu Bong Jang<sup>1</sup>

<sup>1</sup>Korea Institute of Industrial Technology, 7-47, Songdo-dong, Yeonsu-gu, 406-840, Korea

## Abstract:

Metal/ceramic clad materials have been widely used in various electronic industries including micro-electronic packaging, thin film devices, and biomedical devices<sup>[1]</sup>. Recently, Surface activated bonding(SAB) method has been widely used to manufacture metal/metal or metal/ceramic laminate composites. It involves cleaning the contact material surfaces with plasma and then bonding the materials under pressure. However, studies concerning the bonding of metal/ceramic by SAB are still scarce because most of the studies are focused on metal/metal bonding. In this study, we attempted to fabricate a Cu/AlN laminate composite using High Vacuum Surface Controlled Direct Bonding (HV-SCDB) method and investigated the relation between adhesion strength and operating conditions, such as the degree of vacuum, torch power and nano size diffusion layer

**Keywords:** High Vacuum Surface controlled Direct Bonding(HV-SCDB), Surface Activated Bonding(SAB), Cu/AlN laminate, nano size diffusion layer

**Figure 1:** Fig. 1 shows the variation in the adhesion strength for Cu/AlN laminates as a function of working pressure. The adhesion strength is found to increase with increasing working pressure. When the working pressure is 5000 kg/cm<sup>2</sup>, the adhesion strength was estimated to 2.60N/mm. This result correlates well with the expectation that an increase in the working pressure increases the contact area between Cu and AlN, and enhances adhesion strength between them. From these results, it can be concluded that plasma pretreatment and working pressure are very important factors that influence the bonding quality between Cu/AlN laminate.

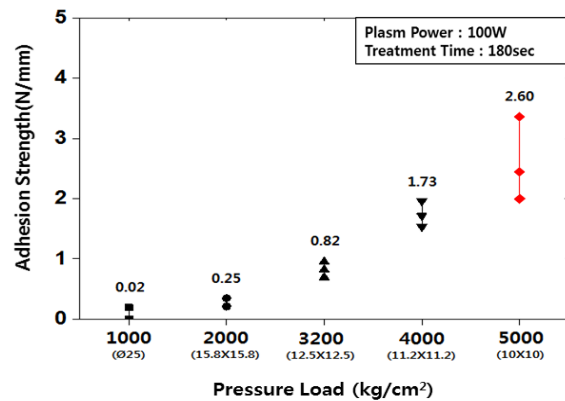


**Figure 1.** Adhesion Strength of Cu/AlN laminates as a function of working pressure

## References:

L. Esposito, A. Bellosi, S. Cuicciardi, and G. De Portu, J. Mater. Sci. 33, 1827 (1998)

# Enhancement of the TFT's performance by slight phosphorus doping: Lower density of states within the grain boundaries and higher stability

Mariem Zaghdoudi<sup>1,\*</sup>, Régis Rogel<sup>2</sup>, Tayeb Mohammed-Brahim<sup>2</sup>, Hatem Ezzaouia<sup>3</sup>

<sup>1</sup>Photovoltaic Laboratory, Research and Technology Center of Energy, Borj-Cedria Science and Technology Park, BP 95,2050 Hammam-Lif, Tunisia

<sup>2</sup>IETR/ Groupe Microélectronique, 263 avenue du général Leclerc, 35042 Rennes cedex, France

<sup>3</sup>High Institute of Environmental Science and Technology; University of carthage, borj cedria, Tunisia  
\*zmeriemtn@yahoo.com

## Abstract

In the present study, we investigate the effect of weak phosphorus doping in polysilicon layers. Films are deposited on glass substrates by Low Pressure Chemical Vapor Deposition (LPCVD) technique and are *in-situ* doped with phosphine adjunction to silane. Doping levels are reported by the phosphine to silane ratio  $\Gamma$  varying from 0 (undoped layer) to  $1.2 \times 10^{-3}$  (heavily doped layer). Films are characterized by different techniques as Photothermal Deflection Spectroscopy (PDS) and photoluminescence measurements. Results give evidence of an optimum doping level to obtain higher polysilicon films quality. Thin Film Transistors (TFTs) are fabricated on glass substrate using a top gate four mask process (Figure 1) at low temperature ( $< 600$  °C). Electrical characterizations highlight significant improvements in the TFTs performances using slightly doped film instead of undoped one as active layer. Indeed, field effect mobility exhibits a gain about 30 % and a lower threshold value is also obtained. Based on Levinson's model, density of states within the grain boundaries is also found to be the lowest. Stability under stress effect is enhanced too. These results give evidence that control of weak phosphorus doping in polysilicon films is a new way to improve polysilicon based devices.

**Keywords:** TFTs,LPCVD, in-situ, field effect mobility.

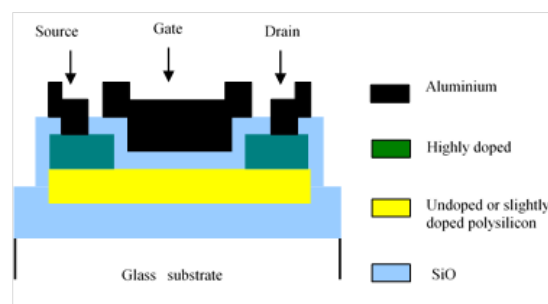


**Figure 1.** Cross section of the four-mask process TFT structure. The active layer is undoped or slightly phosphorus doped.

## References:

1. L. Pichon, K. Mourgues, F. Raoult, T. Mohammed-Brahim, K. Kis-Sion, D. Briand and O. Bonnaud, *Semicond. Sci. Technol.* Vol.16, 2001, 918-924.
2. J Levinson, F.R. Shepherd, P.J. Scanion, W.D. Westwood, G. Este, M. Rider, *J. Appl. Phys.* Vol.53, 1982, 1193-1196.

# The Green Synthesis, Characterization, and Antioxidant Activities of Silver Nanoparticles Synthesized from *Asphodelus aestivus* Aqueous Extract

B. Kuvçak<sup>1</sup>, T. Erdoğan<sup>1</sup>, P. Taştan<sup>1</sup>, B. Sümer Tüzün<sup>1</sup>, M. Özyazıcı<sup>2</sup>

<sup>1</sup>Department of Pharmacognosy, Faculty of Pharmacy, Ege University, Izmir, Turkey

<sup>2</sup>Department of Pharmaceutical Technology, Faculty of Pharmacy, Ege University, Izmir, Turkey

## Abstract:

Nanoparticle synthesis is usually applied some methods such as pyrolysis, laser ablation, vapor deposition, sol gel and lithography electro-deposition (Park *et al.*, 2011). The green nanoparticles synthesis from plant extracts is more easy, relevant, efficient and fast than chemical and physical methods (Kanipandian *et al.*, 2014; Palomares *et al.*, 2013; Rivas *et al.*, 2001; Rodriguez-Leon *et al.*, 2013). Here we present data on the green synthesis of silver nanoparticles from *Asphodelus aestivus* aqueous extract, their physical characterization (Figure 1) and their antioxidant effects *in vitro*.

Ultraviolet-visible spectroscopy, fourier transform infrared spectroscopy (FT-IR), transmission electron microscopy (TEM), particle size (PS) and zeta potential (ZP) were used to characterize the formation of silver nanoparticles (AgNPs). The antioxidant properties of these AgNPs were evaluated using DPPH, and ABTS<sup>+</sup> and hydrogen peroxide scavenging assays. The synthesized AgNPs were noticed through visual colour change from yellow to gray brown. The UV-Vis spectrum exhibited an absorption band at around 440 nm, which is a characteristic band for Ag. FT-IR measurement was carried out to identify the possible biomolecules responsible for capping and reducing agent for the Ag nanoparticles synthesized by *A. aestivus* aqueous extract. XRD results showed peaks at (200), (111), (110), (120), (330) and (210),

which confirmed the presence of AgNPs with monoclinic crystals. The TEM image of silver nanoparticles shown that the morphology of silver nanoparticles was predominantly spherical. It could be concluded that *A. aestivus* extract can be used efficiently in the production of potential antioxidant AgNPs for commercial application.

**Keywords:** *Asphodelus aestivus*, green synthesis, antioxidant activity, silver nanoparticles

## Acknowledgements:

This research was supported by Tübitak (project number SBAG-114S730).

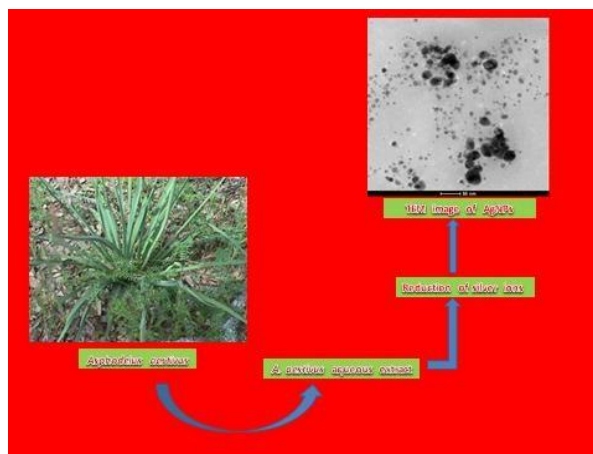


**Figure 1:** TEM image of AgNPs and the green nanoparticles synthesis from *Asphodelus aestivus*

## References:

1. Kanipandian, N., Kannan, S., Ramesh, R., Subramanian, P., Thirumurugan, R. 2014. "Characterization, antioxidant and cytotoxic evaluation of green synthesized silver nanoparticles using *Cleistanthus collinus* extract as surface modifier", *Materials Research Bulletin*, 49, 494-502.
2. Park, H.H., Choi, Y.J. (2011), Direct patterning of SnO(2) composite films prepared with various contents of Pt nanoparticles by photochemical metal-organic deposition, *Thin Solid Films.*, 519, 6214- 6218.
3. Rivas, L., Sanchez-Cortes, S., Garcia-Ramos, J.V. (2001), Growth of silver colloidal particles obtained by citrate reduction to increase the Raman enhancement factor, *Langmuir.*, 17(3), 574-577.
4. Rodriguez-Leon, E., Iniguez-Palomares, R., Navarro, R.E., Herrera-Urbina, R., Tanori, J., Iniguez-Palomares, C., Maldonado, A. 2013. "Synthesis of silver nanoparticles using reducing agents obtained from natural sources (*Rumex hymenosepalus* extracts)", *Nanoscale Research Letters*, 8 (318), 1-9.



# Synthesis of Monodisperse Gold Nanoparticles for Plasmonics

S. Marguet,<sup>1\*</sup> J. Caron,<sup>1</sup> A. Habert,<sup>1</sup> M. Khaywah,<sup>1</sup>

<sup>1</sup> NIMBE, CEA, CNRS, Université Paris-Saclay, CEA Saclay 91191 Gif-sur-Yvette, France

## Abstract:

Our research activities concentrate on the synthesis and assembly of gold nanoparticles for plasmonics that is a rapidly growing discipline at the interface of physics, chemistry and biology with promising applications.

We use a seed-mediated growth method of colloidal chemistry to synthesize gold nano- and micro-particles of controlled shape and size. This morphology control provides a fine tuning of the plasmon resonance wavelength and of the local field enhancement factor. Compared to top-down materials, these gold particles of high crystalline quality offer better surface-confinement of the electromagnetic field.

The figure illustrates some of the monodisperse gold NPs and gold nanohybrids we have been synthesized. Contrary to spherical and rod-shaped NPs that are commercially-available, other shapes such as nanocubes, nanotriangles and micro-plates with tunable sizes are only produced in our lab and in few laboratories worldwide, mainly in Asia. Triangles are of particular interest for ultrasensitive sensing, and plates (hexagonal or triangular) are very attractive for the construction of original plasmon-based optical devices due to their large atomically flat facets. At the present time, the synthesis of highly uniform triangles and plates still required purification steps that render them difficult to produce.

Our research is made in collaboration with various research teams expert in the different field of plasmonics and aims at providing appropriate materials to study enhanced-photochemistry, enhanced-spectroscopy and nanosources of light. In the future, we are eager to widen the application range of these NPs to sensors and metamaterials through new expected collaborations.

**Keywords:** gold nanoparticles, gold nanoplates, gold microplatelets, spontaneous self-assembly, plasmonic applications.

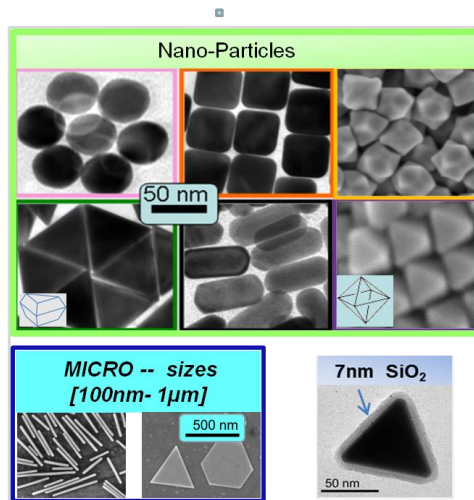


**Figure 1:** illustration of the monodisperse gold NPs and gold nanohybrids we are able to synthesize with tunable sizes and thicknesses. Top to bottom, left to right:

- **Gold Nanoparticles:** perfectly spherical spheres, cubes, stars, triangles, rods, octahedra,
- **Gold Wires and Microplates [100nm-1µm]** Plates with triangular- or hexagonal shape,
- **Gold-silica (Au@SiO<sub>2</sub>) nanohybrids.**

## References:

1. E. Le Moal et al. (2013) "An electrically excited nanoscale light source with active angular control of the emitted light," *Nano Lett.* 13, 4198-4205
2. M. Haggui et al. (2012) "Spatial Confinement of Electromagnetic Hot and Cold Spots in Gold Nanocubes", *ACS Nano.* 6(2), 1299-1307



# Enhanced Mass Activity of Pt as Au@Pt Nanoparticles on reduced Graphene Oxide Support for Methanol and Ethanol Oxidation

P. Gnanaprakasam, S. E. Jeena, T. Selvaraju,\*  
Karunya University, Department of Chemistry, Coimbatore, Tamil Nadu, India

## Abstract:

We present a facile, simple and reproducible method to synthesize a thin layer of platinum on gold as Au@Pt core-shell nanoparticles on the surface of reduced graphene oxide (rGO) using Cu under potential deposition (UPD) followed by the galvanic Pt replacement reaction method. The difference in the reduction potential is the driving force for the reaction where  $\text{Pt}^{4+}$  ions were reduced and deposited simultaneously on the surface of Au by replacing the Cu atoms. The as synthesized catalyst was characterized by scanning electron microscope (SEM), energy dispersive X-ray mapping analysis (EDAX), high resolution transmission electron microscope (HRTEM), high angle annular dark-field scanning/transmission electron microscopy (STEM-HAADF), X-ray diffraction (XRD), Raman spectroscopy and electrochemical studies. Due to the enhanced mass activity of Pt in rGO-Au@Pt the catalyst exhibits an excellent electrocatalytic property for methanol and ethanol oxidation in alkaline medium using cyclic voltametry. Electrochemical method serves as an efficient role in the spawn of a Pt monolayer on the Au surface. In addition, rGO surface acts as a stable platform for the uniform decoration of Au nanoparticles and increasing the electrochemical active surface area of Pt. Further the electrocatalytic activity and the stability of the as synthesized catalyst decorated electrode was compared with the commercial catalysts decorated electrode,  $\text{Pt}_{40}/\text{C}$  and  $\text{Pt}_{20}/\text{C}$  using cyclic voltametry and chronoamperometry, respectively. Thus, the Au@Pt core-shell graphene supported catalyst, rGO-Au@Pt NPs act as promising electrocatalyst for alcohol oxidation which could be used in fuel cell applications.

**Keywords:** Under potential deposition, Galvanic replacement reaction, Core- Shell nanoparticles, fuel cell, ethanol methanol oxidation, reduced graphene oxide.

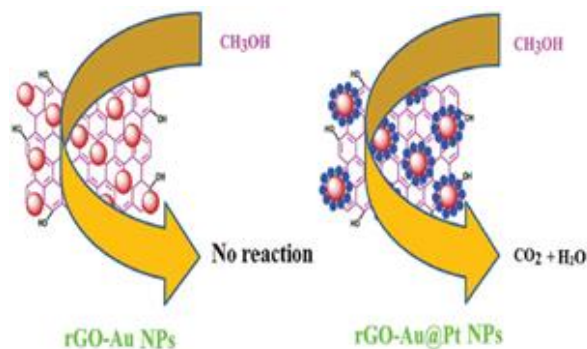


**Figure 1:** Figure is illustrating the hierarchical arrangement of Au nanoparticles and Au@Pt core-shell nanoparticles on the surface rGO. In addition, the figure represents, the alcohol oxidation reaction was feasible only in the presence of Pt thin layers on the surface of Au nanoparticles embedded rGO.

## References:

1. Gnanaprakasam, P., Jeena, S.E., Selvaraju, T. (2015) Hierarchical electroless Pt deposition at Au decorated reduced graphene oxide via a galvanic exchanged process: an electrocatalytic nanocomposite with enhanced mass activity for methanol and ethanol oxidation, *J. Mater. Chem. A.*, 3, 18010.
2. Jeena, S. E., Gnanaprakasam, P., Arun Dakshinamurthy and Selvaraju, T. (2015) Tuning the direct growth of Agseeds into bimetallic Ag@Cu nanorods on surface functionalized electrochemically reduced graphene oxide: enhanced nitrite detection, *RSC Adv.*, 5, 48236.

# Formation of Germanium Analog of The Tubular Aluminosilicate imogolite Containing Fe

M. Ookawa,\* E. Kato, M. Watanabe, K. Osada, M. Yoshikawa, S. Yamane

National Institute of Technology, Numazu College, Dept of Chemistry and Biochemistry, Numazu, JAPAN

## Abstract:

Germanium analog of the tubular aluminosilicate imogolite (Ge-imogolite) has drawn a new attention as a new nano-material. Recently, many studies on synthesis, structure or formation process (Mukherjee et al., 2007, Mallet et al., 2011). Mukherjee et al. indicated that the particle size estimated by dynamic light scattering (DLS) implies the tube length. We synthesized Ge-imogolite containing Fe from the solution with NaOH, AlCl<sub>3</sub>, FeCl<sub>3</sub> and GeO<sub>2</sub> and found that it served as a catalyst of oxidation reactions of benzene (Ookawa, 2012). The tubular structure is formed at the aging step of precursor solution near boiling temperature. We found that the solution with Fe<sup>3+</sup> also colored at this step. In this study, the formation process of Ge-imogolite with Fe<sup>3+</sup> ions was studied using by DLS and UV-VIS spectroscopy. The peak top of particle size distribution obtained by DLS is plotted against aging time. (Figure 1) Without Fe<sup>3+</sup> ions (Fe/(Al+Fe) = 0), the particle size became big gradually and these values are almost same as the those reported by Mukherjee et al.. On the other hands, particle size in the solution with Fe<sup>3+</sup> ions became bigger at the early stage. It is clear that the grown-up rate of tubes was promoted by introducing Fe<sup>3+</sup> ions. The UV-VIS spectra of aging solution at the aging step were shown in figure 2. The absorption at ca. 260 nm decreased and at the region from 300 nm to 350 nm increased with aging. These changes continued for 48h and the isosbestic point was observed. It means the state of Fe<sup>3+</sup> species was changed with the formation of tubular structure.

**Keywords:** imogolite, aluminogermanate, nanotube, dynamic light scattering (DLS), UV-VIS spectroscopy

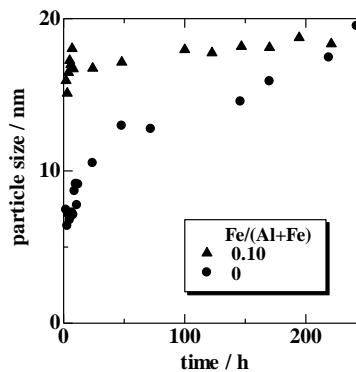


**Figure 1:** Evolution of Particle size of Ge-imogolite with Fe<sup>3+</sup> (Fe / (Al+Fe) = 0 and 0.01) estimated by DLS in aging step at 95°C.

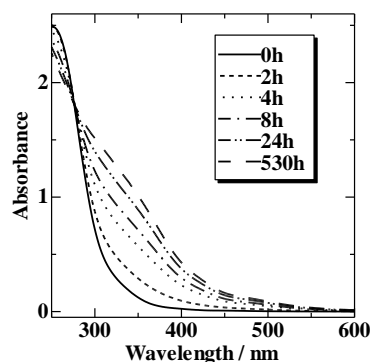


**Figure 2:** UV-VIS spectra of Ge-imogolite with Fe<sup>3+</sup> (Fe / (Al+Fe) = 0.01) in aging step at 95°C.

## References:

1. Mallet, P., et al., (2011), Growth kinetic of single and double-walled aluminogermanate imogolite-like nanotubes: an experimental and modeling approach, *Phys. Chem. Chem. Phys.*, 13, 2682-2689.
2. Mukherjee, S., et al., (2007), Short, highly ordered, single-walled mixed-oxide, Nanotubes assemble from amorphous nanoparticles, *J. Am. Chem. Soc.*, 129, 6820-6826.
3. Ookawa, M., (2012), JAPAN PATENT, 48899010.

# Dispersion Characteristics of Layered Double Hydroxides in the presence of amphipathic macroRAFT agents

M. Pavlovic<sup>1</sup>, V. Prevot<sup>2</sup>, E. Bourgeat-Lami<sup>3</sup>, I. Szilagy<sup>1</sup>

<sup>1</sup> Department of Inorganic and Analytical Chemistry, University of Geneva, 30 Quai Ernest-Ansermet, CH-1205 Geneva, Switzerland

<sup>2</sup> Université Clermont Auvergne, Université Blaise Pascal, Institut de Chimie de Clermont-Ferrand, CNRS, UMR 6296, BP 80026, F-63171 Aubièrre, France

<sup>3</sup> Université de Lyon, Univ. Lyon 1, CPE Lyon, CNRS, UMR 5265, Laboratoire de Chimie, Catalyse, Polymères et Procédés (C2P2), 43 Bvd du 11 Novembre 1918, F-69616 Villeurbanne, France

## Abstract:

Layered double hydroxides (LDHs) have been extensively investigated in the recent years due to their promising applications in drug delivery, catalysis, wastewater treatment and polymer nanocomposites formation. In this last example, it is essential to get good compatibility between the organic and inorganic components in order to achieve improved mechanical, thermal or flammability properties. One of the most currently used strategies to improve the affinity between the organic and inorganic parts is the modification of the inorganic particle with organic molecules, such as polymers. To this respect, determining the proper amount of polymer that can adsorb on the surface of LDH nanoparticles and understanding how polymer adsorption influences colloidal stability of LDH suspensions are of crucial importance. In this communication, the effect of four different macroRAFT copolymers synthesized by reversible addition fragmentation chain transfer (RAFT), composed of acrylic acid (AA) and butyl acrylate (BA) monomers on the colloidal behavior of  $Mg^{2+}$ - $Al^{3+}$  LDH was investigated by determining electrophoretic mobilities and stability ratio values (Figure 1). Strong adsorption of the copolymers occurred, leading to charge neutralisation at the isoelectric point (IEP), and to overcharging at higher concentrations. The LDH particles were moderately stable at low copolymer dose, reaching fast, diffusion limited aggregation close to IEP. Atomic force and transmission electron microscopy revealed that the nanoplatelets preferentially adopted face-to-face orientation in the aggregates. Above IEP, LDH nanoparticles became extremely stable due to substantial charge reversal. Significant effects of the AA-to-BA ratio and polymer molar mass were observed. The macroRAFT copolymers were compared to a pure acrylic acid polymer (PAA) of approximately the same molar mass.

Larger amounts of butyl groups in the copolymers increased the onset of the adsorption saturation plateau (ASP, the maximum amount of copolymer which can adsorb on the LDH particles). In summary, colloidal stability of aqueous LDH dispersions can be fine-tuned by macroRAFTs adsorption. The particles are aggregated at low concentration, but highly stable dispersions can be obtained if one applies the appropriate copolymer dose.

**Keywords:** Layered double hydroxide, macroRAFT, colloidal stability, electrophoretic mobility, nanocomposite

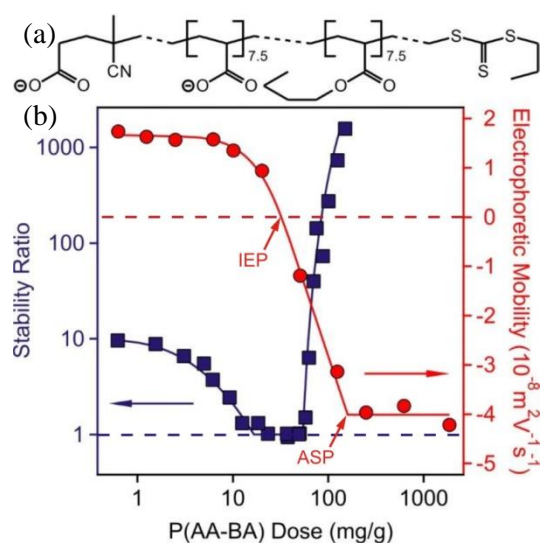


**Figure 1:** Structure of  $P(AA_{7.5}\text{-stat-}BA_{7.5})$  macroRAFT agent (a), stability ratio (■) and electrophoretic mobility (●) of LDH particles coated by macroRAFT copolymers in different doses (b).

## References:

Pavlovic, M., Adok-Sipiczki, M., Nardin, C., Pearson, S., Bourgeat-Lami, E., Prevot, V., Szilagy, I. (2015), *Langmuir*, 31, 12609-12617.

# Tuning the structure and the mechanical properties of epoxy-silica sol-gel hybrid materials

Berta Domènech,<sup>1</sup> Ignasi Mata<sup>1</sup> and Elies Molins<sup>1</sup>

<sup>1</sup> Institut de Ciència de Materials de Barcelona (ICMAB-CSIC), Crystallography Department, Campus UAB, 08193 Bellaterra, Spain.

## Abstract:

Aerogels are materials characterized by an open mesoporous structure, high specific surface area and very low bulk density, usually obtained by a sol-gel procedure. Silica aerogels are by far the most common and are moving into the market for applications mostly related to thermal insulation. Nevertheless, highly porous silica aerogels are brittle and collapse easily, being these poor mechanical properties one of the main drawbacks for their general use. An approach proposed for overcoming this important limitation is the preparation of hybrid materials that combine silica with organic compounds that add flexibility or robustness to the pore structure.

In this work, a new hybrid porous material has been developed from the reaction of an epoxy resin and silicon alkoxides following a new one-pot method and using ethanol as the single solvent. In the preparation route, the epoxy-resin is first included as a co-precursor with silane active groups from which the final material is prepared via sol-gel method and dried with supercritical drying. By this way, the ormosil-material obtained is formed by silica particles bridged by the epoxy resin.

In such material, the characteristics of the pore structure strongly depend on the ratio between silica and epoxy. Scanning and transmission electron microscopy reveals that for most compositions the structure is formed by homogeneous hybrid primary particles (~5-500 nm) agglomerated in large, micrometric particles. A foam-like structure is also observed for a specific composition. This dependence of the pore structure with the amount of resin can be explained in terms of a phase separation process.

Moreover, the measurement of the compression modulus of the different materials obtained reveals that the mechanical properties can be tuned in the range 1-100 MPa just by modifying the molar ratio between alkoxides and epoxy resin (Figure 1), allowing the preparation of materials with tailored modulus.

**Keywords:** sol-gel, ormosil, epoxy, silica, silica-based materials, aerogels, mechanical properties, thermal insulation.



**Figure 1:** Photographs of two samples at the beginning and end of the compression test (force applied 18 N) with low (left) and high (right) amount of epoxy-resin.

## References:

1. Randall, J. P. , Meador, M. A. B., Jana, S. C. (2011) Tailoring Mechanical Properties of Aerogels for Aerospace Applications, *ACS Appl. Mater. Interfaces*, 3, 613-626.
2. Domènech, B., Mata, I., Molins, E. (2016) Tuning the structure and the mechanical properties of epoxy-silica sol-gel hybrid materials, *RSC Adv.*, 6, 10736-10742.



# High performance Transparent Electrode Consisting of Silver and Graphene Hybrid Structure Fabricated by Near-Field Electro-Spinning

D. H. Youn<sup>1</sup>, Y. J. Yu<sup>1</sup>, S. J. Yun<sup>1</sup>, H. K. Choi, J. S. Choi, G. H. Kim<sup>2</sup> and C. G. Choi<sup>1</sup>

<sup>1</sup>Electronics and Telecommunications Research Institute, Deajeon, 305-700, Korea

<sup>2</sup>School of Information and Communication Engineering, and Samsung Advanced Institute of Nanotechnology (SAINT), Sungkyunkwan University, Suwon 440-746, Korea

## Abstract:

Low sheet resistance and high transmittance transparent electrode was fabricated using near-field electro-spinning. We demonstrated that the addition of graphene flakes into silver (Ag) nanowire (NW) resulted in Ag and graphene hybrid with decreased sheet resistance and thermal oxidation. Here graphene acting as two-dimensional pathways for charge transfer between Ag NWs and oxidation resistant layer. We introduced near-field electro-spinning (NFES) method which confines Ag NWs into the narrow line pattern whose width is within 100  $\mu\text{m}$  [1]. The Ag NW density at the same area was increased due to the confinement of Ag NW at the narrow region comparing to that of spin-coated. The percolation efficiency between Ag wires was increased due to the increase in NW density. Therefore, sheet resistance was decreased due to increase in the percolation between Ag NWs. We showed that graphene sheet deposited on top of Ag NWs, protect the Ag NW under neat it from thermal oxidation, preventing the increase in sheet resistance due to thermal oxidation [2-3].

## Results:

Mesh-type transparent electrode was fabricated using NFES whose line width was controlled less than 100  $\mu\text{m}$  as shown in Fig. 1b and 1c. The Ag NW density changed from 25/ 100  $\mu\text{m}^2$  (spin-coated) to 33/ 100  $\mu\text{m}^2$  (electro-spun). Increase in Ag NW density induced the percolation between Ag NWs. After the fabrication of line pattern using NFES, the sheet resistance of Ag NW pattern changed from 79.4  $\Omega/\text{sq}$  (spin-coated) to 3.3  $\Omega/\text{sq}$  (electro-spun) due the increase in percolation at 90 % optical transmittance. The lateral size of graphene sheet may be as large as several  $\mu\text{m}$ . Graphene sheets bridge two or more non-connected Ag NWs. This may result in higher electrical conductive path for charge transfer. The optical transmittance of mesh-type Ag NW patterns were 72.8 % (300  $\mu\text{m}$ ), 84.1 % (100  $\mu\text{m}$ ) and 90.8 % (50  $\mu\text{m}$ ), respectively. Optical transmittance was increased as the line width decreased as shown in the inset of Fig. 1c. We inserted Ag NW line pattern into graphene

dispersive solution for 6 hours at room temperature to add the graphene sheet onto the Ag NWs. Then we took out sample from beaker and placed onto the oven at 70  $^{\circ}\text{C}$  from 0 to 24 hour. After annealing, the  $R_{\text{sh}}$  of spin-coated Ag NW changed greatly from 16.8  $\Omega/\text{sq}$  to 678.5  $\Omega/\text{sq}$  due to thermal oxidation. However, the  $R_{\text{sh}}$  of electro-spun Ag NW changed smaller than that of spin-coated Ag NW from 18.5  $\Omega/\text{sq}$  to 137.4  $\Omega/\text{sq}$ . Here the graphene sheet deposited on top of Ag NW films, acting as an oxidation resistant layer.

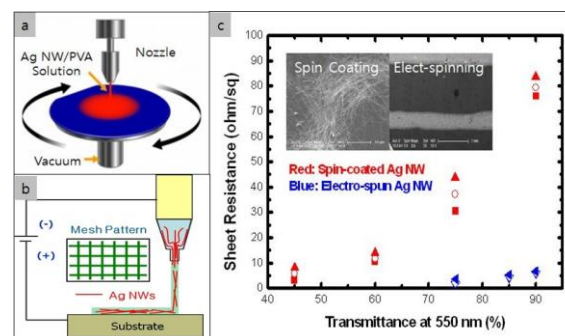


**Figure 2:** Fabrication of Ag NW films on a  $\text{SiO}_2/\text{Si}$  substrate. (a) Schematic process of a spin coating setup. (b) Schematic process of an electrospinning setup. (c) Transmittance and sheet resistance of the spin-coated (red) and electro-spun (blue) Ag NW electrode.

## References

1. Youn D. H., Kim S. H., and Yoo J. B. (2009) Appl. Phys. A 96 933.
2. Kholmanov I. N., Domingues S. H., and Ruoff R. S. (2013) ACS. Nano. 7, 1811 .
3. Wu H., Hu L. B., and Cui Y. (2010) Nano. Lett. 10, 4242.
4. Rizo H. V., Gullon I. M., and Terrones M. T. (2012) ACS Nano. 6, 4565.
5. Rathmell A. R., Nguyen M. N., and Wiley B. J. (2012) Nano. Lett. 12, 3193.
6. Kang D. W., Kwon J. Y., and Shin H. S. (2012) ACS Nano. 6, 7763.



# Plasmonic Ag ultrafine nanoparticle-graphene substrates for Raman enhancement

Esteban Climent-Pascual,<sup>1,\*</sup> Félix Jimenez-Villacorta,<sup>1</sup> Leo Álvarez-Fraga,<sup>1</sup>  
Rafael Ramírez-Jiménez,<sup>2,1</sup> Carlos Prieto,<sup>1</sup> Alicia de Andrés,<sup>1</sup>

<sup>1</sup> Instituto de Ciencia de Materiales de Madrid, CSIC, Madrid, Spain

<sup>2</sup> Departamento de Física, Universidad Carlos III de Madrid, Madrid, Spain

## Abstract:

The biomolecular recognition and characterization, ultrasensitive diagnosis and biodetection, and biomedical imaging are of vital relevance for a diverse array of biomedical applications. In that respect, Raman spectroscopy is a highly specific and label-free technique, allowing multiple parameter analysis of biological samples including individual living cells. The Raman spectrum of every component of a biological sample serves as a molecular ‘fingerprint’, making it possible to differentiate various components without prior knowledge of them. However, a key drawback of Raman spectroscopy is the inherent low-sensitivity in these systems. Recently, progress in significantly enhancing and improving the Raman signal have arisen mainly driven by the significant advances in surface-enhanced Raman scattering (SERS). This is a nanoscale effect, deriving from localized surface plasmon resonances in nanostructured metals which give rise to huge electromagnetic fields at the nanostructured surface. On the other hand, graphene shows some effects when the material interacts with localized surface plasmons. It is known that the plasmon resonance can be tuned by controlling the surrounding media such as a single layer graphene film. Moreover graphene provides a biocompatible substrate.

Our study shows the use of silver ultrafine nanoparticles (~4 nm) onto a transparent graphene-based substrate for generating a SERS-active system.[1] The growth process of silver films of different nanoparticle surface densities and thickness was carried by the sequential stepwise gas aggregation method, which allows control and tunability of the physical properties of these SERS-active graphene-based systems. This is an advanced physical vapor deposition technique to generate continuous flow of ultrafine particles with controlled size and narrow particle size distributions. To seek the Ag-SERS evolution, uniform rhodamine 6G (R6G) films of different molecule surface densities were deposited on the SERS-active systems (nanoparticle-transparent

graphene substrate) by spin coating. R6G molecule surface densities were estimated with the corresponding absorption spectra in the visible region by using a highly diluted R6G solution as reference. This picture (ultrafine nanoparticles and low nanoparticle surface densities) represents the lower bound on the silver nanoparticles enhancement capacity, but even so there is a clear enhancement for the graphene Raman signal which has been correlated to the increased absorption of the silver nanoparticles plasmon. For R6G the Raman enhancement is around three orders of magnitude greater than for graphene. That could be attributed to a geometric effect. R6G molecules are located near the hotspots formed in between these superficially oxidized Ag nanoparticles, while these hotspots are far from graphene and therefore the graphene Raman signal enhancement is lessened.

Moreover, Ag nanoparticles induce carrier doping and weak strains in the graphene lattice.

Future work aims to achieve a rationally designed hotspots for a desired Raman intensity enhancement by advanced nanoscale fabrication.

**Keywords:** metallic ultrafine nanostructures, SERS, biomolecular detection-recognition, plasmons, Raman spectroscopy .

## References:

Jimenez-Villacorta, F., Climent-Pascual, E., *et al.* (2016) Graphene-ultrasmall silver nanoparticle interactions and their effect on electronic transport and Raman enhancement, *Carbon*, In Press.

# Self-cleaning Properties of Nanostructured Polypropylene Foils Fabricated by Roll-to-Roll Extrusion Coating

A. Telecka,\* R. Taboryski

Danish Technical University DTU, Nanotech, Kongens Lyngby, Denmark

**Abstract:** Technologies based on superhydrophobic treatments of artificial surfaces are under a great deal of attention, in both scientific research and manufactory, due to their broad potential applications in industry such as self-cleaning and antifogging materials<sup>1,2</sup>. Fabrication of superhydrophobic surfaces usually follows two conventions: initial structuring the micro/nanopattern to increase surface roughness and then covering a low surface-energy coating to decrease surface free energy of material.

However, the coating treatment can lead to problems in some practical aspects due to the degradation of organic compounds caused by UV radiation, abrasion or mechanical expenditure. Nowadays commercially available polymers like polypropylenes (PP), polyethylenes (PE) or cyclic olefin copolymers (COC) are widely used for direct patterning as low surface free energy materials with advantages of good functionality, flexibility, chemical stability and ease of processing.

In this paper we present systematic wetting properties study of nanostructured polypropylene (PP), functional foils, fabricated by roll-to-roll extrusion coating process (R2R EC). It is a fast and effective manufacture method, so far widely uses for smooth polymer films, which allows to large-scale replication of micro- and nanometric scale arrays onto polymer substrates<sup>3</sup>. In this technique, metal templates used for patterns imprint were prepared through a one step, maskless, black silicon etching process<sup>4</sup>, what led to covering of the whole 4 inch silicon wafer area, and consequent NiV electroplating resulting in nickel shims. By the manipulation of reactive SF<sub>6</sub> and O<sub>2</sub> gas steams, diverse nanograss topographies were generated. Figure 1 presents detailed process flow with images. R2R extrusion was performed under varied imprinting temperatures and extrusion speeds to control nanostructures replication quality. Wetting properties of fabricated PP foils were characterized by contact angle measurements of water sessile drop in static and dy-

namic method. We recorded values of static contact angles above 150° and roll-off angle in a range of 10 - 20°. This results, according to theorie and research experience, indicate on superhydrophobic properties of fabricated surfaces with self-cleaning potential applications.

**Keywords:** nanotechnology, nanofabrication, micro and nanopatterning, polymers and plastics, advanced characterization, surface analysis, materials engineering, materials science, plastics applications

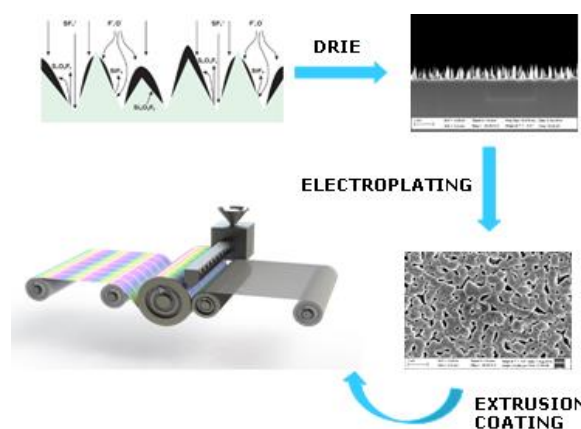


**Figure 1** Figure presents fabrication process flow of nanostructured PP foils. In a first step with the use of fluorine and oxygen plasmas, nanograss patterns were generated on a silicon wafers. Next arrays were transferred on a nickel shims by electroplating process and finally attached on a roll for thermal imprint of nanostructures on a polymer foils with a use of diverse imprint speeds and roll temperatures.

## References:

1. S. H. Anastasiadis, "Development of Functional Polymer Surfaces with Controlled Wettability," *Langmuir*, no. 29, pp. 9277 - 9290, 2013.
2. J. Li, J. Zhu and X. Gao, "Bio-Inspired High-Performance Antireflection and Antifogging Polymer Films," *Small*, vol. 10, no. 13, pp. 2578-2582, 2014.
3. S. Murthy and et. al., "Fabrication of Nanostructures by Roll-to-Roll Extrusion Coating," *Adv.Eng.Mat.*,2015.
4. J. Shieh and et al., "Plasma-made silicon nanograss and related nanostructures," *J. Phys. D: Appl.Phys.*, vol.44,no.17, p.174010(6pp), 2011.

# Chemical and electronic structure profiling in the top few nanometers of hydrothermally prepared and plasma hydrogenated ZnO nanorods

Mubarak J. Al-Saadi, Salim H. Al-Harhi

Sultan Qaboos University, College Of Science, Physics Department, Muscat, Sultanate Of Oman.

## Abstract:

Hydrothermally grown zinc oxide nanorods were investigated by X-ray and ultra violet photoelectron spectroscopy in order to explore the defects and electronic structure at the surface and sub-surface of the nanorods. Upon treating with hydrogen plasma, significant reduction in the metallic bonding between Zn and O atoms was observed with substantial increase in the hydrogen plasma induced OH content of the nanorods. As a result of hydrogenation, 0.20 eV and 0.86 eV shifts in the Fermi level and work function energies were found from the sub-surface to surface respectively. Based on non destructive depth profile analysis a chemical composition distribution model in these nanorods is proposed. The results suggest a plausible mechanism for tailoring of the surface defects and the electronic band structure and demonstrate a direct way to increase the work function but opposite to that based on hydroxylation effect. In addition open up a possible way of OH surface passivation needed to enhance fictionalization of nanomaterials such as quantum dots to the ZnO nanorods essential for solar cell applications.

**Keywords:** Zinc Oxide, Scanning Electron Microscopy, X-ray Diffraction, X-ray Photoelectron Spectroscopy, Ultra-violet Photoelectroscopy, Photoluminescence, Atomic Hydrogen Cracking, Surface and Defects.

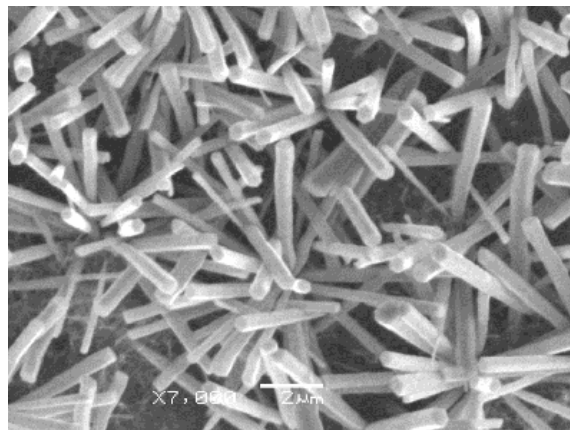


**Figure 2:** SEM of ZnO NR's shows average length of about 1.2 μm and 200 nm width.

## References:

1. Li, Y. Uchino, R. Tokizono, T. Paulsen, A. Zhong, M. Shuzo, M. Yamada, I. Delaunay, J. J., (2009) Effect of hydrogen plasma treatment on the luminescence and photoconductive properties of ZnO nanowires, *Materials Research Society Symposium Proceedings*, 1206, 7-12.
2. Avale, L. Santos, E. Leiva, E. Macagno, V. A., (1992) Characterization of TiO<sub>2</sub> films modified by platinum doping, *Thin Solid Films*, 219, 7-17.

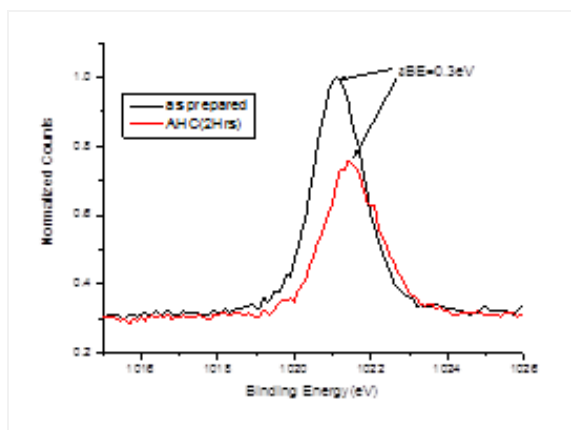


**Figure 1:** Zn 2p<sub>3/2</sub> peak for ZnO nanorods before and after hydrogen treatment.

# Fluorescent Photosensitive Vitroceramics with Silver and Samarium Additives: Improvement of Writing Accuracy and Efficiency for 3D Optical Storage Media

C. Busuioc,<sup>1,\*</sup> S. Jinga,<sup>1</sup> E. Pavel<sup>2</sup>

<sup>1</sup> University POLITEHNICA of Bucharest, Faculty of Applied Chemistry and Materials Science, Bucharest, Romania, RO-011061

<sup>2</sup> Storex Technologies, Bucharest, Romania, RO-020892

## Abstract:

Quantum optical lithography is a technique able to decrease resolution beyond 2 nm by optical means, using new materials (Pavel *et al.*; 2013, 2014, 2015).

Fluorescent photosensitive vitroceramics with different concentrations of silver and samarium were prepared by the classical approach and subsequently mechanically processed in order to achieve optical quality discs (Figura 1). The objective of this study is the improvement of the writing accuracy and efficiency, as well as the obtaining of a higher emission intensity of the fluorescent active centers (Pavel, 2015) which consist in SmF<sub>3</sub> or NaSmF<sub>4</sub>.

The reported material can be also employed for the building of nanorobots through laser nanofabrication. Moreover, by extrapolation, we foresee the possibility of developing metamaterials by writing 3D networks with controlled distances between in-plane lines and planes.

**Keywords:** fluorescent photosensitive glass-ceramics, 3D laser writing, optical disks, data storage.



**Figure 1:** Figure illustrating a fluorescent photosensitive vitroceramic disk during laser irradiation.

## References:

1. Pavel, E., Jinga, S., Andronescu, E., Vasile, B.S., Kada, G., Sasahara, A., Tosa, N., Matei, A., Dinescu, M., Dinescu, A., Vasile, O.R. (2013), 2 nm quantum optical lithography, *Opt. Commun.*, 291, 259–63.
2. Pavel, E., Jinga, S.I., Vasile, B.S., Dinescu, A., Marinescu, V., Trusca, R., Tosa, N. (2014), Quantum optical lithography from 1 nm resolution to pattern transfer on silicon wafer. *Opt. Laser Technol.*, 60, 80–84.
3. Pavel, E., Jinga, S.I., Vasile, B.S., Dinescu, A., Tosa, N., Trusca, R. (2015), 3D direct laser writing of petabyte optical disk, *Opt. Laser Technol.*, 71, 45–49.
4. Pavel, E. (2015), Coherent exciton mechanism of three-dimensional quantum optical lithography, *Appl. Opt.*, 54, 4613–4616.

# Transparent and Hard PTFE-like Coatings by RF magnetron Sputtering of PTFE Polymer Target

Y. S. Song,<sup>1,\*</sup> J. Kim,<sup>2</sup>

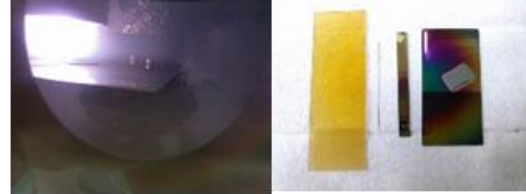
<sup>1</sup>KITECH., Surface Technology R&BD Group, Incheon, Korea(ROK)

<sup>2</sup>Department of Materials and Metallurgical Science, Hanyang University, Ansan, Korea(ROK)

## Abstract:

PTFE (Polytetrafluoroethylene) is a unique material as bulk form and also as thin film. Extremely low friction coefficient, hydrophobic surface property, and chemical inertness make it attractive for various applications. In the form of thin film, about 1-2  $\mu\text{m}$  or below 50 nano meter thickness level, the hydrophobic nature is superior to bulk PTFE according to sputtering conditions. We tried RF (radio-frequency) sputtering with pure PTFE target for thin PTFE film deposition. We can change the PTFE sputtering parameters such as sputter target gun power, process pressure, and RF bias applied to substrate stage and Si wafer or various specimens. We investigated pure PTFE thin films by RF sputtering and compared with bias applied PTFE-like thin films according to the process parameters. Sputtered PTFE coatings have the advantages of contact angle of 100 degrees or more, super water-repellent and high transmittance of more than 90%. There are some problems of low hardness and the adhesion with the substrate, for example Si wafer, in coatings deposited by conventional sputtering using PTFE target. PTFE coating made from a high energy environment shows different characteristics as compared with coatings made by conventional sputtering method. We tried biased RF sputtering of PTFE target for the improvement in hardness and adhesion of PTFE films. We investigated the contact angle, coating transmittance, hardness by nano-indenter, and film adhesion by scratch test. We tried the hardness mechanism of hard PTFE-like coatings by RF sputtering of PTFE polymer target.

**Keywords:** PTFE, RF magnetron sputtering, contact angle, hardness, nano-indenter, transmittance, adhesion, scratch test, PTFE-like coating



Conventional PTFE Sputtering



Hard and Transparent PTFE-like Coating

**Figure 1:** Figure illustrating the RF magnetron sputtering of PTFE polymer target and coating is deposited as substrate bias applied.

## References:

1. O. Kylián, M. Drábik, O. Polonskyi, J. Čechvala, A. Artemenko, I. Gordeev, A. Choukourov, I. Matolínová, D. Slavínská, H. Biederman, *Thin Solid Films*, 519 (2011) 6426-6431.
2. S. Iwamori, *Key Engineering Materials*, 384 (2008) 311-320.



# Mathematical Modeling Process of Sedimentation Magnetic Nanoparticles on the Walls of Blood Vessels

M.A. Shumova,<sup>1,\*</sup> D.V. Korolev,<sup>2,3</sup> O.A. Smolyanskaya<sup>1</sup>, S.A. Chivilikhin<sup>1</sup>

<sup>1</sup>ITMO University, Saint-Petersburg, Russia

<sup>2</sup>North-West Federal Almazov Medical Research Centre, Saint-Petersburg, Russia <sup>3</sup>First Pavlov State Medical University of St.-Petersburg, Saint-Petersburg, Russia

## Abstract:

Catheter embolization is applied widely in medicine. This method is minimally invasive and it is used as for prevention of postoperative bleeding, relapses of tumors and for treatment the various bodies. This method is directed to occlusion of one or a few blood vessels for stop bleeding. In catheter embolization is entered radioactive medication under control of the x-ray computer angiography. The presence of radiative forcing on the human tissue limits the duration and the frequency of this procedure. Magnetic resonance angiography has certain advantage from this point of view, for which holding radioactive substances are not applied and one of the perspective embolic material classes is magnetic colloidal particles on the basis of the iron oxide.

The model for the study process was created, imitating section of the system circulation and allowing apply magnetic influence and also realize registration of the accumulation nano-particles (Fig.1)

On the basis of the experiment mathematical modeling process of sedimentation magnetic nanoparticles on the walls of blood vessels was presented, trajectory of the motion magnetic nanoparticles was built, thickness of the be-sieged layer magnetic nanoparticles was calculated, correlation between growth of the be-sieged magnetic nanoparticles and time was researched.

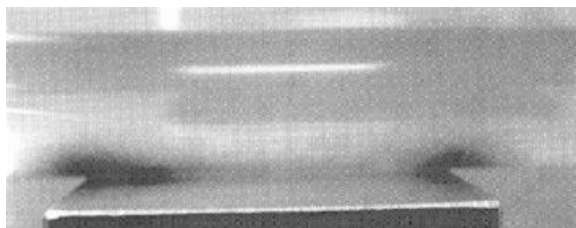


**Figure 1:** The photograph of the accumulation magnetic nanoparticles in the area of motion modeling liquid.

**Keywords:** catheter embolization, angiography, colloidal particles, occlusion, embolic material

## References:

1. Bogachev Yu.V., Chernenco Ju.S., Gareev K.G. et al. The Study of Aggregation Processes in Colloidal Solutions of Magnetite–Silica Nano-particles by NMR Relaxometry, AFM, and UV–Vis-Spectroscopy. *Appl. Magn. Reson.* 2014. V. 45. No. 3. P. 329–337.
2. Smolkova I.S., Kazantseva N.E., Makoveckaya K.N. et al. Maghemite based silicone composite for arterial embolization hyperthermia. *Materials Science and Engineering C.* 2015. V. 48 P. 632–641.

# Grown of silicon nanowires for possible solar cell applications

J. Salazar<sup>1\*</sup>, G. Santana<sup>1</sup>, B. M. Monroy<sup>1</sup>

<sup>1</sup> Instituto de Investigaciones en Materiales, Universidad Nacional Autónoma de México, Ciudad Universitaria, Coyoacán 04510, México D.F., México

## Abstract

The nanowires are structures that have the great advantage of allowing particles such as electrons, holes or photons to propagate freely along the unconfined dimension, which has caused a deep interest for application in solar cells where they could serve as channels of unidirectional conduction through the device. Most methods involve synthesis of nanowires using a metal catalyst "guide" unidirectional growth [1]. In the first years of investigation of silicon nanowires, the growth mechanism leading to a unidirectional orientation was still in discussion. However, in 1964 R.S. Wagner and W.C. Ellis proposed the Vapor-Liquid-Solid mechanism (Figure 1) for crystal growth [2]. This mechanism helps to explain how to carry out the crystal growth in one dimension. The growth is assisted by a metallic material that functions as a catalyst. The metal catalysts must meet the following requirements [3]:

- It should form a liquid solution with a component of the solid phase.
- The limit of solubility of the catalyst component in the liquid phase should be much higher than in the solid phase.
- The vapor pressure of the catalyst component on the molten alloy should be small.
- It must be inert to chemical reactions.
- It does not form a solid intermediate.

Gold has been widely used in this context. In this work the influence of the initial morphology of gold catalyst is discussed in the dimensions and density of silicon nanowires synthesized by PECVD using dichlorosilane ( $\text{SiH}_2\text{Cl}_2$ ) as precursor of silicon. Gold films were deposited by sputtering on p-type silicon,  $\text{Si}_3\text{N}_4$  and  $\text{SiO}_2$  substrates. Subsequently, the growth of silicon nanowires was performed by the VLS mechanism. To study the differences in the morphology of the nanowires on different substrates, scanning electron microscopy (SEM) was used. The differences in terms of the different substrates and the surface chemistries that exist will be discussed.

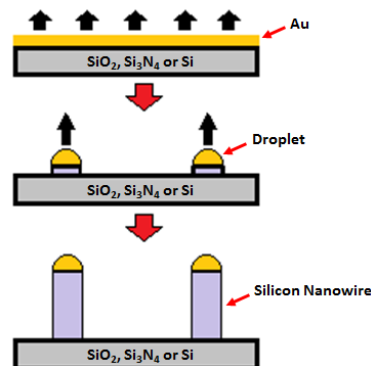


**Figure 1.** A simplified schematic of grown of silicon nanowire.

## Acknowledgements:

Authors thank J.E. Romero-Ibarra and C. Gonzalez for information and technical support. We acknowledge partial financial support for this work from DGAPA-UNAM PAPIIT Projects IN108215 and IN100914, CONACyT Mexico under project 179632, SENER-CONACyT project 151076. A special acknowledgment is due to financial support from CONACyT through scholarship CVU 632679.

## References:

1. Heon-Jin Choi, "Vapor-Liquid-Solid Growth of Semiconductor Nanowires", capítulo 1 en Semiconductor Nanostructures for Optoelectronic Devices NanoScience and Technology, DOI 10.1007/978-3-642-22480-5 1, Springer-Verlag Berlin Heidelberg 2012.
2. R. S. Wagner and W. C. Ellis, "The vapor-liquid-solid mechanism of crystal growth and its application to silicon", Trans. Metall. Soc. AIME, vol. 233, no. June, pp. 1053–1064, 1965.
3. M. Hasan, M. F. Huq, and Z. H. Mahmood, "A review on electronic and optical properties of silicon nanowire and its different growth techniques", Springerplus, vol. 2, p. 151, 2013

# Applications of Positron Probe in polymer nanocomposites

G.B.Xie, J.Zhong, S.Gao, B. Wangf

School of Physics and Technology, Wuhan University, Wuhan, 430072, China

## Abstract:

Positron probe (PP) is a very useful tool to probe the Gong, Z., Gong, J., Yan, X., Wang, B., (2011), Investigation of the effects of temperature and strain on the damping properties of polycarbonate / multiwalled carbon nanotube composites, atomic scale free volume. The principal advantage of PS over other techniques is that the formation and annihilation characteristics of positronium (Ps), i.e., a bound state of  $e^-$  and  $e^+$ , strongly depends on the atomic-scale free-volume hole. Therefore, PP has been widely used in the study of polymeric and nanocomposite materials in recent years. In this work, we report research results using PP, including structural transition, interfacial interaction between the polymer matrix and nano particles doped and its effect on the electronic, damping, mechanic, thermal conductivity and miscibility properties for polycarbonate/multiwalled carbon nanotube composites, polyethylene oxide/lithium perchlorate nanocomposite electrolytes doped with ZnO and graphene oxide, interpenetrating polymer network/MMT, and polypyrrole/graphene oxide polymer and poly(vinyl alcohol)/reduced graphene oxide composites. Based on the experimental measurements, the relationships between positron annihilation parameters and electronic conductivity, ionic conductivity, thermal conductivity, miscibility and damping have been established. The micromechanisms can be explained in terms of positron annihilation parameters.

**Keywords:** positron annihilation, polymer nanocomposites, interfacial interaction, electronic conductivity, thermal conductivity, damping, miscibility, ionic conductivity, free volume, microstructure

## References:

1. Zhu, Y., Wang, B., Gong, W., Kong, M., Jia, Q., (2006) Investigation of the Hydrogen-Bonding structure and miscibility for PU/EP IPN nanocomposites by PALS, *Macromolecules.*, 39, 9441-9445
2. Gong, Z., Gong, J., Yan, X., Wang, B., (2011), Investigation of the effects of temperature and strain on the damping properties of polycarbonate / multiwalled carbon nanotube composites, *J. Phys. Chem. C.*, 115, 18468–18472.
3. Xiao, Y.L., Gong, Z.L., Gong, J., Gao, S., Zhang, Z.L., Wang, B., (2012) Investigation of the rheological and conductive properties of multi-walled carbon nanotube/polycarbonate composites by positron annihilation techniques, *Carbon.*, 50, 2899.
4. Zhou, W., Wang, J.J., Gong, Z.L., Gong, J., Qi, N., and Wang, B., (2009) Investigation of interfacial interaction and structural transition for epoxy/nanotube composites by positron annihilation lifetime spectroscopy, *Appl. Phys. Lett.*, 94, 021904.
5. Gao, S., Yan, X. L., Zhong, J., Xue, G. B., and Wang, B., (2013) Temperature dependence of conductivity enhancement induced by nanoceramic fillers in polymer electrolytes, *Appl. Phys. Lett.*, 102, p. 173903.
6. Gao, S., Zhong, J., Xue, G.B., Wang, B., (2014) Ion conductivity improved polyethylene oxide/lithium perchlorate electrolyte membranes modified by graphene oxide, *J. Membr. Sci.*, 470, 316.
7. Zhong, J., Gao, S., Xue, G.B., and Wang, B., (2015) Study on enhancement mechanism of conductivity induced by graphene oxide for polypyrrole nanocomposites, *Macromolecules.*, 39, 1592.
8. Xue, G.B., Zhong, J., Gao, S., and Wang, B., (2016) Correlation between the free volume and thermal conductivity of porous poly(vinyl alcohol)/reduced graphene oxide composites studied by positron spectroscopy, *Carbon.*, 96, 876

# Modeling and Simulation of P-Type $\text{Cu}_2\text{O}$ Thin-Film Transistors Using COMSOL Multiphysics

S. Alsharif, H. Farhan, H. Aljawhari  
King Abdulaziz University, Department of physics, Jeddah, Saudi Arabia

## Abstract:

Using COMSOL Multiphysics and the Semiconductor Module we were able to build a 3D model for the p-type  $\text{Cu}_2\text{O}$  thin film transistors (TFTs) for the first time. A comparison between three types of  $\text{Cu}_2\text{O}$  bottom gate TFTs was done using strontium titanate  $\text{SrTiO}_3$  (STO) as a gate dielectric, unpatterned, patterned channel and patterned channel and gate. The mechanism of current flow was clarified in each type in addition to transfer and output characteristics. The main objective of this modeling is to investigate the effect of interface traps and gate leakage on the performance of  $\text{Cu}_2\text{O}/\text{STO}$  TFTs. To achieve this goal, an ideal case, with no traps or current leakage, was assumed and modeled. As a result, we built a model which is capable of replicating the experimental results using some external parameters that are linked directly to the physical properties of the deposited  $\text{Cu}_2\text{O}$  films.

Our numerical simulations showed that trap states exist at the  $\text{Cu}_2\text{O}/\text{STO}$  interface are the main reason behind the deterioration of the performance of real  $\text{Cu}_2\text{O}$  transistors. Eliminating such effect could enhance the current on/off ratio by 8 orders of magnitude and boost the TFT mobility up to 5-11 folds.

**Keywords:** p-type  $\text{Cu}_2\text{O}$  TFTs, Ideal case, unpatterned TFTs, patterned channel TFTs, patterned channel and gate TFTs.

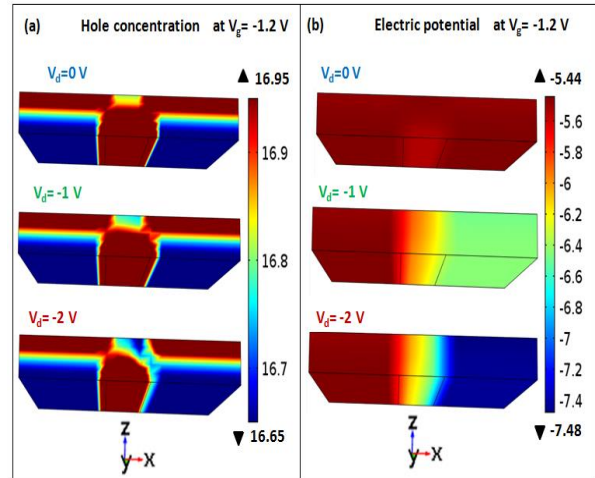


**Figure 1:** Figure illustrating the patterned channel and gate TFT for a gate voltage bias of  $-1.2$  V with changing the drain voltage  $V_d$ . (a) The hole concentration for each  $V_d$  and the pinch-off effect apparent. (b) Electric potential for each  $V_d$ .

## References:

1. Al-Jawhari, H. A., & Caraveo-Frescsa, J. (2014). Effect of Gate Dielectrics on the Performance of P-Type  $\text{Cu}_2\text{O}$  TFTs Processed at Room Temperature. Paper presented at the Advanced Materials Research.
2. Hong, D., Yerubandi, G., Chiang, H. Q., Spiegelberg, M. C., & Wager, J. F. (2008). Electrical Modeling of Thin-Film Transistors. *Critical Reviews in Solid State and Materials Sciences*, 33(2), 101-132. doi: 10.1080/10408430701384808

# MoN-decorated Nitrogen Doped Carbon Nanotubes Anode With High Lithium Storage Performance

Syed Mustansar Abbas<sup>1\*</sup>, Zia-ur-Rehman<sup>2</sup>, Ata-ur Rehman<sup>2</sup>, Nisar Ahmad<sup>1</sup>

<sup>1</sup>Nanoscience and Technology Department, National Centre for Physics, Islamabad, Pakistan

<sup>2</sup>Department of Chemistry, Quaid-e-Azam University, Islamabad, Pakistan

## Abstract:

The MoN nanoparticles in the size range of 20–30 nm are dispersed onto the surface of nitrogen doped CNT (MoN/N-CNT) by annealing at 600 °C kept under a constant flow of nitrogen gas for 4 hrs. The N-doping of CNT is confirmed from the characteristic Raman shift. The as-synthesized nanoparticles display hexagonal MoN phase with sharp mesoporous internal structure and a high surface area of 369 m<sup>2</sup> g<sup>-1</sup>. As an anode material, the composite structure demonstrates high reversible capacity, long cycle life and excellent rate performance. A reversible capacity of 1232 mAh g<sup>-1</sup> is maintained after 200 cycles at a current density of 100 mA g<sup>-1</sup>. When the electrode is tested at higher current densities of 1000, 1200 and 1500 mA g<sup>-1</sup> for 20 cycles each, it still holds a high specific capacity of 1184.7, 1096.5 and 989.5 mAh g<sup>-1</sup>. This electrochemical performance is also compared with bare MoN, N-CNT, MoO<sub>2</sub> and MoO<sub>2</sub>/functionalized-CNT anodes. The superior electrochemical performance is credited to the nitrogen doping of CNT which reduce the charge transfer resistance along with the higher conductivity of MoN due to the substitution of oxygen octahedral sites of MoO<sub>2</sub> with nitrogen atoms.

**Keywords:** Carbon nanotubes, Composites, Lithium ion battery, Raman spectroscopy, Chemical vapour deposition (CVD)

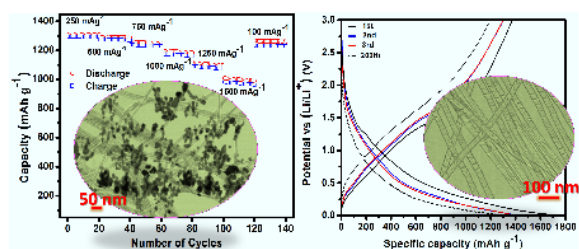


**Figure 1:** (a) Rate capability of MoN/N-doped CNTs at various current densities between 100 and 1500 mA g<sup>-1</sup> while inset represents TEM image of the same, (b) Charge/discharge curves of N-doped CNTs along with their TEM image

## References

1. Afanasiev, P. (2015) New approach to the preparation of highly dispersed transition metals sulfides and nitrides, *Catal. Today.*, 250, 134-44.
2. Fu, Z W., Wang, Y., Yue, X L., Zhao, S L., Qin, Q Z. (2004) Electrochemical reactions of lithium with transition metal nitride electrodes, *J. Phys. Chem. B.*, 108(7), 2236-44.
3. Dong, S., Chen, X., Zhang, X., Cui, G. (2013) Nanostructured transition metal nitrides for energy storage and fuel cells. *Coord. Chem. Rev.*, 257(13), 1946-56.



# Low Frequency Noise Spectroscopy in n-channel UTBOX devices with 20 nm Si film

B. Nafaa<sup>1,4,\*</sup>, B. Cretu<sup>2,3</sup>, N. Ismail<sup>4</sup>, O. Touayar<sup>4</sup>, E. Simoen<sup>5,6</sup>, J.-M. Routoure<sup>1,3</sup>, R. Carin<sup>1,3</sup>, M. Aoulaiche<sup>5</sup>, C. Claeys<sup>5,6</sup>

<sup>1</sup>University of Caen Basse-Normandie, UMR 6072 GREYC, F-14050, Caen, France

<sup>2</sup>ENSICAEN, UMR 6072 GREYC, F-14050, Caen, France

<sup>3</sup>CNRS, UMR 6072 GREYC, F-14032, Caen, France

<sup>4</sup>National Institute of Applied Science and Technology, MMA, Tunis, Tunisia

<sup>5</sup>Imec, Kapeldreef 75, B-3001 Leuven, Belgium

<sup>6</sup>E.E. Dept. KU Leuven, Kasteelpark Arenberg 10, B-3001 Leuven, Belgium

## Abstract:

Low frequency noise is a non-destructive diagnostic tool for predicting device quality. In this work, it was studied in a temperature range of 200 K up to 330 K for n-channel fully depleted UTBOX transistor fabricated on silicon on insulator (SOI) substrate, with gate length of 0.15  $\mu\text{m}$  and a high-k gate dielectric. It was found that the noise spectra contain  $1/f$  and Lorentzian components (figure 1). When performed as a function of temperature, the generation-recombination (GR) noise, corresponding to a Lorentzian type of spectra, was analyzed using the so-called noise spectroscopy (Grassi *et al.*, 2001). These investigations allowed to evaluate the quality of the gate oxide interface, to identify traps in the silicon film and to make a correlation between the observed traps and some device processing steps. It was observed that some additional process steps used to boost the device performances seem to increase the trap densities in the film. For the device already studied, six traps were identified (inset of figure 1): two traps related to hydrogen ( $\text{V}_2\text{H}$ ) and ( $\text{VOH}$ ), that may result from hydrogen incorporation during the selective epitaxial growth (SEG), a trap related to phosphor ( $\text{V-P}$ ), that may originate from highly doped drain implantation (HDD) and three traps related to carbon ( $\text{CiOi}$ ), ( $\text{CiPs}$ ) and ( $\text{BiCs}$ ), that may result from a carbon contamination during the SEG process.

**Keywords:** UTBOX transistors, thin silicon film, low frequency noise, Lorentzian, noise spectroscopy, temperature, traps.

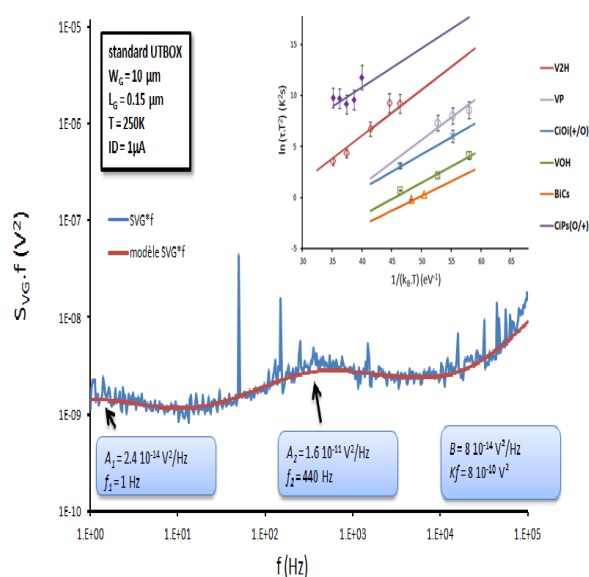


**Figure 1:** Modelling a noise spectrum for UTBOX with physical gate length of 0.15  $\mu\text{m}$  at a temperature of 250K. In the inset: Arrhenius diagram plot for the same structure.

## References:

Grassi, V., Colombo, C.F., Camin, D.V. (2001), Low frequency noise versus temperature spectroscopy of recently designed Ge JFETs, *IEEE Trans. Electron Dev.*, 48, 2899- 2905.

# Aluminum oxide nanopores and nanowires

F. Flores-Gracia, J. Martínez-Juárez, J.A. Luna-López, R.R. González-Jiménez

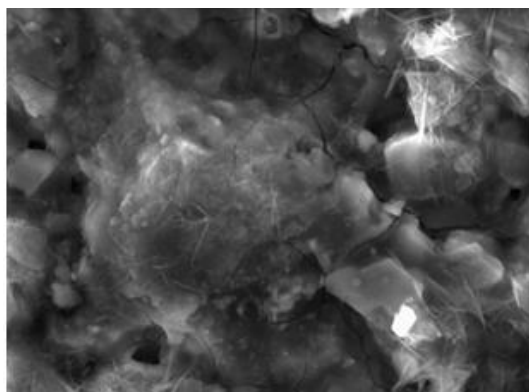
Centro de Investigaciones en Dispositivos Semiconductores. Benemérita Universidad Autónoma de Puebla.  
Puebla, México

## Abstract

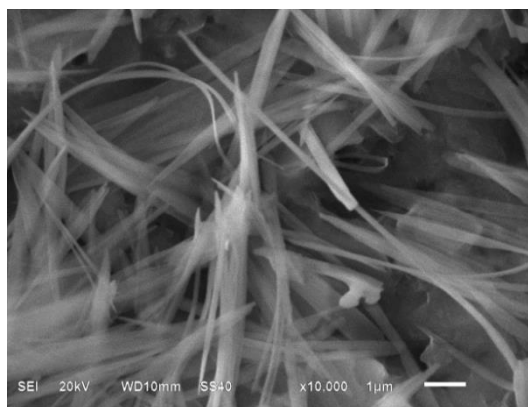
The purpose of this work is the fabrication of anodized aluminum self-organized porous nanostructures by two step anodized oxidation and sol-gel techniques.

A porous anodic aluminium oxide template was prepared by anodizing high purity (99.9%) aluminum film (1 cm<sup>2</sup> area, 0.5 and 0.13 mm thickness) in oxalic acid solution as an electrolyte. In order to investigate the effect of the time of first anodization on the pore diameters, four samples were prepared in different times in sodium oxalate solution diluted in 0.5 to 2M concentrations at 58°C and 10, 20, 30, 60, 120, 180 y 240 minutes of anodizing times. The samples showed structures like fibers, nanowires and nanopores with several characteristics depending on the parameters of fabrication.

Different techniques, such as Scanning Electron Microscopy (SEM), Energy Dispersive Spectrum (EDS) and photoluminescence were employed to study the structure of AAO templates and alumina nanopores and nanowires. The Figure 1b shows the formation of nanowires.



a



b

**Figure 1.** SEM images. 0.5 M concentration, 58°C. a) 20 minutes anodization time, b) 60 minutes anodization time.

## References

1. Azadeh Nazemi, Ahmad Najafian, Seyed Abolfazl Seyed Sadjadi. Aluminium oxide nanowires synthesis from high purity aluminium films via two-step anodization. *Superlattices and Microstructures*. Vol 81, May 2015, pages 1-6
2. Lan Shen, Mubarak Ali, Zhengbin Gu, Bonggi Min, Dongwook Kim, Chinho Park. Preparation of anodic aluminum oxide (AAO) nano-template on silicon and its application to one-dimensional copper nanopillar array formation. *Korean Journal of Chemical Engineering* January 2013, Volume 30, Issue 1, pp 221-227
3. J.H. Chen, C.P. Huang, C.G. Chao, T.M. Chen. The investigation of photoluminescence centers in porous alumina membranes. *Applied Physics A*. August 2006, Volume 84, Issue 3, pp 297-300.
4. S. K. Lazarouk , P. S. Katsuba, A. A. Leshok, V. B. Vysotskii. Effect of the local electric field on the formation of an ordered structure in porous anodic alumina. *Physical Science Of Materials. Technical Physics*. September 2015, Volume 60, Issue 9, pp 1343-1347

# Temperature Controlled Growth of Ag Nanoparticles by Physical Vapor Deposition

Feras G. Alzubi<sup>1</sup>, Reem M. Alrashed<sup>1</sup>

<sup>1</sup>Energy and Building Research Center, Kuwait Institute for Scientific Research, Safat 13109, Kuwait

## Abstract:

Nanoparticles of Nobel metals have shown tremendous breakthrough in enhancing the performance of optoelectronic devices through improving light absorption. Multiple chemical and physical techniques have been used to fabricate the nanoparticles at desired sizes and shapes. Hence, the exceptional properties of these NPs depend on their structure which is affected by the processing conditions. Utilizing physical vapor deposition (PVD) technique to produce thin-films usually is followed by thermal annealing these films to produce uniform NPs. Here in this work, we report the effect of the variation of the annealing temperature on the formation of Silver (Ag) NPs and their structural parameters such as size and distribution. Ag films are produced by PVD with fixed thickness of 4nm, followed by thermal annealing in inert atmosphere at temperatures of (500, 600, 700, 800°C) on silicon substrates for 30 minutes. The absorption spectra of the formed NPs are compared to the as-deposited thin films. UV-Vis absorption and reflectance measurements, atomic force microscopy (AFM), and scanning electron microscope (SEM) studies were carried out. Annealed samples showed clear formation of Ag NPs recognizable in the absorption spectra, which designates the presence of Ag NPs comparing to the un-annealed. Absorption peaks show shifts with wavelength as temperature change. AFM images showed the formation of Ag NPs in annealed films and clearly showed the surface roughness and typography of Ag NPs at diameter variation from 50 to 130nm for temperature of 800 °C. NPs were about 400 nm apart in average with surface roughness of 0.7 nm comparing to the very smooth surface of un-annealed sample. Ag NPs distribution and size varied with varying annealing temperature as illustrated in the paper. Our study provides deep insight on the effect of temperature on the formation of nanoparticles and their optical and structural properties. The produced results herein can be further utilized to determine the proper processing conditions to produce efficient NPs that can be used as enhancers in optoelectronic devices.

**Keywords:** Metallic Nanoparticles, Noble Nanoparticles, PVD, AFM, Absorption spectra, Temperature Annealing.

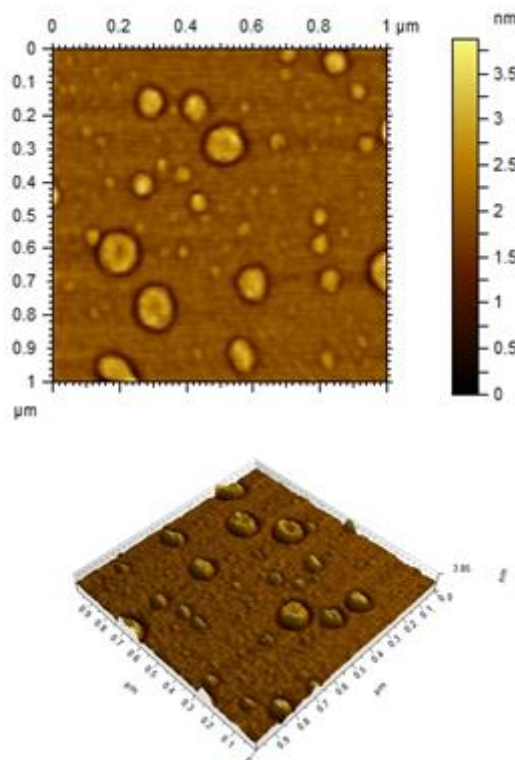


**Figure 1:** Atomic force microscopy topography of annealed Ag films at 800 °C for 30 minutes in inert atmosphere. (a) 1x1 μm surface and (b) Three dimensional image 5x5 μm surface of Ag NPs on Si substrate showing individual NPs.

## References:

1. Atwater, H. A., and Polman, A. 2010. Plasmonics for improved photovoltaic devices. *Nature Materials* **9**: 205-213.
2. Kumar, S. S., Venkateswarlu, P., Rao, V. R., and Rao, G. N. 2013. Synthesis, characterization and optical properties of zinc oxide nanoparticles. *International Nano Letters* **3**: 30, 1-6.

**Posters Session II: June 2<sup>nd</sup>, 2016**

**Nanotech France 2016:  
NanoBioMedecine / NanoSafety**

# Investigation of Biomolecule Release Behaviours From Titanium Surfaces with Controllable Porosity

C. Bayram

Hacettepe University, Advanced Technologies Application and Research Center, Ankara, TURKEY

## Abstract:

Active agent release from metallic implant surfaces has always been a challenge for researchers since the lack of chemical moiety at the surface of the metal. Polymer and organic coatings are also not sufficient efforts and may create major drawbacks such as lamination from the implanted surface after the biodegradation. In the past decade, the release of biologically active molecules directly from the metal surfaces has become one of the extensively studied research topics for the implant bioactivity[1,2]. Nanotubular structures having diameters of less than 100 nm can be originated from the titanium surfaces with controllable length with a technic called anodic oxidation and many studies were conducted by using these structures local active agent releasing reservoirs. The major disadvantage encountered in biomolecule releasing titanium nanotubes is the uncontrollable nature of the release kinetic. Nanotube diameters, which are several times bigger than the biomolecule can become a real disadvantage in releasing, as they interacted with the biologic fluid, releasing more than the half of loaded amount of molecule in the first couple of hours. In this study, nanotube diameters were narrowed by gold sputtering after biomolecule loading into them. Gold sputtering is a non-destructive and cold process which is not harmful for the biological materials. The effect of sputtering time to the releasing time behaviour were investigated in terms of diameter and the hydrodynamic radius of the biomolecule. It was found that as the tube diameters get narrowed, the more release duration was observed; however, this is much more in valid for large biomolecules with higher hydrodynamic radius.

**Keywords:** titanium, implant, anodic oxidation, controlled release.

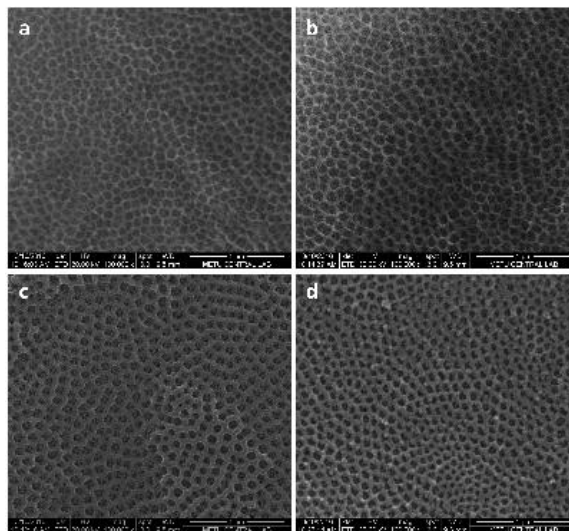


**Figure 1:** TiO<sub>2</sub> surfaces with narrowing diameters after gold sputtering. Anodized only (a) , gold sputtered for 2 min (b), 5 min (c) and 10 min (d)

## References:

1. Aw, M. S., Kurian, M., Losic, D. (2014) Non-eroding drug-releasing implants with ordered nanoporous and nanotubular structures: concepts for controlled drug release, *Biomater. Sci.*, 2, 10.
2. Damodaran, V. B., Bhatnagar, D., Leszczak, V., Popat, K. C., (2015), Titania structures: a biomedical perspective, *RSC Advances*, 5, 37149.



# UV Crosslinkable PLGA-*b*-PEG Nanoparticle Integrated Gel Networks for Topical Drug Delivery

M. Gultekinoglu,<sup>1,3,\*</sup> I. Eroglu,<sup>1</sup> C. Bayram,<sup>2</sup> E.A. Aksoy,<sup>1</sup> K. Ulubayram,<sup>1,2,3</sup>

<sup>1</sup>Department of Basic Pharmaceutical Sciences, Faculty of Pharmacy, Hacettepe University, Turkey

<sup>2</sup>Advanced Technologies Application & Research Center, Hacettepe University, Turkey

<sup>3</sup>Bioengineering Division, Institute for Graduate Studies in Science & Engineering, Hacettepe University, Turkey

<sup>4</sup>Nanotechnology & Nanomedicine Division, Institute for Graduate Studies in Science & Engineering, Hacettepe University, Turkey

## Abstract:

UV crosslinkable gel networks became very popular in biomedical and pharmaceutical approaches thanks to the high yield and easy processing properties. Poly lactic-co-glycolic acid (PLGA) is an oil based hydrophobic polymer, widely used in biomaterials in various forms such as tissue scaffold, membrane and micro-nano particles thanks to its excellent biocompatibility and non-toxic degradation products. Although the advantages of the PLGA is high in number, one of the few major drawbacks of PLGA is the hydrophobicity, which hinders its use in aqueous media. PLGA can be conjugated with poly ethyleneglycol (PEG) and the resulting co-polymer has an amphiphilic character and this property can be exploited in hydrophobic drug encapsulation. Drug and PLGA interact hydrophobically while the PEG part maintain the water solubility of the nanoparticle.

Ibuprofen, is a nonsteroidal anti-inflammatory drug and commonly used for the treatment of pain, fever and inflammation. However, excess amount of ibuprofen may also cause side effects, like other orally administrated drugs, such as rash, acid reflux and even gastrointestinal bleeding. Hence, locally released and effectively dosed ibuprofen should be used in especially topical formulations to avoid aforementioned side effects. The aim of this study, to design PLGA-*b*-PEG nanoparticle integrated gel networks via uv crosslinking method for topical delivery of ibuprofen.

In this study, PLGA-*b*-PEG co-polymer with carboxyl ended functional group was synthesized through the conjugation of PLGA-COOH to COOH-PEG-NH<sub>2</sub>. PLGA-*b*-PEG nanoparticles containing ibuprofen was synthesized via mini emulsion method and an additional step was conducted to introduce a photocrosslinkable moiety into PLGA-PEG block co-polymer after the nanoparticle synthesis. Carboxyl ended

PEG chains were methacrylated with 2-aminoethyl methacrylate via EDC (1-Ethyl-3-(3-dimethylaminopropyl)-carbodiimide) procedure and the resulting particles were further exposed to ultraviolet radiation at 365 nm, in order to create a network both intraparticle and interparticles.

Structural and chemical characterizations of drug encapsulated nanoparticles were carried out with infrared spectroscopy and scanning electron microscopy imaging. The change in the particle size, zeta-potential before and after the applied modifications were also analyzed via dynamic light scattering technique. The mean diameter of nanoparticles were determined as 230 nm; after the uv exposure the resulting nanoparticle cluster network was observed with several micron in size. The resulting network gels impregnated with PLGA-*b*-PEG nanoparticles can be offered as an effective topical formulations for ibuprofen delivery.

**Keywords:** PLGA, PEG, uv crosslink, ibuprofen, mini emulsion, biomedical applications.

## References:

1. Baysal, I., Ucar, G., Gultekinoglu, M., Ulubayram, K., & Yabanoglu-Ciftci, S. (2016). Donepezil loaded PLGA-*b*-PEG nanoparticles: their ability to induce destabilization of amyloid fibrils and to cross blood brain barrier in vitro. *Journal of Neural Transmission*, 1-13.
2. Wu, Y., Wang, L., Guo, B., & Ma, P. X. (2014). Injectable biodegradable hydrogels and microgels based on methacrylated poly (ethylene glycol)-co-poly (glycerol sebacate) multi-block copolymers: synthesis, characterization, and cell encapsulation. *Journal of Materials Chemistry B*, 2(23), 3674-3685.

# New Outlook on Parkinson's Treatment: A Dual Targeting Nanoparticle Complex for More Efficient Delivery of Curcumin Improves Neuroprotection

Nathan Beals<sup>1\*</sup>, Prakash Kharel<sup>1</sup>, Werner Geldenhuys<sup>2</sup>, and Soumitra Basu<sup>1</sup>

Kent State University, Department of Chemistry and Biochemistry<sup>1</sup>  
West Virginia University, School of Pharmacy<sup>2</sup>

## Abstract:

Common features in the pathogenesis and progression of the neurodegenerative disease Parkinson's (PD) has been correlated with oxidative damage and activation of the inflammatory cascade. Therapeutic small molecules have been shown in research to decrease biochemical inflammatory elements (cytokines, cyclooxygenase-2 (COX-2), nuclear transcription factor-kB (NF-kB)) and oxidative damage by decreasing ROS species in neuronal cellular and mouse models. Curcumin, a dietary small molecule seen in the common Indian spice curry, has been established as an encouraging therapeutic for these neurodegenerative precursors but flaws in bioavailability due low blood solubility and low retention in the brain have resulted in little success in recent human trials. To overcome these issues, we developed a novel heptameric nanoparticle drug delivery complex that emphasizes 1) increases in curcumin solubility and 2) two targeting aptamers that look to improve migration across the blood brain barrier and specifically target dopaminergic cells. Our goal is to demonstrate a substantial increase in the therapeutic effect of curcumin in terms of neuroprotection by subsiding negative effects correlated with PD progression. In vitro, confocal microscopy done with SHSY5Y recognized a targeted response when comparing TrkB aptamer and non-aptamer complexes. ROS concentration was measured through DCFDA assays, showing a 15% decrease when treated with the full complex compared to control cells in a high H<sub>2</sub>O<sub>2</sub> environment, a 12-fold improvement compared to free curcumin. In vivo results displayed after 30 minutes, the full complex entered the brain and immunohistochemistry gave evidence to a therapeutic response with reduction of oxidative stress and inflammatory factors.

**Keywords:** Gold Nanoparticles, Parkinson's, Neurodegenerative Diseases, Curcumin, Inflammation, Oxadative Stress, Hyaluronic Acid, Aptamers

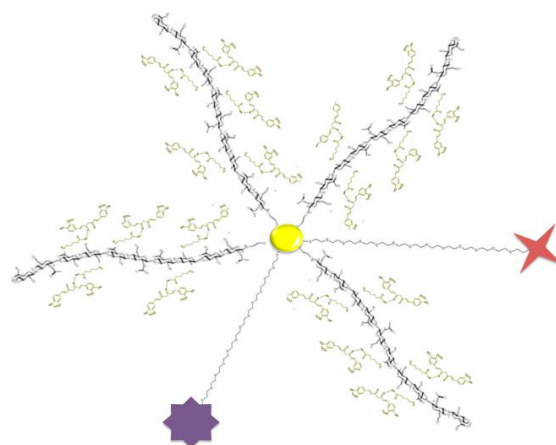


**Figure 1:** Diagram of the heptameric nanoparticle complex utilizing a gold center, curcumin loaded hyaluronic acid, and two different PEGylated targeting aptamers

## References:

1. Darvesh, A *et al.* (2012) *Expert Opin. Investig. Drugs*, 21(8):1123-1140
2. Monroy, A, Lithgow GL, and Alavez. (2013) *S. Biofactors*, 39(1); 122-132
3. Zipp F, Aktas O. (2006) *Trends Neurosci*, 29; 518-27
4. Aggarwal BB and Harikumar KB. (2009) *Int J Biochem Cell Biol*, 41; 40-9

# Biodegradable mesoporous silica nanoparticles from synthesis to anti-cancer application

S. Seré,<sup>1,\*</sup> J. Belmans,<sup>2</sup> B. De Roo,<sup>1</sup> M. Vervaele,<sup>1</sup> S. Van Gool,<sup>3</sup> J. P. Locquet<sup>1</sup>

<sup>1</sup>KU Leuven, Department of Physics and Astronomy, Belgium

<sup>2</sup>KU Leuven, Department of Microbiology and Immunology, Belgium

<sup>3</sup>Pediatric hemato-oncology, Department of Paediatrics, University Hospital RWTH Aachen Germany

## Abstract:

Despite the standard treatment, the prognosis of glioblastoma multiforme patients remains dismal. New therapies, like dendritic cell immunotherapy, are emerging to overcome the limitations of the current treatment. Multiple groups use this therapy and observe long term survival in several patients. Important disadvantages of this patient customized treatment are its high cost and limited efficacy.

Based on our preliminary results from *in vivo* studies with polystyrene nanoparticles, the use of nanoparticles may provide a solution. We report the production of biodegradable mesoporous silica nanoparticles (MSNPs), loaded with tumor lysate, to stimulate the adaptive immune system. The nanoparticles were synthesized using a wet chemistry process, as illustrated in Figure 1. The physicochemical properties of the synthesized MSNPs were investigated with transmission electron microscopy, small angle X-ray scattering, dynamic light scattering and zeta potential measurements. Afterwards, the nanoparticles were loaded with lysate, and the general effect of the nanovaccine was investigated *in vitro* on dendritic cells.

The nanoparticles were determined to be stable at physiological pH due to their negative surface charge. Additionally, the dendritic cells have shown to take up the MSNPs, as well as the vaccine bound to the particles. This uptake was determined to be mostly an ATP-dependent process. Moreover, it was determined that the nanovaccines could induce maturation of dendritic cells, which was not observed for polystyrene nanoparticle based vaccines used in our previous experiments. Therefore, the MSNP vaccines could possibly have an adjuvant effect on the dendritic cells and perhaps the adaptive immune response.

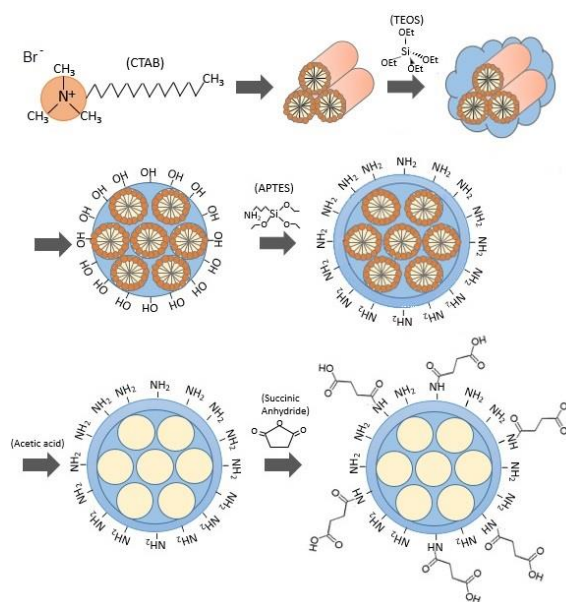


**Figure 1:** Schematic representation of the wet chemistry process for the MSNP synthesis and functionalization.

**Keywords:** Nanoparticles, dendritic cells, nanovaccine, immunotherapy, glioblastoma.

## References:

1. Seré, S. (2015) Unpublished master thesis.
2. Belmans, J. (2016) In press

# Formulation and Characterization of Liposomes Loaded with Resveratrol using Plackett-Burman Experimental Design

Sarmad Al-Edresi<sup>1,2</sup>, Sally Freeman<sup>1</sup>, Harmesh Aojula<sup>1</sup>, Jeffrey Penny<sup>1</sup>

<sup>1</sup> Manchester Pharmacy School, University of Manchester, UK, M13 9PL

<sup>2</sup> School of Pharmacy, University of Kufa, Najaf, Iraq

## Abstract

**Background:** Resveratrol has been reported to possess strong neuroprotective, cardioprotective, anti-inflammatory and powerful antioxidant activities [1]. Liposomes, composed of DSPC and cholesterol, are considered a promising vehicle for transporting resveratrol to the site of action [2]. More than often, the optimisation of liposome composition during early phase research is conducted by trial-and-error. This can be expensive and time consuming due to the large number of variable parameters, in the manufacture procedure, which influences important characteristics ranging from physical size to drug loading efficiency.

**Aim:** The aim of the present study was to investigate and screen eleven variables including: the weight of DSPC, weight of cholesterol, solvent volume, solubilisation temperature, rotation speed, vacuum, freeze-dryer time, re-hydration temperature, re-hydration rotation speed, extrusion pressure and extrusion repetition using Plackett-Burman design to determine which variable(s) significantly affect the particle size (PZ), polydispersity index (PDI), loading capacity (LC%), entrapment efficacy (EE%) and *in vitro* release (R%).

**Method:** Liposomes were prepared by a thin lipid film method and extrusion [3]. Surface response methodology (RSM) (Fig. 1), Pareto chart and half normal plots were used to evaluate the variables. Shapiro-Wilk p-value was used to statistically identify the most effective variable.

**Results:** The 13 liposome preparations had particle sizes ranging between 84-320 nm and a PDI between 0.07-0.4. The LC ranged between 1.3-17% and the EE was between 0.1-1.5%. In general, preparations could be categorised into four types depending on resveratrol release profiles; 6 formulations showing instant release, 2 having release after 18 h, 1 exhibiting delayed release after 24 h, and 4 with no detectable release. The most

effective variables that produced smallest particle sizes, smallest PDI, highest LC%, highest EE% and fastest release were extrusion pressure, solvent volume and re-hydration rotation speed.

**Conclusion:** Plackett-Burman design was proven to be a valuable tool to quickly and precisely optimise liposomes loaded with resveratrol and made from DSPC and cholesterol. The optimum preparation had stable, small particle size, high LC and instant release prepared at short time (~ a week) with low cost could be produced by relying on RSM.

**Keywords:** liposome, resveratrol, Plackett-Burman design

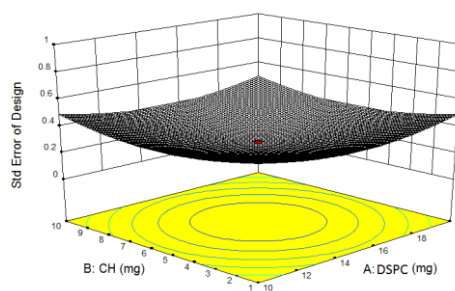


**Fig. 1:** Response surface methodology of the Plackett-Burman design created by Design Expert® software

## References:

1. Caddeo, C., *et al.*, Effect of resveratrol incorporated in liposomes on proliferation and UV-B protection of cells. *Int J Pharm*, 2008. 363(1-2): p. 183-91.
2. Fabris, S., *et al.*, Antioxidant properties of resveratrol and piceid on lipid peroxidation in micelles and monolamellar liposomes. *Biophys Chem*, 2008. 135(1-3): p. 76-83.
3. Isailović, B.D., *et al.*, Resveratrol loaded liposomes produced by different techniques. *Innovative Food Science & Emerging Technologies*, 2013. 19(0): p. 181-189.

# Biological interactions monitoring of B-16 Melanoma cells using electrochemical impedance spectroscopy

Catalin Marculescu, Bianca Tincu, Andrei Avram, Tiberiu Burinaru, Corneliu Voitincu and Marioara Avram  
National Institute for Research and Development in Microtechnologies - IMT-Bucharest, Romania

**Abstract:** The melanoma is one of the most aggressive human cancer types. Its malign nature is characterized by melanoma cells capacity of invading the tissue forming metastasis (Lee et al.; 2014). The current melanomas diagnosis criteria used to determine the treatment choice, include the tumour thickness, invasion, the lymphatic nodules presence and organ metastasis. A problem raised by this diagnose algorithm is that the classified tumours for a certain stage can evolve without any progress in their treatment, meaning a shorter path to metastasis and even death. Therefore, the discovery of biomarkers that can reflect the stage and the evolution of the melanoma with large precision is a necessity. One of the proposed method in this preliminary study for the biological interactions monitoring at tumour cells level implies the use of real time modern characterization techniques of the processes that occur at the sensor interface with the bio-cells: the electrochemical impedance spectroscopy (EIS) (Hu et al.; 2013). This was performed using an electrochemical biosensor with inter-digitised nano-electrodes (Fig. 1). The analyte molecules from the liquid sample in contact with the electrochemical sensor determine the increase of double-layer capacitance and of charge transfer resistance at high frequencies, and the increase of mass molecular transport (diffusion) at low frequencies. The melanoma cells interactions are illustrated and differentiated from a reference solution in Fig. 2 using the Nyquist impedance diagram.

**Keywords:** melanoma, cancer diagnosis, electrochemical biosensor, inter-digitised nano-electrodes, electrochemical impedance spectroscopy, biomedical applications.

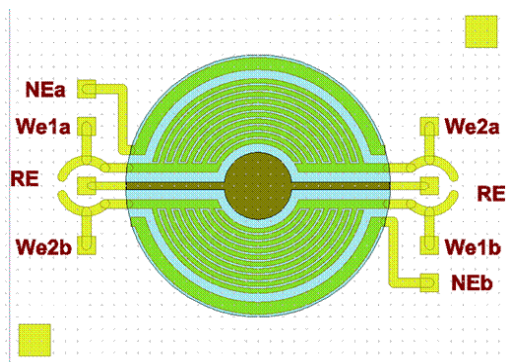


**Figure 1:** Figure illustrating the electrochemical biosensor with inter-digitised nano-electrodes.

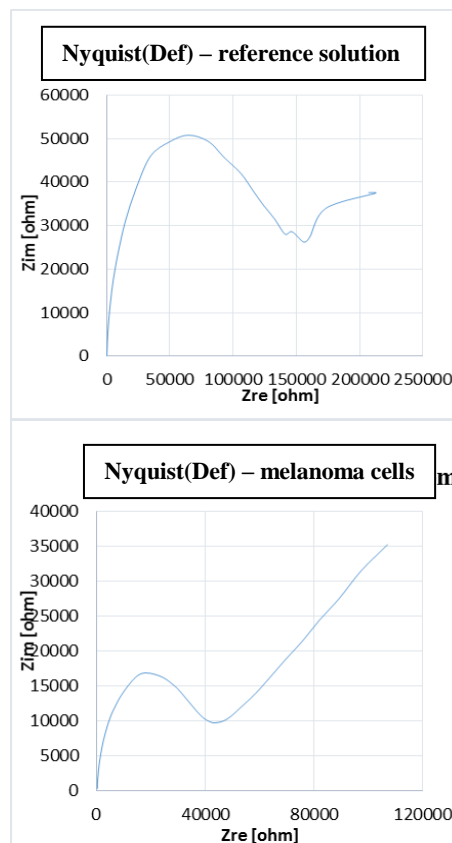


**Figure 2:** Nyquist diagram of reference solution (up) and melanoma cells (down) impedance.

## References:

1. Lee, N., Barthel, S.R., Schatton, T., (2014) Melanoma stem cells and metastasis: mimicking hematopoietic cell trafficking?, *Laboratory Investigation*, 94, 13–30.
2. Hu, Y., Zuo, P., Ye, B.C., (2013) Label-free electrochemical impedance spectroscopy biosensor for direct detection of cancer cells based on the interaction between carbohydrate and lectin, *Biosensors and Bioelectronics*, 43, 79–83.

## Acknowledgements:

This work is funded by UEFISCDI in the Partnership Framework: PN-II-PT-PCCA-2013-4-0366, no. 208/2014 and PN-II-PT-PCCA-2011-3.1-0052, no. 02/2012.



# Formulation and in Vitro Evaluation of Simvastatin Loaded Nanostructured Lipid Carriers

D. Örgül<sup>1</sup>, H. Eroğlu<sup>1</sup>, S. Hekimoğlu<sup>1</sup>

<sup>1</sup>Hacettepe University, Faculty of Pharmacy, Dept. of Pharmaceutical Technology, Ankara, Turkey

## Abstract:

Simvastatin (SV) is a member of the group of 3-hydroxy-3-methylglutaryl coenzyme A reductase (HMG-CoA) inhibitors and commonly used as an effective cholesterol lowering agent. It is well known that regardless of the mechanism of cholesterol lowering effects, simvastatin is also effective on wound healing depending on immune-modulator, anti-inflammatory and angiogenic effects. It is noteworthy that when the limited number for local use of simvastatin is investigated, classical dosage forms such as ointments or creams are generally used. Therefore, in this study nanostructured lipid carrier (NLC) formulations were evaluated for creating a new perspective as an alternative therapeutic option with the aim of topical treatment of diabetic wound healing. NLC formulations were prepared by using the high-pressure homogenization technique and characterized with the parameters of particle size, polydispersity index (PDI), zeta potential, morphology, drug-lipid matrix interaction (DSC, FTIR), drug loading, drug entrapment efficiency and in-vitro release study. In order to prepare formulations having optimum particle size distribution with maximum drug-lipid matrix interaction, high entrapment efficiency and maintaining sustained drug release profile over a certain period of time, several independent variables (different liquid lipids, liquid:solid lipid ratios and amount of simvastatin) were investigated. The resulting NLC formulations were as a suspension of spherical nanosized homogeneous particles with significantly high entrapment efficiency (>99%) (Figure 1). Average particle size for all formulations was within the range of 120-230 nm. Polydispersity index (PDI) values of all formulations were recorded as less than 0.35. The entrapment of simvastatin in the lipid matrix was verified by its high entrapment efficiency and by the absence of endothermic or characteristic peaks according to DSC and FTIR analysis (Figure 2). The release of simvastatin from the NLC formulations was characterized by an initial burst release of approximately 55% within the first hour, which is followed by a sustained release period. As a result of this study, simvastatin loaded NLC

formulations can be considered as suitable candidates for treating diabetic wounds depending on the results of in-vitro characterization studies.

**Keywords:** simvastatin, nanostructured lipid carriers, NLC, wound healing

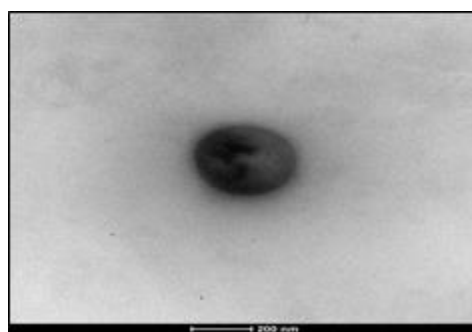


**Figure 1:** Transmission electron microscopic image of SV loaded NLC (x30,000)

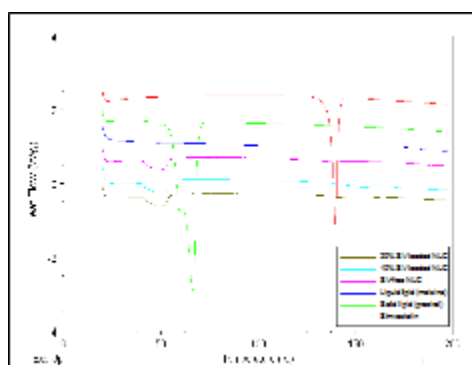


**Figure 2:** DSC thermogram of NLC formulations and ingredients

## References:

1. Asai J., et al. (2012) Topical simvastatin accelerates wound healing in diabetes by enhancing angiogenesis and lymphangiogenesis. *Am J Pathol*, 181, 2217-24.
2. Vitorino, C., et al. (2013a.) Coencapsulating nanostructured lipid carriers for transdermal application: from experimental design to the molecular detail, *J Control Release*, 167(3): 301-314.

# Kinetics of mRNA Onset Time in Single Cell Arrays

N. Mehrotra<sup>1</sup>, A.Reiser<sup>1</sup>, R. Krzyszton<sup>1</sup>, Joachim O. Rädler<sup>1</sup>

<sup>1</sup>Ludwig-Maximilians-University, Faculty of Physics and Center for NanoScience (CeNS, Munich, Germany.

## Abstract:

Since the first non-viral delivery experiment for mRNA transfection, extensive research has been carried out to study and optimize different delivery agents and their efficiency for controlled delivery. There have been some reports on the study of kinetics of mRNA delivery, however the role of transfection agents on the kinetics of mRNA onset time after transfection still needs further exploration. Here we analyze the distribution in mRNA onset time as a function of physicochemical properties of different transfection agents and target cell populations. Automated time-lapse microscopy combined with micropatterned arrays allows the generation of single cell fluorescence curves after mRNA transfection. The single cell time curves obtained have been fitted and analyzed to study the uptake

kinetics followed by different transfection agents.

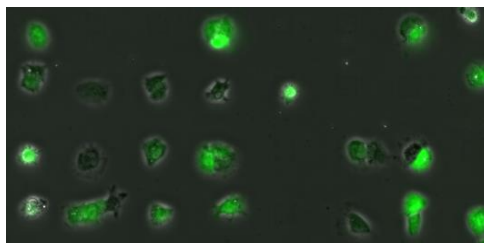


**Figure 1:** Single cell array microscopy images used to analyse eGFP expression to study kinetics of mRNA onset

**Keywords:** mRNA transfection, single cell studies, time lapse microscopy, micropatterning, nucleic acid delivery

# Magnetocaloric effect for inducing hypothermia as new therapeutic strategy for stroke

Ramón Iglesias,<sup>1</sup> Alba Vieites-Prado,<sup>1</sup> Bárbara Argibay,<sup>1</sup> Francisco Campos,<sup>1</sup> Manuel Bañobre-López,<sup>3</sup> Tomás Sobrino,<sup>1</sup> José Rivas,<sup>2,3</sup> José Castillo,<sup>1</sup>

<sup>1</sup>Clinical Neurosciences Research Laboratory, Health Research Institute of Santiago de Compostela (IDIS), Department of Neurology, University Clinical Hospital Hospital, Santiago de Compostela, Spain.

<sup>2</sup>Department of Applied Physics, Technological Research Institute, Nanotechnology and Magnetism Lab—NANOMAG, Universidade de Santiago de Compostela, Spain.

<sup>3</sup>INL - International Iberian Nanotechnology Laboratory, Braga, Portugal.

**Abstract:** Hypothermia is potentially the most effective protective therapy for brain ischemia, although its use in stroke patients is limited due to side effects.[1] The induction of hypothermia is achieved through the systemic reduction of body temperature (using thermal covers, immersion in cooling fluids or endovascular cooling devices) which results in a complex system associated in many cases to severe complications such as, pneumonia and cardiac arrhythmia.[2] However, focal hypothermia, with lower stress effects, represents a promising alternative poorly studied in ischemia.

In order to find alternative strategies based on focal brain hypothermia, without the secondary side-effects associated to systemic hypothermia, the combination of magnetic nanoparticles and electromagnetic fields (EMF) could constitute a suitable candidate for it. In this study, magnetic refrigeration, based on the magnetocaloric effect (MCE), is explored as procedure for the generation of focal hypothermia in the brain. MCE is an intrinsic property of magnetic materials. Near the Curie temperature, changes in the magnetization with the magnetic field are maximized and induce large variation in the entropy of the magnetic material. In adiabatic conditions, this leads to temperature variations (Figure 1A).[3]

As a first approach, we have developed a simple device to evaluate *in vitro* the thermodynamic behavior of different concentrations of commercial gadolinium (Gd) powder as a reference magnetocaloric material (Figure 1B). The samples, properly thermally insulated, were cyclically magnetized and demagnetized at room temperature by 1T permanent magnets in order to induce an adiabatic magnetic effect. This study will allow us to discuss and elucidate the best conditions about the use of new materials and strategies for further *in vivo* experiments.

**Keywords:** biomedical applications, biomaterials, hypothermia, magnetocaloric material, nanomaterials, stroke

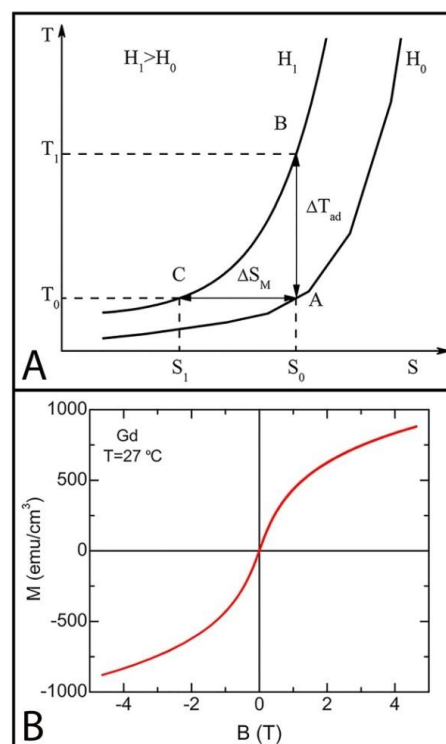


**Figure 1:** (A) Temperature-Entropy diagram illustrating the MCE (adiabatic temperature change,  $\Delta T_{ad}$ ; and isothermal magnetic entropy change,  $\Delta S_M$ ). (B) Hysteresis curve of Gd used in our experiments measured in a SQUID magnetometer.

## References:

1. Campos F, Blanco M, Barral D, Agulla J, Ramos-Cabrer P, and Castillo J. (2012) Influence of temperature on ischemic brain: Basic and clinical principles, *Neurochem Int*, 60:5, 495–505.
2. Darwazeh R, and Yan Y. (2013) Mild hypothermia as a treatment for central nervous system injuries: Positive or negative effects, *Neural Regeneration Research*, 8:28, 2677–2686.
3. Pecharsky VK, and Gschneidner Jr. KA. (2001) Some common misconceptions concerning magnetic refrigerant materials, *Journal of Applied Physics*, 90:9, 4614–4622.

# Lipid membrane anchors in Lipid-Nucleic acid (LiNA) conjugates for liposome fusion

Oliver Ries,\* Philipp M. G. Löffler and Stefan Vogel

<sup>1</sup> University of Southern Denmark, Biomolecular Nanoscale Engineering Center - BioNEC, Department of Physics, Chemistry and Pharmacy, Campusvej 55, 5230 Odense M, Denmark

**Abstract:** Fusion of lipid bilayers is an ubiquitous process in nature. The merging of two biomembranes leading to release of encapsulated content in a controlled way is crucial, e.g. for cell signaling, exocytosis and intracellular trafficking. Initial attempts by Boxer and Höök et al. showed the feasibility of artificial liposome fusion controlled by supramolecular interactions of lipid-nucleic acid conjugates (LiNAs).[1] Thereby LiNAs are able to mimic the basic functional behaviour of the natural SNARE complex.

Assembly as the first step towards fusion has been reported earlier [2] followed by hemifusion and fusion of LiNA-functionalized liposomes.[3] Besides the external trigger temperature, PEGylation of LiNAs and the right choice of the membrane anchoring unit are key parameters of the fusion process. Content and lipid-mixing assays show the influence of these parameters on the fusion process opening the path for reactant mixing and chemistry in liposomal nanoscale reaction containers.

**Keywords:** liposome fusion, lipid-nucleic acid conjugates, content mixing

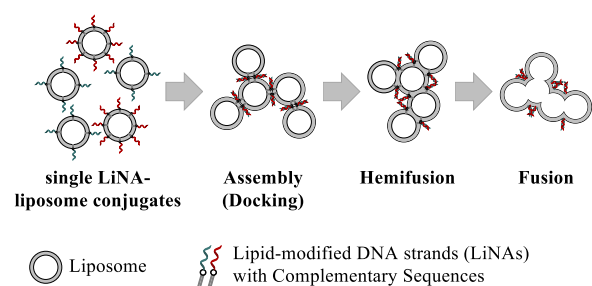


**Figure 1:** Schematic illustration of LiNA-mediated and controlled fusion of liposomes

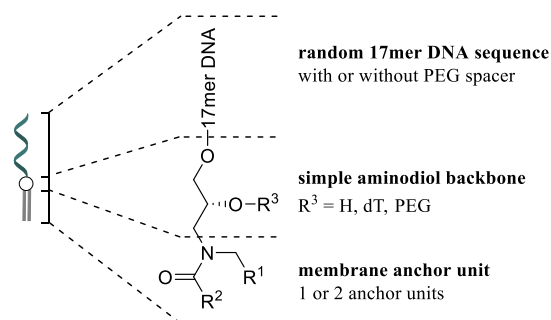


**Figure 2:** General LiNA structure (right).

## References:

- Chan, Y. M.; van Lengerich, B.; Boxer, S. G. (2008), Lipid-anchored DNA mediates vesicle fusion as observed by lipid and content mixing, *Biointerphases*, 3, FA17-21; b) Stengel, G.; Zahn, R.; Höök, F. (2007), DNA-Induced Programmable Fusion of Phospholipid Vesicles, *J. Am. Chem. Soc.*, 129, 9584-9585.
- Jakobsen, U.; Simonsen, A. C.; Vogel, S. (2008), DNA-Controlled Assembly of Soft Nanoparticles, *J. Am. Chem. Soc.*, 130, 10462-10463; b) Jakobsen, U., Vogel, S. (2009), DNA-Controlled Assembly of Liposomes in Diagnostics, *Methods Enzymol.*, 464, 233-248; c) Jakobsen, U., Vogel, S. (2013), Assembly of Liposomes Controlled by Triple Helix Formation, *Bioconjugate Chem.*, 24, 1485-1495.
- Ries, O., Löffler, P. M. G., Vogel, S. (2015), Convenient synthesis and application of versatile nucleic acid lipid membrane anchors in the assembly and fusion of liposomes, *Org. Biomol. Chem.*, 13, 9673-9680.

# One-pot Solventless Preparation of PEGylated Black Phosphorus Nanoparticles for Photoacoustic Imaging and Photo-thermal Therapy of Cancer

Caixia Sun<sup>1,2</sup>, Chongjun Zhao<sup>\*,1</sup>, Zhen Li<sup>\*,2</sup>

<sup>1</sup> Key Laboratory for Ultrafine Materials of Ministry of Education, Shanghai Key Laboratory of Advanced Polymeric Materials, School of Material Science and Engineering, East China University of Science and Technology Shanghai, 200237, China

<sup>2</sup> Center for Molecular Imaging and Nuclear Medicine, School for Radiological and Interdisciplinary Sciences (RAD-X), Soochow University Collaborative Innovation Center of Radiation Medicine of Jiangsu Higher Education Institutions, Suzhou, 215123, China

**Abstract:** Black phosphorus (BP) nanostructures such as nano-sheets and nanoparticles have attracted considerable attention in recent years due to their unique properties and great potential in various physical, chemical, and biological fields.<sup>1-3</sup> In this article, water-soluble and biocompatible PEGylated BP nanoparticles with a high yield were prepared by one-pot solventless high energy mechanical milling technique (HEMM). The resultant BP nanoparticles can efficiently convert near infrared (NIR) light into heat, and exhibit excellent photostability, which makes them suitable as a novel nanotheranostic agent for photoacoustic (PA) imaging and photothermal therapy of cancer. The in-vitro results demonstrate the excellent bio-compatibility of PEGylated BP nanoparticles, which can be used for photothermal ablation of cancer cells under irradiation with NIR light. The in-vivo PA images demonstrate that these BP nanoparticles can be efficiently accumulated in tumors through the enhanced permeability retention effect. The resultant BP nanoparticles can be further utilized for photothermal ablation of tumors by irradiation with NIR light. The tumor-bearing mice were completely recovered after photothermal treatment with BP nanoparticles, in comparison with mice from control groups. Our research highlights the great potential of PEGylated BP nanoparticles in detection and treatment of cancer.

**Keywords:** Black phosphorus, PEGylated nanoparticles, Photoacoustic imaging, Photothermal therapy

## Acknowledgement

This work was supported by the National Natural Science Foundation of China (81471657, 81527901), Jiangsu Provincial Key Laboratory of Radiation Medicine and Protection, A Project Funded by the Priority Academic Program Development of Jiangsu Higher Education Institutions (PAPD), Shanghai Natural Science Foundation (No. 13ZR1411900), the Shanghai Leading Academic Discipline Project (B502), the Shanghai Key Laboratory Project (08DZ2230500).

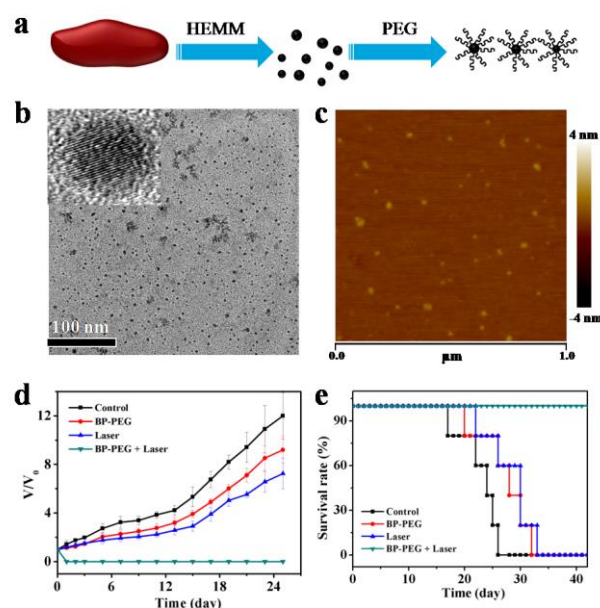


**Figure 1:** a) Sample preparation flowchart of PEG-BP nanocomposites. b) TEM and HRTEM images of BP nanoparticles. c) AFM images. d) Corresponding growth curves of 4T1 tumors in different groups of mice treated in different manners. The relative tumor volumes were normalized to their initial size. e) Survival rates of mice after various treatments as indicated.

## References:

1. L. Li, Y. Yu, G. J. Ye, Q. Ge, X. Ou, H. Wu, et al. Black phosphorus field-effect transistors, *Nat. nanotechnol.* 9 (2014) 372-377.
2. X. Zhang, H. Xie, Z. Liu, C. Tan, Z. Luo, H. Li, et al. Black Phosphorus Quantum Dots, *Angew. Chem. Int. Ed.*, 54 (2015) 3653-3657.
3. Z. Sun, H. Xie, S. Tang, X. F. Yu, Z. Guo, J. Shao, et al. Ultrasmall Black Phosphorus Quantum Dots: Synthesis and Use as Photothermal, Agents, *Angew. Chem. Int. Ed.* 54 (2015) 11526-11530.



# The ultra-structural analysis of antibody conjugated gold nanoparticles on fiber optic particles plasmon resonance (FOPPR) enabled bio-sensor

Ching-Yi Hsieh,<sup>1</sup> Ya-Na Wu,<sup>2</sup> Shang-Rung Wu,<sup>1</sup> Chang-Yue Chiang,<sup>2</sup> Lai-Kwan Chau,<sup>2</sup>

<sup>1</sup>National Cheng Kung University, Institute of Oral Medicine, Tainan, Taiwan

<sup>2</sup>National Chung Cheng University, Department of Chemistry and Biochemistry, Chiayi, Taiwan

## Abstract:

The big issue in critical care patient is that the lag time between sample collection, processing and examining. This may cause potential risk of adverse diversity, also may waste the golden window to treat and take action. Real-time diagnostic on the bedside is an urgent need for clinical health care workers. Following the development of nanotechnology, more and more applications were employed in nowadays. The bio-sensing technique, fiber optic particles plasmon resonance (FOPPR) (Figure 1), based on gold nanoparticles-modified optical fiber with covalently immobilized antibody has successfully demonstrated a major advancement in the field of real-time monitoring of serial biomolecules in complex biological fluids (1). Ultra-fast detection, minimized nonspecific absorption, great stability has enlighten the potential of FOPPR as a novel application *in vitro* diagnostic platform (2). However, it is still unclear where the antibody locates and how the antibody orients in ultra-structural point of view.

To understand the actual ligand binding interaction within FOPPR system (Figure 1), we applied serial micro-analytical tools to dissect the antibody orientation and location *in situ*, including staining techniques, scanning electron microscopy (SEM), focused ion beam (FIB) as well as transmission electron microscope (TEM). By visualizing the distribution and orientation of bio-recognition molecules on FOPPR *in situ*, the curial information to optimize biosensor prototype will be revealed. We anticipate this research will facilitate the systematic design and implementation of FOPPR in the field of clinical diagnostic.

**Keywords:** antibody, biosensor, fiber optic particle plasmon resonance (FOPPR), transmission electron microscopy.

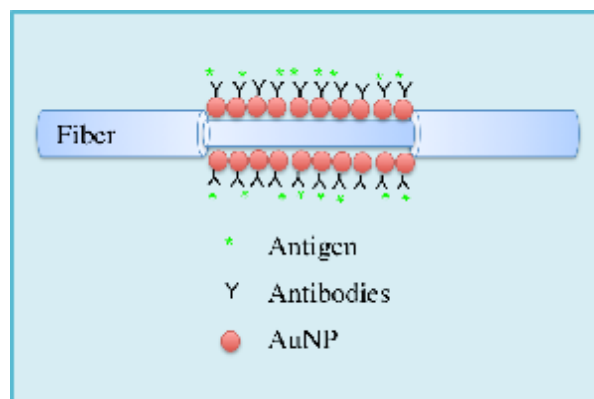


**Figure 1:** The schematic illustration of the FOPPR biosensor. The middle part of fiber was unclad fiber where gold nanoparticles (AuNPs) were coated. The antibodies were then self-assembly on the surface of gold nanoparticles as a monolayer.

## References:

1. C.-Y. Chiang *et al.*, Fiber-optic particle plasmon resonance sensor for detection of interleukin-1 $\beta$  in synovial fluids. *Biosensors and Bioelectronics* **26**, 1036-1042 (2010).
2. Y.-C. Huang *et al.*, Quantification of tumor necrosis factor-[small alpha] and matrix metalloproteinases-3 in synovial fluid by a fiber-optic particle plasmon resonance sensor. *Analyst* **138**, 4599-4606 (2013).

# In situ Synthesis of Nano-copper on Denim Garment for Antibacterial Purposes

D. Zarbaf<sup>1</sup>, M. Montazer<sup>2</sup>, A. Sadeghian Maryan<sup>3</sup>

<sup>1</sup>Islamic Azad University, South Tehran Branch, Department of Textile Engineering, Tehran, Iran

<sup>2</sup>Amirkabir University of Technology, Department of Textile Engineering, Tehran, Iran

<sup>3</sup>Islamic Azad University, Ardabil Branch, Department of Chemical Engineering, Ardabil, Iran

## Abstract:

This study deals with the synthesis of copper nanoparticles on denim garment and its antibacterial properties. In situ synthesis of nano-copper was carried out on denim garment by the reduction of copper(II) sulfate ( $\text{CuSO}_4$ ) with the presence of glucose acting as a reducing agent resulting a simple and cost-effective route. Copper nanoparticles were characterized by UV-visible spectrometer of the remaining solution after treatment. XRD and EDX analyses of the treated garment confirmed synthesis of the copper nanoparticles. Also, the particle size and distribution of nano-copper was studied by SEM observations. Color changes of the denim were determined by  $L^*a^*b^*$  values. The antibacterial properties of the treated denim showed significant reduction in *E. coli* and *S. aureus* bacteria (Figure 1).

**Keywords:** Nano-copper, Antibacterial, Denim Garment, Color changes

## References:

1. Montazer, M., Dastjerdi, M., Azadloo, M., Rad, M., (2015) Simultaneous synthesis and fabrication of nano  $\text{Cu}_2\text{O}$  on cellulosic fabric using copper sulfate and glucose in alkali media producing safe bio- and photo-active textiles without color change, *Cellulose*, vol. 22, Springer
2. Shahidi, S., Wiener, J., (2012) Antibacterial Agents in Textile Industry, *Biochemistry, Genetics and Molecular Biology*, InTech Open Science, 337–404

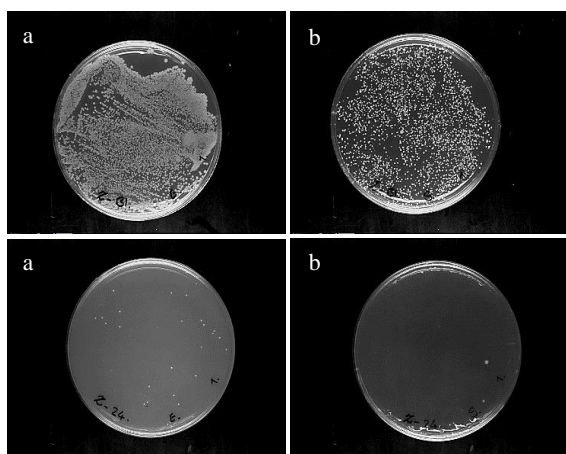


**Figure 1:** Reduction in the amount of bacteria before and after the treatment (a) *E. coli* and (b) *S. aureus*.

# Filtering Pigments from honey by nanofiber membrane

Farzaneh Azizzadeh, Filiz Altay\*

Istanbul Technical University, Faculty of Chemical Metallurgical, Department of Food Engineering, Maslak, 34469, Sarıyer, Istanbul-TURKEY

\*[lokumcu@itu.edu.tr](mailto:lokumcu@itu.edu.tr)

## Abstract:

Honey is a natural food product which has various health benefits. It can be consumed either as is or added to other foods as a sweetener. In the latter case, the pigments in honey can cause some off-color problems in the products. For example, when honey is added to jam or jellies as a sweetener, the brown coloring caused by heat treatment during process affect consumer acceptance adversely. In honey carotenoids, xanthophylls and anthocyanins are present as pigments, whereas carotenoids are the largest occurring one. Due to fact honey is very sensitive to heat and other environmental and process conditions, if the pigments are needed to remove then it must be done without heat or chemical treatments. It is hypothesized that pigments can be removed from honey by nanofiltration. Especially electrospun nanofibers as filter membrane appear to be very suitable for nanofiltration, because of the easiness of modifying the surface of the medium. For instance, the surface characteristics of nanofiber membranes, such as hydrophobicity, porous structure and the pore sizes, can be adjusted depending on the filtration needs by electrospinning parameters. In this study, the objectives were two-folds. First, polyacrylonitrile (PAN) nanofibers were obtained by electrospinning. Then, PAN nanofibers used as filter membrane for removing pigments in honey. PAN nanofibers were obtained from the PAN solution in dimethylformamide (DMF) at 10% by using electrospinning. The feed rate, the applied voltage and the distance to



**Figure1:** electrospinning device which produce nanofibers.

the collector plate were 3 ml/hour, 40 kV and 25 cm, respectively. The electrospinning was conducted for 30 min. The acquired PAN nanofibers were characterized with scanning electron microscope (SEM). In addition, contact angle measurements will be conducted. The honey will be filtrated through a laboratory set-up containing electrospun PAN nanofiber membrane at 1 bar. The physicochemical properties of filtrate such as viscosity, refractive index, pH, electrical conductivity, dielectric parameters will be determined. It is predicted that the hydrophobicity of the filter medium is a crucial factor for removing pigments from honey. Outcomes of this study may help to separate sensitive functional ingredients without getting damaged. The nanofiber membranes seem to have a very high potential utilization in food industry in the future.

**Keywords:** honey, pigment filtration, nanofiltration, nanofiber membrane.

## References:

1. Filatov, Y., Budyka, A., and Kirichenko, V. (2007) Electrospinning of Micro- and Nanofibers, *Fundamentals in Separation and Filtration Processes*, BegellHouse, Inc., Redding, CT, USA. Greiner, A., and Wendorff, J.H. (2007) Electrospinning: a fascinating Method for the preparation of ultrathin fibers. *Angew. Chem. Int. Ed.*, **119**, 5750.
2. Dersch, R., Liu, T., Schaper, A.K., Greiner, A., and Wendorff, J.H. (2003) Electrospun nanofibers: internal structure and intrinsic orientations. *J. Polym. Sci. [A1]*, **41**, 545.

# Physicochemical and mechanical characterization of electrospun poly- $\epsilon$ -caprolactone nanofibers loaded with cilostazol

M. Rychter<sup>1,2,\*</sup>, A. Baranowska-Korczyk<sup>2</sup>, M. Jarek<sup>2</sup>, B.M. Maciejewska<sup>2,3</sup>, L. Emerson Coy<sup>2</sup>, J. Lulek<sup>1</sup>

<sup>1</sup>Department of Pharmaceutical Technology, Poznań University of Medical Sciences, Poznań, Poland

<sup>2</sup>NanoBioMedical Centre, Adam Mickiewicz University, Poznań, Poland

<sup>3</sup>Department of Macromolecular Physics, Adam Mickiewicz University, Poznań, Poland

\* email: mrychter@ump.edu.pl

## Abstract:

Polymer-based nanofibers obtained via electrospinning method constitute the ideal drug delivery system of poorly water-soluble drugs [1]. By applying rotating drum collector electrospinning can produce two- and three-dimensional structures for potential application as biodegradable drug delivery systems [2]. Therefore this method is suitable for covering medical devices used in various fields of medicine.

Electrospun polycaprolactone (PCL) fibers were explored as a novel delivery system for a poorly water-soluble drug – cilostazol (CIL). CIL loaded fibers were successfully produced by applying electrospinning technique. Scanning electron microscopy (SEM) revealed that drug incorporation into electrospun fibers decreased the fibers orientation and the average local coherency. Additionally analysis of SEM micrographs showed that drug addition decreased the standard deviation of average fiber diameter. Mechanical properties of electrospun fibers were also investigated by using nanoindentation technique, which demonstrated that drug loading decreased Young modulus. The crystallinity of the electrospun drug and polymer were assessed by both differential scanning calorimetry (DSC) and Raman spectroscopy. Results obtained from DSC analysis revealed that drug incorporation reduced the overall crystallinity of electrospun fibers. Raman analysis (Fig. 1) confirmed the presence of drug within electrospun fibers and its polymorphic form [3].

Physicochemical characterization showed that drug crystallinity is not changed during the process and its presence has beneficial influence on the morphology of electrospun fibers.

## Acknowledgements:

Financial support from the National Science Centre (UMO-2015/17/N/ST8/00102, UMO-2013/11/D/ST5/02900) is gratefully acknowledged.

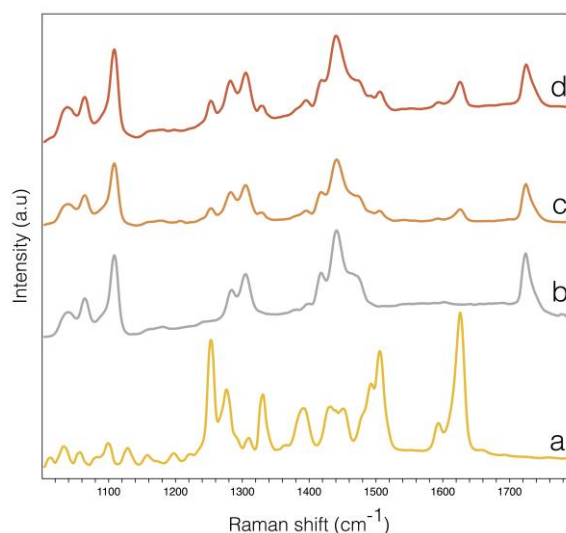


**Figure 1:** Raman spectra of pure CIL [a], PCL nanofibers [b] and PCL nanofibers loaded with 6.25% (wt) [c] and 12.50% (wt) [d] of CIL (with regard to dry weight of PCL).

**Keywords:** electrospinning, drug delivery systems, polymer-based biomaterials, biomedical applications.

## References:

1. Potrč, T., Baumgartner, S., Roškar, R., Planinšek, O., Lavrič, Z., Kristl, J., Kocbek, P. (2015). Electrospun polycaprolactone nanofibers as a potential oromucosal delivery system for poorly water-soluble drugs. *Eur. J. Pharm. Sci.*, 75, 101-113.
2. Puppi, D., Zhang, X., Yang, L., Chiellini, F., Sun, X., Chiellini, E. (2014). Nano/microfibrous polymeric constructs loaded with bioactive agents and designed for tissue engineering applications: A review. *J. Biomed. Mater. Res. B. Appl. Biomater.*, 102, 1562-1579.
3. Stowell, G.W., Behme, R.J., Denton, S.M., Pfeiffer, I., Sancilio, F.D., Whittall, L.B., Whittle, R.R. (2002). Thermally-prepared polymorphic forms of cilostazol. *J. Pharm. S*

S

c

i

.

,

o



# Biomimetic Functionalized Graphene for Biodegradable Bone Implants

A. M. Arnold,\* B. Holt, S. A. Sydlik

Carnegie Mellon University, Department of Chemistry, Pittsburgh, PA

**Abstract:** Bone, like other tissues in the body, is constantly being remodeled,<sup>1</sup> making it well equipped to heal minor injuries even into adulthood. However, bone's regenerative ability diminishes when defects occur above a critical size, resulting in nonunion<sup>2,3</sup> that can lead to severe pain and loss of function.<sup>4,5</sup> Currently, autologous tissue transplantation or implantation of prosthetic devices are used as a therapeutic treatment for large defect areas; yet, both methods pose significant health issues for the patient.<sup>6-8</sup> Tissue engineering has been attempting to address the challenges associated with current bone replacement therapies, but a material that matches the unique mechanical properties and biochemical milieu of bone that is also biocompatible has yet to be realized.<sup>9</sup> Considering this, our laboratory's goal is to use the principles of molecular design to generate a material that mimics the chemical, biological, and mechanical properties of osseous tissue to create a biodegradable bone implant for the treatment of bone injuries. Using graphene oxide (GO) as a scaffold, we can install polyphosphate functionalities that mimic the hydroxyapatite component of native bone onto the basal plane of graphene oxide via modified Arbuzov chemistry (Figure 1).<sup>10</sup> In addition, we have developed the chemistry to control the identity of the counter ion in the resulting phosphate graphene (PG) has generated an exciting new class of materials that exhibit similar compressive mechanical properties to that of bone. It has also been found that PG displays promising cyto-compatibility, making the materials an ideal candidate for a novel, biodegradable bone implant.

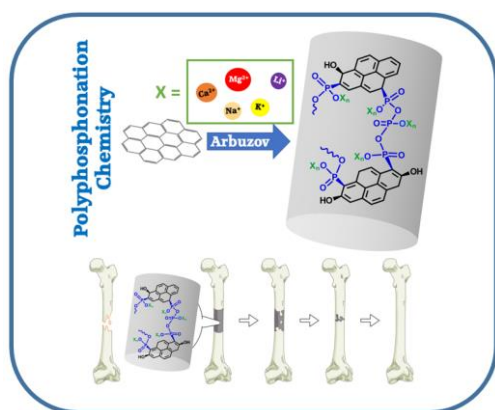


**Figure 1:** Molecular design of a phosphate functionalized graphene composite with varying counter ion

identities synthesized via Arbuzov chemistry to generate materials for a biodegradable bone implant.

**Keywords:** Graphene oxide (GO), phosphate graphene (PG), biodegradable material, bone graft, bone regeneration, bone repair.

## References:

1. Raggatt, L. J. & Partridge, N. C. Cellular and Molecular Mechanisms of Bone Remodeling. *J. Biol. Chem.* 285, 25103–25108 (2010). PMID: 20501658
1. Cooper, G. M. et al. Testing the ‘critical-size’ in calvarial bone defects: revisiting the concept of a critical-sized defect (CSD). *Plast. Reconstr. Surg.* 125, 1685–1692 (2010).
3. Zamurovic, N., Cappellen, D., Rohner, D. & Susa, M. Coordinated Activation of Notch, Wnt, and Transforming Growth Factor- $\beta$  Signaling Pathways in Bone Morphogenetic Protein 2-induced Osteogenesis Notch Target Gene Hey1 INHIBITS Mineralization and Runx2 Transcriptional Activity *J. Biol. Chem.* 279, 37704–37715 (2004). PMID: 15178686
4. Concepts and Cases in Nonunion Treatment. (Thieme: New York, 2011).
5. Neglected Musculoskeletal Injuries. (Jaypee Brothers Publishers: New Dehli, 2011).
6. Damien, C. J. & Parsons, J. R. Bone graft and bone graft substitutes: a review of current technology and applications. *J. Appl. Biomater. Off. J. Soc. Biomater.* 2, 187–208 (1991). PMID: 10149083
7. Principles of Internal Fixation of the Cranio-maxillofacial Skeleton: Trauma and Orthognathic Surgery. (Thieme: New York, 2012).
8. Matsuno, A., Tanaka, H., Iwamuro, H., Takashi, S., Miyawaki, S., Nakashima, M., Nakaguchi, H. & Nagashima, T. Analyses of the factors influencing bone graft infection after delayed cranioplasty. *Acta Neurochir. (Wien)* 148, 535–540; discussion 540 (2006). PMID: 16467959
9. Amini, A. R., Laurencin, C. T. & Nukavarapu, S. P. Bone Tissue Engineering: Recent Advances and Challenges. *Crit. Rev. Biomed. Eng.* 40, 363–408 (2012). PMID: 23339648
10. Goods, J. B., Sydlik, S. A., Walish, J. J. & Swager, T. M. Phosphate Functionalized Graphene with Tunable Mechanical Properties. *Adv. Mater.* 26, 718–723 (2014). PMID: 24114948



# Effect of PEG modification on nebivolol loaded solid lipid nanoparticles for treatment of hypertension: preparation, characterization and pharmacokinetic studies

<sup>1</sup>Evren Homan Gökçe, <sup>1</sup>Aysu Yurdasiper, <sup>2</sup>Neslihan Üstündağ-Okur, <sup>3</sup>Evren Gündoğdu

<sup>1</sup>Ege University, Faculty of Pharmacy, Department of Pharmaceutical Technology, Izmir, Turkey

<sup>2</sup>Istanbul Medipol University, School of Pharmacy, Department of Pharmaceutical Technology, Istanbul, Turkey

<sup>3</sup>Ege University, Faculty of Pharmacy, Department of Radiopharmacy, Izmir, Turkey

## Abstract:

Hypertension is a chronic disease in which the blood pressure in the arteries is elevated. It is a major contributor to vascular morbidity and mortality (1). Nebivolol hydrochloride (NB) is a newly developed third-generation  $\beta$ -adrenergic receptor-blocker approved to be used in hypertension by FDA in 2007 (2). NB loaded solid lipid nanoparticles (SLNs) were modified with polyethylene glycol stearate (PEG) for improvement of its oral bioavailability.

Compritol, poloxamer and lecithin were used for preparation of SLNs by homogenization method. To improve particle size distribution, high pressure homogenizer (Microfluidizer / ML110L) was used at 500 bars for 1 cycle after SLNs were prepared with high shear homogenizer. The obtained SLNs were characterized (Table 1).

PEG modified SLN and commercial formulations were administered at the same doses of NB (240  $\mu$ g/ kg body weight) to rats. NB concentration was analyzed by HPLC and pharmacokinetic parameters were calculated for by Phoenix Win-NonLin. High pressure homogenization for 1 cycle at 500 bars, using 100 mg Compritol as solid lipid, 100 mg poloxamer and 10 mg lecithin together as surfactants led to a narrow size distribution. 0.4 % PEG was added to modify the prepared SLNs (S1). SLNs exhibited a smooth, spherical morphology and they were well dispersed. Table 1 shows characterization of prepared SLNs. The permeability values of NB from SLNs were greater than that of the commercial formulation and the highest permeability value was found with PEG modified SLNs. PEG modified SLNs improved oral bioavailability of NB (Fig.1) ( $P < 0.05$ ). The presented delivery system could provide a new promising strategy for enhancing the oral bioavailability of such drugs with poor hydrophilicity.

**Table 1:** Particle size, PDI, zeta potential, pH, EE, drug loading of SLNs

SLNs	S1	S1NB	PEG-S1NB
Particle size (nm)	365.5 $\pm$ 31.5	428.6 $\pm$ 28.8	269.2 $\pm$ 29.6
PDI	0.427 $\pm$ 0.07	0.445 $\pm$ 0.05	0.308 $\pm$ 0.01
Zeta potential (mV)	-18.8 $\pm$ 0.830	2.29 $\pm$ 0.083	-2.67 $\pm$ 0.303
EE %	-	83.89 $\pm$ 1.8	98.04 $\pm$ 0.2

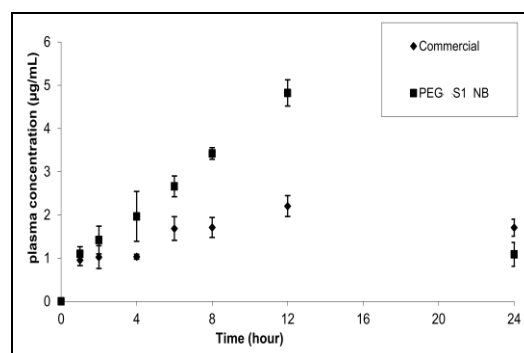


**Figure 2:** Plasma concentration values obtained after administration of PEG-S1NB and commercial formulation

**Keywords:** encapsulation, characterization pharmacokinetic, PEG, SLN

## Acknowledgements

This study (No:112S292) was granted by TUBITAK 1001.

## References:

- Xiong, X., Yang, X., Li, Y, Zhang, Y., Wang, P., Wang, J. (2013), Chinese herbal formulas for treating hypertension in traditional Chinese medicine: perspective of modern science, *Hypertens. Res.* 36, 570–579.
- Kumar, D., Loc, B.P. (2013), Nebivolol a novel somewhat different  $\beta$  adrenergic receptor blocker, *J. Drug Deliv. Ther.*, 3, 185-191.

# Role of the swelling activated chloride current on geno and cytotoxicity of silver nanoparticles on human glioblastoma multiforme

Loredana Latterini<sup>1</sup>, Paola Sassi<sup>1</sup>, Francesco Ragonese<sup>1</sup>, Claudia Tubaro<sup>1</sup>, Marta Gambucci<sup>1</sup>, Luigi Tarpani<sup>1</sup>, Martino Caramia<sup>1</sup>, Loretta Mancinelli<sup>1</sup>, Cataldo Arcuri<sup>2</sup>, Carmen Mecca<sup>2</sup>, Lucio Leonardi<sup>3</sup>, Lanfranco Barberini<sup>1</sup>, Fabio Franciolini<sup>1</sup> and Bernard Fioretti<sup>1\*</sup>

<sup>1</sup> University of Perugia, Dept. of Chemistry, Biology and Biothechnologies, Via Elce di Sotto 8, Perugia, Italy

<sup>2</sup> University of Perugia, Dept of Experimental Medicine, Piazzale Gambuli, Perugia, Italy

<sup>3</sup> S&R Farmaceutici, Via dei Pioppi 2, Bastia Umbra, Perugia, Italy

## Abstract:

The evaluation of therapeutic use of silver nanoparticles (AgNPs) in brain cancer represents a relevant new area of research. Several studies have shown that AgNPs induce inhibition of glioblastoma multiforme (GBM) cell growth in vitro, and this inhibition is correlated to NAD depletion, ROS production and DNA damage. AgNPs are synthesized from silver nitrate reduction with NaBH<sub>4</sub> utilizing as stabilizing agent dodecanthiol (Kang e Kim, 1998). Dodecanthiolate-stabilized silver nanoparticles (AgNP<sub>Sdode</sub>) display homogenous distribution size with mean diameter of about 5 nm, as estimated with TEM analysis in accordance with AgNPs plasmonic resonance properties. Our data show that AgNP<sub>Sdode</sub> at the subnanomolar range decrease mitochondrial activity of U251 glioblastoma cell line, estimated with MTT assay and proliferation rate upon 24 and 48 hours treatment. Under the same conditions, the induction of apoptotic and necrotic processes were observed by Comet test assay and citofluorimetric analysis. Since apoptosis/necrosis process involves ion channels activity, an electrophysiological study was performed during AgNPs application in U251 glioblastoma. Acutely AgNP<sub>dode</sub> application activates a chloride current with biophysical and pharmacological profile similar to that previously found for the swelling activated chloride current (ICl<sub>sw</sub>) in glioblastoma cells (Fioretti et al., 2004). Similar ICl<sub>sw</sub> activation was observed with AgNPs obtained with another synthesis strategy that used citrate as reductive and stabilizing agent, indicating that the biological effect observed is independent from the AgNPs synthesis approach. The chloride current was blocked by DIDS, NPPB and the selective ICl<sub>sw</sub> blocker DCPIB, and displayed significant inactivation at positive membrane voltages. Since the activation of ICl<sub>sw</sub> by AgNPs was preserved upon catalase pretreatment and mimed by hydrogen peroxide application, the involvement of oxygen radical specie (ROS) in the electrophysiological effects of AgNPs is suggested. The involvement of ICl<sub>sw</sub> activity in exerting

the effects of AgNP<sub>Sdode</sub> on cell metabolism and proliferation was further investigated. Our results indicate that the activation of ICl<sub>sw</sub> may represent a new signal to rationalize the effects and thus the use of AgNPs in nanomedicine, namely in GBM therapy.

**Keywords:** Silver nanoparticles, human glioblastoma multiforme, chloride current, cell proliferation and metabolism.

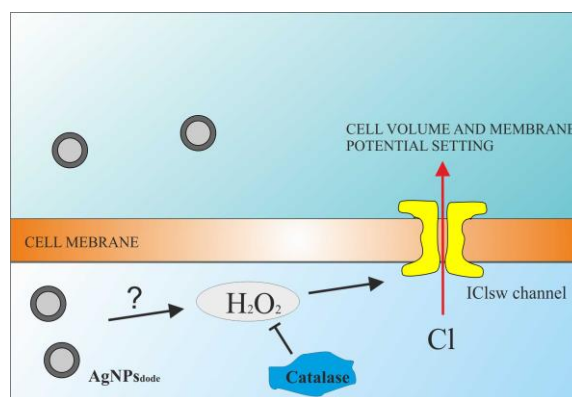


**Figure 1:** Sketch illustrating the signal transduction proposed to be involved in the activation of swelling activated chloride current by silver nanoparticles.

## References:

1. Kang SY and Kim K. (1998) Comparative Study of Dodecanethiol-Derivatized Silver Nanoparticles Prepared in One-Phase and Two-Phase Systems, *Langmuir*, 14: 226–230.
2. Fioretti B, Castigli E, Calzuola I, Harper AA, Franciolini F, Catacuzzeno L. (2004) NPPB block of the intermediate-conductance Ca<sup>2+</sup>-activated K<sup>+</sup> channel. *Eur J Pharmacol*, 497:1-6.

## Acknowledgements

This work has been supported with the funding of the MIUR – SIR 2014 – Fioretti – AgNPs-GBM-IR, RBSI144EUA, Title project: “Novel nanoparticles-based approach to brain cancer therapy” and Fondazione Cassa di Risparmio di Perugia (Project number 2014.0260.021).

# Flexible, Label-Free DNA Sensor using Platinum Dioxide as the sensing element

Nivedita Basu<sup>1\*</sup>, Anil Krishna Konduri<sup>2</sup>, Palash K. Basu<sup>3</sup>, Manoj Varma<sup>1</sup> and Navakanta Bhat<sup>1</sup>

<sup>1</sup>Centre for Nano Science and Engineering, Indian Institute of Science, Bangalore.

<sup>2</sup>Dept. of Neuroscience and Brain Technologies, Istituto Italiano di Tecnologia.

<sup>3</sup>Indian Institute of Space Science & Technology.

**Abstract:** This paper reveals the potential of Platinum Oxide (PtO<sub>2</sub>) as a DNA detector. We have designed arrays of simple, two terminal devices on plastic substrates using CMOS technology in which PtO<sub>2</sub> (80 nm thick) forms the sensing area (8.0 mm X 60 μm) for DNA detection. The sensor array shows a DNA concentration-dependent current change that is linear over a large dynamic range. Flexible acetate sheets were cut into squares containing an array of 20 sensors each. The sensors were fabricated using two layer photolithography. 80 nm PtO<sub>2</sub> and 10 nm Ti/50 nm Pt were deposited using sputtering (Fig. 1). Sequences of oligonucleotides used in this work were: 5' CTT CCT CTT CAT CCT GCT GCT ATG CCT CAT 3', 3'ATG AGG CAT AGC AGC AGG ATG AAG AGG AAG 5', 5'GCT GTA CCA AAC CTT CGG ACG GAA ATT GCA 3' and 5' CTT CCT CTT CAT CCT GCT GCT ATG CCT CAT 3' with Fluorescein tag at 5' end. We compared relative current change among different concentrations of DNA solutions in Milli-Q water ranging from 0.53 nM to 5.25 nM. We obtained a limit of detection (LOD) of 0.5 nM. To confirm adsorption of DNA onto sensor surface and estimate binding affinity of DNA to PtO<sub>2</sub> we used fluorescently labelled DNA. Nonlinear (weighted) least-squares model was used to calculate binding constant  $K_d$  of 7.35 pM/%. We confirmed specificity by performing hybridization of Fluorescein tagged DNA capture probe with complimentary target probe and control probe. The sensor was able to identify a mismatch of one base pair. Present study demonstrates Platinum Dioxide (PtO<sub>2</sub>) thin film devices for label-free electrical sensing of DNA. Advantages of the reported PtO<sub>2</sub> sensor are robustness, label-free operation, ease of fabrication, relevant detection limit, rapid detection and reproducible performance. The sensor can have immense application in diagnosis and prevention of human diseases.

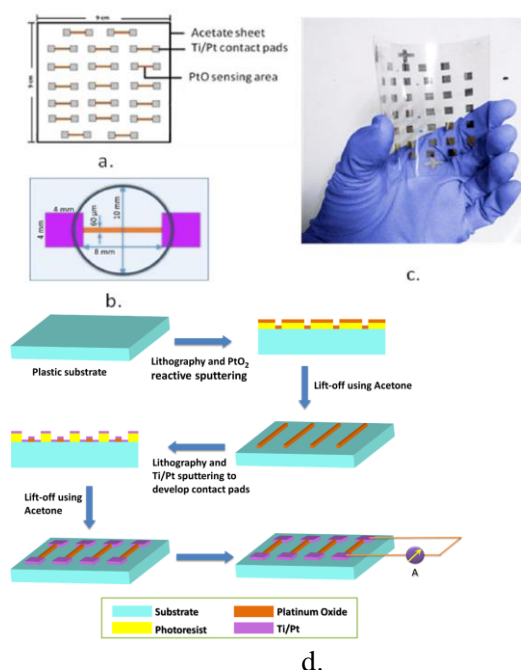


**Figure 1:** (a) Schematic representation of an array of 19 devices on a plastic substrate. (b) A single PtO<sub>2</sub> sensor depicting device dimensions with acrylic O-ring of 10 mm diameter placed around the PtO<sub>2</sub> sensing area to restrict DNA solution within the sensing area and prevent it from interfering with the electrical measurements. (c) Actual image of an array of PtO<sub>2</sub> sensors on a flexible plastic substrate. (d) Schematic representation of the fabrication steps of the PtO<sub>2</sub> sensor.

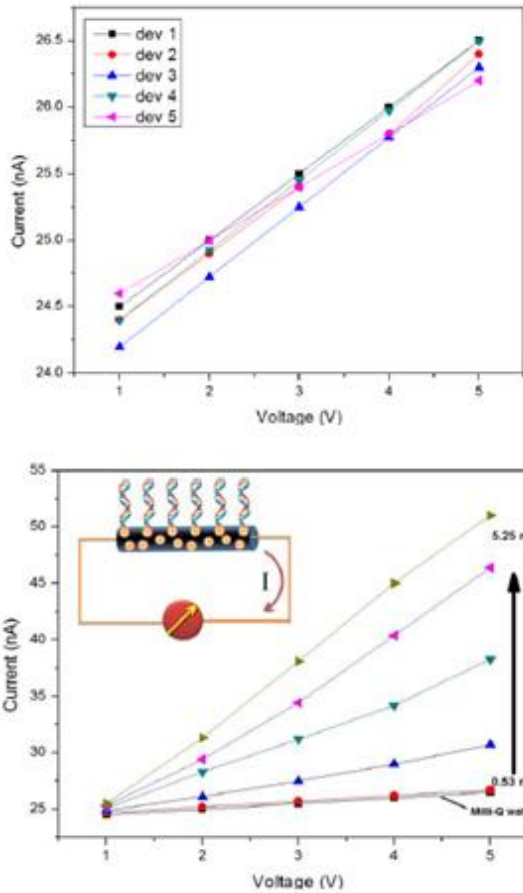
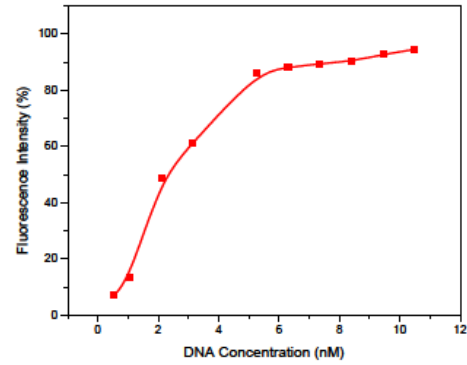
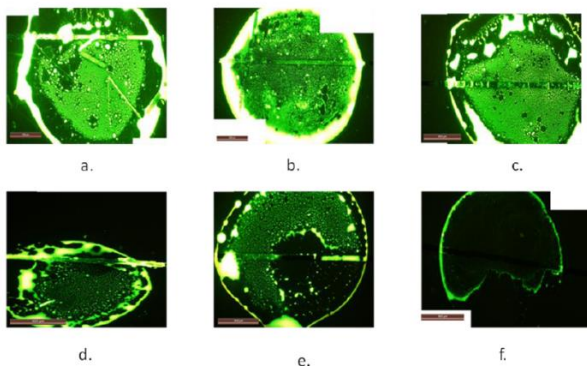


Figure 2: (a) Comparison of I-V curves of a set of five PtO<sub>2</sub> sensors in the array. (b). I-V curves of the sensor for only Milli-Q water and 5 different capture probe concentrations viz., 0.53 nM, 1.05 nM, 2.1 nM, 3.15 nM and 5.25 nM. Inset schematically represents the working principle of our proposed PtO<sub>2</sub> DNA sensor. There is increase in holes at the surface of PtO<sub>2</sub> on introduction of negatively charged DNA (negative charge due to the phosphate back-bone) thus giving rise to an increased conduction.



g.

Figure 3: Fluorescence microscopy images (5X) of different concentrations of Fluorescein tagged DNA solutions dispersed onto the sensor surface for confirmation of DNA adsorption. Figures a-f represent the binding of six different concentrations of Fluorescein tagged DNA (green) to the sensor (the narrow rectangular area) surface viz. 10.5 nM, 8.4 nM, 6.3 nM, 5.25 nM, 3.15 nM and 0.53 nM respectively. (g) Fluorescence titration curve from a plot of fluorescence intensity vs. capture probe (DNA) concentration.

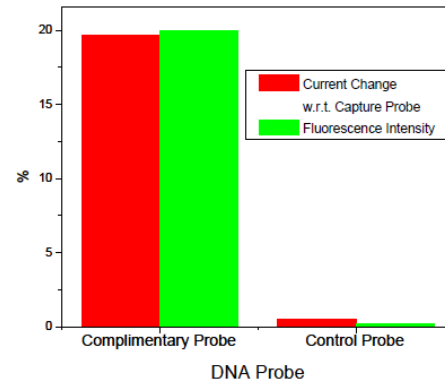


Fig. 4: A plot showing the fluorescence intensities in percentage and changes in current (normalized with respect to the current value obtained when the sensor surface is functionalized solely with single strand DNA capture probe and expressed in percentage) in cases of complimentary target probe and control probe hybridized with capture probe on the sensor surface.

**Posters Session II: June 2<sup>nd</sup>, 2016**

**Nanotech France 2016:  
Nanoelectronics / NanoPhotonics**



# Green Emissive Perovskite Light-Emitting Diodes Via Morphological Control of Perovskite Films

M. H. Song,<sup>1,2,\*</sup> J. C. Yu,<sup>1</sup>

<sup>1</sup>School of Materials Science Engineering/KIST-UNIST Ulsan Center for Convergent Materials, Ulsan National Institute of Science and Technology (UNIST), UNIST-gil 50, Ulsan, 689-798, Republic of Korea

<sup>2</sup>Cavendish Laboratory, UJJ Thomson Avenue, Cambridge, CB3 0HE, United Kingdom

## Abstract:

The organic-inorganic hybrid perovskite materials have been extremely studied because of their excellent electrical and optical properties, a tunable optical bandgap, easy solution processing, and their excellent optical properties with high photoluminescence quantum efficiency (PLQE) as high as 70%, which also raises them promising semiconductor candidates for large area display applications. The crucial work for the highly efficient perovskite LEDs (PeLEDs) and solar cells is to obtain a perovskite layer with a uniform morphology and high crystallinity.

In this study, we present high performance PeLEDs with a uniform morphology of perovskite films by introducing HBr into the perovskite precursor. The introduction of HBr into the perovskite precursor results in a perovskite film with a uniform, continuous morphology because the HBr increases the solubility of the inorganic component in the perovskite precursor and reduces the crystallization rate of the perovskite film upon spin-coating. In particular, PeLEDs fabricated using perovskite films with a uniform, continuous morphology, which were deposited using 6 vol. % HBr in a dimethylformamide (DMF)/hydrobromic acid (HBr) cosolvent, exhibited full coverage of the green EL emission. Finally, the optimized PeLEDs fabricated with perovskite films deposited using the DMF/HBr cosolvent exhibited a maximum luminance of 3,490 cd m<sup>-2</sup> (at 4.3 V) and an external quantum efficiency (EQE) of 0.12 % (at 4.3 V).

**Keywords:** perovskite materials, morphological control, HBr, uniform, continuous morphology, perovskite light-emitting diodes.

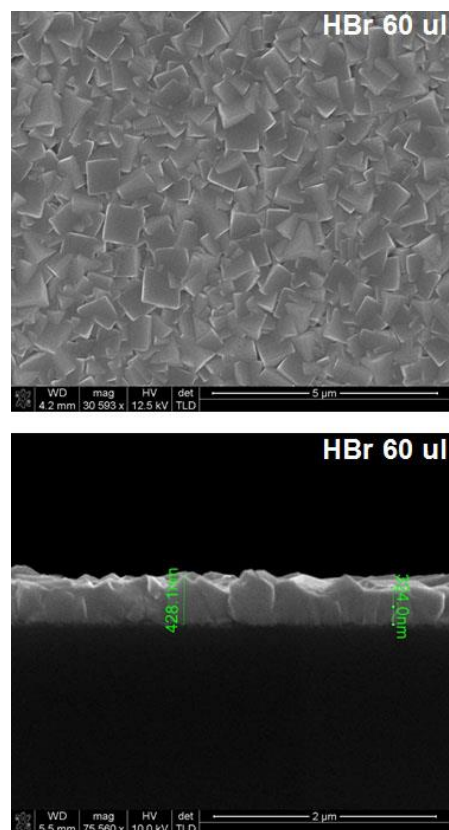


**Figure 1:** Figure illustrating SEM images of the top surfaces and cross section of the MAPbBr<sub>3</sub> layer deposited using 6 vol.% of HBr in the DMF/HBr cosolvent on PEDOT:PSS-coated ITO/glass substrates.

## References:

J. C. Yu, D. B. Kim, E. D. Jung, B. R. Lee, and M. H. Song\*, "High-Performance Perovskite Light-emitting Diodes via Morphological Control of Perovskite Film", *Nanoscale*, In Press.

# Influence of electrical pulses on lithium cobalt oxide thin films : memristive behaviour and potential applications

Van Son Nguyen,<sup>1</sup> Van Huy Mai,<sup>2</sup> Alec Moradpour,<sup>3†</sup> Pascale Auban Senzier,<sup>3</sup> Claude Pasquier,<sup>3</sup> Kang Wang,<sup>3</sup> Pierre-Antoine Albouy,<sup>3</sup> Marcelo J. Rozenberg,<sup>3,4</sup> John Giapintzakis,<sup>5</sup> Christian N. Mihailescu,<sup>5</sup> Charis M. Orfanidou,<sup>5</sup> Efthymios Svoukis,<sup>5</sup> Thomas Maroutian,<sup>6</sup> Philippe Lecoœur,<sup>6</sup> Guillaume Agnus,<sup>6</sup> Pascal Aubert,<sup>6</sup> Sylvain Franger,<sup>7</sup> Raphaël Salot,<sup>8</sup> Katia March,<sup>3</sup> Nathalie Brun,<sup>3</sup> David Alamarguy,<sup>1</sup> Pascal Chrétien<sup>1</sup> and Olivier Schneegans<sup>1</sup>

<sup>1</sup> Lab. de Génie Élect. et Électronique de Paris, CNRS, Upmc&PSaclay Univ., CentraleSupélec, Gif /Yvette, France

<sup>2</sup> CEA, LIST, 91191, Gif Sur Yvette Cedex, France

<sup>3</sup> Laboratoire de Physique des Solides, CNRS, Université Paris-Sud, Orsay, France

<sup>4</sup> Dep. de Física Juan José Giambiagi, FCEN, Univ de Buenos Aires, Buenos Aires, Argentina

<sup>5</sup> Department of Mechanical & Manufacturing Engineering, University of Cyprus, Nicosia, Cyprus

<sup>6</sup> Institut d'Électronique Fondamentale, CNRS, Université Paris-Sud, Orsay, France

<sup>7</sup> Institut de Chimie Moléculaire et des Matériaux d'Orsay, CNRS, Université Paris-Sud, Orsay, France

<sup>8</sup> Liten-CEA de Grenoble, Grenoble, France

## Abstract:

The occurrence of bipolar resistive switching (RS) phenomena has been observed in  $\text{Li}_x\text{CoO}_2$  thin films, using electrode/film/electrode solid-state micrometric devices (see schematic in top-right inset of figure 1), which contain this layered mixed-valence cobalt oxide. Current-voltage curves showed that these devices typically exhibit two resistance states [1] :  $R_{\text{OFF}}$  (which corresponds to the resistance of the pristine cell), and  $R_{\text{ON}}$ , the lowest resistance state, with a  $R_{\text{OFF}} / R_{\text{ON}}$  ratio reaching  $10^4$  to  $10^5$ .

We report preliminary results [2] on these devices, which demonstrate that the application of consecutive electrical pulses (see schematic on bottom left inset of figure 1) leads to resistance states which are tunable as a function of the number of pulses applied (figure 1). Thus, due to their cumulative response to excitations,  $\text{Li}_x\text{CoO}_2$  thin films show promising application potential both towards multilevel non volatile memories, and neuromorphic systems in the field of cognitive computation.

**Keywords:** resistive switching, thin films, cobalt oxides, non volatile resistive memories, multilevel resistance states, memristive behaviour.

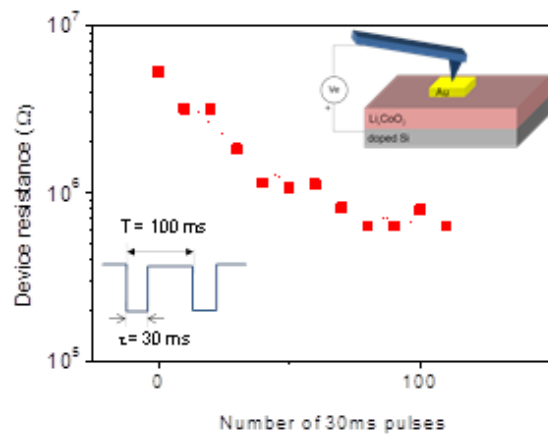


**Figure 1:** Cell resistance as a function of sequential applied voltage pulses, for a  $100 \times 100 \mu\text{m}^2$  upper electrode size. Top right inset : schematic view of an electrode/ $\text{Li}_x\text{CoO}_2$ /electrode device. Bottom left inset : schematic of the applied pulses (-8V pulses, the bias being applied between the bottom electrode and the AFM tip).

## References:

1. A. Moradpour et al (2011), Resistive switching phenomena in  $\text{Li}_x\text{CoO}_2$  thin films, *Adv. Mater.*, 23, 4141-4145
2. V.H. Mai et al (2015), Memristive and neuromorphic behaviour in a  $\text{Li}_x\text{CoO}_2$  nanobattery, *Sci. Rep.*, 5,7761

# Al<sub>2</sub>O<sub>3</sub> passivation effect in HfO<sub>2</sub>-Al<sub>2</sub>O<sub>3</sub> laminate structures grown on InP substrates

Hang-Kyu Kang<sup>1,2,\*</sup>, Yu-Seon Kang<sup>1</sup>, Dae-kyoung Kim<sup>1</sup>, Min Back<sup>1</sup>, Young-Seo, An<sup>3</sup>,  
Jin-Dong Song<sup>2</sup>, Hyounsub Kim<sup>3</sup>, Mann-Ho, Cho<sup>1\*</sup>

<sup>1</sup>Institute of physics and Applied physics, Yonsei University, Seoul, 120-749 Korea

<sup>2</sup>Center of opto-electronic materials, Korea institute of Science and Technology, Seoul 136-791, Korea

<sup>3</sup>School Department of Material science and Engineering Sungkyunkwan University, Suwon 440-746, Korea

## Abstract:

The passivation effect of Al<sub>2</sub>O<sub>3</sub> layer on interfacial and electrical properties were investigated in HfO<sub>2</sub>-Al<sub>2</sub>O<sub>3</sub> laminate structures grown on InP substrate by atomic layer deposition (ALD). HR-XPS data showed that interfacial reactions were dependent on the presence of the Al<sub>2</sub>O<sub>3</sub> passivation layer and its sequence in the HfO<sub>2</sub>-Al<sub>2</sub>O<sub>3</sub> laminate structures.

The Al<sub>2</sub>O<sub>3</sub>/HfO<sub>2</sub>/Al<sub>2</sub>O<sub>3</sub> structure showed the best properties on interfacial and electrical characteristics. The upper Al<sub>2</sub>O<sub>3</sub> layer suppressed the inter-diffusion of oxidizing species into the HfO<sub>2</sub> films, and the lower Al<sub>2</sub>O<sub>3</sub> layer suppressed the out-diffusion of In and P elements. As a result, the formation of In-O bonds (such as In(PO<sub>3</sub>)<sub>3</sub> and InPO<sub>4</sub>) was suppressed effectively in the Al<sub>2</sub>O<sub>3</sub>/HfO<sub>2</sub>/Al<sub>2</sub>O<sub>3</sub> structure as compared to the HfO<sub>2</sub> on InP system. Moreover, the conductance results revealed that the Al<sub>2</sub>O<sub>3</sub> layer passivated on InP reduce the mid-gap to  $2.6 \times 10^{12} \text{ eV}^{-1} \text{ cm}^{-2}$  as compared to that of HfO<sub>2</sub>/InP ( $5.4 \times 10^{12} \text{ eV}^{-1} \text{ cm}^{-2}$ ). These gap states originated from out-diffusion of In elements from the InP substrate, which are well supported by Reflection electron energy loss spectroscopy (REELS) spectra.

**Keywords:** Al<sub>2</sub>O<sub>3</sub> passivation layer, indium phosphide, HfO<sub>2</sub> laminate structure, molar volume.

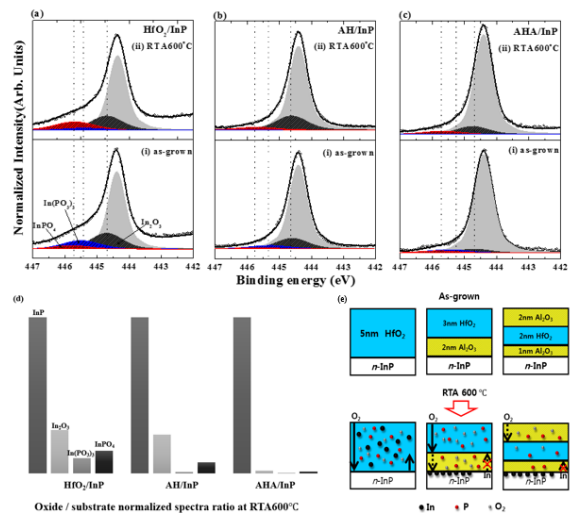


**Figure 1:** XPS In 3d spectra of (a) HfO<sub>2</sub>/InP, (b) HfO<sub>2</sub>/Al<sub>2</sub>O<sub>3</sub>/InP, and (c) Al<sub>2</sub>O<sub>3</sub>/HfO<sub>2</sub>/Al<sub>2</sub>O<sub>3</sub>/InP structure for (i) as-grown (ii) after annealing at 600 °C. In the In3d spectra, the InP, In<sub>2</sub>O<sub>3</sub>, In(PO<sub>3</sub>)<sub>3</sub> and InPO<sub>4</sub> bonding states correspond to binding energies of 444.4, 444.7, 445.4 and 445.7eV, respectively. (d) The ratio of oxidation states/substrate after annealing at 600 °C was calculated using the In 3d core-level spectra. (e) Schematic diagram of interfacial reaction mechanism for generated the oxidation states between dielectric layer and substrate.

## References:

Yu-Seon Kang, Dae-Kyung Kim, Hang-Kyu, Kang, Kwang-Sik, Jeong, Mann-Ho, Cho\*  
Dae-Hong, Ko, Hyounsub Kim, Jung-Hye Seo, and Dong-Chan Kim; ACS Appl. Mater. Interfaces 2014, 6, 3896–3906.

# Flexible Microelectrode Patterning with Thin Polymer Stencils Prepared using PEGDA/Silicate Nanocomposites

Young Ho Kim<sup>1,\*</sup>, Yeon Kyung Lee<sup>1</sup>, Taehyung Kim<sup>1</sup>, Sanket Goel<sup>2</sup>, Hee Jin Kim<sup>3,4</sup>, Sang-June Choi<sup>3,4</sup>

<sup>1</sup>Medical Device Development Center, Daegu-Gyeongbuk Medical Innovation Foundation, Daegu, Korea

<sup>2</sup>Birla Institute for Technology & Science, Pilani, India

<sup>3</sup>Research Institute of Advanced Energy Technology, Kyungpook National University, Daegu, Korea

<sup>4</sup>Department of Environmental Engineering, Kyungpook National University, Daegu, Korea

## Abstract:

A flexible microelectrode patterning with thin polymer stencils has been presented for nano-bio chip applications. The flexible microelectrode patterns on a thin polyester substrate were prepared by soft-lithography using silicate reinforced polyethylene glycol diacrylate (PEGDA) nanocomposites. Recently, miniaturized nano-bio chip devices such as microfluidic chips, lab-on-a-chips, biochips, biosensors have gained high interest in medical and environmental application fields. Moreover, PEG such as PEGDA hydrogel based microfabrication is important for environmentally friendly methods for nanobio-applications.

In this study, biocompatible and UV curable PEG hydrogel, PEGDA, with 0.5-1.0 wt.% of silicate was used to fabricate environmentally friendly microstructures on a substrate. In the fabrication procedures of the microstructured substrates, line-and-space and dot array patterns in the range of 50-800  $\mu\text{m}$  pattern widths were used. PEGDA microstructures were prepared by a simple UV irradiation method. Briefly, UV light for 7 seconds at 26  $\text{mW}/\text{cm}^2$  intensity was irradiated to the PEGDA substrates with a photomask. Then, the prepared PEGDA microstructures on the substrate was used as a micro-mold to prepare a thin polydimethylsiloxane (PDMS) stencil by soft-lithographic procedures. To prepare a flexible microelectrode patterns on a thin polyester substrate, the PDMS stencil was placed on the polyester film. Pt or Au metal was sputtered on the substrate using a sputter. Therefore the flexible microelectrode patterns on a polyester substrate was obtained by removing the thin stencil and characterized. The resistivity of the fabricated flexible Pt microelectrodes was  $3.9 \times 10^{-6} \Omega\text{cm}$ . The present fabrication method of a flexible microelectrode patterning is conventional and simple for nano-bio chip applications.

**Keywords:** microelectrode, flexible electrode, polymer stencil, PEGDA, nanocomposite

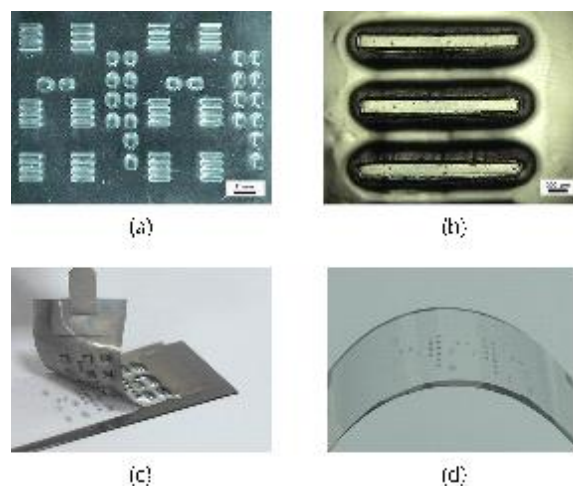


**Figure 1:** Flexible microelectrode patterning using PEGDA/Silicate Nanocomposites. (a,b) Microstructures of PEG Nanocomposites, (c,d) Microelectrode patterning on a thin polyester substrate.

## References:

- Pemberton, R. M., Xu, J., Pittson, R., Biddle, N., Drago, G. A., Jackson, S. K., Hart, J. P. (2009), *Anal. Biochem.* 385, 334.
- Qin, D., Xia, Y., Whitesides, G. M. (2010), Soft lithography for micro- and nanoscale patterning, *Nature protocols*, 5, 491~502.



# Molecular switches - from STM-induced single molecule chemistry to switching of entire layers

T. Leoni,<sup>1,\*</sup> T. Lelaidier,<sup>1</sup> A. Thomas,<sup>1</sup> O. Siri,<sup>1</sup> and C. Becker<sup>1</sup>

<sup>1</sup> Aix Marseille Université, CNRS, CINaM UMR 7325, 13288 Marseille, FRANCE

## Abstract:

Organic semiconductors receive an ever-growing attention because of their applications in solar energy conversion and organic electronics such as OFETs and OLEDs. Molecular order is one of the most important factors for reaching high mobility in organic semiconductors along with a small band gap. In this context we have been exploring aza-acenes like dihydro-tetraazapentacene (DHTAP, scheme 1 in figure 1) on a Au(111) surface by scanning tunneling microscopy (STM) and non-contact atomic force microscopy at low temperature. Our observations clearly demonstrated that intermolecular interaction via hydrogen bonding favors the growth of epitaxial large-scale self-assembled domains of DHTAP.

Moreover, we have found that these molecules can be selectively dehydrogenated via an inelastic electron tunneling process. The comparison of calculated images of the molecular frontier orbitals (MO) of the likely products of the switch with STM images permitted us to identify the molecular structures (scheme 2 and 3 on figure). From this comparison, we interpret one product as the result of a single dehydrogenation of a N-H group and the other as the result of double dehydrogenation (scheme 2). The latter, called tetraazapentacene (TAP), is a very promising analog of pentacene. Interestingly, synthesis of TAP molecule by conventional organic synthesis is still challenging and has yet not been accomplished. We demonstrate here a pathway to the synthesis of TAP on solid surfaces. By using higher current densities, preliminary experiments have shown that it is possible to switch a group of molecules in dense layers while preserving the initial crystallographic order. Further investigation are underway in order to elucidate the mechanism of the dehydrogenation. We expect that this knowledge will allow us to switching entire layers of DHTAP to TAP, and by this way, creating new organic semiconductor layers, which can not be produced using conventional methods.

**Keywords:** organic electronic, STM, nc-AFM, molecular switch, hydrogen-bond, self assembled monolayer, Heteroacene.

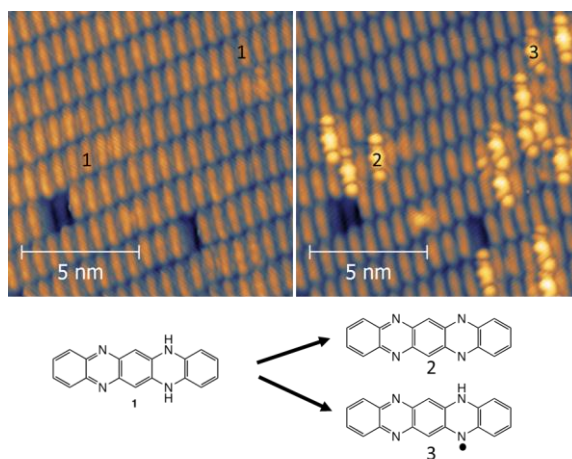


**Figure 1:** left : STM image of DHTAP (scheme 1) layers deposited on Au (111). Holes (dark blue) on the second layer are visible and can be used as landmarks. Right : the same area after a few voltage pulses performed by the STM tip on different molecules. Some DHTAP molecules have been switched (brighter) into new chemical compounds (scheme 2 and 3) which are the result of single dehydrogenation or double dehydrogenation.

## References:

- T. Lelaidier, T. Leoni, P. Arumugam, A. Rangui, C. Becker, O. Siri; Highly Ordered Molecular Films on Au(111): The N-Heteroacene Approach, *Langmuir* (2014) 30, 5700–5704.
- Bunz, U. H. F.; Engelhart, J. U.; Lindner, B. D.; Schaffroth, M. Large N-Heteroacenes: New Tricks for Very Old Dogs? *Angew. Chem., Int. Ed. Engl.* (2013) 52, 3810–21.



**Posters Session II: June 2<sup>nd</sup>, 2016**  
**NanoMatEn 2016**

# Solar charged redox flow battery

K. Wedege<sup>1</sup>, J. Azevedo<sup>2</sup>, A. Khataee<sup>1</sup>, A. Mendes<sup>2</sup>, A. Bontien

<sup>1</sup>Department of Engineering, Aarhus University, Aarhus, 8000, Denmark

<sup>2</sup>Department of Engineering, University of Porto, 4200-465, Portugal

## Abstract:

The intermittent nature of sunlight and the growing necessity for implementing sustainable energy sources drive research in the energy storage field. Direct solar charging of a redox flow battery with an integrated semiconductor photoelectrode could provide a solution to clean and efficient simultaneous harvesting and storage of solar energy. In this work, a solar redox flow battery using stable, low cost and environmentally friendly materials is demonstrated. The flow battery electrolytes consist of an iron complex and an anthraquinone species in sodium hydroxide solution separated by a cation exchange membrane. Battery cycling tests show high coulomb efficiency. Solar charging is facilitated by a thin-film hematite ( $\text{Fe}_2\text{O}_3$ ) semiconductor photoanode immersed directly in the iron complex solution creating a junction for charge collection. The photoelectrochemical charging process requires that the energy levels of the redox reactions are within the bandgap of hematite, if the battery is to be solar charged with no external voltage bias. Upon illumination of the interface, charge separation in the semiconductor material takes place and positive holes oxidize the iron complex while electrons move through external circuit and reduces the anthraquinone species on the other side of the battery, resulting in unbiased solar charging of the redox flow battery. The available photovoltage can be significantly increased following simple surface treatments consisting of pressure annealing and electrodeposition of a layer of a conductive polymer on the hematite surface.

In summary it is shown that it is possible to directly solar charge the electrolytes with a hematite photoanode in a photoelectrochemical process creating a solar redox flow battery using only stable, safe and low cost materials. The solar energy generation and storage approach described here opens up many new possibilities with respect to variation of electrolytes and photoelectrodes. The use of especially organic electrolytes offers a wide range of possibilities in future fully organic solar redox flow batteries

given the many possibilities of tailoring properties through manipulation of functional groups.

**Keywords:** Flow battery; Energy storage; Solar Energy; Photoelectrode

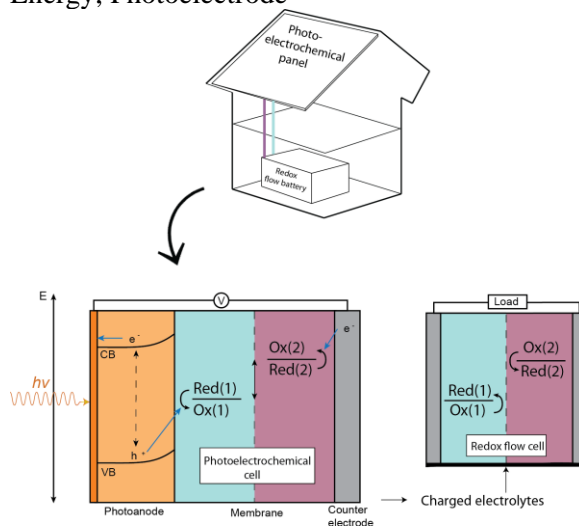


**Figure 1:** Solar redox flow battery and end application in domestic solar energy storage system.

## References:

- Wedege, K., Azevedo, J., Khataee, A., Mendes, A. (2015) Direct Solar Charging of an Organic-Inorganic, Stable and Aqueous Alkaline Redox Flow Battery with a Hematite Photoanode, *Submitted manuscript*.
- Klahr, B., Hamann, T., (2011), Current and voltage limiting processes in thin film hematite electrodes, *J. Phys. Chem.*, 115, 8393-8399.

# Novel Methods for the Deposition of Solution-Processed CdTe Inks for Photovoltaic Applications

Jake C. Russell<sup>1</sup>, J. Matthew Kurley<sup>1</sup>, Hao Zhang<sup>1</sup>, Dmitri Talapin<sup>1,\*</sup>

<sup>1</sup>University of Chicago, Department of Chemistry, Chicago, USA

## Abstract:

Cadmium telluride nanocrystals (CdTe NCs) have received increasing attention in recent years for their use as light absorbers in thin-film photovoltaics. While power-conversion efficiencies (PCE) are still short of silicon, cells fabricated with colloidal CdTe NC inks are cheaper and easier to produce than silicon wafers. Jasieniak et al. developed a layer-by-layer process for high-efficiency CdTe solar cell fabrication, making use of relatively low temperature annealing and a CdCl<sub>2</sub> bath to remove residual organics and encourage grain-growth. ZnO acts as an n-type layer, forming a p-n junction with CdTe. However, their use of spin-coating as the active layer deposition method significantly limits the translatability of the process to industry, because of the low throughput and extremely wasteful nature of spin-coating.

Seeking a more industrially-friendly deposition method while maintaining the same basic device architecture, we have developed a method for spray-coating CdTe NC inks. A novel methanol-based carrier solvent process allows for complete wetting of the substrate surface, leading to smooth and reproducible single layers. This method produces photovoltaic devices with efficiencies rivaling those of spin-coated devices (~12% PCE), while showing 1) higher material efficiency, 2) shorter fabrication times, and 3) potential applicability in industrial roll-to-roll production. Herein we compare and contrast the morphologies and electronic properties of spin- and spray-coated CdTe photovoltaic cells. We also demonstrate the potential for spray-coating various substrate geometries, including rods and lenses. The same solvent system also applies to different deposition methods, such as doctor-blading.

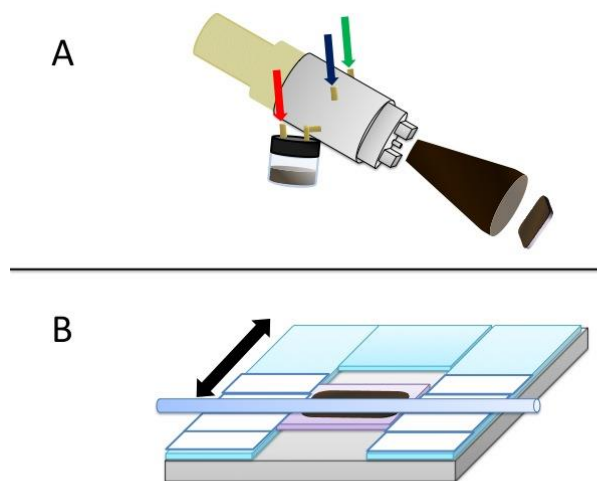


**Figure 1:** Schematic representation of two unique deposition methods for CdTe light absorbing layers in photovoltaic cells: spray coating (A) and doctor blading (B), both making use of a novel methanol-based solvent system.

**Keywords:** CdTe, nanocrystals, photovoltaics, colloidal inks, solution-processed, thin-film deposition, sintering, CdCl<sub>2</sub>, industrial applications.

## References:

Jasieniak, J., MacDonald, B. I., Watkins, S. E., Mulvaney, P. (2011) Solution-Processed Sintered Nanocrystal Solar Cells via Layer-by-Layer Assembly, *Nano Lett.*, 11, 2856-2864.

# Enhancement of power conversion efficiency of dye-sensitized solar cells via incorporation of GaN semiconductor materials synthesized in hot-wall CVD furnace.

M. Baisariyev, R. Iskakov, G. Sugurbekova

National Laboratory Astana, Nazarbayev University, Astana, Kazakhstan

## Abstract:

The current work discusses the study of the enhancement of the power conversion efficiency as well as fill factor (FF) by means of developing a composite photosensitive anode film based on the utilization of GaN (III-V) semiconductor material with 21 nm particle size TiO<sub>2</sub> nanopowder. Furthermore, it discusses how the synthesis conditions of GaN in hot-wall CVD reactor affects the photovoltaic performance of dye-sensitized solar cells as well as it investigates how the usage of GaN powders in different physical configurations in composite anode films affect the power conversion efficiency. SEM, EDX and Raman spectroscopy characterization tools were used to characterize the GaN powders synthesized at two different temperature zones such as Zone 3 and Zone 4 which correspond to 831.5°C-847 °C and 848°C-858 °C temperature ranges, respectively. The EDX and Raman spectra of GaN samples obtained from Zone 4 revealed better crystalline quality and less inclusion of oxygen. The obtained Raman spectra of our samples are shown in Figure 1. The Raman spectra of both Zone 3 and Zone 4 samples show the presence of E<sub>2</sub> (high) and A<sub>1</sub>(LO) modes which are two-symmetry allowed modes of hexagonal wurtzite GaN. The elevated peak intensity of E<sub>2</sub> (high) and A<sub>1</sub>(LO) modes of Zone 4 GaN samples relative to Zone 3 samples indicates the higher crystallinity of the former. As expected, the gallium nitride deposited at 848° C-858° C temperature ranges (Zone 4) demonstrated better fill factor values (0.647) than the powder (0.527) deposited at 831.5°C-847 °C temperature ranges (Zone 3). In order to study the effect of physical structure of anode film, two different configurations were proposed. In first configuration FTO glass gets coated with composite paste of 10wt%GaN/TiO<sub>2</sub> consistency, whereas in second configuration GaN paste gets overlaid on top TiO<sub>2</sub> paste thus forming layered structure. The photovoltaic performance of these two configurations was analyzed and it was revealed that the layered structure produced 11.14%

power conversion efficiency that is almost 2 times the efficiency of the mixed structure 6.62%.

**Keywords:** gallium nitride, dye-sensitized solar cells, fill factor, composite anode films, chemical vapor deposition

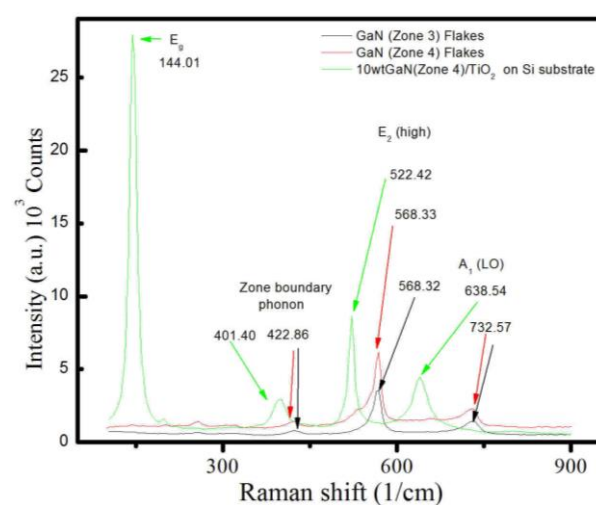


**Figure 1.** Raman spectra of the GaN (Zone 3), GaN (Zone 4) flakes and photoanode film of 10wt%GaN (Zone 4)/TiO<sub>2</sub> mixed composition applied on Si substrate

## References:

1. M. Gratzel, B. O Regan. *Nature (London)*, 1991: 353.
2. A.D. Pasquier, H.Chen and Y. Lu. *Applied Physics Letter*, 2006: 89.
3. B.K.Kang, Y.H.Song, S.M. Kang. *Journal of the Electrochemical Society*, 2011: 158.
4. S.N.Karthick, Hee-Je Kim. *Thin Solid Films*, 2012: 520.

# Fabrication of Hierarchical Nanostructures for Perfect Anti-reflection Coating

S.J. Cho<sup>1</sup>, T. An<sup>\*2</sup>

<sup>1</sup>School of Mechanical Engineering, Chungnam National University, Daejeon, Rep. of Korea.

<sup>2</sup>Department of Mechanical Design Engineering, Andong National University, Andong, Rep of Korea.

\* corresponding authors. Email : tmerias@anu.ac.kr

## Abstract:

In past decade, solar energy have become the focus of increased attention as fossil fuel resources are diminishing.[1] Thus, devices designed to convert sunlight to usable energy, such as a solar cell, have received a great interest. Light absorption is the one of key factors that affect conversion efficiency of solar cell. To improve the absorption, minimizing of reflectance is necessary when transmission is constant because the sum of transmission, reflection, and absorption of the incident flux is equal to unity. Recently, a novel bio-inspired nanostructure which mimics the compound eyes of moth has received a great interest. In previous our work, we fabricated sub-wavelength a silicon pillar array to generate a graded refractive index.[2] Here, we report a hierarchically designed silicon structure consisting of cone-shape micro pillars and nano-hairy structures by using a maskless plasma etching and self-assembly methods. Many of previous AR approaches have focused on fabrication of a simple and mono-scale structure such as a periodic nano-pillar structure or a micro-textured structure. Meanwhile, multi-layered and hierarchically designed structure enhances light absorption and carrier collection efficiency. We believe our fabrication method can be utilized to prepare various optical surfaces such as a solar cell or an optical sensor.

**Keywords:** anti-reflection surface, hierarchical nanostructures, solar energy collection

## References:

1. N. S. Lewis and D. G. Nocera, Proc. Natl. Acad. Sci. U. S. A., 103, 15729–35 (2006).
2. S. J. Cho, T. An, J. Y. Kim, J. Sung, and G. Lim, Chem. Commun., 47, 6108–10. (2011).



# Modeling infrared radiation transport in insulating dielectric nanocomposites to minimize radiative thermal losses

Janika Tang<sup>†</sup>, Vaibhav Thakore<sup>□</sup>, Tapio Ala-Nissilä

COMP Center of Excellence, Department of Applied Physics, Aalto University, Espoo, Finland

Email: \* [vaibhav.thakore@aalto.fi](mailto:vaibhav.thakore@aalto.fi); <sup>†</sup> [janika.tang@aalto.fi](mailto:janika.tang@aalto.fi)

## Abstract:

Thermal insulators focus on preventing heat loss through minimization of thermal conductivity, but suffer significant losses through radiation under high temperature conditions. Increased reflectance from highly scattering nanoparticle inclusions embedded in an insulating dielectric offers a promising method to reduce radiative thermal losses. The modeling of radiation transport in these highly scattering nanocomposites using Maxwell's equations for electromagnetic waves is computationally prohibitively expensive. However, the Monte Carlo modeling of diffusive transport of the incident thermal radiation offers an attractive alternative. Here, we employ Monte Carlo modeling and Mie scattering theory in conjunction with the effective medium theory (EMT) to compute infrared spectra for insulating dielectrics with lead-sulfide (PbS) and lead-selenide (PbSe) nanoinclusions. Similar to metallic nanoparticles [1, 2], these low band-gap semiconducting nanoinclusions in insulating dielectrics enhance reflectance in the infrared regime (see figure 1) due to increased scattering from the localized surface plasmon resonances (LSPR) [3]. The spectra for PbS and PbSe nanocomposites exhibit huge and distinct broad maxima in reflectance and a corresponding decrease in transmittance in the infrared regime for thermal radiation (Figure 2). Further, we identify optimum size, shape and volume fractions of the PbS and PbSe nanoinclusions to obtain maximal infrared reflectance. The results presented here are thus highly relevant to the development of advanced thermal insulators for high-temperature applications that seek to minimize radiative thermal losses.

**Keywords:** thermal radiation, Monte Carlo modeling, Mie scattering, effective medium theory, nanocomposites, nanoparticle inclusions, thermally insulating dielectrics, low band gap semiconductors, lead sulfide, lead selenide

## Acknowledgements:

Academy of Finland, Center of Excellence Programme (2015-2017), Project # 284621; Aalto Energy Efficiency Research Program EXPECTS; Aalto Science-IT project.

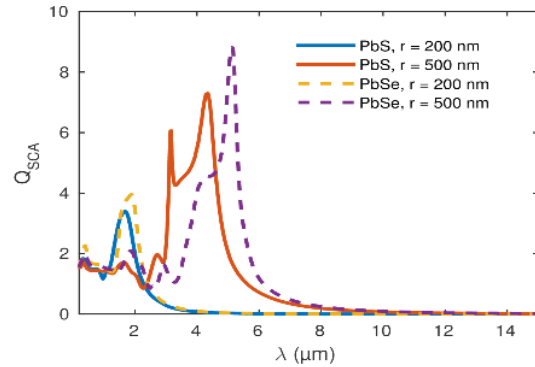


**Figure 1:** Scattering efficiency factor  $Q_{SCA}$  for PbS and PbSe particles of different radii embedded in a dielectric medium of refractive index  $n_m = 1.5$ .

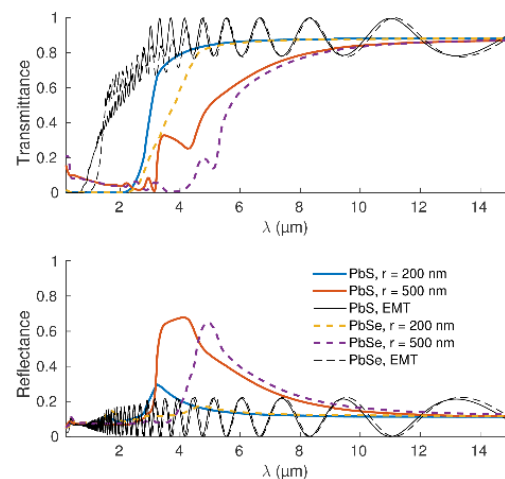


**Figure 2:** Reflectance and transmittance spectra of insulating nanocomposite dielectrics with PbS and PbSe inclusions in a host medium of refractive index  $n_m = 1.5$ , thickness  $d = 10 \mu\text{m}$  and volume fraction of nanoinclusions  $f = 0.1$ .

## References:

1. K. Laaksonen, S. Suomela, S. R. Puisto, N. K. J. Rostedt, T. Ala-Nissilä, R. M. Nieminen, *J. Opt. Soc. Am. B* **30** (2013) 338-348.
2. K. Laaksonen, S.Y. Li, S.R. Puisto, N.K.J. Rostedt, T. Ala-Nissilä, C.G. Granqvist, R.M. Nieminen, G.A. Niklasson, *Sol. Energ. Mat. Sol. C* **130** (2014) 132-137.
3. J.M. Luther, P.K. Prashant, T. Ewers and A.P. Alivisatos, *Nature Materials* **10** (2011) 361-366.

# Numerical Investigations of Heat Transfer in Rectangular Micro-Channels during Single Phase Fluid Flow using Cooling Nanoliquids

L. Snoussi<sup>1,2\*</sup>, N. Ouerfelli<sup>3</sup>, F.B.M. Belgacem<sup>4</sup>, A. Guizani<sup>1</sup>,

<sup>1</sup>Thermal Process Laboratory Research and Technologies Centre of Energy, Borj-Cedria Science and Technologies Park, BP 95, 2050 Hammam-lif, Tunisia

<sup>2</sup>High Institute of Environmental Science and Technology; University of carthage, borj cedria, Tunisia

<sup>3</sup>Université de Tunis El Manar, Laboratoire de Biophysique et Technologies Médicales, LR13ES07, Institut Supérieur des Technologies Médicales de Tunis, 9 Avenue Dr. Zouhaier Essafi 1006 Tunis, Tunisia

<sup>4</sup> Department of Mathematics, Faculty of Basic Education, PAAET, Al-Ardhiya, Kuwait.

## Abstract:

Studying fluid flow characteristics at microscale levels, using nanofluids, is gaining importance and momentum with shrinking device sizes. Better understanding of fluid flow and heat transfer in microchannels has important implications in electronic chip cooling, heat exchangers, MEMS, and microfluidic devices [1-3]. In this study, the three-dimensional fluid flow and heat transfer phenomena in a copper-based rectangular microchannel heat sink (MCHS) are analyzed numerically using nanofluids. The (MCHS) has 215  $\mu\text{m}$  width, 821  $\mu\text{m}$  depth, and 4.48 cm length under the boundary conditions of constant heat flux and laminar flow with uniform inlet velocity. The distributions of the particles in base fluid are assumed to be uniform (Figure 1). A three-dimensional Computational Fluid Dynamics (CFD) model was built using the commercial package, FLUENT.

This work shows temperature and velocity distributions in the investigated MCHS. For verification of the used CFD method, the results obtained were compared with available experimental data for both pure water and the nanofluids in different volume fractions in terms of convective heat transfer coefficients, wall temperature and pressure drops, analysis shows that the nanofluids enhance heat transfer while the Reynolds number and the volume fractions are increasing. A very weak effect on the heat transfer coefficient for pure water, but an appreciable effect for the nanofluid. We observe that the pressure drop of the nanofluids increases with increment in the Reynolds number, while there is a notable but small increase with increasing nanofluids volume fraction.

**Keywords:** Commercial CFD code FLUENT, Heat transfer coefficient, Heat transfer enhancement, Reynolds number, Rectangular microchannel heat sink (MCHS), Nanofluids.

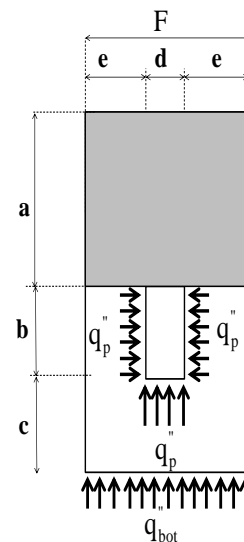


**Figure 1:** Computational Domain.

## References:

- [1] Tuckerman D.B., Pease R.F.W., (1981) High Performance Heat Sinking for VLSI, *IEEE Elect. Dev. Lett.*, vol. 2, pp 126-129.
- [2] Peng, X.F. and Peterson, G.P., (1995), The effect of thermofluid and geometrical parameters on convection of liquids through rectangular microchannels, *Int. J. Heat Mass Transfer*, Vol. 38(4), 755-758.
- [3] Snoussi L., Chouikh R., Ouerfelli N., Guizani A. (2016) Numerical simulation of heat transfer enhancement for natural convection in a cubical enclosure filled with Al<sub>2</sub>O<sub>3</sub>/water and Ag/water nanofluids. January 2016, *Physics and Chemistry of Liquids*.

# The performance of Zn/Ni battery using $\text{Ni}_x\text{Zn}_{(1-x)}\text{O}$ as anodic material to suppress Zn dendrite

Younghwan Im<sup>1</sup>, Kyung Su Park<sup>2</sup>, Tae Woo Cho<sup>2</sup>, Jin-Sik Lee<sup>2</sup>, Misook Kang<sup>1,\*</sup>

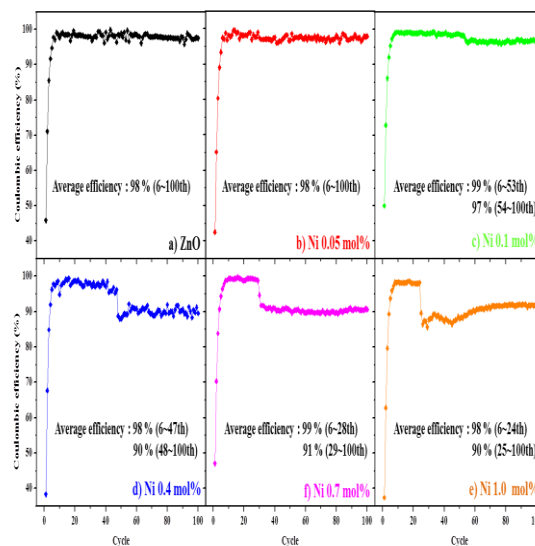
<sup>1</sup>Yeungnam University., Department of chemistry, Gyeongsan, Gyeongbuk38514, Republic of Korea

<sup>2</sup> Research & Development center, Vitizro cell, Yesan-gun, Chungnam 23535, Republic of Korea

## Abstract:

The energy storage system (ESS) has widely been developing to improve the efficiency of electric load management. Because the electricity consumption is imbalanced according to a time of a day, season and so on. Moreover, generated renewable energies also are intermittent and often unpredicted under weather condition and other factors. Without special device like the energy storage system [1]. Therefore, among many ESSs, the redox flow batteries (RFBs) has been focused as promising electric energy storage device and studied [2]. In this study, the Zn/Ni redox couple's properties have been investigated, especially, focusing Zn dendrite growth on the anode side that limits its performance.

The nanoparticles of ZnO and  $\text{Ni}_x\text{Zn}_{(1-x)}\text{O}$  (Ni 0.05 mol%, 0.1 mol%, 0.4 mol% 0.7 mol%, 1 mol%) were synthesized by sol-gel method adding Oxalic acid as chelate agent. X-ray diffraction (XRD), transmission electron microscope, scanning electron microscope (SEM), energy dispersive X-ray spectroscopy (EDX), cyclic voltammetry (CV), and galvanostatic charge-discharge cycle test were used in this study. The ZnO and  $\text{Ni}_x\text{Zn}_{(1-x)}\text{O}$  nanoparticles have spherical shape with about 20 nm size and hexagonal wurtzite crystalline structure. In the galvanostatic charge-discharge test, the cells were fabricated with a  $\text{Ni}(\text{OH})_2$  electrode as cathode and Ni metal plate as an anode. The electrolyte was the dissolved ZnO or  $\text{Ni}_x\text{Zn}_{(1-x)}\text{O}$  of 0.01 mole into 6 M KOH of 10 mL. The cells using pure ZnO and  $\text{Ni}_x\text{Zn}_{(1-x)}\text{O}$  show efficiencies of 90 % above during entire cycle. Simultaneously, The more Ni ion had been added, the more Zn and ZnO dendrite were suppressed. However, there was an efficiency's drop according to Ni content. Considering the conflicting factors,  $\text{Ni}_x\text{Zn}_{(1-x)}\text{O}$  of 0.1 mol% is the most appropriate cell among the others.



**Keywords:** ZnO, Zn dendrite, Zn/Ni redox flow battery, Zn/Ni redox couple

**Figure 1:** The coulombic efficiencies' plots of Zn/Ni cells using ZnO and  $\text{Ni}_x\text{Zn}_{(1-x)}\text{O}$  as the anodic active materials.

## References:

- [1] Siraj Sabihuddin., Aristides E., Kiprakis, Markus Mueller. (2015) A Numerical and Graphical Review of Energy Storage Technologies, *Energies.*, 8, 172-216.
- [2] Adam Z. weber., Matthew M. Mench., Jeremy P. Meyers., Philip N. Ross., Jeffrey T. Gostick., Qinghua Liu. (2011) Redox flow batteries: a review., *J. Appl. Electrochem.*, 41, 1137-1164.

# Kinetic mechanisms of hydrogen sorption in nanocrystalline magnesium (hydride)

S. Shrinivasan<sup>1\*</sup>, A. Gangrade<sup>1</sup>, N.K. Gor<sup>1</sup>, H.-Y. Tien<sup>2</sup>, M. Tanniru<sup>2</sup>, F. Ebrahimi<sup>2</sup>, S.S.V. Tatiparti<sup>1,2</sup>

<sup>1</sup> Indian Institute of Technology Bombay, Department of Energy Science and Engineering, Mumbai-400076, India.

<sup>2</sup> University of Florida, Materials Science and Engineering Department, Gainesville, FL 32611, USA.

## Abstract:

Magnesium (hydride) is a very promising material for hydrogen storage with very high gravimetric capacity (7.6 wt.%). However, its slow kinetics of hydrogen absorption/desorption (sorption) hinders its application. Strategies such as particle size reduction, catalyst addition are employed to improve the kinetics of sorption. To devise the strategies for improving the kinetics, it is essential to unravel the mechanisms of hydrogen sorption. The kinetics of hydrogen sorption in ball milled nanocrystalline magnesium (hydride) powders are investigated using the popular Johnson-Mehl-Avrami-Kolmogorov (JMAK) equation ( $\alpha = 1 - \exp(-kt^n)$ ) at different temperatures (180 °C-400 °C). The exponent  $n$  indicates the dimensionality of the growth of Mg (during desorption) or MgH<sub>2</sub> (during absorption).  $n$  decreases with time from a high value (>1) to a negligible value (<0.5) suggesting that the growth of the phase (Mg or MgH<sub>2</sub>) decreases with time. The cross-sectional observation of these powders using SEM and TEM revealed that the depth of the growing phase from the particle surface increases with time rendering a core-shell structure during sorption. The estimated hydride/metal interface velocity ( $U$ ) for growth of these phases shows two clear regimes of high and low velocities in the  $n > 0.5$  and  $n < 0.5$  regimes respectively. The former velocity is at least 2 orders of magnitude higher than the latter. The diffusion coefficients ( $D$ ) are also estimated using Fick's 2nd law (transient) for hydrogen diffusion through the magnesium hydride phase. The estimated diffusion coefficients are at least 4 orders of magnitude higher in the  $n > 0.5$  regime than in those in the  $n < 0.5$  regime. Moreover, the diffusion coefficients in the  $n < 0.5$  regime are closer to the expected values from literature. The estimated activation energy for hydrogen diffusion through hydride is 91 kJ/mol H and is close to the literature reported value of 100±10 kJ/mol H. The combined  $n$ - $U$ - $D$  analysis supported by the microstructural examinations suggests that the growth of the magnesium or hydride is gov-

erned by hydride/metal interfacial movement in the  $n > 0.5$  regime and by hydrogen diffusion through hydride in the  $n < 0.5$  regime. The present analysis distinguishes growth by the interfacial velocity from that by diffusion during hydrogen sorption in magnesium (hydride). The present analysis contributes to the advancement of the understanding on the kinetic mechanisms of hydrogen sorption of MgH<sub>2</sub>.

**Keywords:** MgH<sub>2</sub>, hydrogen sorption, JMAK, interfacial growth, diffusional growth.

## References:

1. S. Shrinivasan, H.-Y. Tien, M. Tanniru, F. Ebrahimi, S.S.V. Tatiparti, *Mater. Lett.*, **161** (2015), 271-274.
2. S. Shrinivasan, H. Goswami, H.-Y. Tien, M. Tanniru, F. Ebrahimi, S.S.V. Tatiparti, *Int. J. Hydrogen Energy*, **40** (2015), 13518-13529.
3. K. Nogita, X.Q. Tran, T. Yamamoto, E. Tanaka, S.D. McDonald, C.M. Gourlay, K. Yasuda, S. Matsumura, *Sci. Rep.*, **5** (2015) 8450.

# Hydrogen production from propane steam reforming over $30\text{Ni}_x\text{Fe}_{1-x}\text{O}/70\text{Al}_2\text{O}_3$ catalysts

Kang Min Kim<sup>1</sup>, Byeong Sub Kwak<sup>1</sup>, No-Kuk Park<sup>2</sup>, Tae Jin Lee<sup>2</sup>, Misook Kang<sup>\*1</sup>

<sup>1</sup>School of Chemistry, Yeungnam University, Gyeongsan, Gyeongbuk 38541, Rep. of Korea

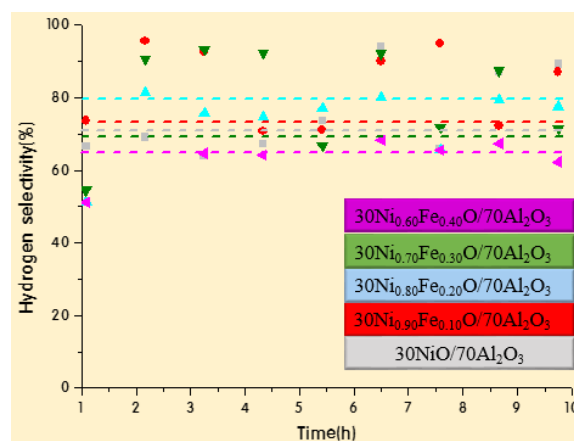
<sup>2</sup>School of Chemical Engineering, Yeungnam University, Gyeongsan, Gyeongbuk 38541, Rep. of Korea

## Abstract:

Hydrogen energy is highly effective as renewable source that can be produce the electricity in the fuel cell. There are several methods of producing the hydrogen. Among the methods, hydrocarbon reforming method is the most effective and cheap[1]. Propane Steam Reforming(PSR) is versatile method to produce hydrogen as hydrogen 10 mole per propane 1 mole[2]. Particularly, Propane plays a major role in the LPG component. Moreover, A huge requirement of LPG fuel is becoming strong in day to day life in Korea. Thus, in this study, the main constituent of the propane in LPG was to produce hydrogen. We use the main catalyst that is known as effective catalyst NiO/Al<sub>2</sub>O<sub>3</sub> in Methanol Steam Refroming(MSR)[3]. Moreover, We examined the catalytic activities of  $30\text{Ni}_x\text{Fe}_{1-x}\text{O}/70\text{Al}_2\text{O}_3$  ( $x = 0.6, 0.7, 0.8, 0.9, 1$ ) catalysts as well as the promotion between NiO and FeO ratio on propane steam reforming(PSR). Propane conversion and H<sub>2</sub> yield increased and carbon coke deposition and CO emission have been suppressed by substituting FeO[4]. Synthesized catalysts' physical characteristics are analysed by XRD, TEM, TPD, H<sub>2</sub>-TPR and TGA. PSR reaction measured from 500 °C to 800 °C for reduced catalysts in 700 °C for 10 h. In the temperature range from 700 °C it showed the highest hydrogen selectivity. Among these catalysts,  $30\text{Ni}_{0.8}\text{Fe}_{0.2}\text{O}/70\text{Al}_2\text{O}_3$  is the best hydrogen production selectivity and propane conversion in 700 °C Figure 1.

**Keywords:** Propane Steam reforming, PSR, water gas shift reaction, Hydrogen production,  $30\text{Ni}_x\text{Fe}_{1-x}\text{O}/70\text{Al}_2\text{O}_3$ .

**Figure 1:** Hydrogen selectivity curved for  $30\text{Ni}_x\text{Fe}_{1-x}\text{O}/70\text{Al}_2\text{O}_3$  catalysts



## References:

1. Paula O.-V., Nicolás A. F.-G., Rufino M. N., Jose L.G. F., Cristian H. C., Patricio R., (2015), Improved stability of Ni/Al<sub>2</sub>O<sub>3</sub> catalysts by effect of promoters (La<sub>2</sub>O<sub>3</sub>, CeO<sub>2</sub>) for ethanol steam-reforming reaction, *Catal. Today*, 259, 27–38
2. Maki M., Kazuki S., Tatsumi I., (2014), Comparative study of propane steam reforming in vanadium based catalytic membrane reactor with nickel-based catalysts, *Int. J. Hydrogen Energ.*, 39, 14792-14799
3. A.A. Lytkina, N.A. Zhilyaeva, M.M. Ermilova, N.V. Orekhova, A.B. Yaroslavtsev, (2015), Influence of the support structure and composition of Ni-Cu-based catalysts on hydrogen production by methanol steam reforming, *Int. J. Hydrogen Energ.*, 40, 9677-9684
4. Y. Jiao, J. Zhang, Y. Du, D. Sun, J. Wang, Y. Chen, J. Lu, (2015), Steam reforming of hydrocarbon fuels over M(Fe, Co, Ni, Cu, Zn)-Ce bimetal catalysts supported on Al<sub>2</sub>O<sub>3</sub>, *Int. J. Hydrogen Energ.*, xxx, 1-10



# Hydrogen production by propane steam reforming over transition metal (A = Fe, Co, Ni, Cu) in Mn-based metal oxide structure

Jeong Yeon Do<sup>1</sup>, Misook Kang<sup>#</sup>

<sup>1</sup>Yeungnam University, Department of chemistry, Gyeongsan, Gyeongbuk, (38541) Republic of Korea

<sup>#</sup>Misook Kang/ E-mail: mskang@ynu.ac.kr, TEL: +82-53-2363, FAX: +82-53-4617

## Abstract:

Humanity's main energy source, fossil fuels caused a lot of environmental problems. So worldwide attention is focusing on renewable energy sources, particularly hydrogen. Due to Hydrogen has environmental benefits compared to current fossil fuel or nuclear power, it is being evaluated as a new generation of clean energy. Even if there are several ways for producing hydrogen, most economical and environmental method is a steam reforming reaction.

In this study, it was used for LPG gas (in particular propane) as a source of reforming fuel. It is closely connected in our life and can be obtained more easily very economical fuel source. Previously used a conventional catalyst for steam reforming reactions are mainly precious metals. But these catalysts have disadvantage that the price is too high compared to the energy efficiency

Therefore, the purpose of this study was development of the new catalysts which has low-cost, heat-resistant and excellent durability by dispersing a transition metal on the supporting material.

Catalyst  $X_2MnO_4$  ( $X = Fe, Co, Ni, Cu$ ) was first synthesized in a molar ratio, then it was impregnated in the supporting materials,  $\gamma-Al_2O_3$  with 3 in a ratio of about 7. Finally it was used as a catalyst for the steam reforming reaction for producing hydrogen. In order to determine the physical and chemical properties of the catalysts, we used to various techniques such as XRD, BET, XPS and so on. The steam reforming reaction was conducted at GHSV  $5300h^{-1}$ . When I perform the reaction while increasing the temperature ( $450\sim 800\text{ }^\circ C$ ), the hydrogen production amount of all of the catalyst is usually most at high temperature. To find the best catalyst performance, the experiment was performed under the same conditions (at 973K for 10h). As a result, a catalyst having a spinel structure was  $Ni_2MnO_4$  generate most hydrogen during the reaction for 10h (Fig 1). Propane conversion was closely to 100%, and by-products has been identified as methane, ethane, acetylene. Among the catalysts, hydrogen selectivity of  $Ni_2MnO_4$  was highest about 80%. Therefore, spinel structure and Mn as

oxygen carrier contributes to catalyst performance.

**Keywords:**  $Ni_2MnO_4$ , hydrogen production, Propane steam reforming,  $X_2MnO_4$ , spinel structure

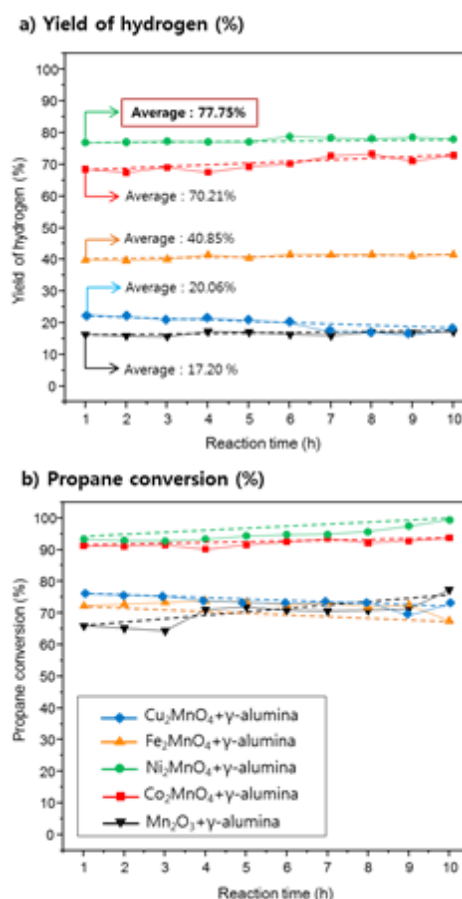


**Figure 1:** (a) Yield of hydrogen(%) and (b) Propane conversion during propane steam reforming reaction at 973K for 10h.

## References:

1. B.T. Schädel, M. Duisberg, O. Deutschmann, Steam reforming of methane, ethane, propane, butane, and natural gas over a rhodium-based catalyst, *Catal Today* **142** (2009) 42-51.
2. M. Matsuka, K. Shigedomi, T. Ishihara, comparative study of propane steam reforming in vanadium based catalytic membrane reactor with nickel-based catalysts, *Int J Hydrogen Energy* **39** (2014) 14792-14799.

# Three-metallic Mn-based Ni<sub>1-x</sub>Co<sub>x</sub>MnO<sub>4</sub>/γ-Al<sub>2</sub>O<sub>3</sub> (X=0.2, 0.3, 0.4, 0.5) catalysts for hydrogen production via steam reforming of propane gas

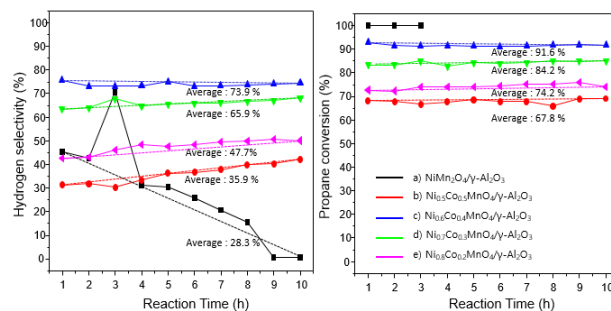
SeungWon Jo,<sup>1</sup> Misook Kang<sup>1,\*</sup>

<sup>1</sup>Yeungnam University., Department of chemistry, Gyeongsan, GyeongBuK38514, Republic of Korea

\*Misook Kang/E-mail: [mskang@ynu.ac.kr](mailto:mskang@ynu.ac.kr), TEL: +82-53-2363, FAX: +82-53-4617

**Abstract:** Research developments for utilization of alternative energies have become a Big deal now a days due to increasing environmental problems such as air pollution, ozone layer depletion and global warming. It is well known that hydrogen can serve as a renewable energy carrier due to its non-polluting nature. Among the various methods, Reforming is superior one for producing the hydrogen production using fuel like hydrocarbon.[1] View of research, selection of fuel plays a pivotal role in reforming process.[2] Propane or LPG are attractive fuels because of their connectivity in our a day to life.[3] Here, We report the results regarding investigation on propane steam reforming over the three-metallic catalysts. Various techniques such as X-ray diffraction (XRD), temperature-programmed reduction (TPR) etc were used to characterize the as-prepared catalysts in order to the catalyst structure-performance relationship. We have been made a comprehensive comparative analysis of hydrogen selectivity over Mn-based three-metallic catalysts (Ni<sub>1-x</sub>Co<sub>x</sub>MnO<sub>4</sub>/γ-Al<sub>2</sub>O<sub>3</sub> (X=0.2, 0.3, 0.4, 0.5 mol-%) on the same temperature 973K (GHSV 5300h<sup>-1</sup>). Propane conversion was identified to be converted up to 91%. when compared with hydrogen selectivity among the catalysts, Ni<sub>0.6</sub>Co<sub>0.4</sub>MnO<sub>4</sub>/γ-Al<sub>2</sub>O<sub>3</sub> catalyst was measured up to 75.7 % against other catalysts as show in Figure 1 This selectivity of hydrogen production was formed to be 75.7 % during 10-h accompanying with byproducts of CH<sub>4</sub>, acetylene and ethylene. The enhancement of catalytic activity and stability are ascribed due to selective metal composition and structure.

**Keywords:** Steam reforming of propane gas, Three-metallic catalysts, hydrogen production,



propane conversion, selectivity, alternative energy.

**Figure 1:** Hydrogen selectivity over Ni<sub>1-x</sub>Co<sub>x</sub>MnO<sub>4</sub>/γ-Al<sub>2</sub>O<sub>3</sub> (X=0.2, 0.3, 0.4, 0.5 mol-%) during steam reforming of propane gas :

To improve the hydrogen selectivity, What are the most important thing to solve the problem of carbon deposition. To solve this problem, We added Mn as the oxygen carrier and changed mol-ratio of Ni and Co

## References:

1. Chunfeng Song., Qingling Liu., Na Ji., Yasuki Kansha., Atsushi Tsutsumi, (2015), Optimization of steam methane reforming coupled with pressure swing adsorption hydrogen production process by heat integration, *Applied Energy.*, 154, 392-401
2. Tengfei Hou., Bo Yu., Shaoyin Zhang., Jianghua Zhang., Dazhi Wang., Tongkuan Xu., Li Cui., Weijie Cai, (2015), Hydrogen production from propane steam reforming over Ir/Ce<sub>0.75</sub>Zr<sub>0.25</sub>O<sub>2</sub> catalyst, *Applied Catalysis B: Environmental.*, 168-169, 524-530
3. M. Matsuka., K. Shigedomi., T. Ishihara., (2014), Comparative study of propane steam reforming in vanadium based catalytic membrane reactor with nickel-based catalysts, *Int J Hydrogen Energy.*, 39, 14792-14799

# Effective hydrogen production from propane stream reforming on $\text{Co/Ce}_x/\gamma\text{-Al}_2\text{O}_3$

Minkyu Park,<sup>1</sup> Misook Kang,\*

<sup>1</sup>Yeungnam University, Department of Chemistry, Gyeongsan, Gyeongbuk, (38541) Rep. of Korea.

\*Misook Kang/ E-mail : [miskang@ynu.ac.kr](mailto:miskang@ynu.ac.kr), TEL: +82-53-2363, FAX: +82-53-4617

## Abstract:

Recently, due to fossil fuel use, natural resource depletion and environmental pollution has become a serious problem. Hydrogen energy in renewable energy is attention as a clean energy with no secondary pollution. Ethanol steam reforming reaction has been widely studied. So, we focused on the study using steam reforming reaction of propane[1].

This study examined the catalytic activities on propane steam reforming (PSR). When using a propane fuel of the hydrocarbon steam reforming method for producing hydrogen has the advantage of mass production of hydrogen of 1 to 10 moles per molecule. To produce hydrogen efficiently by using a Co-based catalyst with excellent oxidation rate and high-temperature durability. Using a  $\gamma\text{-Al}_2\text{O}_3$ , supporting material, was impregnated with Co and Ce to produce a  $\text{Co/Ce}_x/\gamma\text{-Al}_2\text{O}_3$  ( $X=0.03, 0.09, 0.15, 0.21, 0.3$ ) catalyst in the form of a thermal treatment under an oxygen flow[2]. Synthesis of five different ratio of cerium by sol-gel method. X-ray diffraction measurement in order to confirm the crystal structure.

The PSR catalytic tests for hydrogen production were performed in a fixed bed reactor catalyst at 973K and  $6,500 \text{ h}^{-1}$  GHSV after Hydrogen-pre treatment and reaction for 10 hour. Propane conversion was identified to be converted about 100 %. When compared with hydrogen selectivity among the catalysts,  $\text{Co/Ce}_{0.09}/\gamma\text{-Al}_2\text{O}_3$  catalyst was measured up to 80 %.

**Keywords:** Propane steam reforming (PSR), Hydrogen production,  $\text{Co/Ce}_x/\gamma\text{-Al}_2\text{O}_3$

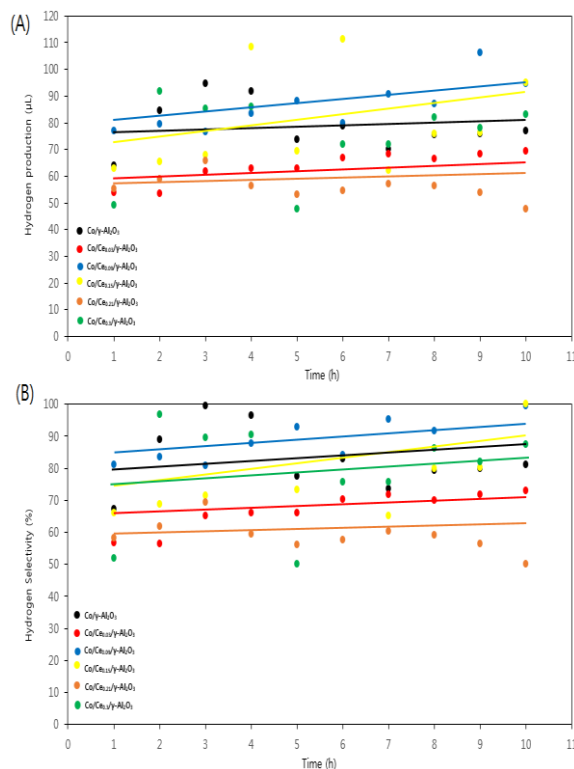


**Figure 1:** (A) Hydrogen Production, (B) Hydrogen Selectivity over  $\text{Co/Ce}_x/\gamma\text{-Al}_2\text{O}_3$  ( $X=0.03, 0.09, 0.15, 0.21, 0.3$  wt-%) during steam reforming of propane gas.

## References:

1. Hydrogen: the energy source for the 21<sup>st</sup> century. Brenda Johnston, Michael C. Mayo, Anshuman Khare\*, Technovation 25 (2005) 569-585.
2. Hydrogen production from propane steam reforming over  $\text{Ir/Ce}_{0.75}/\text{Zr}_{0.25}\text{O}_2$  catalyst. Tengfei Hou, Bo Yu, Shaoyin Zhang, Jianghua Zhang, Dazhi Wang, Tongkuan Xu, Li Cuo, Weijie Cai, Applied Catalysis B: Environmental, 168-169 (2015) 524-530.

# Oxygen Reduction Reaction Catalyzed by Manganese Dioxide Nanoflowers

L.R. Aveiro,<sup>1\*</sup> V.S. Antonin,<sup>1</sup> A.G.M. da Silva,<sup>2</sup> E. G. Candido,<sup>2</sup> P.H.C. Camargo,<sup>2</sup> M.C. dos Santos,<sup>1</sup>

<sup>1</sup>Federal University, UFABC, Lab. Electroch. and Nanostructured Materials, St André, Brazil

<sup>2</sup>University Sao Paulo, USP, Institute of Chemistry, São Paulo, ABC Brazil

## Abstract:

Manganese dioxide is one of the most promising candidates to replace Pt as an efficient cost-effective catalyst for the oxygen reduction reaction (ORR) in alkaline medium. Among various advantages offered by manganese dioxide one can point out that are low-cost materials found in abundance from natural ores. Moreover, they present environmental compatibility and eco-friendly feature, with high electrocatalytic activity for the ORR being extensively investigated by different researchers and research groups<sup>1</sup>. In this work, the nanoflowers dioxide manganese - NFMnO<sub>2</sub> were obtained by a hydrothermal approach and supported on carbon – Vulcan XC-72R in different compositions (1-3-5-7 and 10% w/w) for RRO electrocatalytic activity evaluation. The NFMnO<sub>2</sub> were physically characterized by scanning electron microscopy (SEM). **Figure 1** shows the nanoflowers displayed well-defined shapes and uniform sizes, petals being  $15 \pm 5$  nm in width and  $> 1$   $\mu$ m in diameter. Polarization curves obtained for the ORR using rotating ring-disk electrode, at 1600 rpm, on the NFMnO<sub>2</sub>/C electrocatalysts, and the corresponding currents for the HO<sup>-2</sup> oxidation in the ring are presented in **Figure 2A**. Note that the material which showed highest ring current in the ORR was NFMnO<sub>2</sub>/C 3 % ( $\sim 23 \mu$ A) while the ring current for the same process with carbon without nanoflowers showed  $\sim 16 \mu$ A current. Furthermore, the slope in Koutechy - Levich plot for ORR of this same material was close to the one determined for the same process using Vulcan, (**Figure 2B** - slope 102 - Vulcan XC-72R and 103- NFMnO<sub>2</sub>/C 3 %) thus indicating a 2- electrons transference in ORR, to H<sub>2</sub>O<sub>2</sub> formation. The results presented here indicate that NFMnO<sub>2</sub>/C 3 % is a promising material as electrocatalyst for H<sub>2</sub>O<sub>2</sub> electrogeneration and it can be employed in the degradation of organic pollutants in Advanced Oxidative Processes .

**Keywords:** manganese dioxide, nanoflowers, oxygen reduction reaction, electrocatalyst, peroxide hydrogen.

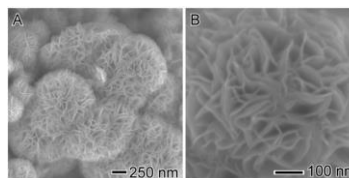


**Figure 1:** (A-B) SEM images of NFMnO<sub>2</sub> obtained by hydrothermal method.

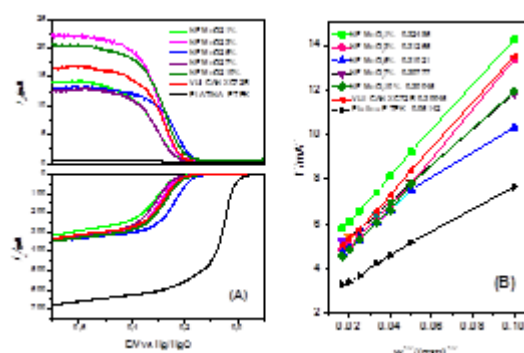


**Figure 2:** (A) Polarization curves for the oxygen reduction reaction on different electrocatalysts in oxygen saturated NaOH (1.0 mol.L<sup>-1</sup>) aqueous solution,  $\omega = 1600$  rpm;  $\nu = 5$  mV.s<sup>-1</sup>. (B) Koutechy - Levich diagram for ORR using electrocatalysts NFMnO<sub>2</sub> 1-3-5-7-10 % and materials reference Pt/C 20wt.% (E-TEK) and Vulcan XC-72R.

## References:

1. Valim, R.B., Santos, M.C., Lanza, M.R.V., Machado, S.A.S., Lima, F.H.B., Calegari, M.L. (2012) Oxygen reduction reaction catalyzed by  $\epsilon$ -MnO<sub>2</sub>: Influence of the crystalline structure on the reaction mechanism, *Electrochimica Acta*, 85, 423-431.
2. Wang, X., Li, Y. (2002) Selected-Control Hydrothermal Synthesis of  $\alpha$ - and  $\beta$ -MnO<sub>2</sub> Single Crystal Nanowires, *J. Am. Chem. Soc.*, 124, 2880-2881.
3. Yu, L.L., Zhu, J.J., Zhao, J.T. (2014) Beta-manganese dioxide nanoflowers self-assembled by ultrathin nanoplates with enhanced supercapacitive performance, *J. of Mat. Chem. A*, 2, 9353-9360.



# W@Au nanostructures as catalysts for H<sub>2</sub>O<sub>2</sub> electrogeneration

V. S. Antonin<sup>1\*</sup>, L.S. Parreira<sup>1</sup>, F.L. Silva<sup>2</sup>, R.B. Valim<sup>2</sup>, P. Hammer<sup>3</sup>, M.R.V. Lanza<sup>2</sup>, M. C. Santos<sup>1</sup>

<sup>1</sup> Universidade Federal do ABC, UFABC, Santo André, SP, Brazil.

<sup>2</sup> Universidade de São Paulo, São Carlos, SP, Brazil.

<sup>3</sup> Universidade Estadual Paulista, Araraquara, SP, Brazil

**Abstract:** The use of nanostructures core-shell type has attracted considerable interest for research field on alternative power sources because of their conductive and versatile compositions for bulk metals and for its corresponding monometallic particles<sup>1</sup>. In addition, both coating high cost metal (e.g., Au, Pt or Pd) and a monolayer on the surface of non-precious metal-based nanostructures (e.g., Ni, Fe or Co) imply a reduction in costs and may even increase the catalytic efficiency<sup>2</sup>. In this work, we report a facile strategy for the synthesis of W@Au structures (**Figure 1**) followed by a comparative study of two proportions of the core-shell nanoparticles supported on carbon (1% and 2%) as electrocatalysts for the oxygen reduction reaction (**Figure 2**). The main goal of this work was to know how the W@Au loading could affect the electrocatalytic activity of the Vulcan XC-72R carbon. The use of W@Au materials led to higher activity compared to pure carbon and commercial Pt/C, and the optimal load corresponded to 1% which presented the higher ring current for the ORR using the rotating ring-disk electrode technique. Exhaustive electrolysis using a W@Au/C 1% gas diffusion electrode (GDE) was employed to verify the real amount of H<sub>2</sub>O<sub>2</sub> electrogenerated comparing to Vulcan XC-72R GDE (**Figure 3**). We verified that the W@Au/C 1% material is able to generate 50% more H<sub>2</sub>O<sub>2</sub> than carbon. These results can be explained based on synergistic interactions presented by the W@Au/C 1% material and also by conductivity differences provided by the nanostructures loaded on supported. All electrochemical measurements indicated that the electrocatalyst based on W@Au/C 1% is a promising material for H<sub>2</sub>O<sub>2</sub> electrogeneration and consequently can be applied on advanced oxidation processes on the degradation of organic pollutants in water.

**Keywords:** Hydrogen peroxide electrogeneration, oxygen reduction reaction, core-shell, W@Au.

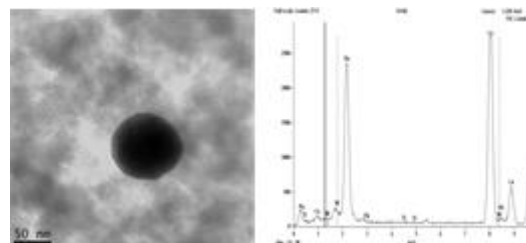


**Figure 1:** (A) TEM images of 1% W@Au/C electrocatalyst and (B) EDS spectrum of 1% W@Au/C prepared.

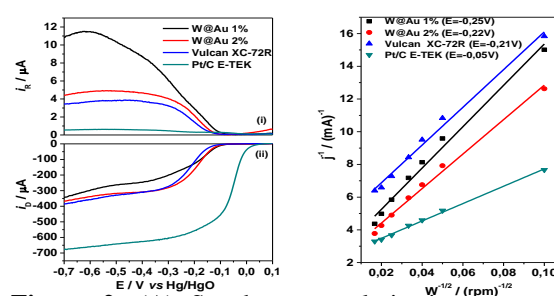


**Figure 2:** (A) Steady-state polarization curves for the ORR of different proportion of W@Au supported on Vulcan XC-72R carbon and (B) Koutecky–Levich plots for the ORR on W@Au based materials in NaOH 1 mol L<sup>-1</sup>. The plots for Vulcan XC-72R and Pt/C E-TEK were also included for comparison.

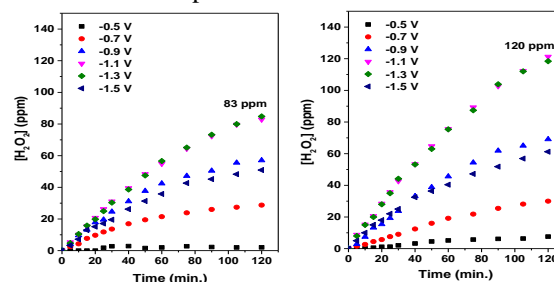


**Figure 3:** H<sub>2</sub>O<sub>2</sub> concentration as a function of electrolysis time using (A) Vulcan XC-72R GDE and (B) W@Au/C 1% GDE.

## References:

1. Mazloum-Ardakani, M., Hosseinzadeh, L., Taleat, Z. (2015) Synthesis and electrocatalytic effect of Ag@Pt core-shell nanoparticles supported on reduced graphene oxide for sensitive and simple label-free electrochemical aptasensor, *Biosensors and Bioelectronics* 74, 30-36.
2. Gawande, M.B., Goswami, A., Asefa, T., Guo, H., Biradar, A.V., Dong-Liang P., Zboril, R., Varma, R.S. (2015) Core-shell nanoparticles: synthesis and applications in catalysis and electrocatalysis, *Chem. Soc. Rev.* 44, 7540-7590.



## Selective removal of lead using a nanocompound based on diatomite and graphene oxide

E. Flores,<sup>1</sup> O. Enriquez,<sup>1</sup> J. De la Cruz<sup>1</sup>, A. López,<sup>1</sup> G. Poma<sup>1,2</sup>, M. Quintana<sup>1,2</sup>

<sup>1</sup>Engineering and Technological University, Department of Chemical Industrial Engineering, Medrano St. 165, Lima, Peru; tel.+5112305000, e-mail: cfloresb@utec.edu.pe;<sup>2</sup>National University of Engineering, School of Physical Engineering, Faculty of Science, Tupac Amaru Av. 210, Lima, Peru; tel. +5114811070

### Abstract:

There is a wide variety of techniques for the removal of heavy metals from wastewater. These techniques are useful but some of them are not economically available.

In this research we study the capacity of lead decontamination in water using a novel compound based on diatomite and graphene oxide. Diatomite earth was taken from Piura (northern coast of Peru) and graphene oxide was synthesized in a lab from Merck graphite.

Chemical analysis by atomic absorption show that diatomite nanocarbon material removes almost 100% of lead in contaminated water with concentration between 50-200 ppm.

Preparation of this compound demands easy steps which can be scalable, becoming an important alternative for lead removal in wastewater.

Keywords: wastewater, diatomite, graphene oxide, nanocarbon



Figure 1 : Synthesis of Graphene oxide

### References:

M. Hirata, T. Gotou, S. Horiuchi, M. Fujiwara, M. Ohba, Carbon 42 (2004) 2929- 2937.

D.C. Marcano, D. Kosynkin, J. Berlín, A. Sinitskii, Z. Sun, A. Slesarev, L.Aleman, W.Lu, J.Tour, ACS Nano (2010) 4806-4814

# Hybrid Nanocomposite of Nanocellulose-Silver Nanoparticles-Graphene Oxide for Environmental Remediation Purposes

S.W. Chook,<sup>1,\*</sup> C.H. Chia,<sup>1</sup> S. Zakaria<sup>1</sup>

<sup>1</sup>Bioresources and Biorefinery Laboratory, School of Applied Physics, Faculty of Science and Technology, Universiti Kebangsaan Malaysia, 43600 Bangi, Selangor, Malaysia

## Abstract:

Cellulose is the world most abundant biopolymers on earth. By nature, cellulose exhibits non-specific functional properties and could be benefited by functionalisation of silver nanoparticles (AgNPs) which expands the practical applicability of cellulose. The high surface area and abundant reactive functional groups of nanocellulose emerged as an attractive candidate that possesses many advantages for immobilization of AgNPs. In this study, cellulose nanofibril (CNF) was functionalised with AgNPs via a one pot *in situ* hydrothermal synthesis approach. The presence of active functional groups on the CNF favours the direct synthesis of AgNPs on the nanofibrils without the use of reducing agent. Additionally, graphene oxide was introduced for the synthesis of the nanocomposite. The produced AgNPs were immobilized onto both CNF and GO surfaces (as shown in Figure 1), where both GO and CNF has contributed to the simultaneous reduction of AgNPs. In recent years, numerous studies have demonstrated that AgNPs-GO nanocomposite exhibited an excellent enhancement of functionalities as compared to the AgNPs and GO, respectively. The produced aerogel nanocomposites exhibited highly porous structure, with an advantage of allowing the more interactions between immobilized nanoparticles and foreign molecules. Rhodamine B (RhB) was chosen to investigate the characteristics of the produced nanocomposite for environmental remediation applications. The nanocomposite showed significant enhancement in detection of signal for RhB in aqueous solution, as compared to the neat CNF, which is attributed to the surface-enhanced Raman scattering effect (SERS) owing to the synergistic effect of both GO and AgNPs. In addition, the nanocomposite exhibited a notable catalytic effect on the degradation of RhB in the presence of sodium borohydride.

**Keywords:** Silver nanoparticles, graphene oxide, cellulose nanofibrils, nanocomposite, environment remediation, SERS, catalysis

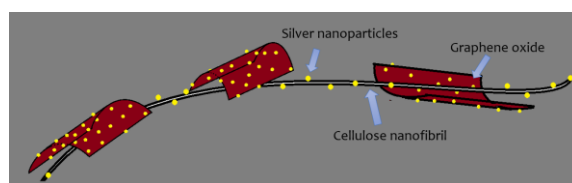


Figure 1. One pot synthesized hybrid nanocomposite of nanocellulose-graphene oxide-silver nanoparticles.

## References:

- Khin, M. M., A. S. Nair, V. J. Babu, R. Murugan & S. Ramakrishna (2012). A review on nanomaterials for environmental remediation. *Energy & Environmental Science* 5, 8, 8075-8109.
- Carpenter, A. W., C.-F. de Lannoy & M. R. Wiesner (2015). Cellulose Nanomaterials in Water Treatment Technologies. *Environmental Science & Technology* 49, 9, 5277-5287.
- Sreeprasad, T. S., S. M. Maliyekkal, K. P. Lisha & T. Pradeep (2011). Reduced graphene oxide-metal/metal oxide composites: Facile synthesis and application in water purification. *Journal of Hazardous Materials* 186, 1, 921-931.

# Study of degradability of starch-based films mixing with nano-Titanium dioxide

J. Komasatitaya,<sup>1,\*</sup> S. Mataweechotikul,<sup>1</sup> A. Simprasert

<sup>1</sup>King Mongkut University of Technology Thonburi, Department of Printing and Packaging Technology, Bangkok, Thailand

**Abstract:** The study of degradability of starch-based films mixing with nano-Titanium dioxide was aimed to prepare the starch film which made from Tapioca flour mixed with nano-TiO<sub>2</sub> and study the degradability of starch film by 3 and 30 percent weight of nano-TiO<sub>2</sub> based by starch weight. The starch film are formed into thin and thick sheets. The degradation of the nano-TiO<sub>2</sub> and starch film was studied by weighing lost, spectrum infrared, micrograph and tensile strength. The results showed that the degradability of 30 percent of nano-TiO<sub>2</sub> starch film was higher than 3 percent of nano-TiO<sub>2</sub> starch film for 1.13 of weight lost. The thin starch film was degraded more than the thick starch film and the weight of the thin film reduced approx 0.18 times of initial weight. The weight of the thick starch film reduced approx 0.16 times of initial weight. The spectrum infrared of before and after UV exposure of the nano-TiO<sub>2</sub> starch film was changed at frequency of 3500-3250 cm<sup>-1</sup> (OH) and 1200-1000 cm<sup>-1</sup> (COH)

**Keywords:** nanotitaniumdioxide, starch, IR spectrum, degradation

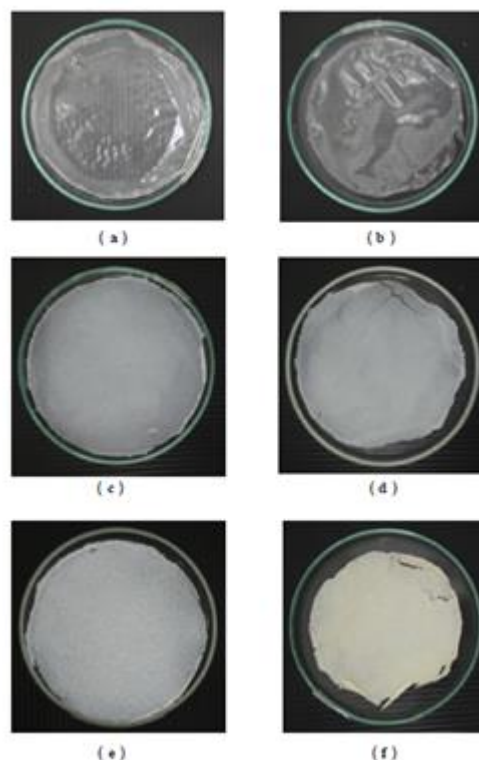


**Figure 1:** Figure shows degradation of starch film with nano-TiO<sub>2</sub>

## References:

Changjun Yanga, Chuqing Gongga, Tianyou Penga, Kejian Dengb ,andLing Zana , “High photocatalytic degradation activity of the polyvinyl chloride (PVC)–vitaminC (VC)–TiO<sub>2</sub> nano-composite film” , Journal of Hazardous Materials 178 (2010) 152–156.

# Synthesis and Characterization of Superparamagnetic Magnetite/Modified Magnetite Nano-Particles ( $\text{Fe}_3\text{O}_4@\text{SiO}_2@\text{L}$ )

H. ÇİFTÇİ,<sup>1</sup> B. ERSOY,<sup>1,2\*</sup> A. EVCİN<sup>2</sup>

<sup>1</sup>Afyon Kocatepe University, Engineering Faculty, Mining Engineering Department, Afyonkarahisar, Turkey

<sup>2</sup> Afyon Kocatepe University, Engineering Faculty, Material Science and Engineering Department, Afyonkarahisar, Turkey

## Abstract:

In this study, nano sized magnetite ( $\text{Fe}_3\text{O}_4$ ) was synthesized by chemical co-precipitation method at first (Massart, 1981), then nano sized magnetite particles were coated with silica by modified Stöber process, and the surface of silica coated magnetite nano-particles ( $\text{Fe}_3\text{O}_4@\text{SiO}_2$ ) were further functionalized by 3-aminopropyl-triethoxysilane (Stöber *et al.*, 1968, Deng *et al.*, 2005). Finally, attained nano sized products were characterized by Fourier transform infrared spectroscopy (FT-IR), X-ray diffraction (XRD), transmission electron microscopy (TEM), Brunauer-Emmett-Teller (BET), vibrating sample magnetometer (VSM) and Zeta-Meter devices/methods. Some of the results can be arranged as following: (i) Mean size of synthesized nano magnetite was about 12 nm and its specific surface area was around  $89.5 \text{ m}^2\text{g}^{-1}$ ; (ii) FT-IR and TEM results prove that the magnetite nano-particles have been successfully coated with silica in the core-shell form; (iii) The superparamagnetic property of magnetic nano-particles was confirmed by VSM. (iv) This facile and low cost method of synthesis and functionalization is promising for large production of magnetite/modified magnetite nano-particles to use in many industrial applications such as medicine, drug and adsorption processes for environmental protection.

**Keywords:** nano particles, magnetite, sol-gel, core-shell

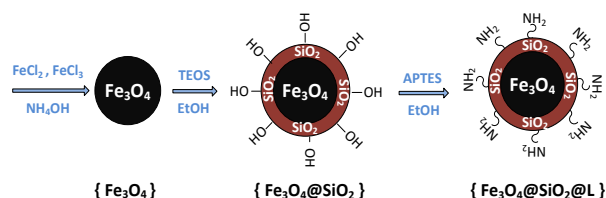


**Figure 1:** Illustration of magnetite/modified magnetite nano-particles synthesis process.

## References:

- Deng, Y.H., Wang, C.C., Hu, J.H., Yang, W.L., Fu, S.K. (2005) Investigation of formation of silica-coated magnetite nanoparticles via sol-gel approach, *Colloids and Surfaces A: Physicochem. Eng. Aspects.*, 262, 87–93.
- Massart, R. (1981) Preparation of aqueous magnetic liquids in alkaline and acidic media, *IEEE Transactions on Magnetics.*, 17(2), 1247-1248.
- Stöber, W., Fink, A., Bohn, E. (1968) Controlled growth of monodisperse silica spheres in the micron size range, *Journal of Colloid and Interface Science.*, 26-1, 62–69.

# Determination of the equilibrium constant of 1,3,5-nickel benzenetricarboxylate, Ni-HKUST-1

J. Vargas, J. Balmaseda, R. Salcedo

Departamento de polímeros, Instituto de Investigaciones en Materiales, Universidad Nacional Autónoma de México D.F., C.P. 04510

## Abstract:

The polymers of porous coordination (PCP's) and metal organic frameworks (MOF's) are formed by metal ions are coordinated multidentate organic molecules, forming highly crystalline structures and with size of nanometric pores. One of the polymers of coordination more studied as for physical properties and applications refers is the HKUST-1 [Cu<sub>3</sub>(BTC)<sub>2</sub>(H<sub>2</sub>O)<sub>3</sub>] (BTC = 1,3,5-benzenetricarboxylate). Between the series isoreticular the HKUST-1 of 1,3,5-nickel benzenetricarboxylate is of great interest as intermediary in the generation of clean energies, due to its high hydrogen storage capacity and other gases with high power energy[2,3].

As proof of this, the BASF company develops "nanocubes" of MOFS for the storage of hydrogen and natural gas in vehicles. However, in spite of the extensive labor of investigation that has been realized in the last decade, there is no systematization of knowledge to implement any of these applications on an industrial scale. For the study of the physical and chemical properties and the development of some of its applications, it is essential to know the energy of formation and equilibrium constant. In this work was replicated the HKUST-1 (Ni) synthesis reported by Maniam et al[1], the system was characterized by X-ray powder diffraction, infrared spectroscopy and Raman, thermogravimetric analysis, mass spectroscopy, pH and voltammetry. It also took out the calculation of the equilibrium constant and the energy of formation of Ni-HKUST-1. For this purpose it was performed quantum-mechanical calculations by the method of isodesmic reactions[4], and finally by thermal analysis. Moreover adsorption studies were performed on different types of gases.

With these results it is possible to create a thermodynamic hypersurface and designing a predictive method for the synthesis of PCP's, which would facilitate the implementation will any of its applications.

**Keywords:** Nanocubes, PCP's, MOF's nanometric pores, adsorption, clean energies.

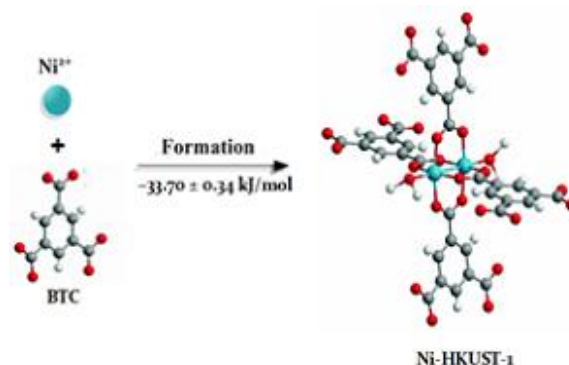


**Figure 1:** illustrates the formation of HKUST. The value of the enthalpy of formation experimental ( $\Delta H_f$ ) of Ni-HKUST-1 is  $-33.70 \pm 0.34$  kJ.

## References:

1. Maniam and N. Stock, *Inorg. Chem.*, 50 (2011) 5085–5097.
2. M. Forster et al., *J. Am. Chem. Soc.*, 128 (2006) 16846–16850.
3. C. Lamberti et al., *S. Chem. Soc. Rev.*, 39 (2010) 4951–5001.
4. P. George et al., Homodesmotic reactions for the assessment of stabilization energies in benzenoid and other conjugated cyclic hydrocarbons. *J. Chem. Soc. Perkin Trans. 2*. 1976, 11, 1222–1227.



# Nanocomposite films as a gas sensor for organic compounds

S.Ali\*, B. Horrocks\* and A. Houlton\*

\*Bedson building, Chemical Nanoscience Laboratories, Chemistry school,  
Newcastle University, NE1 7RU

## Abstract:

This research concerns the physical and structural properties of carbon nanotube /conductive polymer composites and their use in gas sensors. A good sensor should be sensitive, reliable, low cost, with fast response and a short recovery time. Carbon nanotubes (CNTs) are well-suited because of their unique properties; their small size, hollow centre, large surface area and good electric conductivity. However, it has been shown that pristine carbon nanotubes have a low response for volatile organic compounds – our target analyse - therefore we attempted to improve this property of CNTs by templating pyrrole on CNTs. Polypyrrole is simple to prepare by oxidation of the monomer and its resistance is very sensitive to organic vapours, although much larger than that of CNTs. TEM and AFM of polypyrrole/CNT composites prepared from single-walled carbon nanotubes (SWCNTs) and multi-walled carbon nanotubes (MWCNTs) show polypyrrole coated the CNTs successfully. There are significant changes in the range of diameters of nano tubes for SWCNTs from (7-10) nm to (8-35)nm and from (2-10) to (21-50)nm for MWCNTs. The composites were tested for the variation in their resistance upon exposure to a range of organic vapours (acetone, chloroform) and to water. The sensing devices comprised simple two-terminal devices over which a layer of the composite was applied by drop-coating. We investigated the effect of the CNT : polypyrrole ratio on the sensor response,  $S = (R - R_0) / R_0$  where  $R_0$  is the resistance in an air atmosphere and  $R$  is the resistance at steady-state after exposure to an air/analyte mixture. In general, pure CNTs show a rapid response time, but very low response (typically  $S < 0.1$ ) at room temperature. As the amount of polypyrrole in the composite is increased,  $S$  increases, the response time deteriorates. Interestingly, the response of the composites may even change sign as a function of target analyse concentration; this suggests that a simple mechanism based on swelling and its effect on the percolation behaviour of CNTs in the polypyrrole matrix is insufficient to explain the data.

**Keywords:** Gas sensors, CNTs/Ppy, Conductive polymers.

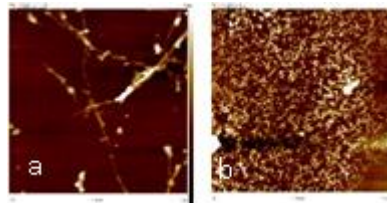


**Figure1:** AFM height images of (a) height distribution of SWCNTs after templated by Ppy. (b) height distribution of MWCNTs after templated by Ppy. The heights were calculated by AFM.



**Figure 2:** TEM images of (a) hybrid MWCNTs (Mag11x), (b) SWCNTs after templated by Ppy.

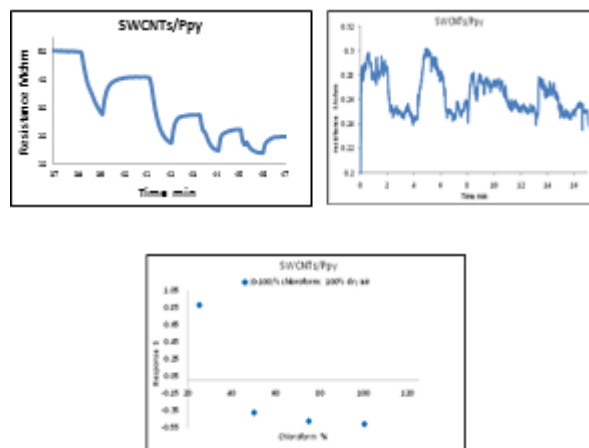


**Figure3:** (a & b) show the sensitivity of the electrical resistance  $R$  of SWCNTs/Ppy films to chloroform (0-100)% exposure at 17°C; (c) The device sensitivity  $S = (R - R_0) / R_0$  as a function of chloroform concentration.

## References:

1. King, V.B. (2007) Nanotechnology research advances. New York: Nova Science Publishers.
2. Richard, K., F., Lee, Barry, J., Cox and James, M., Hill (2010) 'The geometric structure of single-walled nanotubes', *Nanoscale*, 2, pp. 859-872.

# Synthesis and characterization of ZnO-Ag nanoparticles supported on MCM-41 as a photocatalyst for degradation Congo Red

E. M. Barrera-Rendón<sup>1</sup>, G. García-Rosales<sup>1</sup>, J. Jiménez-Becerril<sup>2</sup>

<sup>1</sup>Instituto Tecnológico de Toluca, Posgrade and Investigation Studies Division, Metepec, Mexico.

<sup>2</sup>Instituto Nacional de Investigaciones Nucleares, Department of Chemistry, Ocoyoacan, Mexico

## Abstract:

Currently, in textile industry, dyes are used as raw material, which generates 525,000 tons per month of waste in Mexico; as example of dye used in the past, is the Red Congo. Nanotechnology through obtaining new materials with specific properties such as the photocatalytic activity is a viable option for the degradation of organic pollutants [1]. An example is the ZnO photocatalyst; the presence of Ag improves their photocatalytic properties [2]. In this research MCM-41 is used as a support, nanoparticles of ZnO-Ag was synthesized by wet method and was characterized and evaluated their ability to photodegradation of Congo Red [3]. The material obtained was characterized by scanning electron microscopy (JEOL JSM-6610LV). In Figure 1, the structure of ZnO-Ag/MCM-41 present agglomerated particles of spherical morphology with an average size of 56 nm. EDS analysis indicates the presence of: C 54.5%, O 44.6%, Zn 0.79% and Ag 0.08%.



**Figure 1:** Micrograph of ZnO-Ag/MCM-41

A FT-IR equipment, Varian 640-IR was used. Spectrum of MCM-41 present, five peaks; the first corresponds to the O-H group in water  $3373\text{ cm}^{-1}$ ; the second is at  $2350\text{ cm}^{-1}$  which corresponds to the vibrational bands of C-H environmental  $\text{CO}_2$ . The third is at  $1055\text{ cm}^{-1}$  corresponding to the asymmetric Si-O-Si group.

The fourth is at  $973\text{ cm}^{-1}$  belonging to Si-OH groups and  $805\text{ cm}^{-1}$  which is characteristic of the symmetric Si-O group. In the spectrum of ZnO-Ag, two distinct bands were observed; the first is at  $2350\text{ cm}^{-1}$ , which belongs to the C-H vibrational band of  $\text{CO}_2$ . The second at  $561.42\text{ cm}^{-1}$  was assigned to the vibration of Zn-O. For ZnO-Ag/MCM-41, were observed peaks that correspond of MCM-41 and ZnO-Ag materials. The specific area material of ZnO-Ag/MCM-41 is  $1429.3\text{ m}^2\cdot\text{g}^{-1}$  and an average pore diameter of 2.75 nm.

A UV lamp was used to  $\lambda = 218\text{ nm}$  for evaluating the ability of photodegradation of ZnO-Ag/MCM-41, using 100 mg/L of material with a solution of Congo Red 50 mg/L concentration; to determine the degradation of dye UV-vis spectrophotometer, Thermo Spectronic, GENEYS 10 UV was used. The results show that ZnO-Ag/MCM-41 material is organic pollutant viable to photodegrade the Congo Red.

**Keywords:** ZnO-Ag/MCM-41, nanoparticles, chemical method.

## References:

- 1 Ohama, Y., Van Gemert, D. (2011). Application of titanium dioxide photocatalysis to construction materials. First Edit. *Springer Sci. Editor.*, 5, 1.
- 2 Zhao, Z., Wang, M., Liu, T. (2015). Tribulus terrestris leaf extract assisted green synthesis and gas sensing properties of Ag-coated ZnO nanoparticles. *Mater. Lett.*, 158, 274-277.
- 3 Yin, A., Wen, C., Dai, W., Kangnian, F. (2011). Ag/MCM-41 as highly efficient mesostructured catalyst for the chemoselective synthesis of methyl glycolate and ethylene glycol. *Appl. Catal., B: Environmental.*, 108-109, 90-99.

# Synthesis and Evaluation of a Carbon-TiO<sub>2</sub>-CeO<sub>2</sub> composite for the degradation of phenol

Y. Lara-López,<sup>1</sup> G. García-Rosales,<sup>1</sup> J. Jiménez-Becerril,<sup>2</sup>

<sup>1</sup>Instituto Tecnológico de Toluca, División de estudios de Posgrado e Investigación, Metepec, Mexico

<sup>2</sup>Instituto Nacional de Investigaciones Nucleares, Departamento de Química, Ocoyocac, Mexico

## Abstract:

The presence of phenol in waste water is because its use as raw material and is considered to be highly toxic and slightly biodegradable, beside being known for being carcinogenic [1,2]. The technology of heterogeneous photocatalysis is based on the absorption of energy across the semiconductor, which gets excited of two forms. In this work was realized the synthesis of bimetallic nanoparticles of TiO<sub>2</sub>-CeO<sub>2</sub> supported in carbon obtained by means of the pyrolysis of orange peel for the photodegradation of phenol obtaining favorable results.

Firstly, termogravi-metric analysis (STAP PT 1600 LINSEIS) was used to determine the temperature of pyrolysis to obtain carbon. To obtain carbon-TiO<sub>2</sub>-CeO<sub>2</sub> composite it was prepared a solution of (NH<sub>4</sub>)<sub>2</sub>Ce(NO<sub>3</sub>)<sub>6</sub>-NH<sub>4</sub>OH and was kept in agitation, then it was added to a dispersion with the orange peel and a solution of C<sub>12</sub>H<sub>28</sub>O<sub>4</sub>Ti. Obtained materials were characterized by electronic microscopy (JEOL I model 6610 LV), infrared spectroscopy (VARIAN model 640-IR), and specific surface area (Belsorp® Max III). Figure 1 shows the micrography of the carbon-TiO<sub>2</sub>-CeO<sub>2</sub>.

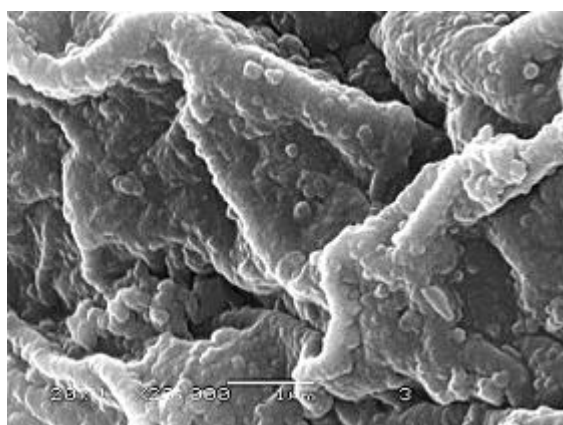


**Figure 1.** Morphology of the composite carbon-TiO<sub>2</sub>-CeO<sub>2</sub>

It can be observed spherical particles which average diameter is of 96 nm deposited in the surface of the carbon. The analysis realized by

EDS shows the presence of the elements Ti 4% and Ce 2% besides the own elements of the support C 70%, O 10%, K 3% and Ca 11%. The FTIR's spectra of orange peel present the bands typical of the hidroyl groups at 3294cm<sup>-1</sup> from cellulose, the band at 2910 cm<sup>-1</sup> and between 900-600 cm<sup>-1</sup> that are attributed to the vibrations of the bond C-H, at 1727 cm<sup>-1</sup> to the double bond C=O of the carboxylic acids. The band located at 1588 cm<sup>-1</sup> corresponds to C=C. At 1420 cm<sup>-1</sup> and 1356 cm<sup>-1</sup> it is find the band corresponding to the vibrations of the bond C-O. The band located at 1213 cm<sup>-1</sup> could be assigned to CO<sup>-</sup> and OH<sup>-</sup>, nevertheless once obtained the composite carbon-TiO<sub>2</sub>-CeO<sub>2</sub> the vibrations are attributed to bonds of O-H (3723 cm<sup>-1</sup>), -C≡C- (2353 cm<sup>-1</sup>), C-H (2100 cm<sup>-1</sup>) and C-C (635 cm<sup>-1</sup>). Presence of particles of TiO<sub>2</sub>-CeO<sub>2</sub> in the carbon increases their specific surface area from 6.19 m<sup>2</sup>/g to 25.16 m<sup>2</sup>/g. In a test of photo-degradation of phenol, using composite as catalyst, show that obtained materials have a major capacity of photodegradation, compared of photodegradation separately, then the material is suitable for the water treatment that they contain organic contaminants.

**Keywords:** TiO<sub>2</sub>-CeO<sub>2</sub> particles, carbon, photocatalytic degradation

## References:

1. Gar, A. M., Tawfik, A. (2014), Solar Photocatalytic Degradation of Phenol in Aqueous Solutions Using Titanium Dioxide, *J. Chem. Nuc. Metall. Mater.*, 8, 144-147.
2. Seftel, E. M., Niarchos, M., Mitropoulos, Ch., Mertens, M., Vasant, E. F., Cool, P. (2014), Photocatalytic removal of phenol and methylene-blue in aqueous media using TiO<sub>2</sub>@LDH clay nanocomposites, *Catal. Today.*, 252, 120-127.

# Low Cost and Free TCO Porous Coal as a Counter Electrode (CE) for Dye Sensitized Solar Cell (DSSC)

M.Y. Feteha, Shaker Ebrahim and Laila Saad  
Department of Materials Science, Institute of Graduate Studies and Research,  
Alexandria University, P.O Box 832, Egypt

## Abstract:

Carbonaceous materials are quite attractive to be applied as a counter electrode for DSSCs due to their high electronic conductivity, corrosion resistance towards  $I_2$ , high reactivity for tri-iodide reduction and low cost. In this work, two types of CEs are fabricated using carbon material, 1) Porous coal and 2) Porous coal after electrodepositing of platinum nano particles (NPs). SEM micrographs of porous coal and porous coal /platinum counter electrodes (Figure 1) are performed for studying the morphologies of the carbon counter electrodes and the distribution of platinum NPs within it. The catalytic activity of the prepared electrodes toward the reduction of  $I_3^-/I^-$  was investigated by cyclic voltammetry technique. The Nequist impedance spectra of the DSSC structures (glass/ITO/TiO<sub>2</sub>(NPs)-N3/electrolyte/(porous coal) or (porous coal/Pt(NPs))) were performed. Using of coal as a material for counter electrode in DSSC offers a cheap, light weight, suitable catalytic activity and simple way of treatment cell relative to platinum as material for counter electrode. On the other hand, depositing of the platinum NPs on the coal electrode surface enhanced the cell efficiency by 56 %, due to a reduction in cell's resistance components values.

**Keywords:** DSSC, counter electrode, Pt nanoparticles, porous coal.

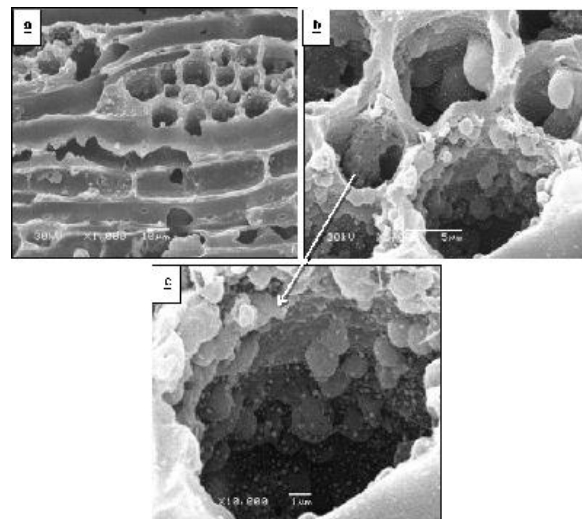


**Figure 1:** SEM micrographs of (a) Porous coal, (b) Porous coal /platinum nanocomposite and (c) magnification of porous coal /platinum nanocomposite counter electrodes.

## References

1. Grätzel M, (2001), "Photoelectrochemical Cells: Insight Review Articles", *Nature*, Vol. **414**, P: 338-344.
2. Yimhyun J., *et al*, (2012), " Highly Interconnected Ordered Mesoporous Carbon–Carbon Nanotube Nanocomposites: Pt-free, highly efficient, and durable counter electrodes for dye-sensitized solar cells", *Chem. Commun.*, Vol. **48**, P 8057-8059.

# Facile formation of fullerene nanostructures and their application to polymer solar cells

S. Woo,<sup>1,\*</sup> W.-H. Kim,<sup>1</sup> and S.-J. Sung,<sup>1</sup>

<sup>1</sup>DGIST (Daegu Gyeongbuk Institute of Science & Technology), Solar Energy Convergence Research Center, Daegu, South Korea

## Abstract:

Polymer solar cells (PSC) have been considered as attractive candidate for next generation renewable energy sources due to their potentials such as low material cost, easy processability over large area via roll-to-roll coating process, and unique flexibility [1,2]. The performance of PSC based on bulk heterojunction (BHJ) structure has been gradually increased by the development of new materials such as low-bandgap donor polymers, high lowest unoccupied molecular orbital (LUMO) level fullerene derivatives, new device structures and processing conditions. Although the efficiency of PSC improved above 10% in single stack structures [3], there are still many issues to improve such as long-term stability and large area module efficiency. As an excellent electron acceptor, fullerenes and their derivatives are mainly applied in organic/polymer solar cells [4,5]. For this purpose it is further required that fullerenes should be tuned into one-dimensional nanostructures, that is, nanorods within a thin conjugated polymer film, which would simultaneously satisfy both efficient exciton dissociation and transportation of free charge carriers by forming interconnecting networks. Here, we have prepared fullerene nanorods/clusters directly from solution by self-assembly routes (Figure 1). In this study, we checked the effect of 1-dimensional nanostructure embedded in the bulk heterojunction active layer. This nanostructure, obtained by a careful solvent treatment of photoactive solution, is expected to be useful for the formation of charge transfer path and eliminating the post thermal or solvent treatment to produce well-ordered morphology. The UV-Vis absorption and device performance properties will be discussed fully.

**Keywords:** fullerene, solvent-treatment, self-assembly, one-dimensional nanostructures, polymer solar cells.

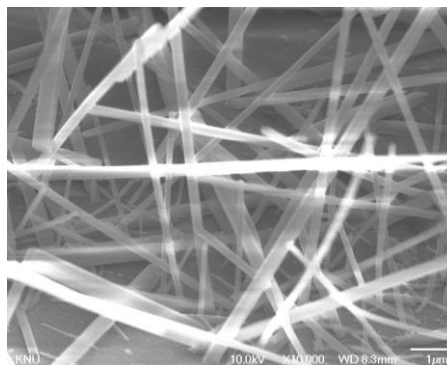


**Figure 1:** Scanning Electron Microscopy image of fullerene nanorods prepared by solvent treatment of fullerene thin film on glass substrate.

## References:

1. Gunes, S., Neugebauer, H., Sariciftci, N. S. (2007) Conjugated polymer-based organic solar cells, *Chem. Rev.*, 107, 1324.
2. Brabec, C. J., Gowrisanker, S., Halls, J. J., Laird, D., Jia, S., Williams, S. P. (2010) Polymer–fullerene bulk-heterojunction solar cells, *Adv. Mater.*, 22, 3839.
3. Nam, S., Seo, J., Woo, S., Kim, W. -H., Kim, H., Bradley, D. D. C., Kim, Y. (2015) Inverted polymer fullerene solar cells exceeding 10% efficiency with poly(2-ethyl-2-oxazoline) nanodots on electron-collecting buffer layers, *Nat. Commun.*, 6, 8929.
4. Yang, X., Loos, J., Veenstra, S. C., Verhees, W. J. H., Wienk, M. M., Kroon, J. M., Michels, M. A. J., Janssen, R. A. J. (2005) Nanoscale morphology of high performance polymer solar cells, *Nano Lett.*, 5, 579.
5. Sariciftci, N. S., Smilowitz, L., Heeger, A. J., Wudl, F. (1992) Photoinduced electron transfer from a conducting polymer to buckminsterfullerene, *Science*, 258, 1474.



# Comparison of the systemic nanoherbicide Imazamox-LDH obtained by direct synthesis and reconstruction: preliminary results

R. Khatem<sup>1</sup>, A. Bakthi<sup>1</sup>, M.C. Hermosin<sup>2\*</sup>

<sup>1</sup>Laboratory of Biodeversty and Conservation of Soil and Water. University of Abdel hamid Ibn badis Mostaganem. Algeria

<sup>2</sup>Environmental Agrochemistry. Instituto de Recursos Naturales y Agrobiologia de Sevilla. Consejo Superior de Investigaciones Científicas (IRNAS-CSIC). Sevilla. Spain

**Abstract:** Pesticides are widely used in modern agriculture but their needed intensive use causes environmental problems with toxicity and carcinogenicity consequences. This concern has generated research efforts to reduce pesticide environmental risks by developing formulations which gradually release the active ingredient supported on diverse materials (Perez-de-Luque & Hermosin 2013). This type of slow-release formulation is fundamental for anionic herbicide as Imazamox, because its high soil mobility. The concept of nanopesticide has very recently appeared in the phytopathology (Kah et al. 2013, Perez-de-Luque&Hermosin 2013, Cabrera et al. 2015) being specially interesting for the systemic pesticide, which are those needing to enter in the plant by leaves or roots to act versus pest. The objective of this work is to prepare Imazamox-LDH as nanocomponent, to be used as smart delivery system that allows to remain imazamox in the target site (rizosphere at subsoil) and to minimize its environmental risk.

The complexes are prepared by direct synthesis (DS) or coprecipitation and by regeneration (RE) of calcined HT at 500°C in aqueous solution containing herbicide at appropriated pH. The imazamox content in the nanoherbicides are determined by dissolving in acid and then quantified by HPLC. The content of Imazamox in those samples was 35% for DS and 10% (w/w) for RE. Fig. 1 shows the XRD patterns of both nanoherbicide obtained, where the most important diffraction peaks of the hydrotalcite-like structure are developed.

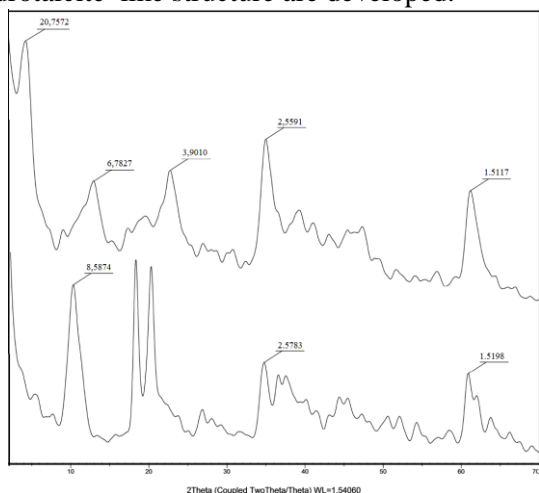


**Figure 1:** The XRD patterns for LDH-Imazamox RE (a) and LDH-Imazamox SD (b).

The imazamox anion would compensate 33% of the anion exchange capacity (AEC) for RE and 10% for DS. The large imazamox content of RE-nanoimazamox oblies to those anions to conform a steeply position in the interlamellar spaces rendering large  $d_{002}$  value. FT-IR and SEM/TEM characterization confirms that structure. The nanoimazamox stability is also checked. The release kinetic of both nanoimazamox samples (RE and DS) was measured in distilled water and Fig. 2 shows good slow release profile for both, slightly better for RE. The release rate was found to be faster in the first 30min where the released amount represents 70% of the total content for both nanoherbicides. After 144hrs the RE-nanoimazamox reached 98%, while the DS only did 80%. However, both nanoherbicides shows good performance as slow delivery systems in water, allowing to maintain two different dose levels.

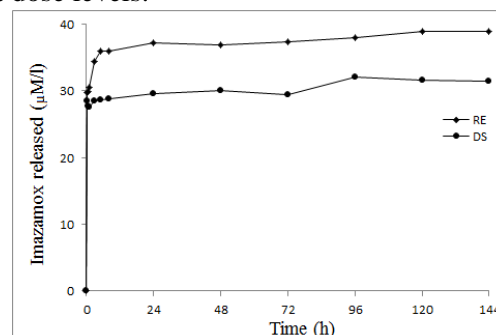


**Figure2:** Water release Kinetic curves of imazamox from HDL complexes. (DS) direct synthesis; (RE) regenerated method

**Keywords:** Clays, layered double hydroxide (LDH), nanopesticide, nanoformulation, pesticide, release, water.

**Acknowledgments:** PO11-AGR-7400 (Junta de Andalucía) & RECUPERA 2020 (MINECO-CSIC)

## References:

1. Kah, M., Beulke, S.s Tiede, K., Hofmann, T. (2013) Nanopesticides: state of knowledgge, environmental fate, and exposure modeling. *Crit Rev Environ Sci Technol* 43:1823-1867
2. Perez-de-Luque, A And Hermosin, MC.(2013) Nonotechnology and its use in agricultura, *In*

*Bio-nanotechnology. A Revolution in Food, Biomedical and health Sciences. Part3*, ed Bagachi D. Wiley-Blackwell, Chichester, UK, pp. 383-398.

3. Cabrera, A., Celis, R., Hermosin, M.C. (2015) Imazamox-clay complexes with chitosan- and iron(III)- modified smectites and their use in nanoformulations, *Pest Manag Sci*. DOI 10.1002/ps.4106

**Posters Session II: June 2<sup>nd</sup>, 2016**  
**European Graphene Forum**  
**EGF 2016**

# Formation of Continuous Few-layer MoS<sub>2</sub> Nanosheet Film for Sensing and Detection Applications

M. Demydenko<sup>1</sup>, M. Jergel<sup>1</sup>, D. Kostiuk<sup>1</sup>, Y. Halahovets<sup>1</sup>, M. Kotlar<sup>2</sup>, P. Siffalovic<sup>1</sup>, K. Vegso<sup>1</sup>, E. Majkova<sup>1</sup>

<sup>1</sup>Institute of Physics, Slovak Academy of Sciences, Bratislava, Slovakia

<sup>2</sup>Slovak University of Technology, Bratislava, Slovakia

## Abstract:

Recently there has been considerable interest in the 2D materials because of their unique properties, such as MoS<sub>2</sub>, that differ from their bulk form. We present a simple and low-cost technique of fabrication of continuous few-layered MoS<sub>2</sub> nanosheet film. The ethanol based solution of few-layered MoS<sub>2</sub> nanosheets was obtained by liquid exfoliation [1] using sonication of the mesh powder with 40 μm grains followed by centrifugation up to 21000 rpm. The structural properties of the nanosheets were analyzed using XRD, GISAXS, SEM, HRTEM, AFM, Raman microscopy. The layers exhibited well developed crystalline structure with the lateral size of 100 nm (Fig. 1c). The MoS<sub>2</sub> exfoliation into nanosheets proved to be optimal for 21000 rpm as Raman spectrum confirms (Fig. 1a), the nanosheet average thickness being around 3 monolayers.

The large-area film of the few-layered MoS<sub>2</sub> was prepared by modified Langmuir-Schaeffer technique onto Si substrate with 500nm of SiO<sub>2</sub>. The obtained film is uniformly stretched over the whole substrate as proved by SEM (Fig. 1b) with a minimum folding of nanosheets. The electrical measurements were performed using silver interdigitated contacts of 100 nm thickness that were deposited through the mask by vacuum thermal evaporation. The first annealing up to 650K to remove impurities decreased the resistance from 100GΩ to 10kΩ. The I-V characteristics show a typical semiconducting behaviour with the resistance change of 10-1000kΩ during annealing.

The preparation method presented above is applicable on large-scale substrates. The film morphology and its electrical properties stemming from our analyses show potential of such large-area films as nanoplatform for tailored functionalization towards advanced detecting, sensing and catalysis applications.

**Keywords:** few-layered MoS<sub>2</sub> nanosheets, Langmuir-Schaeffer film deposition, thermal treatment, conductivity.

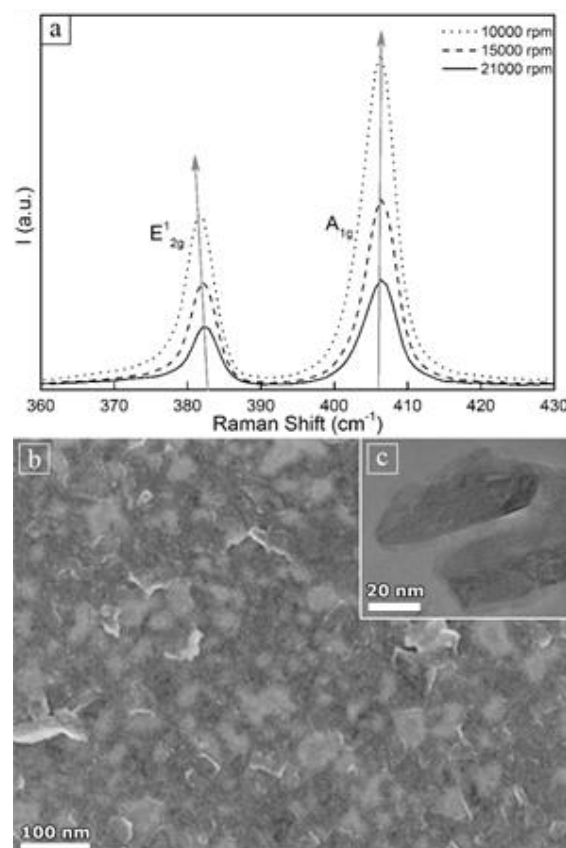


**Figure 1:** Figure illustrating the Raman spectrum of E<sub>2g</sub><sup>1</sup> and A<sub>1g</sub> modes for three size separation forces (a) and shows the changing of the difference between peaks maximum that is correspond to nanosheet thickness; SEM image of the prepared film (b); HRTEM image of individual nanosheets (c).

## References:

Coleman J. N., et al. (2011) Two-Dimensional Nanosheets Produced by Liquid Exfoliation of Layered Materials, *Science*, 331, 568 – 571.

# Grain Boundary Structures and Electronic Properties of Hexagonal Boron Nitride on Cu (111)

Qiucheng Li, Yanfeng Zhang\*, Zhongfan Liu\*

Center for Nanochemistry (CNC), Academy for Advanced Interdisciplinary Studies, Peking University, Beijing 100871, People's Republic of China, [liqc-cnc@pku.edu.cn](mailto:liqc-cnc@pku.edu.cn)

## Abstract:

Grain boundaries (GBs) possess attractive properties related to electronic,<sup>[1, 2]</sup> magnetic,<sup>[3]</sup> and mechanical<sup>[4]</sup> aspects in graphene, where great scientific concerns have been devoted in this area. However, the GB investigation in two-dimensional hexagonal boron nitride (*h*-BN), a structural analogue to graphene, is still in its infancy.<sup>[5, 6]</sup> We have performed a systematic STM/STS studies on the GBs of *h*-BN towards an understanding of their atomic configurations and electronic properties. The first experimental evidence of the GBs composed of square-octagon pairs (4|8 GBs) was given, together with those containing pentagon-heptagon pairs (5|7 GBs). Of particular interests are the remarkably different electronic properties of the 4|8 and 5|7 GBs, where the band gap of the 5|7 GB was dramatically decreased as compared with that of the 4|8 GB by STS measurement. This fact is consistent with the local density of states (LDOS) calculations by density functional theory (DFT). Our finding offers a deeper insight into the grain boundary structures formed in CVD-grown *h*-BN film, which also provides a possibility of tuning the inert electronic property of *h*-BN via grain boundary engineering.

**Keywords:** hexagonal boron nitride, chemical vapor deposition, STM/STS, grain boundary, electronic properties

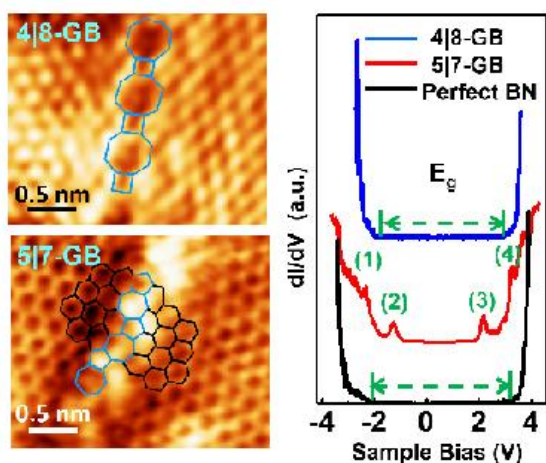


**Figure 1:** Figure illustrating the two typical grain boundary structures of hexagonal boron nitride on Cu (111), together with their local electronic properties.

## References:

1. Yazyev, O. V.; Louie, S. G. *Nat. Mater.* **2010**, *9* (10), 806-809.
2. Ma, C. X.; Sun, H. F.; Zhao, Y. L.; Li, B.; Li, Q. X.; Zhao, A. D.; Wang, X. P.; Luo, Y.; Yang, J. L.; Wang, B.; Hou, J. G. *Phys. Rev. Lett.* **2014**, *112* (22).
3. Cervenka, J.; Katsnelson, M. I.; Flipse, C. F. *J. Nat. Phys.* **2009**, *5* (11), 840-844.
4. Yang, B.; Xu, H.; Lu, J.; Loh, K. P. *J. Am. Chem. Soc.* **2014**, *136* (34), 12041-12046.
5. Liu, Y. Y.; Zou, X. L.; Yakobson, B. I. *Acs Nano* **2012**, *6* (8), 7053-7058.
6. Gibb, A. L.; Alem, N.; Chen, J.-H.; Erickson, K. J.; Ciston, J.; Gautam, A.; Linck, M.; Zettl, A. *J. Am. Chem. Soc.* **2013**, *135* (18), 6758-6761.



# Large-scale Synthesis of Defects-selective Graphene Quantum Dots for Cell Imaging by Ultrasonic-assisted Liquid-Phase Exfoliation

Liqiang Lu, Y.T. Pei\*

University of Groningen, Advanced Production Engineering, Engineering and Technology Institute Groningen, Groningen, Netherlands

## Abstract:

Graphene quantum dots (GQDs) exhibit unique physical and chemical properties due to their quantum confinements and edge defects. In this paper, a facile, green and fast method was developed for large-scale synthesis of GQDs via an ultrasonic-assisted liquid-phase exfoliation technique. GQDs with different sizes and structures were obtained through this exfoliation method with different graphitic carbon precursors, such as nano-graphite, acetylene black and even graphite powder. The luminescent properties of as-synthesized GQDs have been investigated. Different light absorption and photoluminescence (PL) properties were identified relevant to the defect characters, namely high-defects GQDs (HD-GQDs) or low-defects GQDs (LD-GQDs). The variable edges and sizes of GQDs are responsible for the variation of luminescent properties induced by changing the excitation wavelength and the pH values of the GQDs dispersions (Figure1). Attributed to the high water dispersancy, excellent biocompatibility, controllable fluorescent performances, as well as the low toxic properties, the as-synthesized HD-GQDs show high potential as fluorescence nanoprobes for bioimaging.

**Keywords:** graphene quantum dots, photoluminescence, ultrasonication, defects, bioimaging

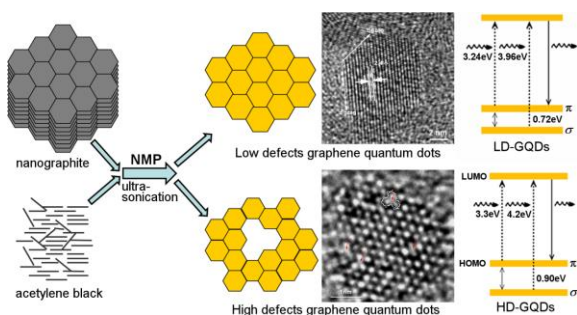


**Figure 1** illustrating the method of the large-scale synthesis of GQDs via an ultrasonic-assisted liquid-phase exfoliation technique. By using this method, high-defects GQDs and low defects GQDs could be obtained by selecting various raw carbon materials. The photoluminescence proper-

ties for high-defects GQDs and low-defects GQDs at different excitation wavelengths and pH values of GQDs dispersion are investigated. The cell imaging performances and biocompatibility are detected.

## References:

Pan, D., Zhang, J., Li Z., Wu, M. (2010), Hydrothermal Route for Cutting Graphene Sheets into Blue-Luminescent Graphene Quantum Dots, *Adv. Mater.*, 22,734-738.

Liu, Q., Guo, B., Rao, Z., Zhang, B., Gong, J. (2013), Strong Two-Photon-Induced Fluorescence from Photostable, Biocompatible Nitrogen-Doped Graphene Quantum Dots for Cellular and Deep-Tissue Imaging, *Nano Lett.*, 13, 2436-2441

# CVD growth of large single crystal graphene

Li Lin, Huaying Ren, Jiayu Li, Ning Kang, H. Q. Xu, Hailin Peng\*, and Zhongfan Liu\*

Center for Nanochemistry, Beijing Science and Engineering Center for Nanocarbons, College of Chemistry and Molecular Engineering, Peking University, Beijing 100871, China. Email: hlpeng@pku.edu.cn; zfliu@pku.edu.cn

## Abstract:

Graphene is the two-dimensional atomic crystal made of  $sp^2$ -hybridized carbon atoms with extraordinary electronic and optical properties<sup>[1]</sup>, which has motivated the rapid development of various methods for the preparation of high-quality graphene. Chemical vapor deposition (CVD) on transitional metals, especially on copper, has been considered as one of the most promising techniques for production of graphene with high quality and in large scale<sup>[2]</sup>. However, due to its high nucleation density, CVD-grown graphene typically suffers from a high density of domain boundaries, affecting graphene's electronic properties<sup>[3]</sup>. Thus, great efforts have been devoted to produce large-size single-crystal graphene to minimize the adverse impact of graphene boundaries<sup>[4,5]</sup>. As we know, the copper boundary is highly active spots for graphene nucleation resulting in the high nucleation density of graphene especially at extremely low methane concentration<sup>[6]</sup>. Here we develop a facile method to suppress the graphene nucleation number by occupancy of active nucleation sites, such as copper boundaries, by pretreatment of copper substrate using the organonitrogen molecules. Centimeter-size hexagon single-crystal graphene domains were successfully grown on copper foil. Transmission electron microscopy (TEM) and electron diffraction studies were conducted to confirm the single crystal nature of the large hexagonal graphene domains. Moreover, Hall measurements demonstrate that our graphene single crystals on  $\text{SiO}_2$  substrate exhibit excellent electronic properties with the carrier mobility up to  $24000 \text{ cm}^2\text{V}^{-1}\text{s}^{-1}$ .

## References:

1. H. C. Neto, F. Guinea, N. M. R. Peres, K. S. Novoselov and A. K. Geim, *Rev. Mod. Phys.* **81**, 109 (2009).
2. X. Li, W. Cai, J. An, S. Kim, J. Nah, D. Yang, R. Piner, A. Velamakanni, I. Jung, E. Tutuc, S. K. Banerjee, L. Colombo and R. S. Ruoff, *Science*. **324**, 1312-1314 (2009).
3. Q. Yu, L.A. Jauregui, W. Wu, R. Colby, J. Tian, Z. Su, H. Cao, Z. Liu, D. Pandey and D. Wei, *Nature materials*. **10**, 443-449 (2011).
4. Y. Hao, M. S. Bharathi, L. Wang, Y. Liu, H. Chen, S. Nie, X. Wang, H. Chou, C. Tan, B. Fallahzad, H. Ramanarayan, C. W. Magnuson, E. Tutuc, B. I. Yakobson, K. F. McCarty, Y. W. Zhang, P. Kim, J. Hone, L. Colombo and R. S. Ruoff, *Science*. **342**, 720-723 (2013).
5. H. Zhou, W. J. Yu, L. Liu, R. Cheng, Y. Chen, X. Huang, Y. Liu, Y. Wang, Y. Huang and X. F. Duan, *Nat. Commun.* **4**, 2096 (2013).
6. G. H. Han, F. Güneş, J. J. Bae, E. S. Kim, S. J. Chae, H. -J. Shin, J. -Y. Choi, D. Pribat and Y. H. Lee, *Nano letters*. **11**, 4144-4148 (2011).

# Fabrication and Characterization of Near Infrared Detectors based on MoS<sub>2</sub> Few-layers Grown with Chemical Vapor Deposition

X. Wang,<sup>1</sup> L.L. Shiau,<sup>1</sup> B.K. Tay,<sup>1,\*</sup>

<sup>1</sup>Nanyang Technological University, NOVITAS Center, School of Electrical and Electronic Engineering, Singapore

## Abstract:

As a semiconductor, molybdenum disulfide (MoS<sub>2</sub>) monolayers has attracted much attention recently due to its good performance in electronic devices, including high mobility and high on/off ratio, and novel properties, such as valleytronics. When its thickness increases from monolayer to bilayer and thicker, its band gap will decrease from 1.9 eV to 1.2 eV because of the quantum confinement effect.<sup>1</sup> This crossover makes MoS<sub>2</sub> few-layers suitable to work in the near infrared region (750 nm to 1,000 nm). Previously, MoS<sub>2</sub> few-layers are mainly achieved by micro-mechanical exfoliation with adhesive tape. Although many groups have reported the growth of MoS<sub>2</sub> monolayer with various methods, such as chemical vapor deposition,<sup>2</sup> sulfurization of metal film,<sup>3</sup> few works have been on the growth of MoS<sub>2</sub> few-layers. In this work, MoS<sub>2</sub> few-layers are synthesized on SiO<sub>2</sub>/Si substrate with chemical vapor deposition. Their thickness will be confirmed with atomic force microscope, and their performance in near infrared detectors are characterized by fabricating devices on these as-grown MoS<sub>2</sub> few-layers with standard UV lithography. These detectors adopt a field effect transistor structure (figure 1) in which two metal electrodes work as source and drain electrodes, while the Si substrate works as global back gate to tune the current passing the MoS<sub>2</sub> channel. As a result, the performance of the detectors can be tuned by the Si back gate.

**Keywords:** near infrared detector, MoS<sub>2</sub>, few-layer, chemical vapor deposition.

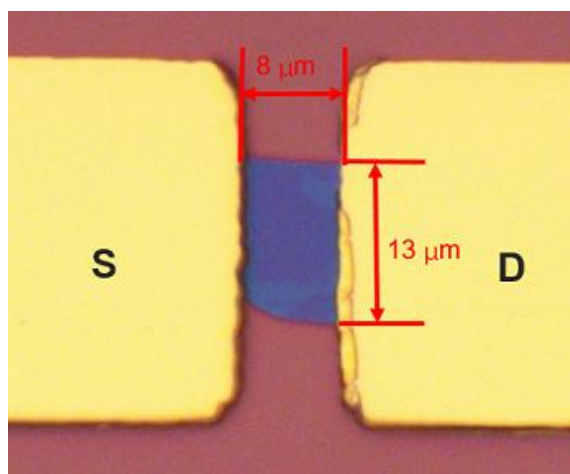


**Figure 1:** Top view of the near infrared detectors based on CVD grown MoS<sub>2</sub> few-layer. The metal electrodes work as source and drain, while the Si substrate works as global back gate to tune the current passing the MoS<sub>2</sub> channel. The responsivity of the device to near infrared light can be tuned as well.

## References:

1. Mak, K. F.; Lee, C.; Hone, J.; Shan, J.; Heinz, T. F., Atomically Thin MoS<sub>2</sub>: A New Direct-Gap Semiconductor. *Physical Review Letters* **2010**, *105* (13).
2. Najmaei, S.; Liu, Z.; Zhou, W.; Zou, X.; Shi, G.; Lei, S.; Yakobson, B. L.; Idrobo, J.-C.; Ajayan, P. M.; Lou, J., Vapour phase growth and grain boundary structure of molybdenum disulphide atomic layers. *Nature Materials* **2013**, *12*, 6.
3. Zhan, Y.; Liu, Z.; Najmaei, S.; Ajayan, P. M.; Lou, J., Large-area vapor-phase growth and characterization of MoS<sub>2</sub> atomic layers on a SiO<sub>2</sub> substrate. *Small* **2012**, *8* (7), 966-71.

# Silver/nitrogen-doped reduced graphene oxide as an electrocatalyst for oxygen reduction in alkaline medium

L.T. Soo<sup>1</sup>, K.S. Loh<sup>1</sup>, A.B. Mohamad<sup>1</sup>, W.R.W. Daud<sup>1</sup> & W.Y. Wong<sup>2</sup>

<sup>1</sup>Universiti Kebangsaan Malaysia, Fuel Cell Institute, Selangor, Malaysia

<sup>2</sup>Taylor's University's Lakeside Campus, School of Engineering, Selangor, Malaysia

## Abstract:

The utilisation of costly and scarcity noble metal such as platinum as an electrocatalyst is one of the obstacles in fuel cells commercialisation. In this work, silver incorporated nitrogen-doped reduced graphene oxide (Ag/N-rGO) was synthesized by a facile, catalyst-free thermal method by annealing metal salts with graphene oxide and melamine. The obtained Ag/N-rGO, an electrocatalyst for oxygen reduction reaction (ORR), was characterized by X-ray photoelectron spectroscopy (XPS), energy dispersive spectroscopy (EDS) and transmission electron microscope (TEM). Both XPS and EDS analyses have confirmed the presence of Ag element and higher Ag particles loading on the N-rGO surface compared with rGO. Transmission electron microscope (TEM) images revealed a wide size distribution of Ag particles loaded on the N-rGO surface. Electrochemical studies via cyclic voltammetry (CV) and linear sweep voltammetry (LSV) proved that Ag/N-rGO is a potential candidate for ORR catalyst in alkaline medium, giving an onset potential of -0.15 V vs. Ag/AgCl and limiting diffusion current density of -4.38 mA cm<sup>-2</sup> with four electron pathways. In addition, Ag/N-rGO also showed better methanol tolerance than that of Pt/C.

**Keywords:** Silver/nitrogen-doped, reduced graphene oxide, electrocatalyst, alkaline medium

# Adsorption Abilities of TiO<sub>2</sub>-R-OH-rGO Nanocomposites

E. Kusiak-Nejman,<sup>1,\*</sup> A. Wanag,<sup>1</sup> J. Kapica-Kozar,<sup>1</sup> Ł. Kowalczyk,<sup>1</sup> A.W. Morawski,<sup>1</sup> L. Lipińska,<sup>2</sup> M. Aksienionek,<sup>2</sup>

<sup>1</sup> Institute of Chemical and Environmental Engineering, West Pomeranian University of Technology, Szczecin, Pułaskiego 10, 70-322 Szczecin, Poland

<sup>2</sup> Institute of Electronic Materials Technology; Wólczyńska 133, 01-919 Warszawa, Poland

**Abstract:** Graphene, a two-dimensional (2D) monolayer of carbon atoms, has attracted great attention due to its excellent chemical and physical properties and wide potential applications in sensors and biosensors, electronic devices, liquid crystalline displays, capacitors solar cells, H<sub>2</sub> production, energy storage and nanocomposites including TiO<sub>2</sub>/graphene materials. Nanocomposites TiO<sub>2</sub>/graphene offer new opportunities in photocatalysis by the hybrid structures with a variety of nanomaterials, due to their excellent charge carrier mobility, a large specific surface area, and good electrical conductivity. TiO<sub>2</sub> combined with graphene acts as an electron trap, which promotes electron-hole separation and facilitates interfacial electron transfer [Kim et al. 2012, Liang et al. 2010, Zhang et al. 2010, Huang et al. 2013].

In this work the adsorption abilities of different TiO<sub>2</sub>-reduced graphene oxide nanocomposites were discussed. Industrial titanium dioxide from sulphate technology supplied by Grupa Azoty Zakłady Chemiczne "POLICE" S.A. was used as a starting material. Reduced graphene oxide was prepared according to Hummers' method. Two different kinds of aliphatic alcohols (methanol and 1-butanol) were used in order to form better connection between graphene sheets and titania nanoparticles. Firstly, the role of alcohol addition and secondly, the kind of used alcohol on the adsorption abilities of new nanocomposites were checked. The TiO<sub>2</sub>-R-OH and TiO<sub>2</sub>-R-OH-rGO were prepared using hydro-thermal method (under elevated pressure). A monoazo dye Reactive Red 198 (anionic dye) was used as a model organic water contamination in the adsorption process.

In Figure 1 the SEM image of TiO<sub>2</sub>-1ButOH-rGO (1wt.%) nanocomposite is presented. As it can be seen the TiO<sub>2</sub> agglomerates cover the thin graphene flake. According to XPS studies the reduction of graphene oxide was performed with quite high efficiency. However, the peak characteristic for C-O bands for reduced graphene oxide were found.

**Table 1.** Adsorption capacity values

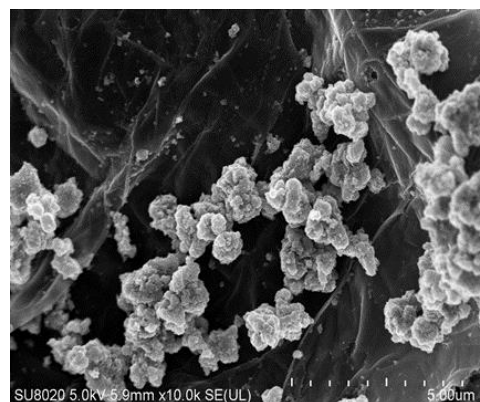


**Figure 1.** SEM image of reduced graphene oxide decorated-TiO<sub>2</sub> (sample prepared in the presence of 1-butyl alcohol)

It was found that the several features (specific surface area, presence and kind of aliphatic alcohol, zeta potential values of prepared sorbents) influence on the adsorption abilities.

**Keywords:** photocatalysis, titanium dioxide, reduced graphene oxide, TiO<sub>2</sub>-rGO nanocomposites, adsorption abilities.

**Acknowledgments:** This work was supported by grant Maestro 3 No. DEC-2012/06/A/ST5/ 00226 from the National Science Centre (Poland).

## References:

- Huang, Q., Tian, S., Zeng, D., Wang, X., Song, W., Li, Y., Xiao, W., Xie, C. (2013), Enhanced photocatalytic activity of chemically bonded TiO<sub>2</sub>/graphene composites based on the effective interfacial charge transfer through C-Ti bond *ASC Catalysis*, 3, 1477-1485.
- Kim, C. H., Kim, B.H., Yang, K.S. (2012) TiO<sub>2</sub>
- nanoparticles loaded on graphene/carbon composite nanofibers by electrospinning for increased photocatalysis *Carbon* 50, 2472-2481.
- Liang, Y., Wang, H., Casalongue, H.S., Chen, Z., Dai H. (2010) TiO<sub>2</sub> Nanocrystals grown on graphene as advanced photocatalytic hybrid materials *Nano Res.* 3, 701-705.
- Zhang, H., Lv, X., Li, Y., Wang, Y., Li, J. (2010) P25-graphene composite as a high performance photocatalyst *ACS Nano* 4, 380-386.

Sample code	Freundlich model of adsorption isotherm		Langmuir model of adsorption isotherm	
	R <sup>2</sup>	C <sub>p</sub> [mg/g]	R <sup>2</sup>	C <sub>p</sub> [mg/g]
TiO <sub>2</sub> -1ButOH	0.973	72.27	0.825	83.73
TiO <sub>2</sub> -1ButOH-rGO (1 wt.%)	0.996	82.37	0.804	109.43
TiO <sub>2</sub> - MetOH	0.990	58.38	0.907	98.46
TiO <sub>2</sub> -MetOH-rGO (1 wt.%)	0.999	53.67	0.914	67.28



# Preparation and Tribological Performance of Nickel-Graphene Oxide Composite Coatings

Shaojun Qi,\* Xiaoying Li and Hanshan Dong

\*Corresponding author. [Sxq355@bham.ac.uk](mailto:Sxq355@bham.ac.uk)

School of Metallurgy and Materials, University of Birmingham, United Kingdom

## Abstract:

The tribological studies in literature have revealed the excellent anti-friction property of graphene at nano scale and its great potential as a nano solid lubricant. For macro-scale applications, graphene-based composites, in forms of either bulk materials or surface coatings, are attracting growing interest due to the improved mechanical performance and durability. In this work, nickel-graphene oxide (GO) composite coatings were fabricated on steel by electrobrush plating. The morphology and structure of the coatings were characterized and the effects of GO on the mechanical & tribological properties were investigated. Graphene oxide sheets have been incorporated into the nickel matrix successfully as evidenced by scanning electron microscopy (SEM) (**Figure 1**) and Raman spectra. The nickel-GO composites possess improved micro-hardness, due to the reduced average grain size after introducing GO, which has been confirmed by X-ray diffraction (XRD). When sliding against a hardened steel ball under a normal load of 1 N, the composite coatings showed much lower friction (coefficient of friction  $\sim 0.4$ ) than pure nickel coating (COF  $\sim 0.7$ ). As the GO content increases, the wear rate of the composite can be reduced significantly (**Figure 2**). This can be attributed to the hardening effect and the formation of GO lubricating film during sliding. The results also indicate that brush plating is a technique capable for novel nanocomposite coating.

**Keywords:** graphene oxide, composite coating, brush plating, tribology.

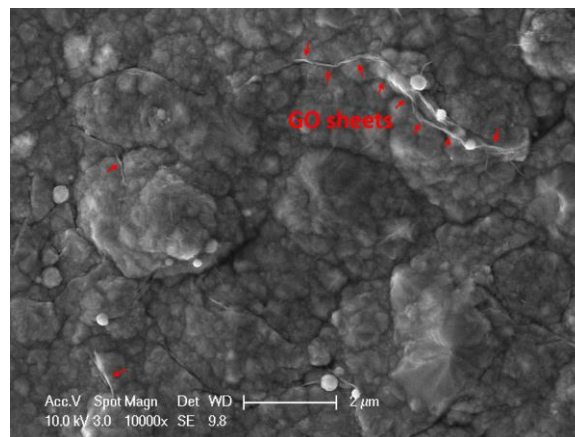


**Figure 1:** Morphology of a nickel-graphene oxide composite coating, showing the silk-like, transparent GO sheets incorporated in the metallic matrix. The GO sheets intersect the nickel crystals randomly and provide extra nucleating sites, thus reducing the nickel grain size.

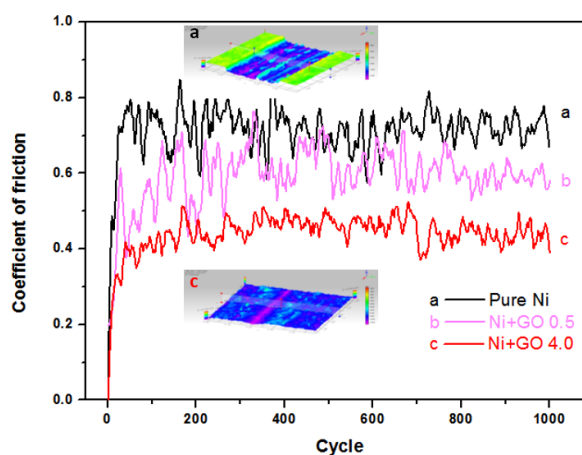


**Figure 2:** Friction of (a) pure nickel, (b and c) composite coatings with different GO contents. 0.5 and 4.0 designate the concentration of GO in the plating solution, in mg/ml. The two insets are 3D profiles of the wear tracks of sample (a) and (c), respectively.

# Reduced graphene oxide on/in metallic substrates: coating and composite

M.A. Rodríguez-Escudero<sup>1</sup>, A. Argumanez<sup>1,2</sup>, I. Llorente<sup>1</sup>, O. Caballero-Calero<sup>3</sup>, M.S. Martín González<sup>3</sup>, R. Fernandez<sup>1</sup>, M.C. García-Alonso<sup>1\*</sup>

<sup>1</sup> Consejo Superior de Investigaciones Científicas (CSIC), Centro Nacional de Investigaciones Metalúrgicas (CENIM), Madrid, Spain

<sup>2</sup> Current address: Universidad Complutense de Madrid (UCM), Facultad de Física, Madrid, Spain

<sup>3</sup> Consejo Superior de Investigaciones Científicas (CSIC), Instituto de microelectrónica de Madrid (IMM), Madrid, Spain

## Abstract:

The surface and bulk performances of metallic materials when are respectively coated by a graphene layer or processed as composite materials are considerably modified. Since its first mechanical exfoliation from graphite in 2004, several physical and chemical methods have been developed for the synthesis of graphene, which include among others chemical vapour deposition (CVD), and reduction of graphene oxide (GO) produced via graphite oxide. Among these approaches to synthesise graphene, one of the most popular is the reduction from GO due to its high yield and low cost. The presence and quantity of epoxy and carbonile groups in the structure of the network strongly depends on the preparation method of GO and have certain influences on its properties. Consequently, deoxygenation is required in order to restore some of the original properties of pristine graphene. Nevertheless, it is difficult to fully dehydrate a GO sample. GO can be thermally, chemically or electrochemically reduced to get reduced GO. In this work, two different approaches have been chosen to get reduced graphene oxide: as coating, Electrochemical Reduced Graphene Oxide (ERGO) on a Co alloy from an aqueous suspension; and, as a RGO/metal composite material, where copper particles have being coated by reduced graphene oxide, using a route that combines chemical process hidrazine and thermal treatments in a protective atmosphere. The results include the electrochemical characterization of the ERGO coatings on Co alloys and the characterization of the RGO/Cu composite material by xps, zeta potential and electrical conductivity.

**Keywords:** reduced graphene oxide, electrochemical reduced graphene oxide coating, XPS, zeta potential, electrical conductivity.

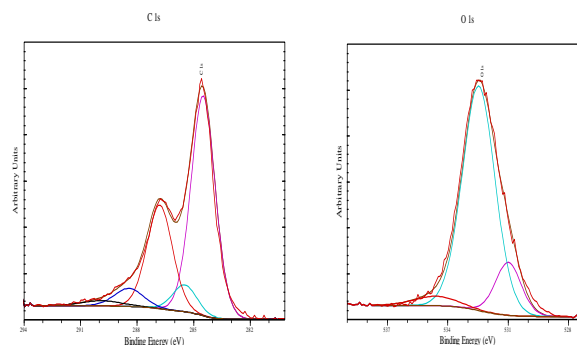


**Figure 1:** High resolution peaks appearing at approximately 284 eV and 530 eV correspond to the C1s and O1s spectra, respectively. C 1s peak is corresponding to the sp<sup>2</sup>-sp<sup>3</sup> bonded carbon network. The ratio of peak intensity between O1s and C1s can be used to determine the oxygen content in the oxygenated graphenes.

## References:

Hilder, M., Winther-Jensen, O., Winther-Jensen, B., & MacFarlane, D. R. (2012), Graphene/zinc nanocomposites by electrochemical co-deposition. *Physical Chemistry Chemical Physics*, 14, 14034-14040.

Mattevi C, Eda G, Agnoli S, Miller S, Mkhoyan KA. (2009), Evolution of electrical, chemical, and structural properties of transparent and conducting chemically derived graphene thin films. *Adv. Funct. Mater.* 19, 2577-2583.

# High orientation degree of graphene nanoplatelets in spark plasma sintered silicon nitride composites

Orsolya Tapasztó<sup>a</sup>, Levente Tapasztó<sup>a</sup>, Victor Puchy<sup>b</sup>, Jan Dusza<sup>b</sup>, Csaba Balázsi<sup>c</sup>, Katalin Balázsi<sup>a</sup>

<sup>a</sup>Center for Energy Research, Institute of Technical Physics and Materials Sciences, 1121 Konkoly

Thege Miklós str. 29-33, Budapest, Hungary

<sup>b</sup>Institute for Material Research, Slovak Academy of Sciences, Watsonova 47, 40001 Kosice, Slovakia

<sup>c</sup>Department of Advanced Materials, Engineering Division, Bay Zoltán Nonprofit Ltd. for Applied Research, 1116 Fehérvári str. 130, Budapest, Hungary

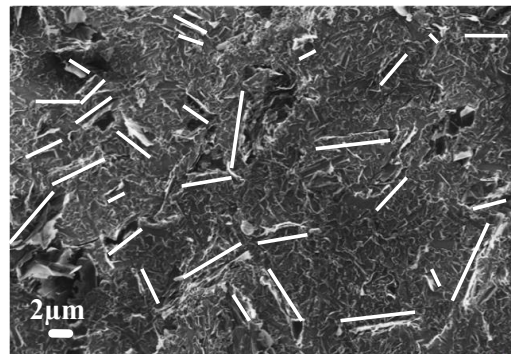
## Abstract:

Silicon nitride ceramics reinforced with exfoliated few-layer graphene nanoplatelets have been prepared by various sintering methods. In the present work we compare two sintering processes (hot isostatic pressing -HIP- and spark plasma sintering -SPS) to consolidate and tailor the microstructure of graphene nanoplatelets/silicon nitride ceramic composites. We have investigated the influence of the sintering processes on the dispersion patterns of the graphene nanoplatelets inside the ceramic matrix.

Scanning electron microscopy investigations revealed strikingly different distribution patterns of the graphene platelets, indicating a preferred orientation of the graphene flakes in the SPS sintered samples, in contrast to HIP sintered samples where a random orientation has been found.

X-ray diffraction and ultra-small angle neutron scattering experiments have been also involved, to provide detailed information on the dispersion of the nano-scale carbon fillers throughout the volume of the ceramic matrix. A clear difference in the distribution patterns of the filler material as a function of the sintering method has been confirmed by these experiments.

**Keywords:** nanocomposites, graphene nanoplatelets, ceramics, spark plasma sintering, self-assembly, microstructure, mechanical properties, scanning electron microscopy, neutron scattering.

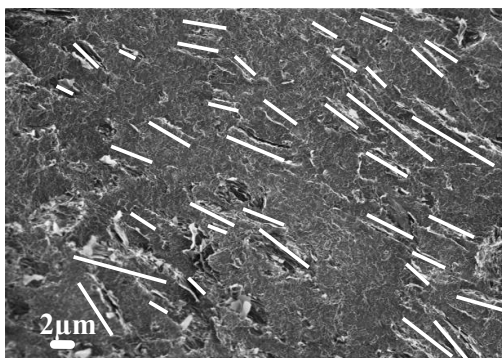


b.

SEM micrographs of fracture surfaces of few  $\text{Si}_3\text{N}_4$  composites containing 3wt% graphene nanoplatelets prepared using SPS (a) and HIP (b). The GNPs can be clearly identified in the micrographs. White lines mark the position and orientation of various GNPs. It is apparent that GNPs in the SPS sintered samples display a preferred orientation direction within each image, in contrast to HIP sintered samples where a closely random orientation is revealed in all of the images.

## References:

Tapasztó O., et al (2016) High orientation degree of graphene nanoplatelets in silicon nitride composites prepared by spark plasma sintering. *Ceramic International* 42, 1002-1006



a.

# Observation of Alkali Metal Adsorption on Freestanding Graphene by Means of LEEPS Microscopy

M. Lorenzo,<sup>1\*</sup> J. Vergés,<sup>1</sup> C. Escher,<sup>1</sup> J.-N. Longchamp,<sup>1</sup> H.-W. Fink<sup>1</sup>

<sup>1</sup>University of Zurich, Department of Physics, Zurich, Switzerland

## Abstract:

The Low-Energy Electron Point Source (LEEPS) microscope is a lens-less setup based on Dennis Gabor's proposition in the year 1948. An ultrasharp field emission point source emits a bright divergent beam of coherent electrons with an energy in the range of 50-250 eV, corresponding to wavelengths of 0.17-0.08 nm. The interference between the electron reference wave and the wave elastically scattered off the sample, produces an hologram on the detector.

Low-energy electrons are particularly sensitive to electromagnetic fields, therefore holography with low-energy electrons allows for probing related phenomena.

We have recently developed a new LEEPS microscope with improved mechanical stability that allows to investigate the adsorption of alkali metals on freestanding graphene.

Thanks to the high transparency (>70%) to low energy electrons, the graphene is an optimal substrate for LEEPS investigations.

Here we present the studies we have just started on Cs adsorption on freestanding graphene with the LEEPS microscope (Figure 1). In particular our studies are focused on the adsorption characteristics as a function of coverage and the influence of defects or wrinkles. Along with these studies we will also investigate the alkali intercalation between two graphene layers.

**Keywords:** electron holography, alkali metals, freestanding graphene, LEEPS microscopy.

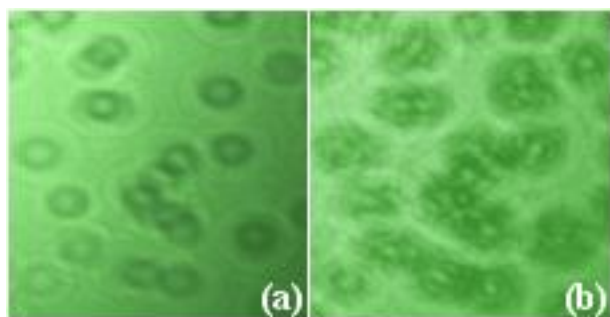


**Figure 1:** Holograms of adsorbates on freestanding graphene (a) and of the Cesium clusters grown around adsorbates (b). The energy of the electron

beam is 160eV and the magnification is  $1.1 \times 10^5$ . The field of view is  $160 \times 160 \text{ nm}^2$ .

## References:

1. Gabor D. (1948) A New Microscopic Principle, *Nature*, 161, 777-778
2. Fink H.-W., Stocker W., Schmid H. (1990) Holography with low-energy electrons, *Phys. Rev. Lett.*, 65, 1204-1206
3. Mutus J. Y., Livadaru L., Robinson J. T., Urban R., Salomons M. H., Cloutier M., Wolkow R. A. (2011) Low-energy electron point projection microscopy of suspended graphene, the ultimate 'microscope slide', *New J. Phys.*, 13, 063011
4. Longchamp J.-N., Latychevskaia T., Escher C. (2012) Low-energy electron transmission imaging of clusters on free-standing graphene, *Appl. Phys. Lett.*, 101, 113117
5. Longchamp J.-N., Escher C., Fink H.-W. (2013) Ultraclean freestanding graphene by platinum-metal catalysis, *J. Vac. Sci. Technol. B*, 31, 020605



# 3D nanodendrites consisting of Pd and N-doped carbon nanoparticles as bifunctional catalyst

H. K. Sadhanala, R. Nandan, and K. K. Nanda\*

Materials Research Centre

Indian Institute of Science, Bangalore – 560012, India.

## Abstract:

Novel self-assembled architectures have received immense research interest over the years owing to their versatile applications as they offer effective material utilization and enhanced stability. For instance, Pt-based nanostructures have widely been explored to facilitate the fuel oxidation as well as oxygen reduction reaction (ORR) as anode and cathode materials in fuel cells. Similarly, various metallic and bimetallic nanostructures have been employed to improve the reaction kinetics of 4-nitrophenol reduction as well. In this regard, Pd-based nanocatalysts with unique morphologies have gained interest, especially for the oxidation of fuels because of their lower cost and greater tolerance to CO in comparison with Pt-based catalysts.

We demonstrate room temperature electroless synthesis of highly active 3D nanodendrites (Figure 1a) consisting of N-doped carbon nanoparticles (N-CNPs) and Pd NPs. The dendrites exhibit superior catalytic activity for methanol oxidation in alkaline media (1M NaOH) which is ascribed to the large electrochemical active surface area and the enhanced mass activity with repeated uses (Figure 1b). Further mass activity improvement has been realized after acid-treatment of dendrites, which is attributed to the increment in –OH functional group (Figure 1c). The dendrites show higher mass activity, better operational stability, superior CO tolerance over commercial Pt-carbon/Pd-carbon (Pt-C/Pd-C) and may serve as a promising alternative to commercial Pt-C catalysts for anode application in alkaline fuel cells. To ensure the adaptability of our 3D-nanodendrites for other catalytic activities, we studied 4-nitrophenol reduction at room temperature (Figure 1d). The 3D-nanodendrites show excellent catalytic activity toward 4-nitrophenol reduction as well.

**Keywords:** nitrogen doped carbon nanoparticles, electroless deposition, Pd nanoparticles, nanodendrites, methanol oxidation and nitrophenol reduction.

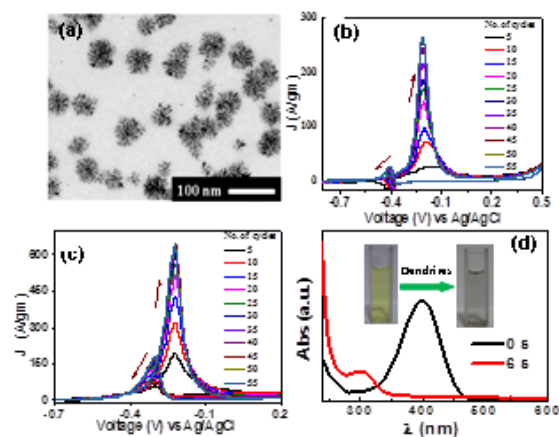


**Figure 1:** (a) TEM image of 3D nanodendrites. (b and c) Cyclic voltammogram of methanol (0.5M) electrooxidation with as-synthesized and acid-treated dendrites. (d) Time-dependent UV-visible spectra of 4-nitrophenol reduction in the presence of dendrites. Inset shows optical image of color change from 4-nitrophenol (yellow) to 4-aminophenol (colorless).

## References:

1. C. Li, Y. Yamauchi (2013), Facile solution synthesis of Ag@Pt core shell nanoparticles with dendritic Pt shells, *Phys. Chem. Chem. Phys.*, 15, 3490-3496.
2. L. Wang, Y. Yamauchi (2013), Metallic nanocages: synthesis of bimetallic Pt-Pd hollow nanoparticles with dendritic shells by selective chemical etching, *J. Am. Chem. Soc.*, 135, 16762-16765.



# Graphene growth and transfer towards flexible substrates for microwave applications

J. Njeim<sup>1,2</sup>, A. Madouri<sup>3</sup>, A. Cavanna<sup>3</sup>, P. Chrétien<sup>2</sup>, A. Jaffré<sup>2</sup>, Z. Ren<sup>1</sup> and D. Brunel<sup>1,2</sup>

<sup>1</sup>L2E | Laboratoire d'Electronique et d'Electromagnétisme, UR2, Université Pierre et Marie Curie-Sorbonne Universités, Campus Jussieu, 75252 Paris Cedex 05, France

<sup>2</sup>GeePs | Group of Electrical Engineering – Paris, UMR CNRS 8507, CentraleSupélec, Université Paris-Sud, Université Pierre et Marie Curie Sorbonne Université, 11 rue Joliot Curie, 91192 Gif-Sur-Yvette Cedex, France

<sup>3</sup>LPN | Laboratoire de Photonique et Nanostructures, CNRS – UPR20, coussis Cedex, France

## Abstract:

Flexible electronics has recently attracted much attention because of its revolutionary potential in offering new paradigms using low production costs, low energy consumption, and environmentally friendly processes. Flexible electronics also sparks high expectations in biomedical applications due to flexibility, biocompatibility and durability of some plastic substrates, qualities that cannot be combined with silicon-based technologies.

Graphene is now well known as an efficient candidate for flexible electronics due to its extraordinary electronic and mechanical properties<sup>1</sup>. Another field where graphene is highly competitive is when flexible is combined with radiofrequency applications such as communicating devices on non-flat surfaces.

Here we present the chemical vapor deposition (CVD) growth from high quality copper foils<sup>2</sup>, transfer and electrical characterization of large area and high quality graphene. To improve the quality of CVD graphene, ideal conditions of growth have to be found by starting from hexagonal single domains. The growth parameters for CVD systems are generally temperature, pressure, gas flow-rate and of course the used gases. High quality monolayer graphene have been successfully grown and transferred towards several targets such as inorganic substrate like silicon dioxide (SiO<sub>2</sub>) or flexible substrates like polyethylene terephthalate (PET) substrates.

A great challenge consists in improving electrical characteristics by nanostructuring the graphene layer after transfer. Graphene nanomeshes (GNM) and graphene Nanoribbons (GNR) are then realized on flexible substrates and results will be discussed in this presentation.

Several characterization techniques have been realized such as Raman Spectroscopy (RS) and combined Atomic Force Microscopy – RS. Moreover, a unique AFM technique named

Resiscope® has been used to measure graphene local resistance.

Very low sheet resistance has been measured around 300 Ω/□ and electron mobility as high as 2000 cm<sup>2</sup>/V.s.

Finally, static and radiofrequency measurements have been performed showing promising results in the field of flexible and communicating devices.

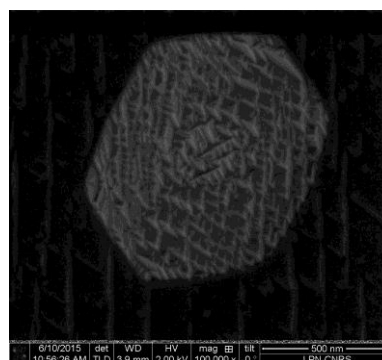


**Figure 1:** First step, graphene growth on a hexagonal single domain of a copper foil.

**Keywords:** graphene, CVD, transfer, flexible electronics, Raman spectroscopy, atomic force microscopy, Resiscope, transistor, radiofrequency.

## References:

1. A.C. Ferrari *et al.* *Nanoscale* **7**, 11, 4587 (2015)
2. Z. Han *et al.* *24*, 7, 964 (2013)
3. O. Schneegans *et al.* Brevet national FR1001940 (2010)

# Multi-layered graphene interface for enhancing the stretchability of brittle conductive layers

Sejeong Won,<sup>1</sup> Yun Hwangbo,<sup>1,\*</sup> Kwang-Seop Kim<sup>1</sup>, Hak-Joo Lee<sup>1</sup>, Jae-Hyun Kim<sup>1</sup>  
<sup>1</sup>Department of Nanomechanics, Nano-Convergence Mechanical Systems Research Division, Korea Institute of Machinery & Materials (KIMM), 156 Gajungbuk-ro, Yuseong-gu, Daejeon 305-343, Republic of Korea.

**Abstract:** Oxide materials are important for potential applications in flexible and stretchable electronics because of their excellent electrical properties and the wide range of possible material combinations. However, the intrinsic brittleness has been an obstacle to their widespread usage in flexible and stretchable electronics (Won *et al.*; 2014, 2015). In this report, we propose the use of a multilayered graphene interface to improve the stretchability of the oxide layer for applications in flexible electronics. Electromechanical tensile tests of indium tin oxide (ITO) layers on polymer substrates were performed with in situ optical microscopy observations. The electromechanical stretchability of the ITO layer was increased by inserting a graphene interface between the ITO layer and the substrate. To investigate the mechanism by which the graphene interface improves the electromechanical stretchability, we experimentally measured the electrical resistance and the crack density of the ITO, and the electromechanical behavior of the graphene interface was analyzed using a shear lag model. We find that the main reason for the improved electromechanical stretchability is reduction of the transferred strain from the substrate to the ITO layer due to interlayer sliding in the graphene interface (Won *et al.*; 2015). The multilayered graphene interface provides a useful pathway for realizing flexible and stretchable electronic applications based on oxide layers.

**Keywords:** graphene, indium tin oxide, stretchability, shear lag model, electromechanical behavior.

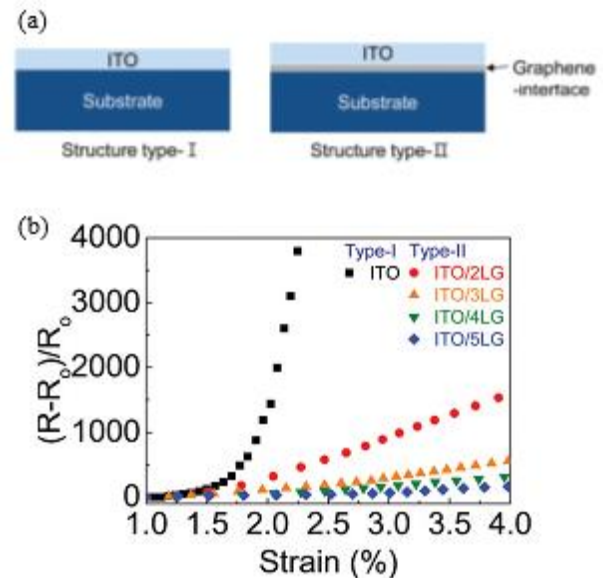


**Figure 1:** Electromechanical behavior of the type-I and type-II structures as a function of strain. (a) Schematics of the type-I (ITO/PET) and type-II (ITO/multilayer graphene/PET) structures (b) The normalized electrical resistance of the type-I and type-II structures as a function of the tensile strain.

## References:

1. S. Won, Y. Hwangbo, S.-K. Lee, K.-S. Kim, K.-S. Kim, S.-M. Lee, H.-J. Lee, J.-H. Ahn, J.-H. Kim and S.-B. Lee. (2014), Double-layer CVD graphene as stretchable transparent electrodes, *Nanoscale*, 6, 6057-6064.
2. S. Won, J.-W. Jang, H.-J. Choi, C.-H. Kim, S. B. Lee, Y. Hwangbo, K.-S. Kim, S.-G. Yoon, H.-J. Lee, J.-H. Kim, S.-B. Lee. (2015), A graphene meta-interface for enhancing the stretchability of brittle oxide layers, *Nanoscale*, DOI: 10.1039/c5nr05412e.

# Experimental study of the electrical properties of multilayer graphene-fullerene C<sub>60</sub>-multilayer graphene junctions

E. Benítez, D. Mendoza.

Instituto de Investigaciones en Materiales, Departamento de Materia Condensada y Criogenia, Universidad Nacional Autónoma de México, México D. F., México.

**Abstract:** Carbon based nano-materials has been studied since the last part of the past century, in particular graphene as one of the most promising materials to function as the successor for Silicon. The recent discovery of graphene (Novoselov et al. 2004) has provided a large amount of fascinating physics [1,2].

Graphene is topic of current research interest due to its excellent properties e.g. transmittance of about 97% of the visible light [3] and the high thermal conductivity of the order of  $5 \times 10^3$  W/mK [4].

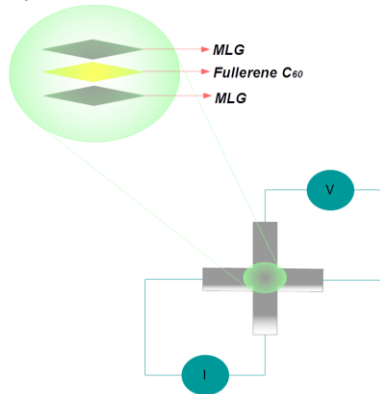


**Figure 1:** Diagram of the cross junction configuration: an electrical current  $I$  is injected and a voltage drop  $V$  is measured in the opposite arms.

Using the technique of Chemical Vapor Deposition (CVD), we obtained the multilayer graphene (MLG) onto copper substrates, after copper foil was dissolved the MLG films were transferred on to a glass substrates.

Cross junction devices of the form MLG-C<sub>60</sub>-MLG were made, where the sandwiched thin film of C<sub>60</sub> was obtained by thermal evaporation (see *figure 1*).

Electrical conductance as a function of light intensity as well as a function of temperature were measured in these devices.

The most notorious result is that the electrical conductivity of the junction increases under illumination and also by increasing its temperature; such as is shown in *figure 2*.

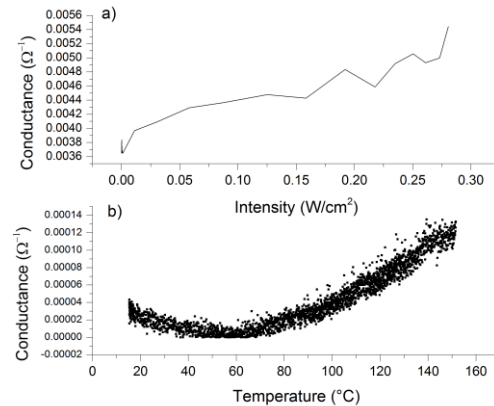


**Figure 2:** a) Conductance vs. light intensity using a red laser diode (650nm of wavelength) b) conductance vs. temperature with 250nA of injected current in both cases.

We may conclude that the observed photoconductive effect is related to the electron-hole pairs generated in the C<sub>60</sub> layer and transferred to the MLG electrodes; in a similar way to the reported effect observed in the C<sub>60</sub>-MLG junction [5].

**Keywords:** graphene, fullerene C<sub>60</sub>, photoconductivity, cross junction device.

## References:

1. Geim, A. K., Novoselov, K. S. (2007), The Rise of Graphene, *Nature Materials*, 6, 183–191.
2. Katsnelson, M. I. (2007), Graphene: Carbon in Two Dimensions, *Materials Today*, 10(1-2), 20 – 27.
3. Nair, R. R., Blake, P., Grigorenko, A. N., Novoselov, K. S., Booth, T. J., Stauber, T., Peres, N. M. R., Geim A. K. (2008), Fine Structure Constant Defines Visual Transparency of Graphene, *Science*, 320.
4. Balandin, A. A., Ghosh, S., Bao, W., Calizo, I., Teweldebrhan, D., Miao, F., Lau, C. N. (2008), Superior thermal conductivity of single-layer graphene, *Nano Letters*, 8(3), 902-907.
5. Bautista-Flores, C., Sato-Berrú, R. Y., Mendoza, D. (2014), Charge transfer in the fullerene C<sub>60</sub>-few layer graphene system and the existence of negative photoconductivity, *Applied Physics Letters*, 105(191116).

# Spin transport in fully hexagonal boron nitride encapsulated graphene

M. Gurram,<sup>1\*</sup> S. Omar,<sup>1</sup> S. Zihlmann,<sup>2</sup> P. Makk,<sup>2</sup> C. Schönenberger,<sup>2</sup> and B.J. van Wees<sup>1</sup>

<sup>1</sup>Physics of Nanodevices, Zernike Institute for Advanced Materials, University of Groningen, Groningen, The Netherlands

<sup>2</sup>Department of Physics, University of Basel, Basel, Switzerland

## Abstract:

In a quest to figure out the sources limiting the intrinsic spin transport in graphene, there have been several experiments, which suggest that the role of underlying substrate and the quality of tunnel barrier is crucial[1].

We study fully hexagonal boron nitride (hBN)-encapsulated graphene spin valve devices, fabricated to overcome the shortcomings of the substrate and the tunnelling barrier. The device consists of a graphene channel encapsulated between two crystalline hBN flakes; thick-hBN flake as a bottom gate dielectric substrate which masks the charge impurities from SiO<sub>2</sub>/Si substrate and single-layer thin-hBN flake as a tunnel barrier. Full encapsulation prevents the graphene from coming in contact with any polymer/chemical during the lithography and thus gives homogeneous charge and spin transport properties across different regions of the encapsulated graphene. Further, even with the multiple electrodes in between the injection and the detection electrodes which are in conductivity mismatch regime, we observe spin transport over 12.5 μm long distance under the thin-hBN encapsulated graphene channel, demonstrating the clean interface and the pin-hole free nature of the thin-hBN as an efficient tunnel barrier.

**Keywords** nitride, Tunnel barrier, Full encapsulation: Spintronics, Graphene, Boron.

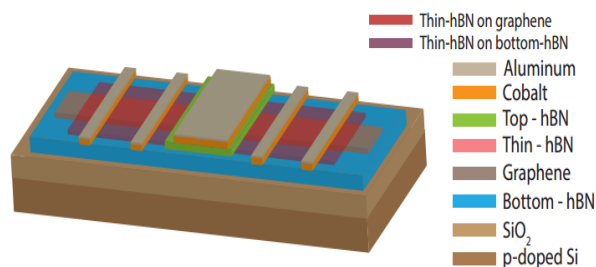


**Figure 1:** Schematic of the proposed fully hBN encapsulated graphene spin valve device to overcome the challenges due to i) the influence of underlying substrate, ii) the influence of tunnel barrier interface, and iii) the inhomogeneity in graphene channel.

## References:

1. Roche, S., and Valenzuela, S. O. (2014), Graphene spintronics: puzzling controversies and challenges for spin manipulation, *Journal of Physics D: Applied Physics* 47, 094011.
2. Gurram, M., *et al.*, (2016), Spin transport in fully hexagonal boron nitride encapsulated graphene., *Submitted*.

# Ultra-Broadband Strong Absorption Enhancement in Graphene with Plasmonic Light Trapping

Feng Xiong, Jianfa Zhang

College of Optoelectronic Science and Engineering, National University of Defense Technology, Changsha 410073, China

## Abstract:

Graphene shows very high carrier mobility and exhibits a nearly universal optical absorption of about 2.3% in the spectral range from the ultraviolet to infrared, which makes it a promising material for high speed and broadband photodetectors. However, even though such an absorption is quite remarkable considering its atomic thickness, it is too weak for practical applications. So lots of research efforts have been made to enhance its interactions with light. Many approaches have been proposed to enhance the absorption in graphene, including using F-P cavities, photonic crystals as well as plasmonic nanostructures[1-2]. However, realizing both broadband and strong absorption enhancement remains a challenge. Here we study the absorption enhancement in graphene with light trapping by plasmonic absorbers and show that  $> 30\%$  light absorption by monolayer graphene can be realized in an ultra-broad spectral range from 940 to 1950 nm with a proposed design.

**Keywords:** Graphene, absorption enhancement

Figure 1a shows the schematic illustration and geometric parameters of our proposed structures for plasmonic light trapping. The metallic structure consists of arrays of periodical metallic crosses backed by a metallic mirror, which is a well-known design for plasmonic absorbers. The structure contains two crosses with different dimensions in each unit cell, which is specially designed to expand the absorption bandwidth. The side width of the large cross is 410 nm and that of the small cross is 330 nm. The incident light excites localized plasmons in the metallic structure, which traps light in the near-field and leads to strong absorption. As the graphene film is now integrated in the structure, a significant proportion of light will be absorbed by the graphene which will far exceed the absorption by a free standing graphene film. Figure 1b shows the spectra of absorption in the graphene. It exhibits  $> 30\%$  light absorption by monolayer graphene in an ultra-broad spectral range from 940 to 1950 nm (the red solid curve).

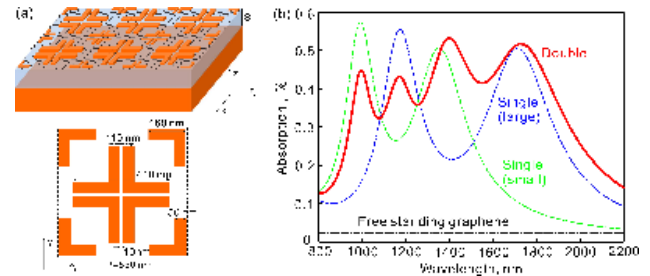


**Figure 1:** Plasmonic light trapping and absorption enhancement in graphene. (a) Scheme of the proposed design with geometric parameters. From the top to the bottom are an array of metallic crosses, the monolayer graphene, an insulator layer with a thickness of  $s = 80$  nm and a metallic reflection mirror, respectively. The metallic crosses have 10 nm wide cross gaps in the middle. The period is  $P = 550$  nm. (b) Simulated spectra of absorption in the graphene (red solid line). The absorption for the structures with just one type of crosses is described by the dashed blue line (large crosses) and dashed green line (small crosses). The flat dashed line shows the absorption ( $\sim 2.3\%$ ) in a free standing graphene without enhancement.

In summary, we have investigated plasmonic absorber designs for light trapping and absorption enhancement in graphene. Absorption enhancements up to tens of times in an unprecedented broad spectral range are realized. The design may significantly improve the efficiency of optoelectronic devices based on graphene and other two-dimensional materials [3].

## References:

1. T. Echtermeyer, L. Britnell, P. Jasnó, A. Lombardo, R. Gorbachev, A. Grigorenko, A. Geim, A. Ferrari, and K. Novoselov, "Strong plasmonic enhancement of photovoltage in graphene," *Nature Communications* 2, 458, 2011.
2. S. Song, L. Wen, and Q. Chen, "Graphene photodetector based on metamaterial perfect absorber," *Session 2P8 SC2&3: Light Harvesting for Energy and Optoelectronic Applications* p. 847, 2014
3. F. Koppens, T. Mueller, P. Avouris, A. Ferrari, M. Vitiello, and M. Polini, "Photodetectors based on graphene, other two-dimensional materials and hybrid systems," *Nat. Nanotechnol.* 9, 780–793 (2014).



# Novel Aerosol Synthesis of Pt Nanoparticles-Laden Graphene via Microwave Plasma Spray Pyrolysis and Their Enhanced Methanol Oxidation Reaction

Hankwon Chang,<sup>1,2,\*</sup> Eun Hee Jo,<sup>1,2</sup> Sun Kyung Kim,<sup>1</sup> Hee Dong Jang,<sup>1,2</sup>

<sup>1</sup>Mineral Resources Research Division, Korea Institute of Geoscience and Mineral Resources (KIGAM), Daejeon, Korea

<sup>2</sup>Nanomaterials Science and Engineering Major, University of Science and Technology (UST), Daejeon, Korea

## Abstract:

Graphene (GR), a two-dimensional monoatomic carbon sheet, has received much attention due to its unique and interesting properties and its potential applications include transparent conducting electrodes, biosensors, fuel cells, and energy storage devices (Krishnan et al., 2012). Especially, GR can be applied as a catalyst support for the direct methanol fuel cell (DMFC) due to its excellent electrical conductivity and extremely high specific surface area. In addition, the platinum (Pt) catalyst has been used as electrocatalysts in DMFCs because it is very effective in reducing oxygen in cathodes and methanol oxidation in anodes. Thus, GR-supported Pt nanoparticles can be a promising materials for the enhanced methanol oxidation reaction (Jang et al., 2012).

Here, we suggest a new aerosol process for the synthesis of Pt nanoparticles-laden GR from a solution of platinum acid and ethanol via microwave plasma spray pyrolysis with advantage of simple and continuous process. We prepared the Pt nanoparticles-laden GR (Figure 1) with different concentrations of platinum acid and characterized their particle properties such as morphology, crystal structure, the number of graphene layer, Pt contents in the composites and specific surface area by using TEM, EDS, XRD, Raman spectrometry, TGA and BET. Further we analyzed the methanol oxidation reaction by the as-prepared Pt/GR. The Pt nanoparticles-laden GR having a high specific surface area ( $402 \text{ m}^2/\text{g}$ ) and an electrochemical surface area ( $77 \text{ m}^2/\text{g}$ ) showed the more enhanced catalytic performance for methanol oxidation compared with a commercial Pt/carbon black

**Keywords:** platinum nanoparticles-laden graphene, microwave plasma spray pyrolysis, methanol oxidation reaction, direct methanol fuel cell, electrochemical catalyst.

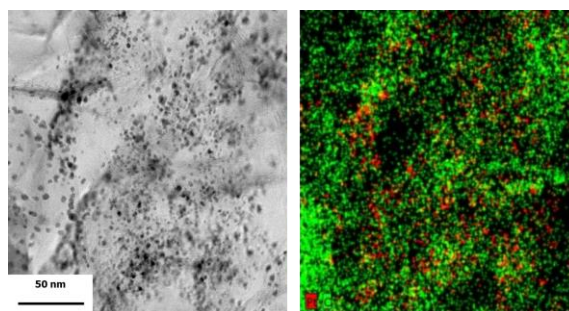


**Figure 1:** TEM and EDS mapping images of Pt nanoparticles-laden graphene prepared by microwave plasma spray pyrolysis.

## References:

Jang, H. D., Kim, S. K., Chang, H., Choi, J. W., Luo, J., Huang, J. (2012) One-step synthesis of Pt-nanoparticles-laden graphene crumples by aerosol spray pyrolysis and evaluation of their electrocatalytic activity, *Aerosol Sci. Technol.*, 47, 93-98.

Krishnan, D., Kim, F., Luo, J., Cruz-Silva, R., Cote, L. J., Jang, H. D., Huang, J. (2012), Energetic graphene oxide: Challenges and opportunities, *Nanotoday*, 7, 137-152.

# Diverse anisotropy of phonon transport in two-dimensional group IV-VI compounds: A comparative study

Guangzhao Qin,<sup>1</sup> Ming Hu<sup>1,2,\*</sup>

<sup>1</sup>Institute of Mineral Engineering, Division of Materials Science and Engineering, Faculty of Georesources and Materials Engineering, RWTH Aachen University, Aachen 52064, Germany

<sup>2</sup>Aachen Institute for Advanced Study in Computational Engineering Science (AICES), RWTH Aachen University, Aachen 52062, Germany

## Abstract:

The four novel monolayer compounds of *GeS*, *GeSe*, *SnS* and *SnSe*, which attracted tremendous interest recently, have great potential applications in nanoelectronics, optoelectronics and thermoelectrics, calling for fundamental study of the phonon transport properties. A complete and comparative prediction and understanding of the underlying phonon transport properties is the key to expand the range of their applications in nanoelectronics, optoelectronics and thermoelectrics. In this paper, we conduct comprehensive investigations of the diverse phonon transport properties of the 2D orthorhombic group IV-VI compounds. It is found that all the four monolayer compounds possess rather low thermal conductivity compared to lots of other 2D materials. The most intriguing phenomenon is that, the four monolayer compounds, although possessing similar hinge-like structure along the armchair direction as phosphorene, show diverse anisotropic properties in many aspects, such as phonon group velocity, Young's modulus and lattice thermal conductivity ( $k$ ), etc. We present a detailed analysis on the phonon transport and focus on the anisotropy. Besides the discussions in the framework of BTE theory, we also provide convincing understandings of the underlying mechanisms from the scattering channels and the more fundamental physical properties, i.e. electron localization functions (ELF). It is concluded that the anisotropic behavior of the ELF reflecting the bonding characteristics is the physical origin of the anisotropic properties. Furthermore, we found that the  $k$  could be effectively lowered and the anisotropy could be effectively modulated by nanostructuring. This study not only give detailed information of the phonon transport properties of the new family of 2D compounds (*GeS*, *GeSe*, *SnS* and *SnSe*), but also reveal their unexpected diverse anisotropy of phonon transport by providing discussions and analysis on the physical origins, which enriches the understanding of nanoscale phonon transport in 2D materials and would be of significance for thermal modulation and thermal management in the application fields of nanoelectronics and nanoenergy.

**Keywords:** 2D materials, hinge-like, phonon transport, thermal conductivity, anisotropy, first-principles

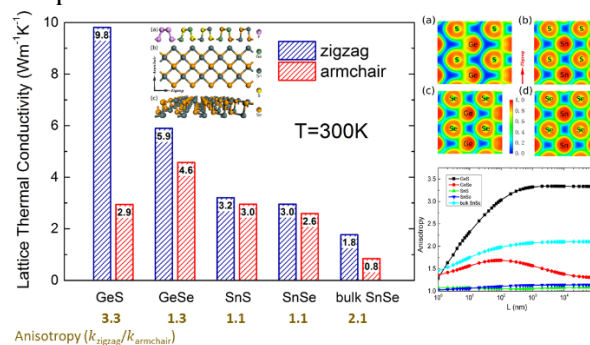


**Figure 1:** The four monolayer group IV-VI compounds (*GeS*, *GeSe*, *SnS* and *SnSe*), although possessing similar puckered (hinge-like) structure along the armchair direction as phosphorene, show diverse anisotropic properties in phonon transport.

## References:

1. Zhao, L. D., Lo, S. H., Zhang, Y., Sun, H., Tan, G., Uher, C., ... & Kanatzidis, M. G. (2014). Ultralow thermal conductivity and high thermoelectric figure of merit in SnSe crystals. *Nature*, **508(7496)**, 373-377.
2. Qin, G., Yan, Q. B., Qin, Z., Yue, S. Y., Cui, H. J., Zheng, Q. R., & Su, G. (2014). Hinge-like structure induced unusual properties of black phosphorus and new strategies to improve the thermoelectric performance. *Scientific Reports*, **4**, 6946.
3. Qin, G., Yan, Q. B., Qin, Z., Yue, S. Y., Hu, M., & Su, G. (2015). Anisotropic intrinsic lattice thermal conductivity of phosphorene from first principles. *Physical Chemistry Chemical Physics*, **17(7)**, 4854-4858.

# Effect of modified Graphene and Montmorillonites and their mixtures on the properties of biodegradable PLA/PCL blend

Abderrahmane HABI<sup>1,\*</sup>, Boubkeur Seddik BOUAKAZ<sup>1,2</sup>, Yves GROHENS<sup>2</sup>, Isabelle PILLIN<sup>2</sup>

<sup>1</sup>Laboratoire des Matériaux Organiques (LMO), Université A. MIRA de Béjaia, Route de Targa Ouzemour 06000, Bejaia, Algérie.

<sup>2</sup>Laboratoire d'Ingénierie des Matériaux de Bretagne, EA4250, Université de Bretagne Sud, Rue de Saint Maudé, F-56100 Lorient, France.

**Abstract:** Nowadays, polylactide (PLA), a renewable and biodegradable polymer obtained through bio conversion and polymerization, is considered as the most promising biopolymer due to its excellent mechanical properties, comparable to those of conventional polymers, and its low cost. The main drawbacks of this polymer are its brittleness and poor thermal stability, which significantly limit its expansion into new trading application areas. To improve PLA's properties, blending with ductile polymers such as poly ( $\epsilon$ -caprolactone) and/or nanofillers was widely reported in the literature. In this work, we report the effect of nanofiller mixtures on the morphology, thermal and barrier properties of PLA/PCL (70/30 wt.%) prepared using twin screw extruder machine. A transition from liquid-like to solid-like behavior and a high value of elastic modulus, loss modulus and complex viscosity (at the terminal region) for quaternary nanoblends (PLA /PCL /Cloisites<sup>®</sup> /Graphene), attributed to the better dispersion of hybrids clay mineral/graphene in the PLA/PCL blend, were observed using rheological technique and confirmed on transmission electronic microscopy (TEM) images. The thermal stability (TGA) and water vapor properties (WVP) of unfilled blend and ternary nanocomposites were significantly enhanced via melt blending of PLA/PCL matrix with hybrids Cloisites<sup>®</sup>/graphene, indicating the high level of dispersion and also the existence of a synergy between the Cloisites<sup>®</sup> and graphene fillers. Scanning electronic microscopy (SEM) characterization showed that the blend morphology was influenced by nanofillers incorporation to immiscible blend, indicating some improvement of PLA/PCL compatibility.

**Keywords:** PLA/PCL blend, Miscibility, Cloisites<sup>®</sup>, Graphene, Nanocomposites, Properties.

## References:

1. Södergård, A., Stolt, M., (2002), Properties of lactic acid based polymers and their correlation with composition, *Prog Polym Sci.* 27, 1123-63.
2. Forouharshad, M., Gardella, L., Furfaro, D., Galimberti, M., Monticelli O., (2015), A low-environmental-impact approach for novel biocomposites based on PLLA/PCL blends and high surface area graphite, *Eur. Polym. J.*, 70, 28-36.
3. Li, Q., Yoon, J., Chen, G., (2011), Thermal and Biodegradable Properties of Poly(l-lactide)/Poly( $\epsilon$ -Caprolactone) Compounded with Functionalized Organoclay, *J. Polym. Environ.*, 19, 59-68.
4. Bouakaz, B. S., Pillin, I., Habi A., Grohens Y., (2015), Synergy between fillers in organo-montmorillonite/graphene-PLA nanocomposites, *Appl. Clay Sci.*, 116-117, 69-77.

# Magneto-optical characterization of super-lattices in graphene

T. Wolf, I. P. Levkivskyi, O. Zilberberg, G. Blatter

ETH Zurich, Institute for Theoretical Physics, Zurich, Switzerland

## **Abstract:**

The unique electronic and optical properties of graphene are often compromised by impurities and disorder, a difficulty that can be overcome by using boron nitride as a substrate. Such a substrate introduces new physical effects in graphene due to the formation of a super-lattice structure caused by the nearly 2% difference in lattice constants of graphene and hexagonal boron nitride. The super-lattice structure manifests itself by several peculiar phenomena, such as a Hofstadter's butterfly appearing in a magnetic field, trigonal warping of the band structure, etc. The low-energy physics of graphene on a boron nitride substrate is conveniently described by an effective theory that contains all relevant terms allowed by the super-lattice symmetries. We find, in analytic form, the infra-red optical transmission in the presence of a magnetic field, with the goal to infer the parameters of the superlattice potential from measured data.

**Keywords:** Graphene, hexagonal boron nitride, super-lattice, super-potential, Dirac Fermions, Optical absorption, Infra-red, Magnetic fields.

# Development of Graphene-based Barriers for Solar Cells

Gabriella Rossi<sup>1,\*</sup>, Maria Sarno<sup>1,2</sup>, Claudia Cirillo<sup>1</sup> and Loredana Incarnato<sup>1,2</sup>

<sup>1</sup>University of Salerno, Department of Industrial Engineering, Fisciano (SA), Italy

<sup>2</sup>University of Salerno, Centre NANO\_MATES, Fisciano (SA), Italy

## Abstract:

Conventional transparent electrodes of solar cells make use of tin oxide (ITO) or Fluorine Tin Oxide which have optical transparency of 90% and of 82.4%, respectively and unlimited scalability. Nevertheless, ITO films are expensive due to the high cost of the current ITO vacuum fabrication method and the high cost of Indium materials (Bae et al., 2010).

Graphene films may be considered an effective alternative as window electrode because of their excellent transmittance of 97.7% per layer of graphene (Nair, R. R. et al., 2008). Indeed, graphene is recently attracting great attention not only for its outstanding electrical and optical properties (Novoselov, K. S. et al., 2012), but also for the gas barrier properties (Bunch J. S. et al., 2008). This last characteristic is particularly suitable for photovoltaic (PV) application, since it is well known that the protection of flexible solar cells from the atmospheric degradation agents still represents a challenge for ensuring an acceptable lifetime.

In this study, a transparent barrier film was produced of PET-graphene, thought to be applicable with a double functionality of window electrode and of barrier film for flexible solar cells.

Few-layer graphene have been synthesized via ambient pressure Catalytic Chemical Vapour Deposition of methane on a copper foil at temperature of 950°C. After synthesis graphene was transferred on the PET substrate: first of all gluing on the carbon layer a thermal release tape by applying soft pressure; followed by an etching to remove the Cu foil; and finally transferring the few layers graphene film on substrate applying uniform pressure at 80°C.

The optical characterization of the obtained PET-graphene film revealed a percent transmittance of 86% with a small reduction of 4% in transparency in comparison with the uncoated substrate. Furthermore, the measurement of the oxygen transmission rate highlighted an outstanding increase of 84% of the O<sub>2</sub> barrier properties of the PET films that were coated with graphene. Thus, thermal characterization and X-ray diffraction analysis were performed to assess if a PET crystallinity increase occurred consequently to the graphene deposition process conditions. Even though the preliminary data indicate a crystallinity growth up to Xc approximately 12%, this value does not justify such a relevant increase of the barrier properties that can be essentially attributed to the presence of the graphene coating. The surface morphology of the ob-

tained samples, investigated with Atomic Force Microscopy, revealed the presence of ripples, where it can be seen that areas covered with few layer of graphene coexist with islands with a higher number of layers (Fig. 1). The measured arithmetic average roughness R<sub>a</sub> (15.8 nm) needs to be optimised since a smooth surface is necessary for electrodes in organic solar cells.

Concluding, the preliminary results indicate that the developed system has a great potential to effectively act as a transparent electrode for solar cells while at the same time protecting the PV device from the oxygen induced degradation.

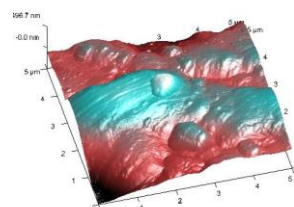


**Figure 1:** AFM 3D Tapping mode image of PET/Graphene sample with surface area of 5 x 5 µm<sup>2</sup>

**Keywords:** flexible solar cells, PET-graphene films, oxygen barrier, transparent electrode.

## References:

1. Bae, S., Kim, H., Lee, Y., Xu, X., Park, J.-S., Zheng, Y., Balakrishnan, J., Lei, T., Kim, H. R., Song, Y., Kim, Y. J., Kim, K. S., Ozyilmaz B., Ahn J-H, Hong, B.H., Iijima S. (2010), Roll-to-roll production of 30-inch graphene films for transparent electrodes, *Nature nanotechnology* 5, 574–578.
2. Nair, R. R., Blake, P., Grigorenko A. N., Novoselov K. S., Booth T. J., Stauber T., Peres N.M.R., Geim A. K. (2008), Fine structure constant defines visual transparency of graphene, *Science*, 320, 1308.
3. Novoselov, K. S., Fal'ko, V. I., Colombo, L., P.R. Gellert, P. R., Schwab M. G., Kim, K. (2012), A roadmap for graphene, *Nature* 490, 192.
4. Bunch J. S., Verbridge S. S., Alden J. S., B., van der Zande A. M., Parpia J.M., Craighead H. G., McHeuen, P. L (2008), Impermeable atomic membranes from graphene sheets, *NanoLett.* 8, 2458-246.



# Green chemistry process for the synthesis of next generation of photocatalyst based on graphene nanocomposites

Ouarda Fellahi<sup>1\*</sup>, Faouzya Khili<sup>2</sup>, Nouh Belalia<sup>3</sup>, Bilal Khenfous<sup>3</sup>, Zeggane Belaid<sup>4</sup>, Toufik Hadjersi<sup>1</sup>, Rabah Boukherroub<sup>2</sup>

<sup>1</sup>Technology Research Centre of Semiconductors for Energy,  
02 Bd Frantz fanon , BP 140 7-merveilles-Algiers, Algeria;

<sup>2</sup>Interdisciplinary Research Institute, Campus CNRS - Parc de la haute-borne  
50 avenue de Halley, BP 70478, Villeneuve d'Ascq Cédex, France;

<sup>3</sup>Laboratory of Reaction Engineering, Faculty of Mechanical Engineering and Process Engineering, Bp 32.El Alia.Bab Ezzouar-16111, Algiers, Algeria.

<sup>4</sup>Université Saad Dahlab Blida, Algérie

\*Corresponding author: fellahiouarda@crtse.dz

**Abstract:** Graphene-based materials have received significant attention in recent years since their discovery in 2004 due to their unique two-dimensional structure, high conductivity, superior electron mobility and extremely high specific surface area, and can be produced on a large scale at low cost [1]. Thus, it has been regarded as an important component for making various functional composite materials. Especially, graphene-based semiconductor photocatalysts have attracted extensive attention because of their usefulness in environmental and energy applications.

A green chemical approach, to synthesize metal-graphene (Me-G) nanocomposites in the water-reducing agent system, using graphene oxide and metal salt were usually used as the precursors of both components.

The incorporation of graphene into the composites can provide unique properties and possibly induces new functions based on synergetic effects, providing a new opportunity for designing and developing next-generation catalysts [2]. Graphene-based semiconductor photocatalysts have been extensively applied to photocatalytic degradation of organic compounds. These, photocatalysts possess high dye adsorption capacity, extended light absorption range, and enhanced charge separation and transportation properties [3].

In this work, we used silicon nanowires modified with Metal (Ag, Cu) –graphene nanocomposites as photocatalysts for the degradation of pollutant molecules in an aqueous solution under visible irradiation. The nanocomposites have been prepared by a facile one-step reduction method using graphene oxide, copper sulfate and silver nitrate. SiNWs samples were elaborated by Ag-assisted electroless etching method. It is shown that higher photocatalytic activity is obtained when Cu nanoparticles are used as nanocomposites with the graphene. Indeed, Fig.1 clearly depicts that the degradation rate is

higher for SiNWs modified with the nanocomposites of Cu-G than that for Ag-G. A photodegradation of 93% after 150 min of visible irradiation was obtained. The different photocatalysts were characterized by WXRf analysis, X-ray diffraction, Fourier transform infrared spectrum (FT-IR), photoluminescence (PL) and scanning electron microscopy (SEM).

**Keywords:** Keywords: Graphene oxide; silicon nanowires; heterogeneous photocatalysis; graphene nanocomposite.

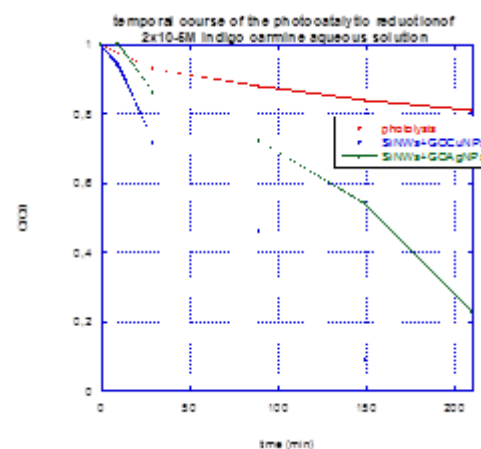


**Figure 1:** Temporal course of the photocatalytic reduction of  $2 \times 10^{-5} \text{M}$  Indigo Carmine aqueous solution.

## References:

1. Ouarda Fellahi & al, Silicon nanowire arrays-induced graphene oxide reduction under UV irradiation, *Nanoscale*, 2011, 3, 4662.
2. Bruno F.Machado & al, Graphene-based materials for catalysis, *Catal.Sci.Technol.*, 2012,2,54-75.
3. Quanjun Xiang & al, Graphene-based semiconductor photocatalysts, *Chem.Soc.Rev.*,2012,41,782-796

# FlexeGRAPH: Graphene and 2D Materials Production at The Australian National University

Shannon M Notley

Department of Applied Mathematics, Research School of Physics and Engineering, The Australian National University, Acton ACT 2601 Australia

**Abstract:** The Australian National University (ANU) holds a unique IP portfolio in the production of pristine graphene and other 2D material particles. At the heart of the technology, is the ability to control stabilization in water and non-aqueous solvents as well as the flexibility to improve compatibility with a range of materials such as thermosets and thermoplastics to enhance dispersion.

FlexeGRAPH [1] is the recently launched brand for 2D materials manufactured at ANU. It is produced via a scalable method resulting in graphene and other atomically thin particles ideally suited for use in many applications. The facile technique leads to large defect free particles with very low thickness (typically 90% less than 2nm) with high electrical and thermal conductivity. The production facility was commissioned in October 2015 with a capacity of 2 tonnes per year however this process is easily scaled to larger volumes. The process itself is non-toxic and environmentally friendly.

Supply certainty using the low cost in-house production facility coupled with the ability to control interfacial properties of the 2Ds has allowed us to focus on validating the use of graphene in downstream high volume applications centred on thermal management. This presentation will concentrate on the use of graphene and hexagonal-boron nitride to render inherently thermally insulating materials heat conducting. Our main areas of attention to date are:

- Phase change materials with high thermal conductivity for use in energy storage, transport and construction.
- Thermosets such as urethanes, acrylates, epoxies and benzoxazines tailored for applications including thermal interface materials and structural composites.
- Heat transfer fluids for solar thermal co-generation systems and coolants for engines.

We have used the laser flash technique (LFA) in order to determine the thermal properties of the diverse systems described above in addition to the extensive characterization of the raw 2D materials (Figure 1).

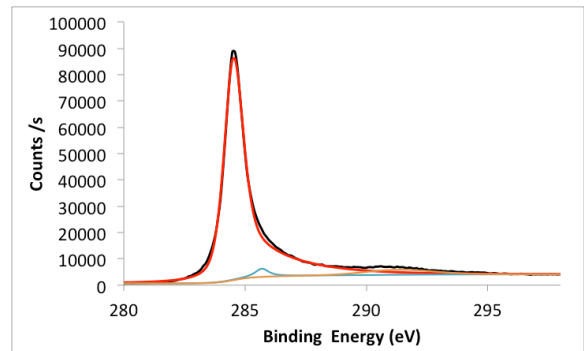
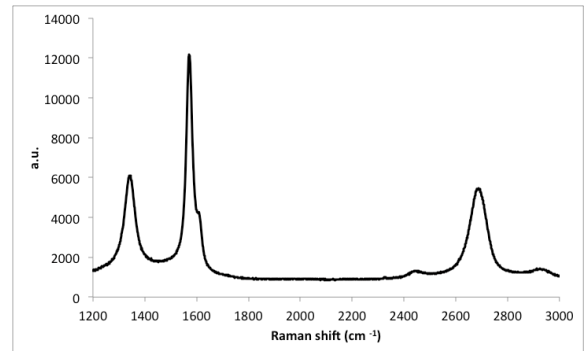
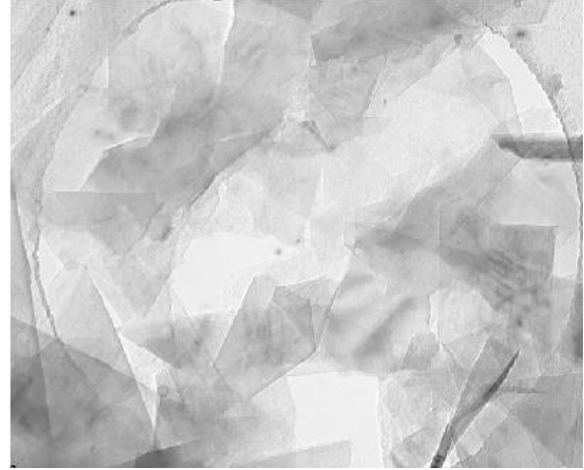


**Figure 1:** Top: TEM image of FlexeGRAPH graphene (image scale 1  $\mu\text{m}$  across). Middle: Raman Spectrum of FlexeGRAPH graphene. Bottom: XPS C1s peak of FlexeGRAPH graphene with a C:O of 60:1.

**Keywords:** graphene production, thermal management, phase change materials, thermoset, heat transfer fluid.

## References:

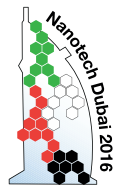
1. <https://graphene.anu.edu.au>



## Allied Events



**nano tech  
2016**  
International Nanotechnology  
Exhibition & Conference



**NANO KOREA 2016**

July 13 (Wed.) ~ 15 (Fri.), **KINTEX**, Gyeonggi-do, Korea

## With the support of



## Media Partners



[www.nanopro.biz](http://www.nanopro.biz)  
PROMOTING NANOTECHNOLOGIES

